WADC-TN-59-365

PROJECT PLUTO

Volume III

The Marquardt Corporation

NOVEMBER 1959
Final Report

Approved for public release; distribution unlimited.

See additional restrictions described on inside pages

AIR FORCE RESEARCH LABORATORY
AEROSPACE SYSTEMS DIRECTORATE
WRIGHT-PATTERSON AIR FORCE BASE, OH 45433-7541
AIR FORCE MATERIEL COMMAND
UNITED STATES AIR FORCE

NOTICE AND SIGNATURE PAGE

Using Government drawings, specifications, or other data included in this document for any purpose other than Government procurement does not in any way obligate the U.S. Government. The fact that the Government formulated or supplied the drawings, specifications, or other data does not license the holder or any other person or corporation; or convey any rights or permission to manufacture, use, or sell any patented invention that may relate to them.

This report was cleared for public release by the USAF 88th Air Base Wing (88 ABW) Public Affairs Office (PAO) and is available to the general public, including foreign nationals.

Copies may be obtained from the Defense Technical Information Center (DTIC) (http://www.dtic.mil).

WADC-TN-59-365 HAS BEEN REVIEWED AND IS APPROVED FOR PUBLICATION IN ACCORDANCE WITH ASSIGNED DISTRIBUTION STATEMENT.

*//Signature//

ROBERT A. MERCIER
Deputy for Technology
High Speed Systems Division
Aerospace Systems Directorate

This report is published in the interest of scientific and technical information exchange and its publication does not constitute the Government's approval or disapproval of its ideas or findings.

*Disseminated copies will show "//Signature//" stamped or typed above the signature blocks.

REPORT DOCUMENTATION PAGE

Form Approved
OMB No. 0704-0188

1. REPORT DATE *(DD-MM-YY)*	2. REPORT TYPE	3. DATES COVERED *(From - To)*
November 1959	Final	01 March 1959 – 15 November 1959

4. TITLE AND SUBTITLE
PROJECT PLUTO
Volume III

5a. CONTRACT NUMBER
AF 33(616)-6214

5b. GRANT NUMBER

5c. PROGRAM ELEMENT NUMBER
N/A

6. AUTHOR(S)

5d. PROJECT NUMBER
N/A

5e. TASK NUMBER

5f. WORK UNIT NUMBER
N/A

7. PERFORMING ORGANIZATION NAME(S) AND ADDRESS(ES)
The Marquardt Corporation

8. PERFORMING ORGANIZATION REPORT NUMBER
30002

9. SPONSORING/MONITORING AGENCY NAME(S) AND ADDRESS(ES)

1959 NOMENCLATURE:
Wright Air Development Center, with the
Aeronautical Research Laboratory
Air Force Materials Laboratory
Research and Technology Division
Air Force Systems Command
Wright-Patterson Air Force Base, OH 45433

2016 NOMENCLATURE:
Air Force Research Laboratory
Aerospace Systems Directorate
Wright-Patterson AFB, OH 45433-7541
Air Force Materiel Command
United States Air Force

10. SPONSORING/MONITORING AGENCY ACRONYM(S)
AFRL/RQH

11. SPONSORING/MONITORING AGENCY REPORT NUMBER(S)
WADC-TN-59-365

12. DISTRIBUTION/AVAILABILITY STATEMENT
Approved for public release; distribution is unlimited.

13. SUPPLEMENTARY NOTES
PA Case Number: 88ABW-2016-2977; Clearance Date: 10 June 2016.
This version of the 1959 report is the best quality available. Approval for public release was obtained as a result of a Freedom of Information Act (FOIA) request for this report.

14. ABSTRACT
This report volume was produced by the Nuclear Systems Division of The Marquardt Corporation and includes the fourteenth quarterly progress report.

Two series of irradiation programs were conducted in 1959 to investigate the effects of combined environments on materials and components of control systems that operate in piloted nuclear propulsion aircraft. The tests were performed in environmental chambers, which were air-irradiated primarily with gamma photons and neutrons. Because the tests did not reach desired temperatures or maximum integrated fluxes, no definite conclusions could be drawn regarding the effectiveness or safety levels of radiation exposure for a PLUTO-type environment.

15. SUBJECT TERMS
silicon semiconductor diodes, infrared sensors, ion chamber, capacitor, shielding, irradiate, dosimetry

16. SECURITY CLASSIFICATION OF:			17. LIMITATION OF ABSTRACT:	18. NUMBER OF PAGES	19a. NAME OF RESPONSIBLE PERSON (Monitor)
a. REPORT	b. ABSTRACT	c. THIS PAGE			Robert A. Mercier
Unclassified	Unclassified	Unclassified	SAR	157	19b. TELEPHONE NUMBER *(Include Area Code)* N/A

(TITLE UNCLASSIFIED)

AIRCRAFT NUCLEAR PROPULSION SYSTEMS,

PROJECT PLUTO
TECHNICAL SUMMARY REPORT

(INCLUDING THE FOURTEENTH QUARTERLY PROGRESS REPORT)

NUCLEAR SYSTEMS DIVISION
THE MARQUARDT CORPORATION

CONTRACT AF 33(616)-6214

15 NOVEMBER 1959

WRIGHT AIR DEVELOPMENT CENTER
AIR RESEARCH AND DEVELOPMENT COMMAND
UNITED STATES AIR FORCE
WRIGHT-PATTERSON AIR FORCE BASE, OHIO

U.

155

The Marquardt Corporation

WADC-TN-59-365
Marquardt Report No. 30002

Volume III
No. of Pages 151 & i

(Title -- Unclassified)

PROJECT PLUTO
TECHNICAL SUMMARY REPORT
(Including the Fourteenth Quarterly Progress Report)

"MATERIALS SECTION (TABLE LXXV)"

Nuclear Systems Division
The Marquardt Corporation

Contract AF 33(616)-6214

15 November 1959

Approved by: John W Gruber
A. R. Gruber
Director

Wright Air Development Center
Air Research and Development Command
Wright-Patterson Air Force Base, Ohio

CONTENTS

SECTION I

SUMMARY

Two series of irradiation programs were conducted under Contract AF 33(616)-6214 during 1959 to investigate the effects of the following combined environments on materials and components:

1. 300°F temperature, 10^{11}nv, and 10^{16}nvt
2. 500°F temperature, 10^{11}nv, and 10^{16}nvt
3. 100 to 150°F temperature, 10^{12}nv, and 10^{17}nvt
4. 3000°F temperature, 5×10^{13}nv, and 10^{19}nvt

Items 1 and 2 were performed at the Ground Test Reactor of Convair, Fort Worth, Texas during March 1959. The irradiations included the following items:

1. Silicon semiconductor diodes
2. Infra-red sensors
3. Ion chambers
4. Capacitors
5. Potting compounds

The tests were made in specially designed environmental chambers. The chambers were instrumented and checked outside the reactor area, and moved into position on a special system of skids, as shown in Figure 1. The irradiation environment consisted primarily of gamma photons and neutrons with energies grater than 0.48 ev since the reactor operated in a borallined chamber and the irradiations took place in air. Data were taken periodically during the irradiation as well as pre-and-post test. Thus, both transient as well as permanent effects were established. Two tests, each of ten-hours duration at 40 KW and twenty-hours duration at 3 MW were conducted. A plot of the irradiation exposures is shown in Figures 2 and 3. In addition, a separate test was run for 10 hours at 40 KW, and 12 hours at 3 MW to determine the shielding properties of the potting compounds. Initial processing of the test data, including dosimetry was performed by Convair; the final evaluation was made by Marquardt.

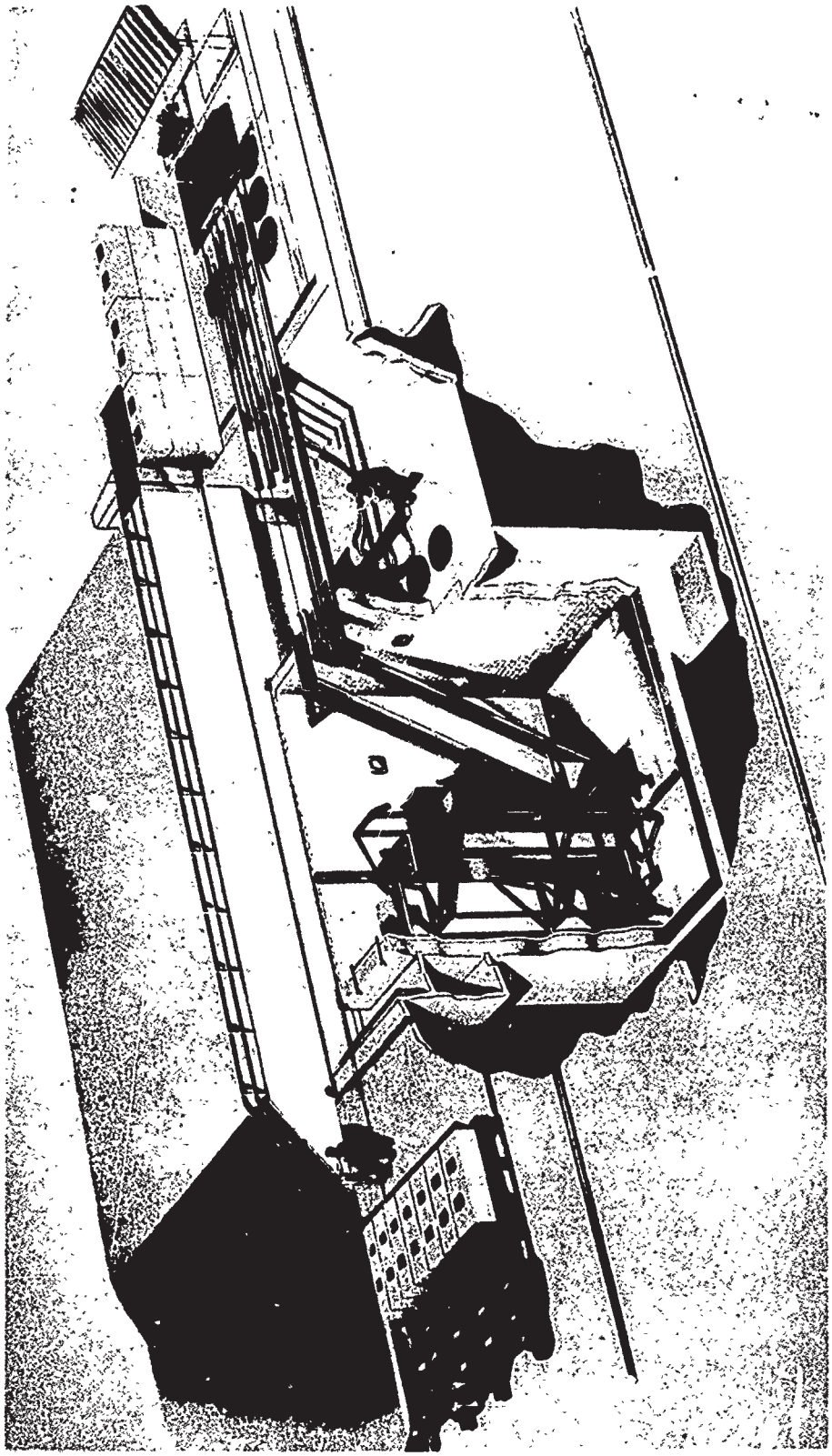

CONVAIR, FT. WORTH GETR FACILITY

FIGURE 1

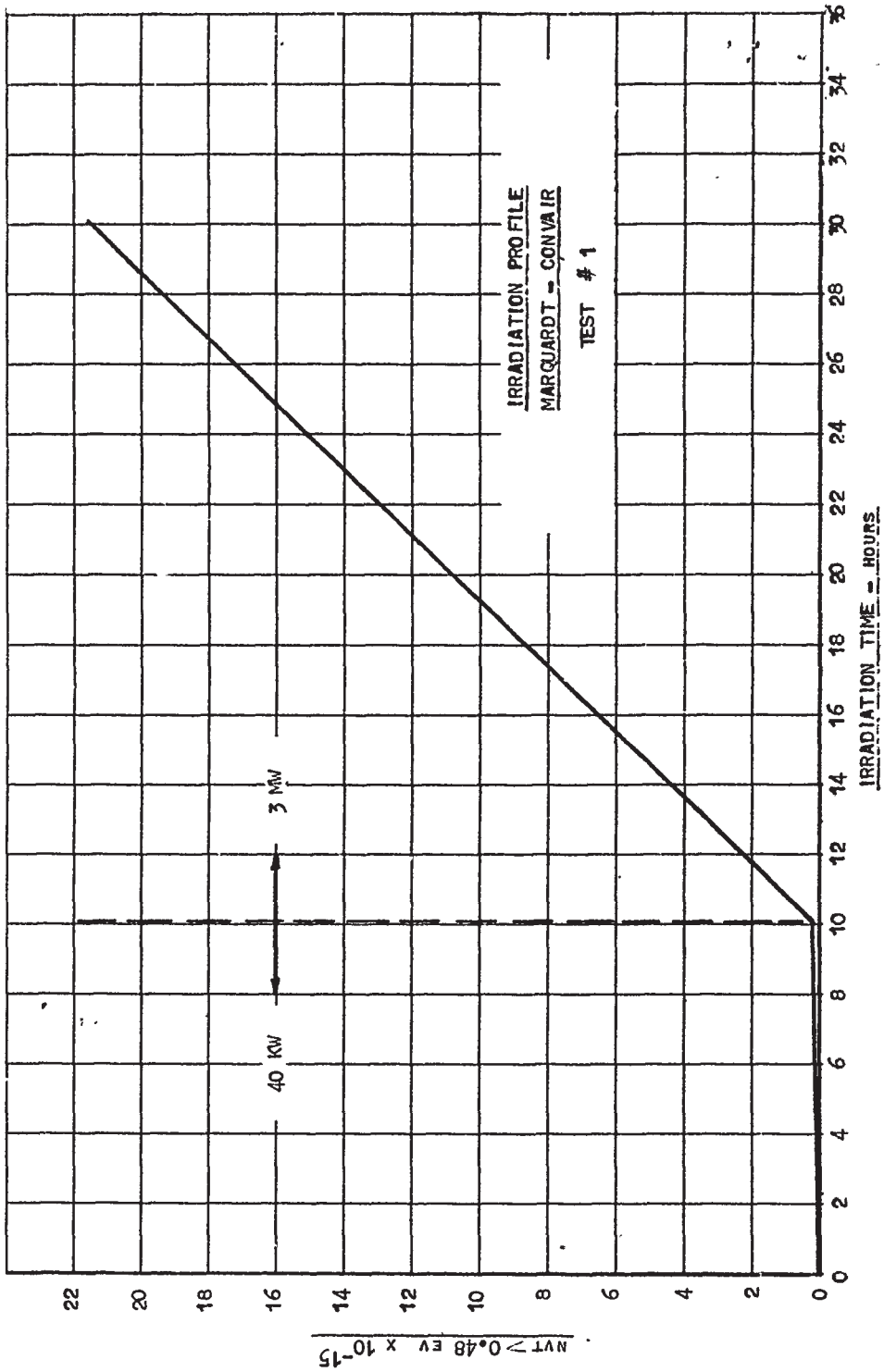

FIGURE 2

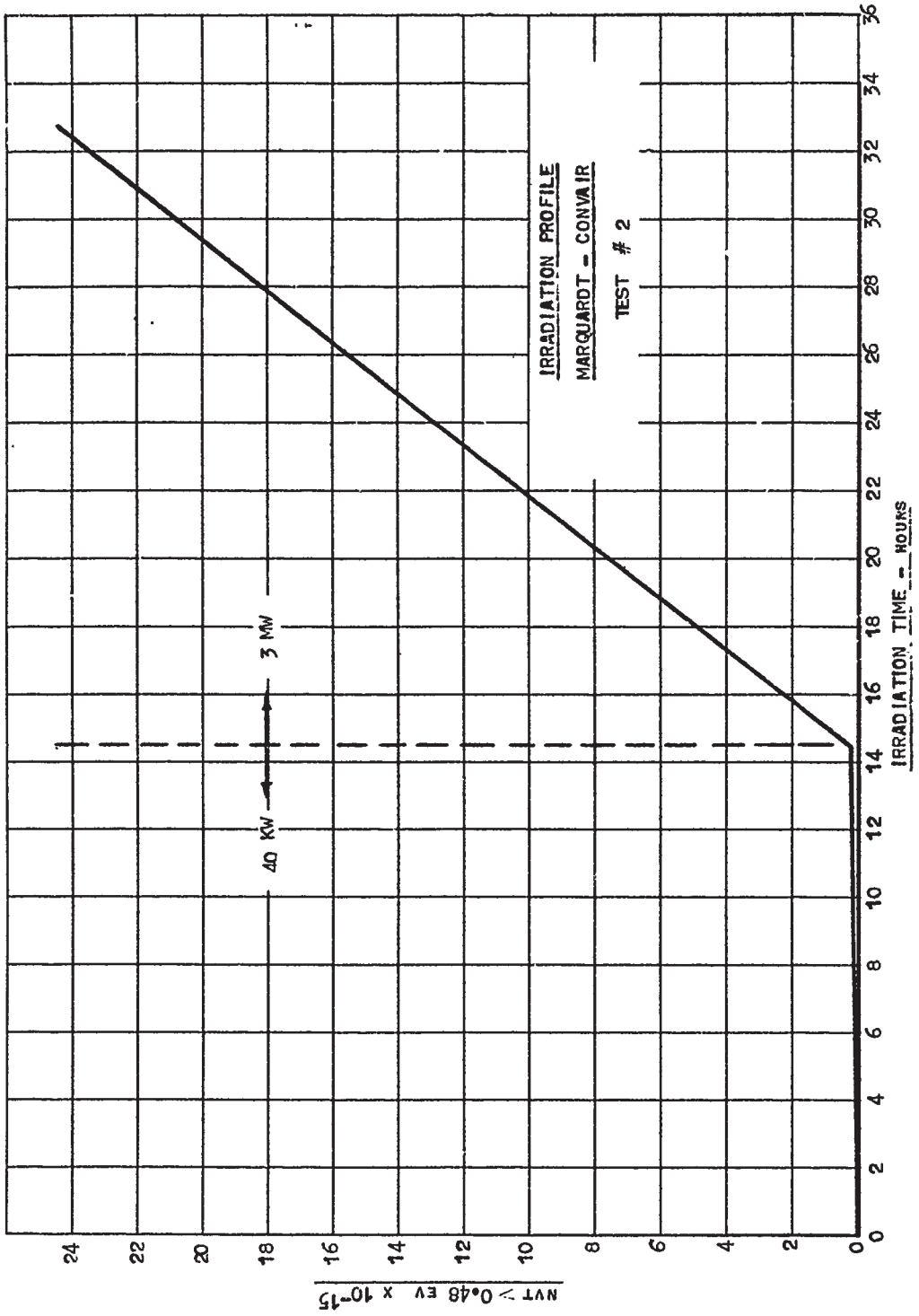

A second series of tests was performed at the General Electric Testing Reactor, Vallecitos Road, Pleasanton, California during September 1959. This series covered the following items:

1. Ceramic insulators
2. Ceramic vacuum tubes
3. Subminiature vacuum tubes
4. Gallium arsenide semiconductor diodes
5. Thermistors
6. High-temperature ion chambers
7. Silicon semiconductor reference diodes

The test was designed and, to a large extent, operated by Marquardt. A special curved guide tube, approximately 31-feet long was furnished by Marquardt (Figure 4) and installed in the reactor. The lower end of the tube was adjacent to the reactor core in the pool area, while the upper end was accessible at all times from the third floor of the reactor. This enabled a series of capsules to be inserted and withdrawn into special casks (Figure 5) without interfering with reactor operations. Two types of capsules were furnished by Marquardt. One capsule was designed to operate with internal temperatures of 3000°F in an air-cooled reactor (Figures 6 and 7). The capsule was then adapted to operate in the cooling water furnished to the guide tube. These capsules were used to test the insulation resistance of ceramic insulators at high temperatures. A second type of capsule (Figures 8 and 9) was used to irradiate electronic components at higher fluxes than available during the Convair reactor tests. The individual capsules were designed to operate from eight to ten hours in the guide tube next to the reactor core. Actual operating times varied, caused in some cases by capsule failure, and in others by the desire to irradiate certain components to failure. Typical exposure data are shown in Figures 10 and 11. The greatest test duration was 31-hours, for an integrated exposure of 1.3×10^{17} nvt $> 0.4^{8}$ev. During this series of tests some of the data were recorded continuously while the remainder were taken periodically, as during the Convair tests. A total of ten tests were made during a 20-day operating cycle. In addition to actual irradiation data on the test specimens, data were obtained which will aid in the design of future test capsules. In general, the test date confirmed the anticipated effect of gamma heating and activation of materials; however, the need for improvement in test leads and seals was demonstrated by failures that occurred during the tests.

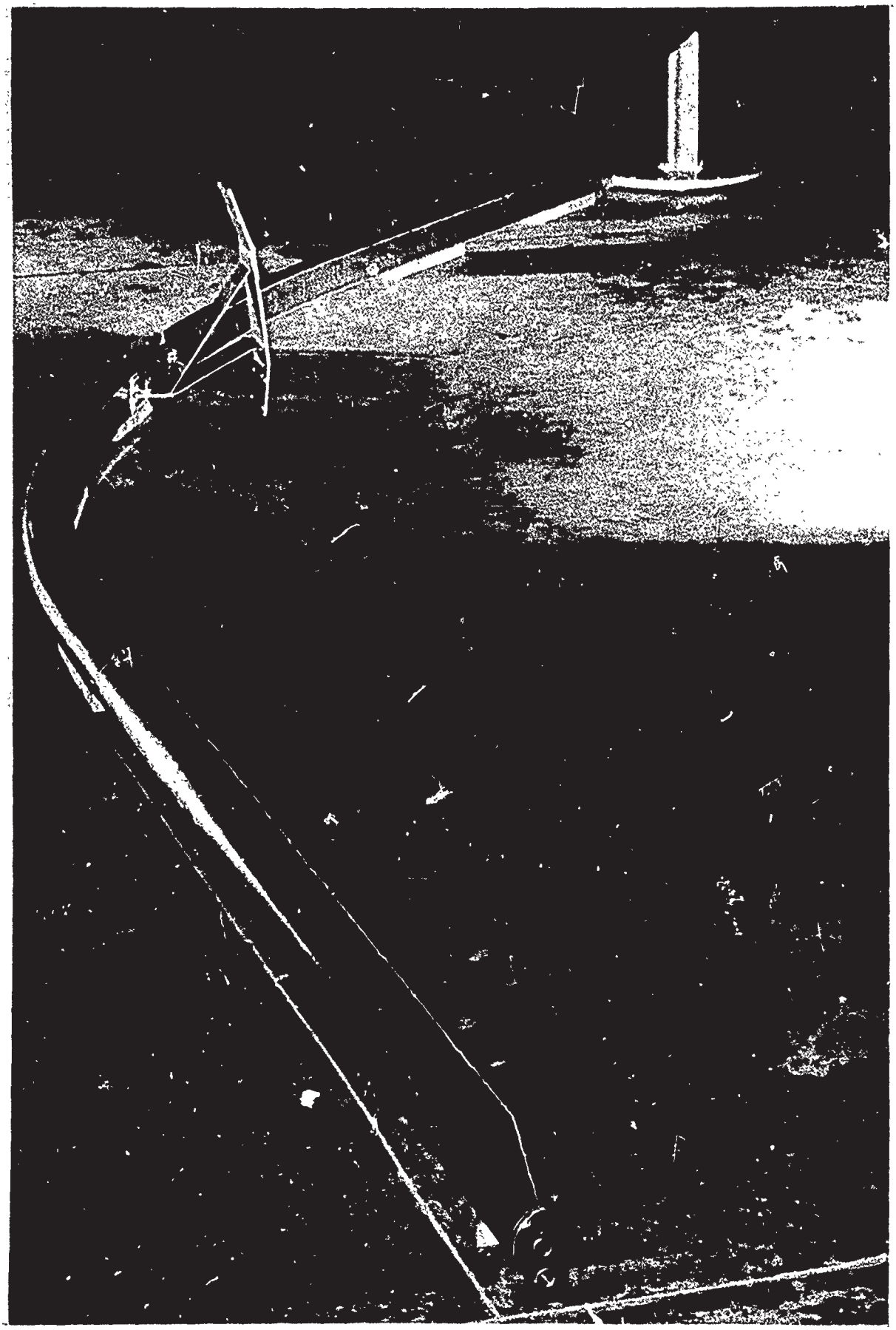

RADIATION GUIDE TUBE

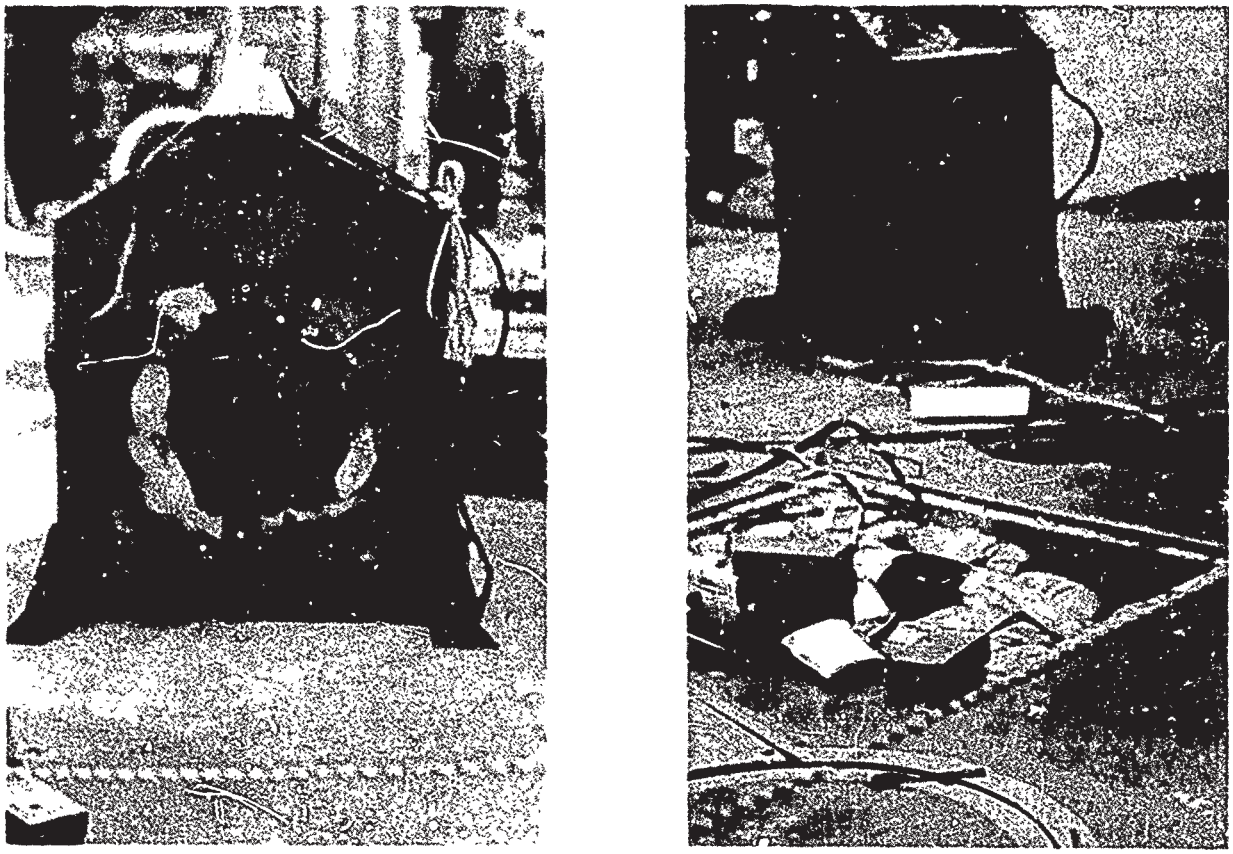

TRANSFER CASKS FOR
GETR 1 AND 1A TESTS

FIGURE 5

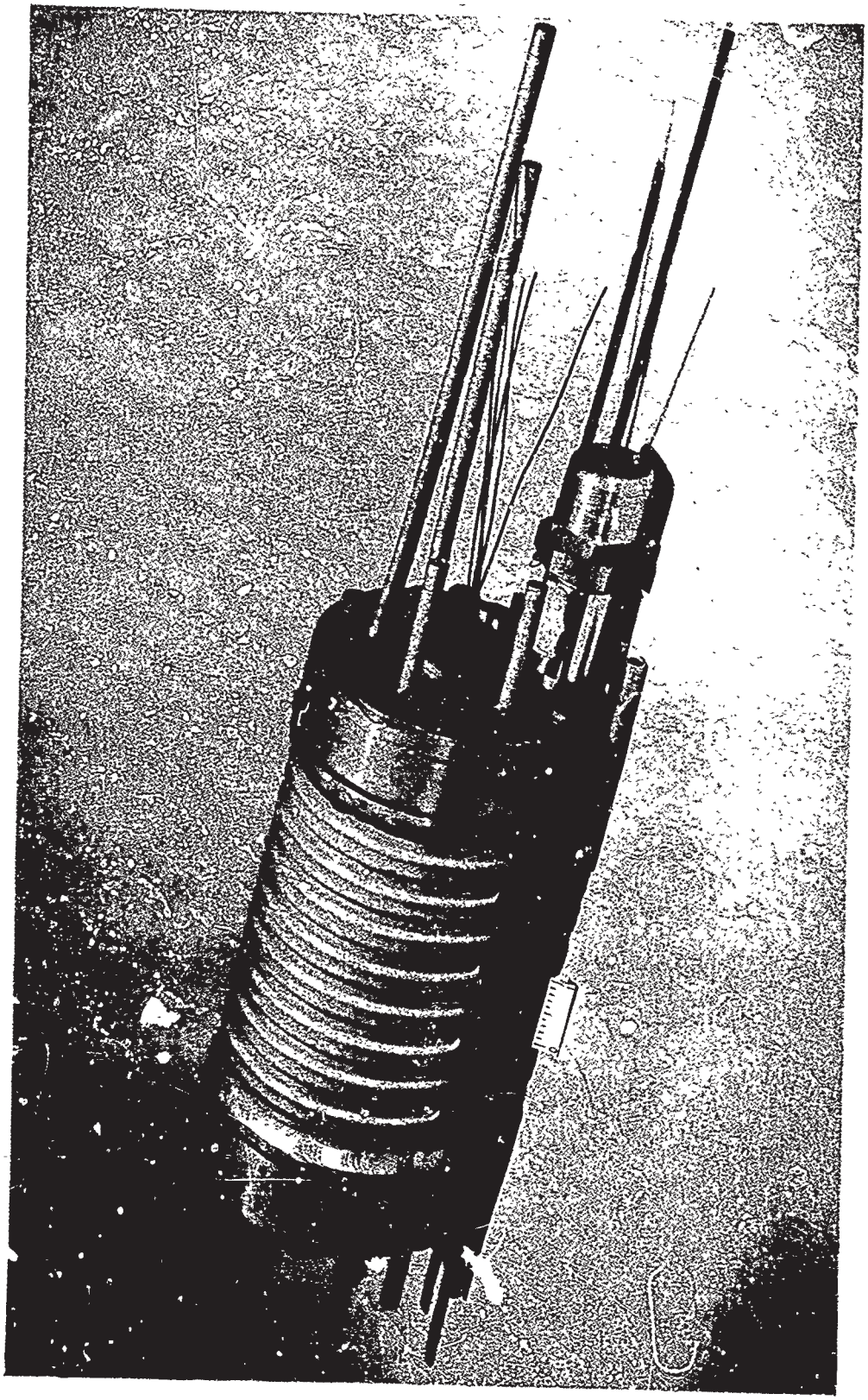

IN-PILE FURNACE ASSEMBLY X-2925

FIGURE 6

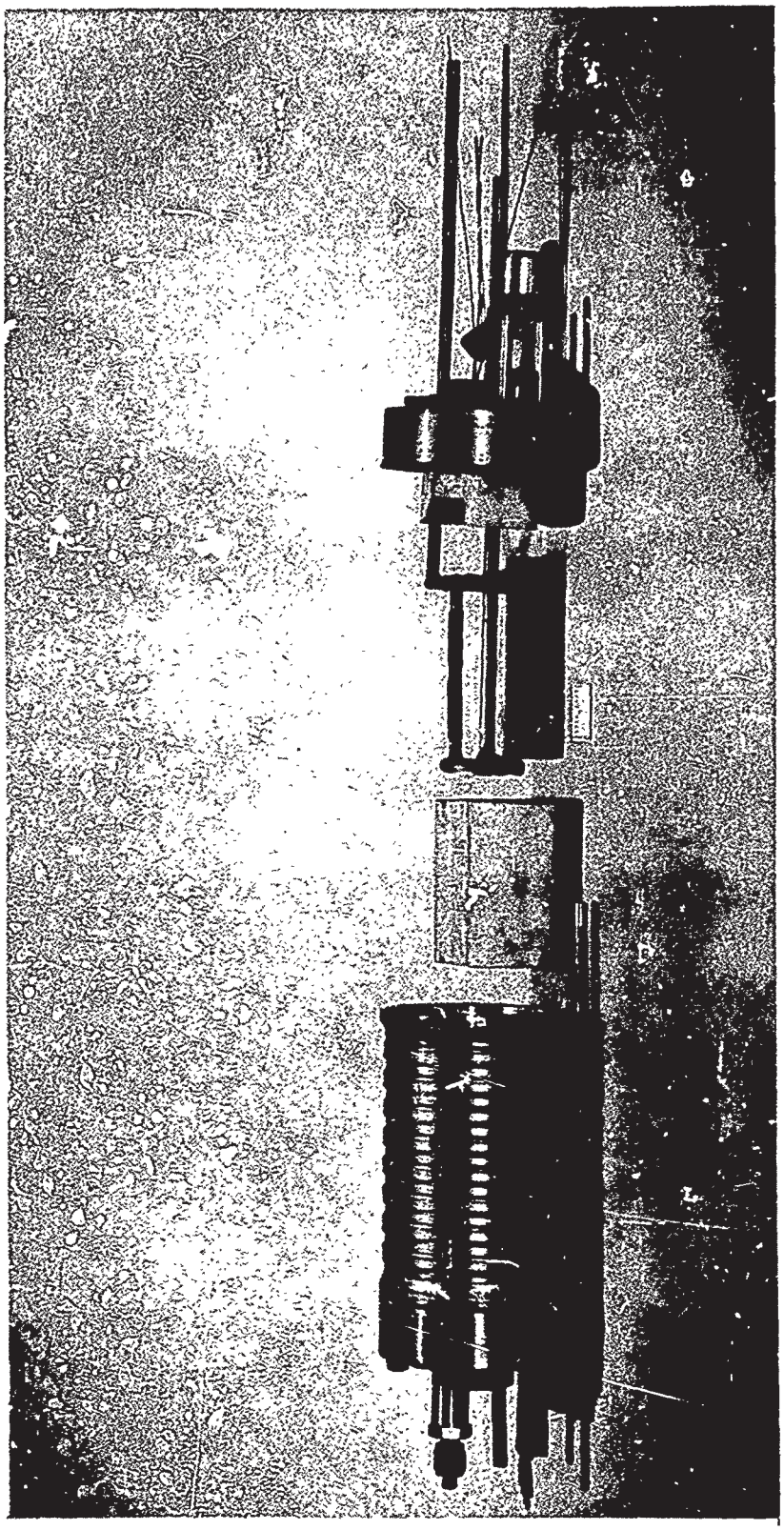

IN-PILE FURNACE ASSEMBLY DISSASSEMBLED X-2925

FIGURE 7

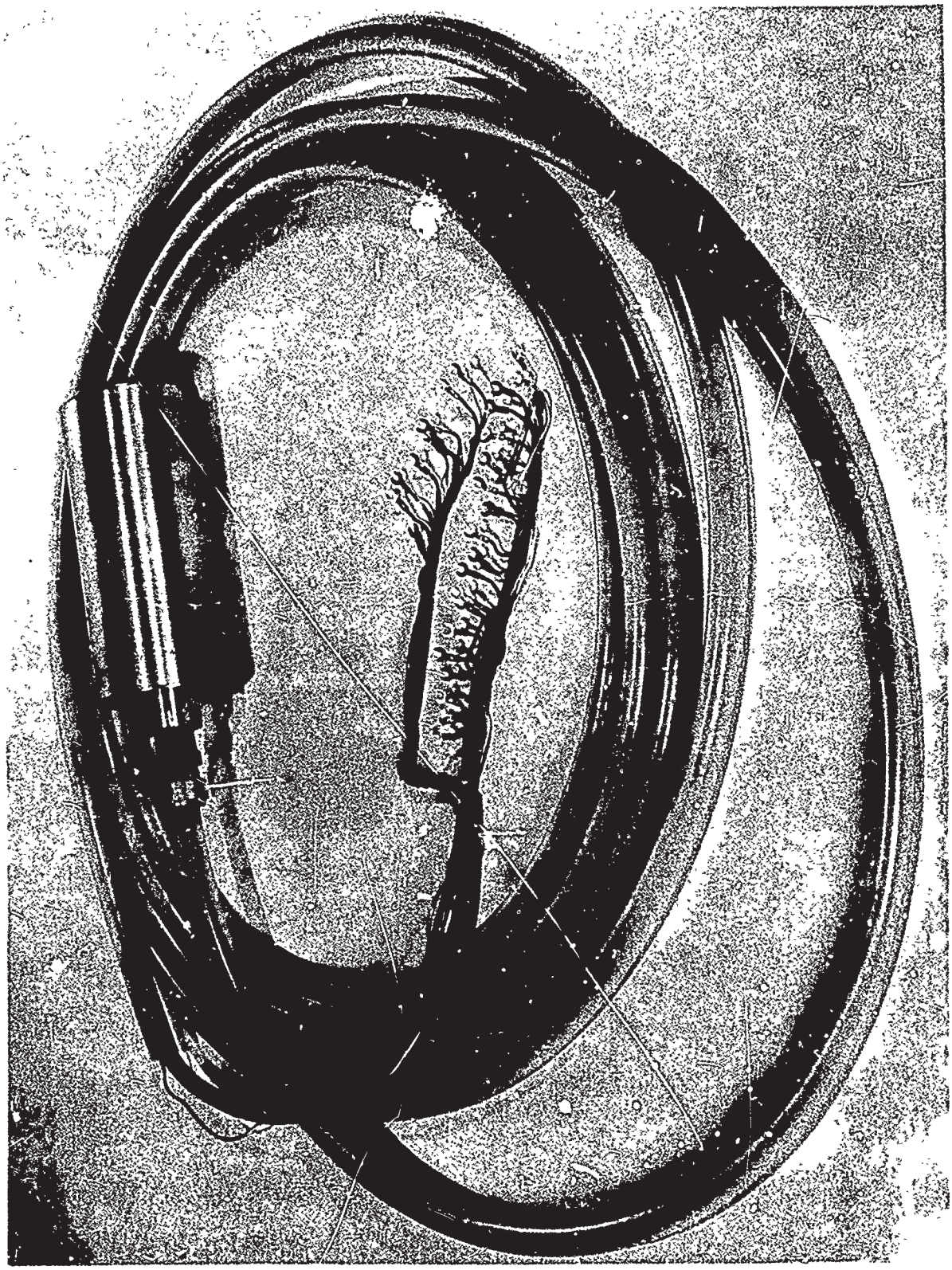

COMPLETE CAPSULE AND CABLE ASSEMBLY

FIGURE 8

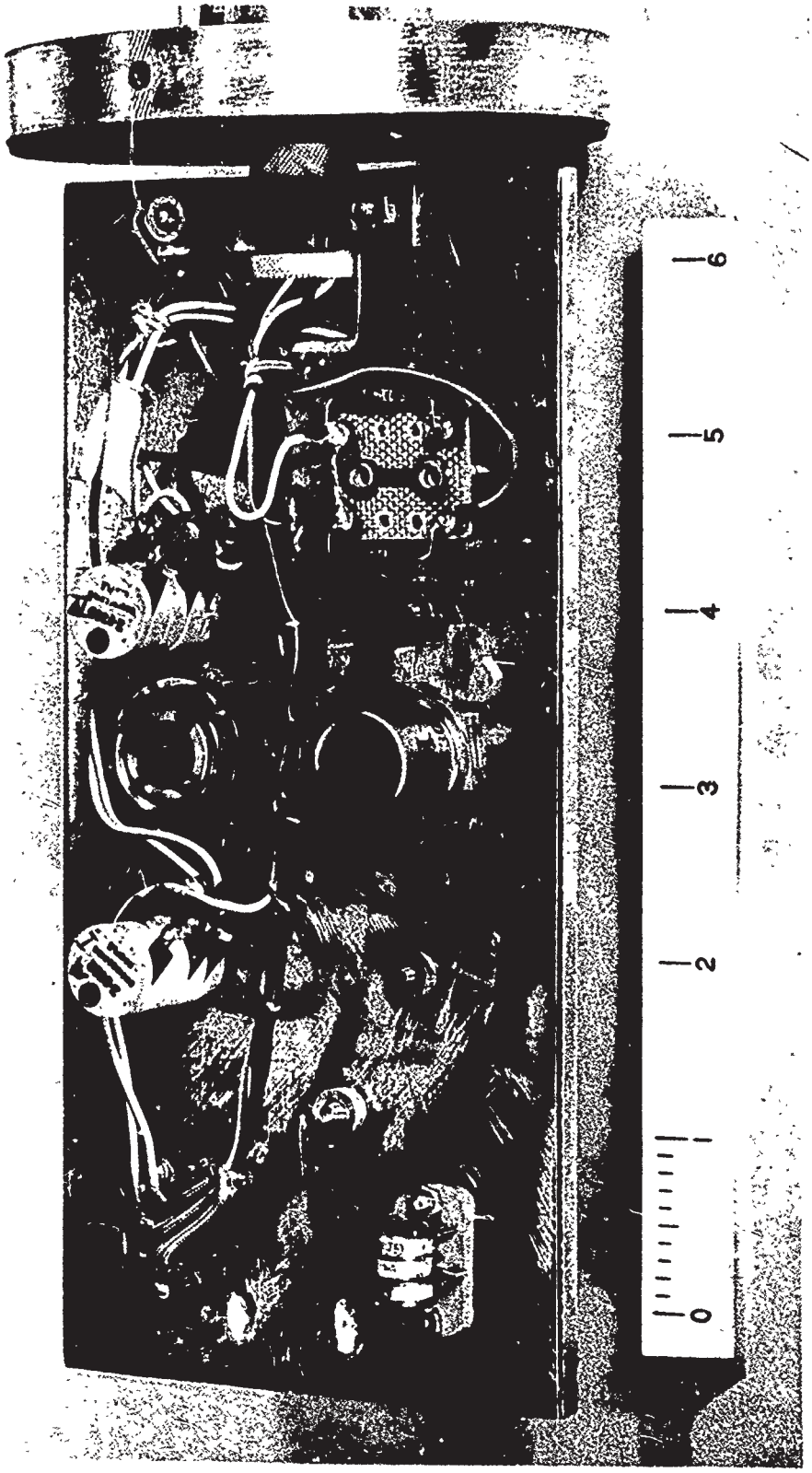

INTERIOR VIEW OF CAPSULE NO. 1

FIGURE 9

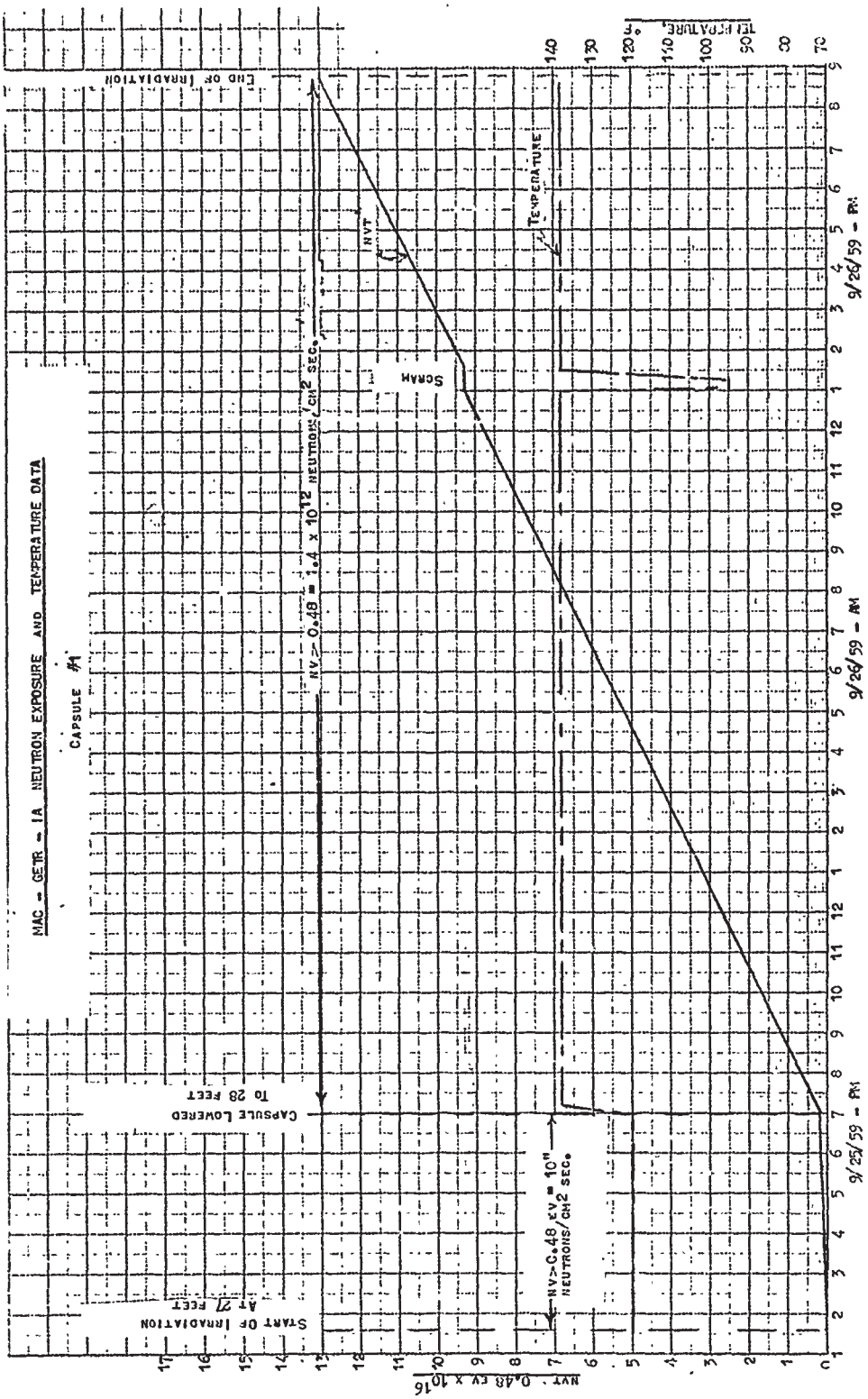

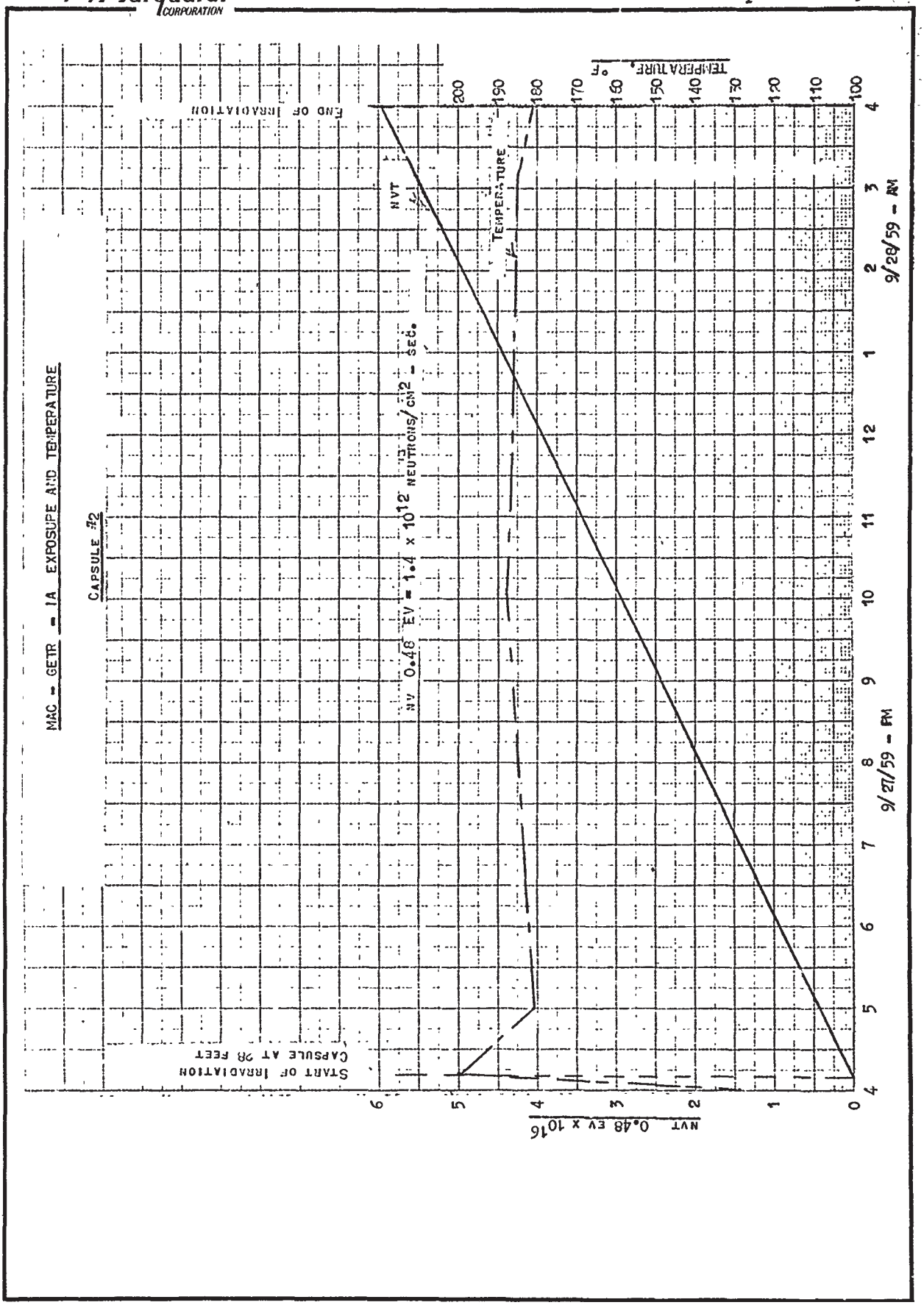

SECTION II

INTRODUCTION

A. PURPOSE

To provide accurate and reliable control of a nuclear ramjet, it is necessary to provide materials and components for the control system which will operate in an environment dictated by the nuclear characteristics of the system. A similar problem is encountered in providing nuclear propulsion for manned aircraft. Much work has been done on establishing reliabile components for this purpose; however, the environment to be encountered in missile applications is more severe. Thus, it was necessary to accumulate as much available data as possible on radiation effects and then extend the data experimentally to cover the particular problems encountered with PLUTO.

B. SURVEY OF AVAILABLE INFORMATION ON RADIATION EFFECTS

Two methods were used to provide a basis for the preliminary choice of materials and components to be used in a nuclear ramjet control system. The first, and most extensive, consisted of a literature search which actually covered radiation and environmental effects on virtually every possible item. Two sources were used as the primary listing of documents: (1) the abstracts furnished by the Radiation Effects Information Center and, (2) the Nuclear Science Abstracts. Additional information was obtained from technical periodicals and manufacturers bulletins.

From these sources, several hundred documents were used to establish potential materials and components to meet the particular needs of the PLUTO program and establish an experimental program.

This information was supplemented by attendance at meetings and symposia or radiation effects, as well as personal contacts with manufacturers' representatives.

SECTION III

MATERIALS

A. CERAMICS

1. Types Tested

A total of nine different ceramics were included in the tests. Because of test capsule leakage, resistivity data were obtained on only four types:

a. 99.6 percent Pure Al_2O_3

b. Pure MgO

c. Pure BeO

d. Pure ZrO_2

The MgO specimens were single crystal; the others were polycrystalline.

Testing was to be conducted at temperatures to 3000°F and an integrated epicadmium flux of 10^{18} in the capusles shown in Figures 6 and 17. The maximum temperature achieved was 10000°F and the maximum integrated flux was 8×10^{17}.

2. Results

Although actual test conditions were not achieved, sufficient information was obtained to indicate trends of resistivity changes during irradiation as shown in Figure 12. In addition, annealing effects during and immediately following reactor shutdowns were noticed in BeO and Al_2O_3. The effect was much more pronounced in Al_2O_3. No shutdowns occurred prior to ultimate capsule failure for the other two specimens and it is impossible to determine whether similar annealing effects would be found with MgO and ZrO_2.

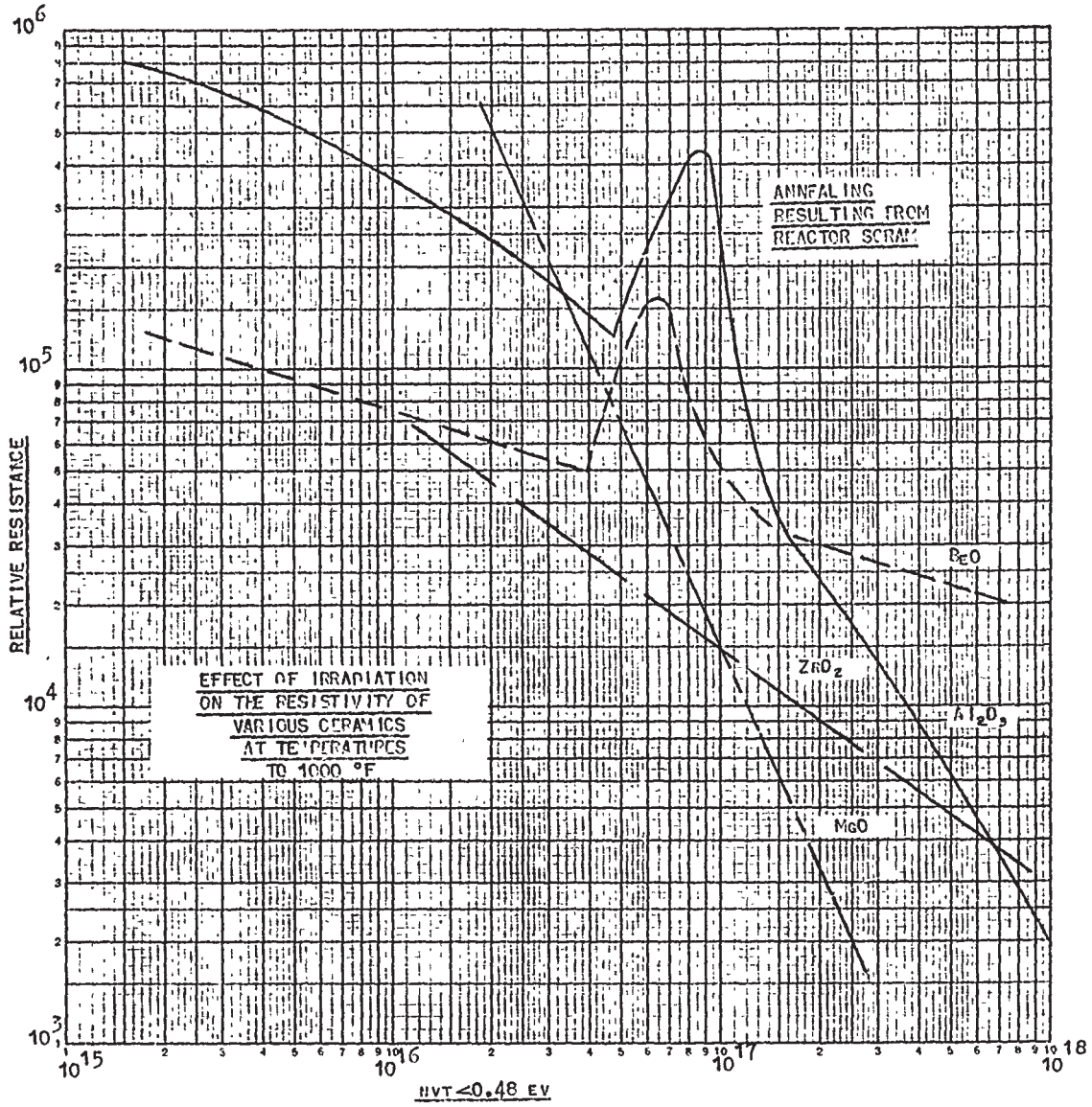

EFFECT OF IRRADIATION ON THE RESISTIVITY OF VARIOUS CERAMICS AT TEMPERATURES TO 1000°F

3. Conclusions

Because the tests did not reach the desired temperatures or maximum integrated fluxes, no definite conclusion can be drawn as to their ultimate use in a PLUTO-type radiation and temperature environment. However, sufficient data were obtained to indicate that the two major insulators presently used in similar non-nuclear applications, i.e., Al_2O_3 and MgO might suffer serious changes in a nuclear environment and should be investigated further. Experience at lower temperatures in various reactor tests with actual thermocouples tends to bear out this assumption. To date, BeO appears to be the most promising material; however, further testing will be required to verify BeO suitability and provide information at higher temperatures.

B. POTTING COMPOUNDS

1. Types Tested

Three types of potting compounds were tested. The basic compound, Epocast-275, is a commercial compound with the properties shown in the Table below. The other compounds manufactured by the same company, and incorporating shielding fillers, were also tested. Their formulas are also listed below.

Material	Composition, Weight Percent			Density, gms/cc	Volume Resistivity at 300°F ohm-cm
	Resin	Hardener	Shield Material		
Epocast-275	95	5.0	--	1.66	2.2×10^{11}
H-1107-A	24	3.9	57.7 Pb, 14.4 B_4C	3.0	--
H-1107-A	38.2	6.54	8.46 Pb, 57.7 B_4C	1.66	--

The tests included measurements of gamma and neutron shielding properties, volume resistivity, nuclear heating, and actual encapsulation of components. The lack of sufficient amounts of each compound prevented tests from being made on all the compounds. Some extrapolation of data was necessary in order to make comparisons.

2. Results

The epoxy-type resins used in this test showed good mechanical stability to combined neutron and gamma irradiation at temperatures for which the resins were formulated. In addition, the shielding properties agree with calculated properties and correlate reasonably well with nuclear heating data (i.e., the amount of nuclear heating corresponds to the amount of energy absorbed in shielding). Figure 13 shows the comparison of calculated and measured values of neutron and gamma absorbtion for H-1107-B. Table III-1 lists the following items:

1. Neutron and gamma absorbtion coefficients (calculated and experimental)
2. Nuclear heating rates (calculated and experimental)

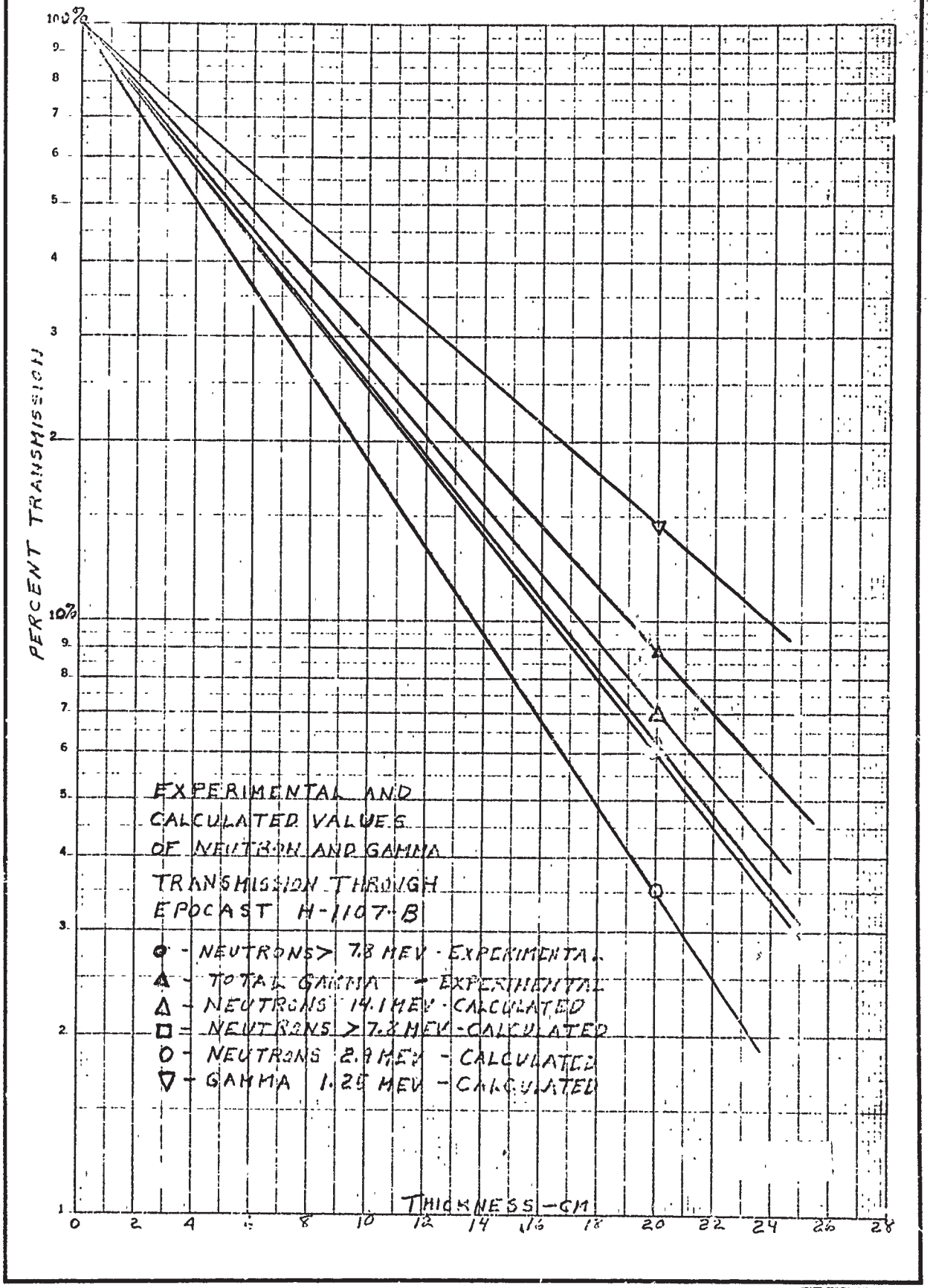

FIGURE 13

TABLE 1

NUCLEAR PROPERTIES OF SHIELDING COMPOUNDS

Material	Neutron Adsorbtion		Gamma Adsorbtion		Nuclear Heating	
	Coefficient Cm^{-1}		Coefficient Cm^{-1}		in Watts/Gm	
	Experimental	Calculated	Experimental	Calculated	Experimental	Calculated
H-1107-A	--	(1)0.258	--	(2)0.188	0.073	(1) (2)0.049
H-1107-B	(3)0.1365	(3)0.139	(4)0.1163	(2)0.1064	--	(1) (2)0.032

(1) Neutrons 2.9mev

(2) Gammas at 1.25mev

(3) Neutrons 7.8mev

(4) Total Gammas

The calculations of absorbtion coefficients were performed by Convair using a flux spectrum determined by measuring the undistorted spectrum (no boral shield) using standard foil and cadmium ratio techniques and then calculating the attenuated spectrum. The nuclear heating calculations were also performed by Convair using rate of rise data and equilibrium heat transfer data. The formula used in rate of rise calculations was as follows:

$$d\phi = A_s F_{sw} \sigma (\Theta_s^4 - \Theta_w^4),$$

where:

ϕ = temperature, °K

t = time, sec

A_s = area of specimen surface, cm^2 (200 cm^2)

σ = Stefan-Boltzmann constant, 5.67×10^{-5} ergs/cm^2-sec-$(°K)^4$

Θ_s = specimen surface temperature, °K

Θ_w = chamber wall surface temperature, °K

F_{sw} = combination view factor and gray-body reradiation factor:

$$F_{sw} = \frac{1}{(1/\epsilon_s) + (A_s/A_w)(1/\epsilon_w - 1)}$$

In this relation, A_w = area of chamber wall (642 cm^2), and ϵ_s and ϵ_w denote the emissivity of the specimen and chamber walls, respectively. In the calculations, values from WADC Rep 56-222 of 0.79 for ϵ_s and 0.21 for ϵ_w were used.

Equilibrium values were calculated using radiant and conductive heat transfer. Actual pressure in the chamber following irradiation was 1.87 mm of Hg; thus, considerable conductive transfer took place. Comparisons between nuclear heating and shielding data were made at Marquardt on the basis of Convair figures for gamma and neutron adsorbtion factors at 1.25 Mev gamma and 2.9 Mev neutron, plus incident flux values during the nuclear heating test.

The volume resistivity data cannot be definitely evaluated for the high flux run because of test fixture breakdown. However, in both cases, the post-irradiation results were much higher than initial results and probably represent a change in contact resistance rather than true resistance value for the resins. It is probably safe to assume that the changes represent a minimum, and that the actual resistance decreases could be much greater.

The effect of shielding on the encapsulated components was probably nullified to a large extent by the increased operating temperatures caused by gamma heating (Figure 14-15) since their performance was no better, and in some cases worse, than similar unshielded performance.

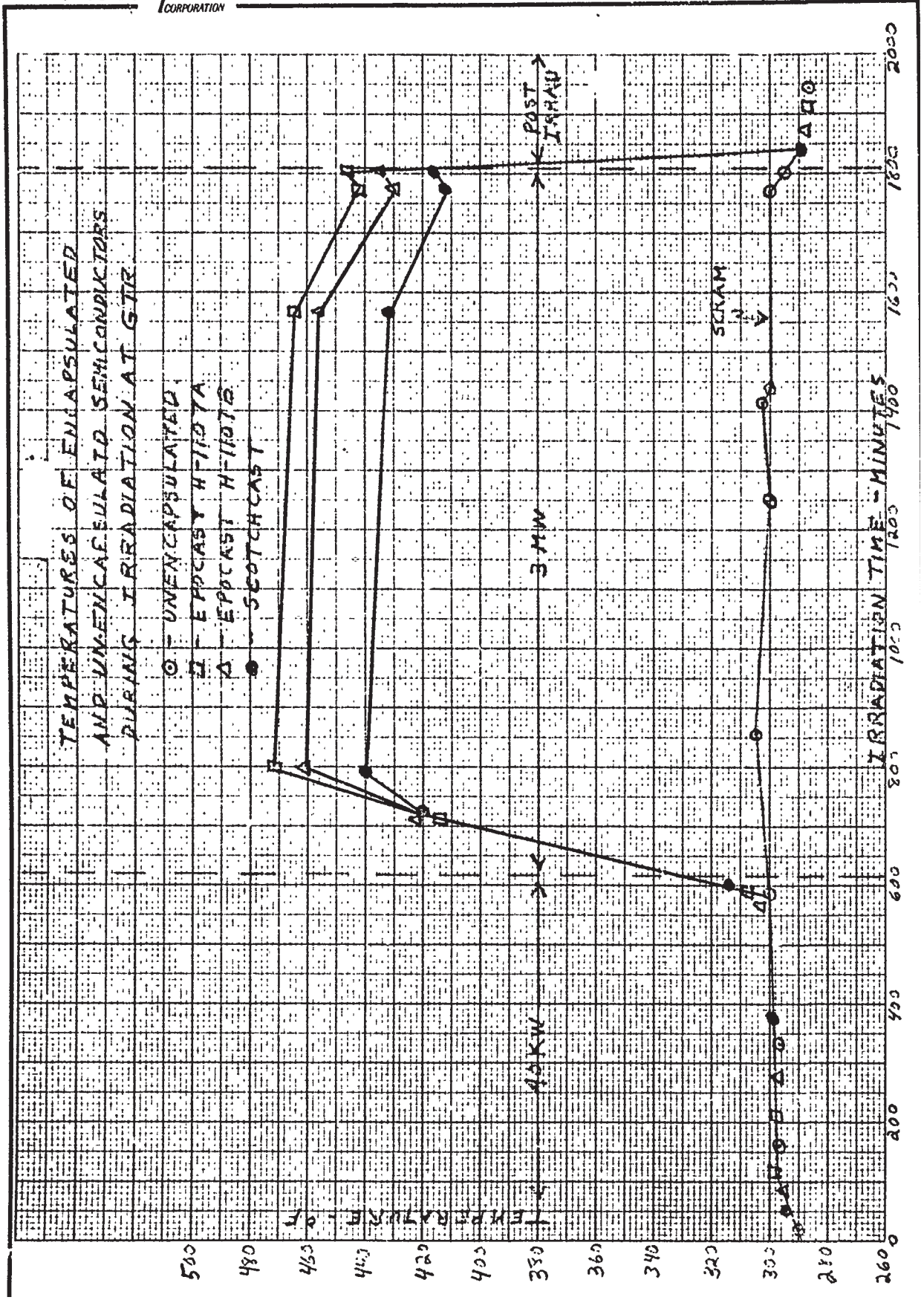

3. Conclusions

Potting compounds of the type tested and similar types are probably of limited usefulness because of the effects of nuclear heating. This cannot be overcome in a direct potting application at the flux used here, since the nuclear heating is directly related to the amount of shielding provided. Shielding-type potting compounds could be used at lower incident flux levels to provide protection from neutron and gamma damage without overheating the component. Probably, a reduction of one decade from the level used here would be satisfactory.

Alternately, shielding at higher flux levels can be used if cooling of the encapsulated component is provided. Both of these methods should be verified experimentally.

SECTION IV

ELECTRONIC COMPONENTS

A. SEMICONDUCTOR DIODES

1. Types Investigated

The diode test program was initiated by the need for data on the combined effects of nuclear irradiation and temperature environments on a variety of diodes contemplated for use in control amplifier circuitry. As such, the primary interest was in the behavior of the reverse current characteristics, with secondary emphasis on the forward characteristic behavior.

No attempts have been made at this time to evaluate the effects observed in terms of crystal lattice disorders and thus, predict and formulate the theoretical behavior of the tested semiconductors.

2. Components Tested

Two hundred and two diodes including 13 types and representing 10 manufacturers were irradiated in two test sequences. The diodes irradiated in Test No. 1 are listed in Table III-2; those irradiated in Test No. 2 are shown in Table III-3. The various types were selected from the standpoint of their applicability to perform specific circuit functions in the control amplifier systems.

All diodes to be irradiated were tested prior to exposure to nuclear radiation operating temperatures for fulfillment of the manufacturers specifications. Those diodes which did not meet specifications at the operating temperatures were replaced.

The forward and reverse characteristics were recorded prior to the irradiation, during the radiation periods, and after irradiation. These characteristics were recorded sequentially on Mosely X-Y plotters. The system was designed to be as nearly automatic as practicable. An automatic switchbox simultaneously selected a component, the appropriate maximum current and voltage sweeps for the forward and reverse tests, and the appropriate temperature in the case of the 1N-430B zener diodes.

Voltage was applied to a component only during the interval of curve plotting (approximately 15 seconds). The forward and reverse curves were plotted on separate plotters for each component before the selection of another component was made.

TABLE 2
DIODES IRRADIATED IN TEST NO. 1

Number Tested	Manufacturer	Type	Identification Numbers		Controlled Temp. (°F)	Remarks
5*	Hoffman	IN430B	25-1	25-5	150	
5**	International Rectifier	IN430B	26-1	26-5	150	
10	Hoffman	IN212	27-1	28-5	300	Components 27-1 through 27-5 were encapsulated in Furane 1107A.
10	Semcor	IN212	29-1	30-5	300	
5	Hoffman	IN430B	31-1	31-5	200	
5**	International Rectifier	IN430B	32-1	32-5	200	
3	Pacific	IN617	33-1	33-3	300	Encapsulated: 33-1; Epocast 1107A. 33-2; Epocast 1107B. 33-3; Scotchcast resin.
3	Hoffman	IN210	33-4	34-1	300	Encapsulated: 33-4; Epocast 1107A. 33-5; Epocast 1107B. 34-1; Scotchcast Resin.
10	Semcor	IN210	34-2	36-1	300	
5*	Hoffman	IN430B	37-1	37-5	300	
5**	International Rectifier	IN430B	38-1	38-5	300	
3	Radio Receptor	16J1T	39-1	39-3	300	Encapsulated: 39-1; Epocast 1107A. 39-2; Epocast 1107B. 39-3; Scotchcast Resin.
2	Radio Receptor	16J1T	39-4	39-5	300	Selenium Rectifiers.
10	Fansteel	TEC276-1	40-1	41-5	300	Selenium Rectifiers.
3	Transitron	IN483B	42-1	42-3	300	Encapsulated: 42-1; Epocast 1107A. 42-2; Epocast 1107B. 42-3; Scotchcast Resin.
10	Pacific	IN660	42-4	44-3	300	
10	Texas Instruments	IN660	44-4	46-3	300	

* These components are the same five Hoffman IN430B's.

** These components are the same five International Rectifier IN430B's.

TABLE 3

DIODES IRRADIATED IN TEST NO. 2

Number Tested	Manufacturer	Type	Identification Numbers	Controlled Temp. (°F)	Remarks
9	General Electric	IN538	1-1 ⟶ 2-4	300	
10	Hoffman	IN538	3-1 ⟶ 4-5	300	Components 3-1 - 3-5 were encapsulated in Furane 1107A.
9	Hughes	IN538	5-1 ⟶ 6-4	300	
10	International Rectifier	IN538	7-1 ⟶ 8-5	300	
10	Radio Receptor	IN538	9-1 ⟶ 10-5	300	
10	Texas Instruments	IN538	11-1 ⟶ 12-5	300	
10	Transitron	IN538	13-1 ⟶ 14-5	300	
10	Pacific	IN645	15-1 ⟶ 16-5	300	
10	Texas Instruments	IN645	17-1 ⟶ 18-5	300	
10	Transitron	IN645	19-1 ⟶ 20-5	300	
10	General Electric	IN441B	21-1 ⟶ 22-5	300	
10	Pacific	IN485B	23-1 ⟶ 24-5	300	

As indicated in the "Remarks" column of the Tables, some diodes were individually encapsulated; others were encapsulated in the form of an assembly, with a thermocouple embedded to measure temperature.

Photographs of two of the diode test assemblies and the diode test equipment are shown in Figures 15, 16, and 17, respectively.

4. Summary of Results

During the two test sequences for the 202 diodes, approximately 3300 curves of forward and reverse characteristics were obtained. A detailed statistical analysis of the change in characteristics with integrated flux has not yet been made. The trend in the different types and diodes of different manufacture was similar. There was an accelerating increase in the forward resistance, and a corresponding decrease in the reverse resistance with integrated flux. This effect, as indicated by the curves of Appendix A, continued even during the post-irradiation period.

To more significantly evaluate the large volume of data, it was necessary to re-plot the forward and reverse characteristics on a single graph for the conditions of pre-irradiation, post-irradiation, and three increasing values of integrated flux selected to show the deterioration of the diode. The number of diodes analyzed was further reduced on the basis of most probable use. Ten units of each type and manufacture were tested. Of the ten units tested, three units representing the two extremes and the middle variation in the forward and reverse characteristics were selected. The diodes selected for re-plotting from the lot of ten are designated by the dashed number (e.g. 1-2, 1-3, and etc.). This reduction in data resulted in the re-plotting of five curves each for the forward characteristics and five curves each for the reverse characteristics of each unit for the diodes listed below:

Type 1N-538

a. General Electric
b. Hoffman
c. Hughes
d. International Rectifier
e. Radio Receptor
f. Texas Instrument
g. Transitron

Type 1N-645

a. Pacific Semiconductor
b. Texas Instrument
c. Transitron

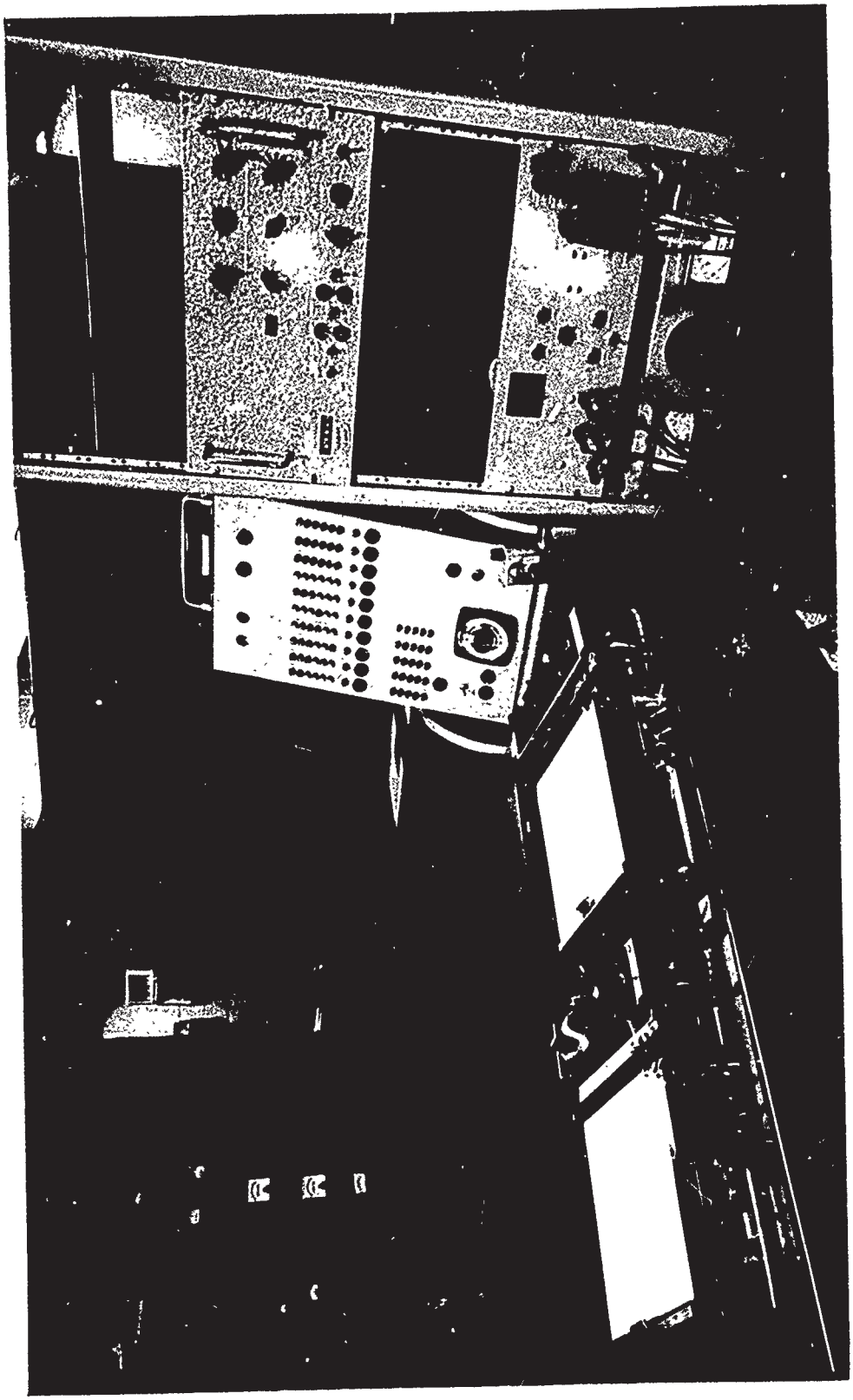

FIGURE 15

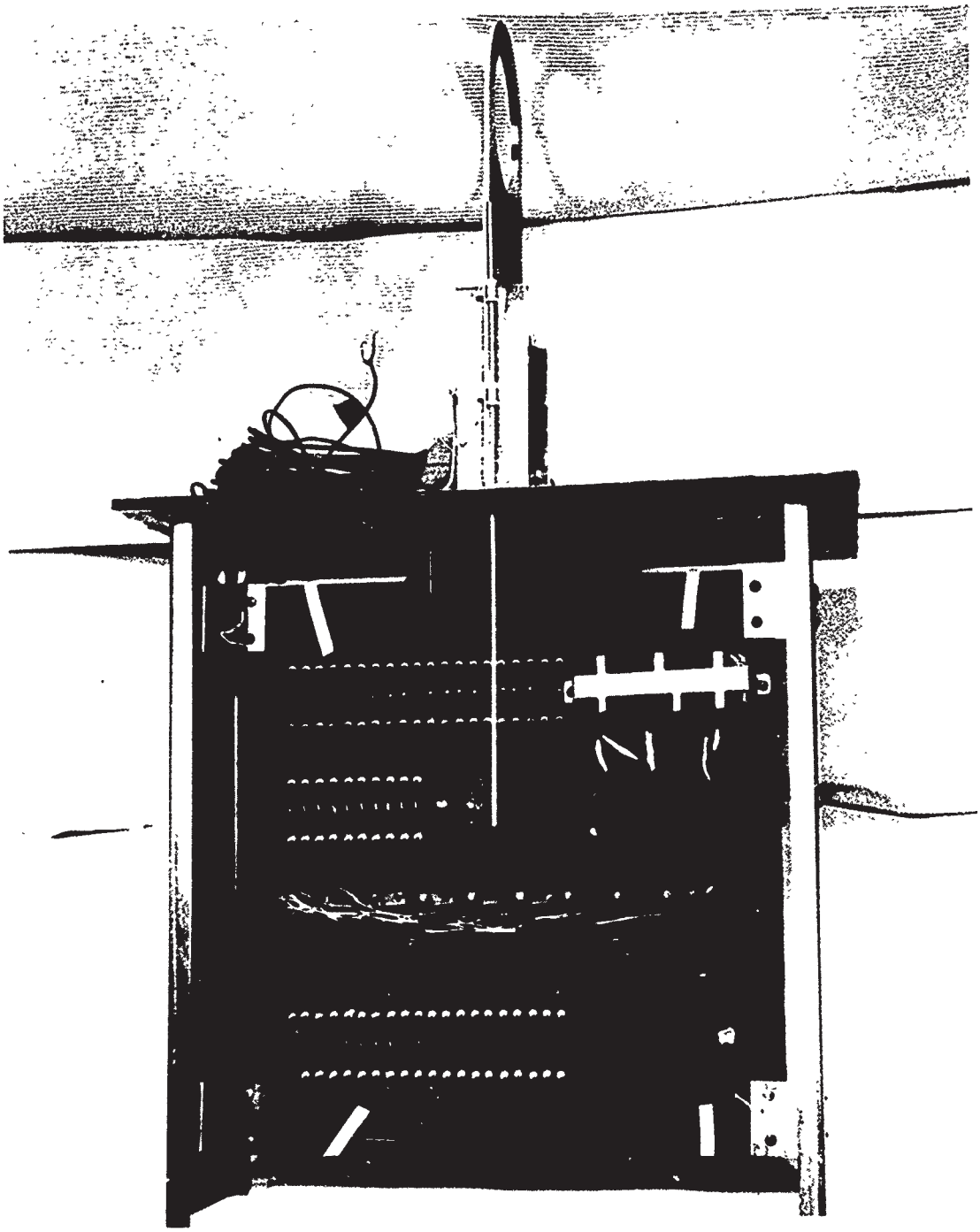

FIGURE 16

DIODE TRAY TEST NO. 1
FRONT VIEW
CONVAIR FT. WORTH TEXAS

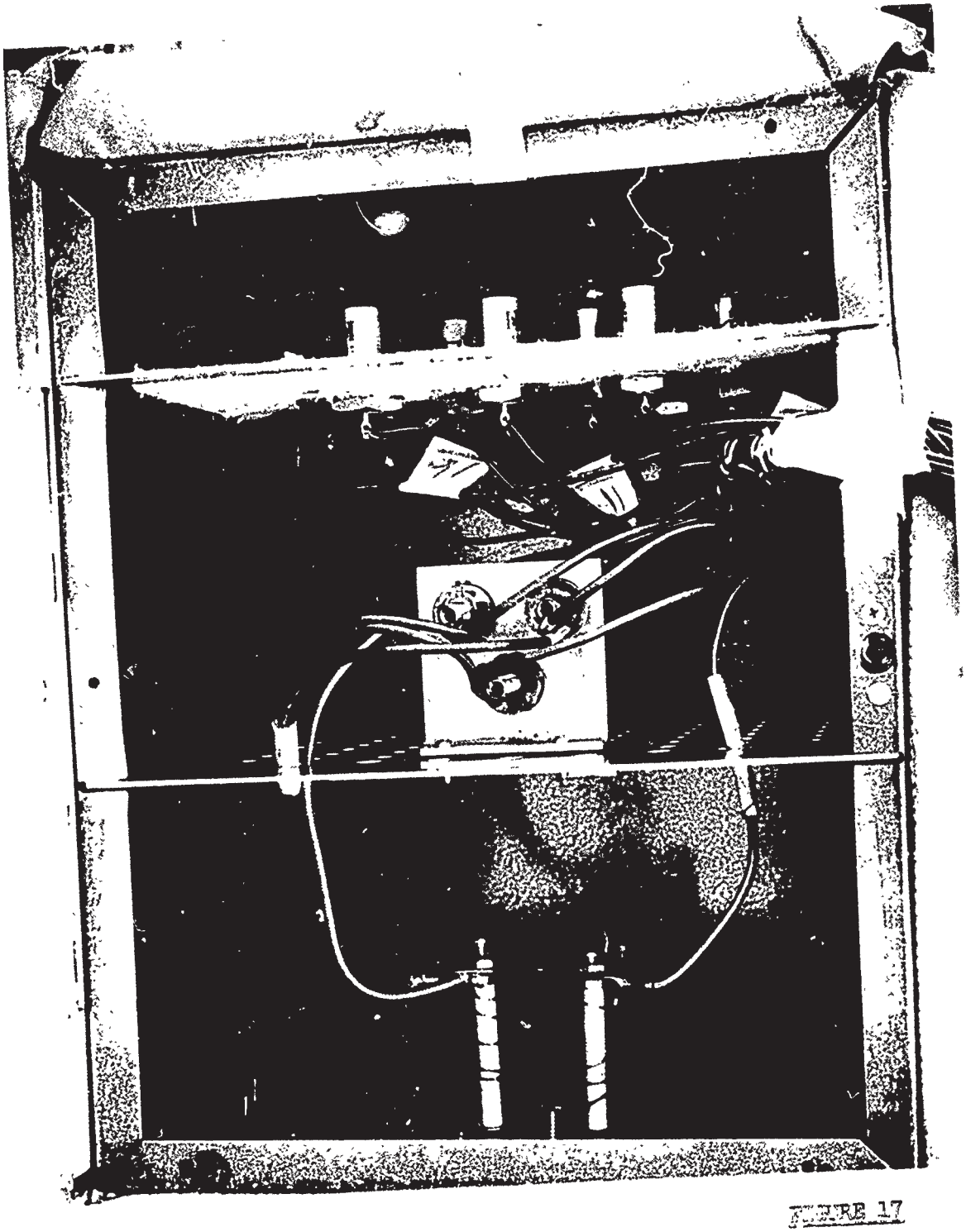

FIGURE 17

ZENER DIODE CHAMBER CONVAIR FT. WORTH TEXAS

Type 1N-441B

a. General Electric

Type 1N-485B

a. Pacific Semiconductor

Type 1N-212

a. Hoffman

b. U.S. Semiconductor

Type 1N-210

a. Hoffman

b. U.S. Semiconductor

Type 1N-660

a. Pacific Semiconductor

b. Texas Instrument

Diode Rectifier Types

a. Fansteel TEC 276-L

b. Radio Receptor 16JIT

The total number of curves thus re-plotted totaled 200, and these are included in the Appendix A for further reference and study. To illustrate typical trends, several curves are included in the body of this report. These are shown in Figures 18 and 19. Reference to the re-plotted curves will show that the radiation tolerance for typical diodes for the service expected in this project, ranges from 1.2×10^{14}nvt ($E > 0.48$ev) to 1.8×10^{15}nvt ($E > 0.48$ev) for the forward characteristics, and 4.2×10^{13}nvt ($E > 0.48$ev) to 1.5×10^{14}nvt ($E > 0.48$ev) for the reverse characteristics. These ranges are also applicable to the rectifier types.

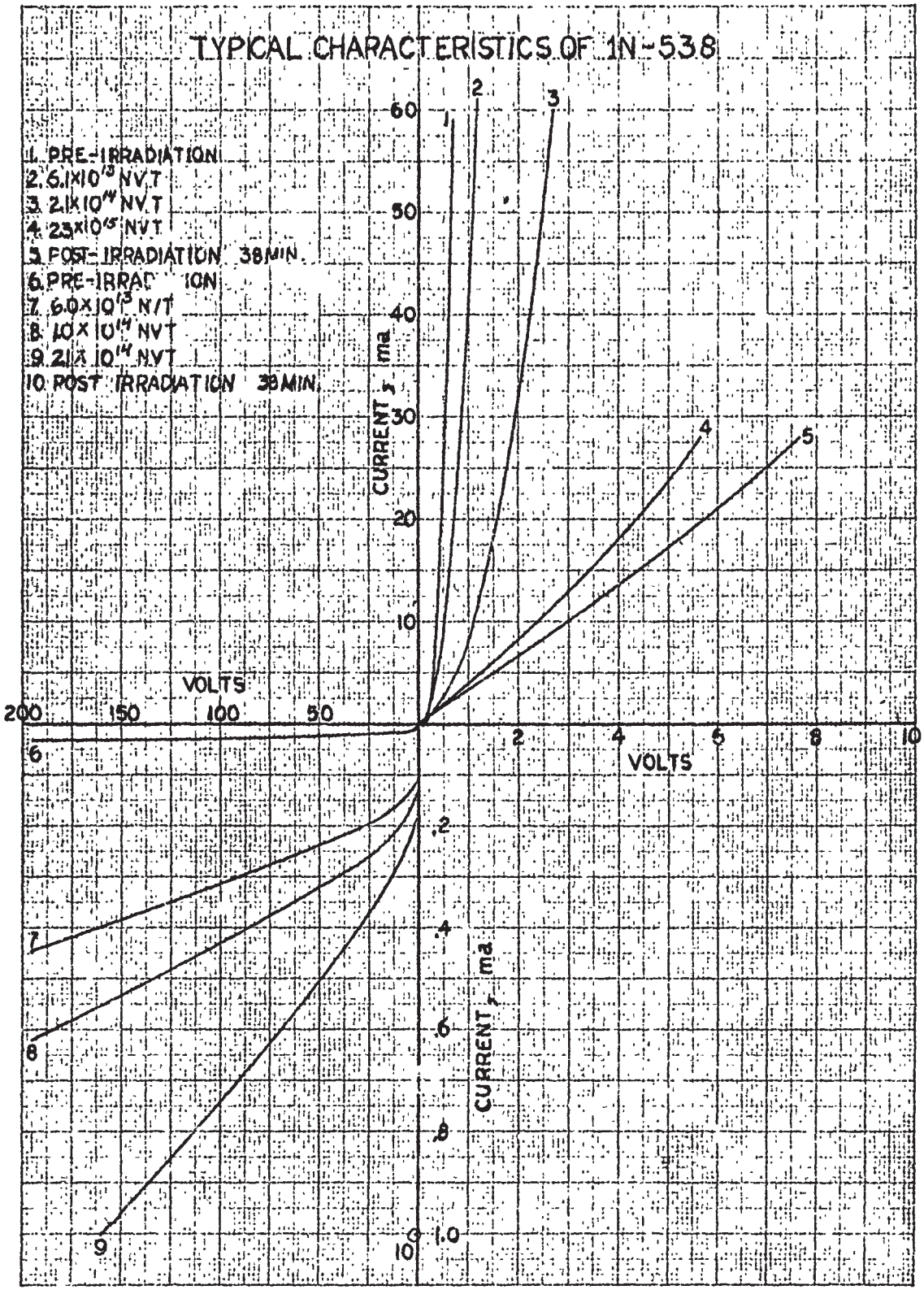

FIGURE 18

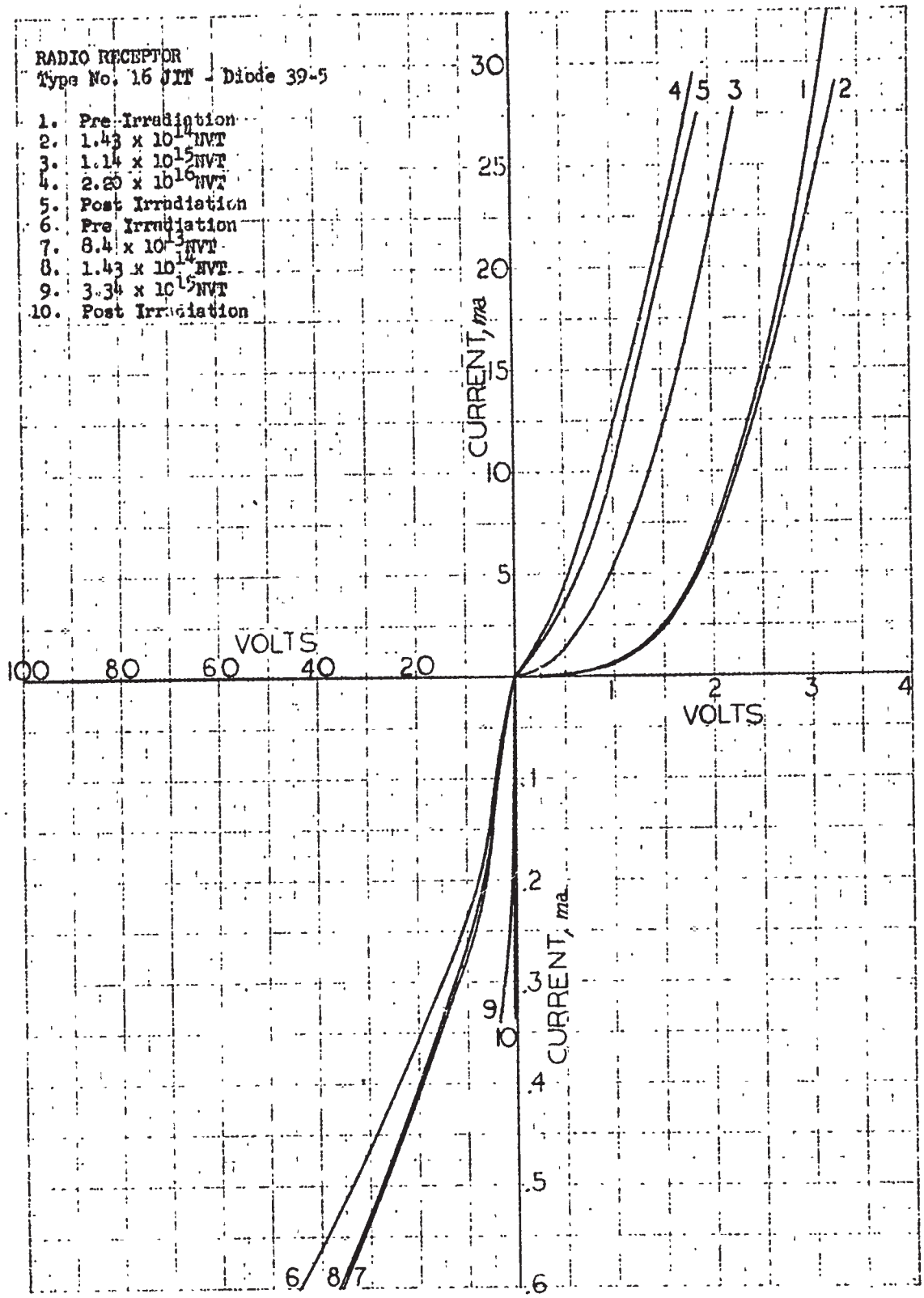

FIGURE 19

In the case of the zener diodes, the International Rectifier Type 1N-430B deteriorated as rapidly as other diode types, while the Hoffman 1N-430-B zener diode showed considerably less deterioration. Typical characteristic curves of the Hoffman and International Rectifier 1N430B types are shown in Figures 20 and 21, respectively.

In addition to the diodes tested at Convair, two Hoffman 1N-430-B zener diodes and two Texas Instrument type XDI gallium arsenide diodes were irradiated in the Marquardt GETR-1A tests at Vallecitos. The Hoffman zener reference voltage had increased 20 percent at 7.4×10^{16} nvt > 0.48ev and failed completely before 1.3×10^{17}nvt > 0.48ev. One gallium arsenide diode showed little or no change to 2.8×10^{15}nvt > 0.48ev and failed before > 7.3×10^{16}nvt. A plot of this diode is shown in Figure 22. The other gallium arsenide diode behaved abnormally during the preirradiation tests.

B. INFRA-RED SENSORS

1. Components Tested

Interest in infra-red detectors stems from their possible application as sensors in the use of radiation techniques for the temperature of nuclear reactors. The detectors tested were selected because of ready availability, fast response, and the possibility of adaption for ambient high-temperature (500°F) operation

Fourteen infra-red detectors of the photoconductive and semiconductive type were irradiated. The types, manufacturers, and numbers are shown in Table 4.

The detectors were arranged radially around an infra-red source consisting of a nichrome-wire element. Surrounding the infra-red source was a drum-shaped chopper with three slits, spaced 120 degrees about the periphery. Infra-red rays were conducted from the source to the detectors by slits in two concentric shields around the chopper and cylindrical tubes. Details of the arrangement are shown in Figure 23. The thermistor bolometer, lead selenide, and indium antimonide (PEM) detectors required preamplifiers at the detector location. These were specially constructed to be free from radiation effects. In addition, a bias voltage was supplied to all but the PEM detector. The response signals generated in the detectors and detector-amplifier combinations were transmitted by a 100-foot coaxial cable to measuring instruments in the control room. The relative signal level, signal-to-noise ratio, and the resistance of each detector were measured as a function of the integrated flux. In addition, the temperature of the air near the detector was monitored and controlled to the approximate values shown in Table 4. It was not possible to secure post-irradiation data on any of the detectors.

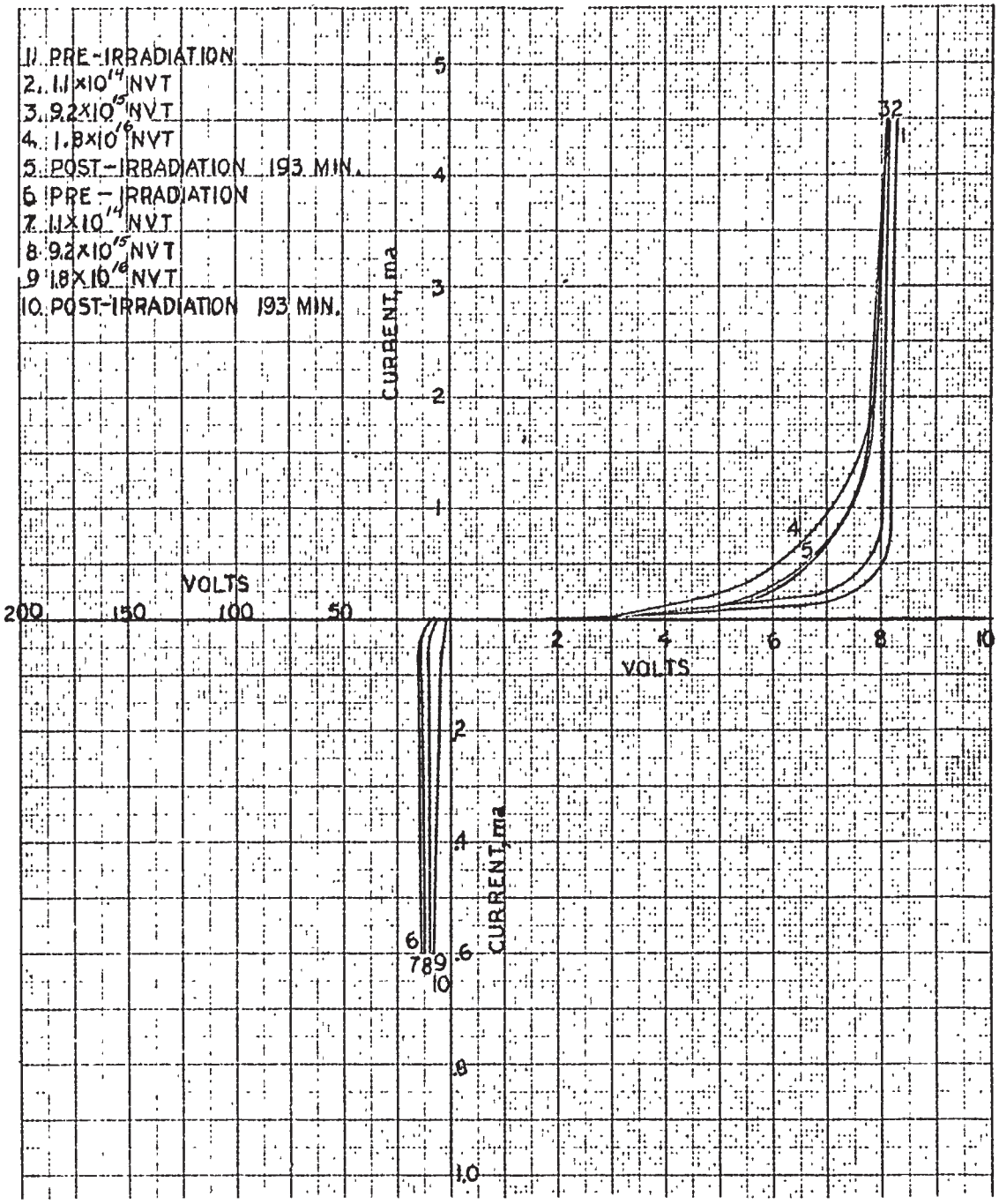

TYPICAL CHARACTERISTICS OF HOFFMAN IN 430-B

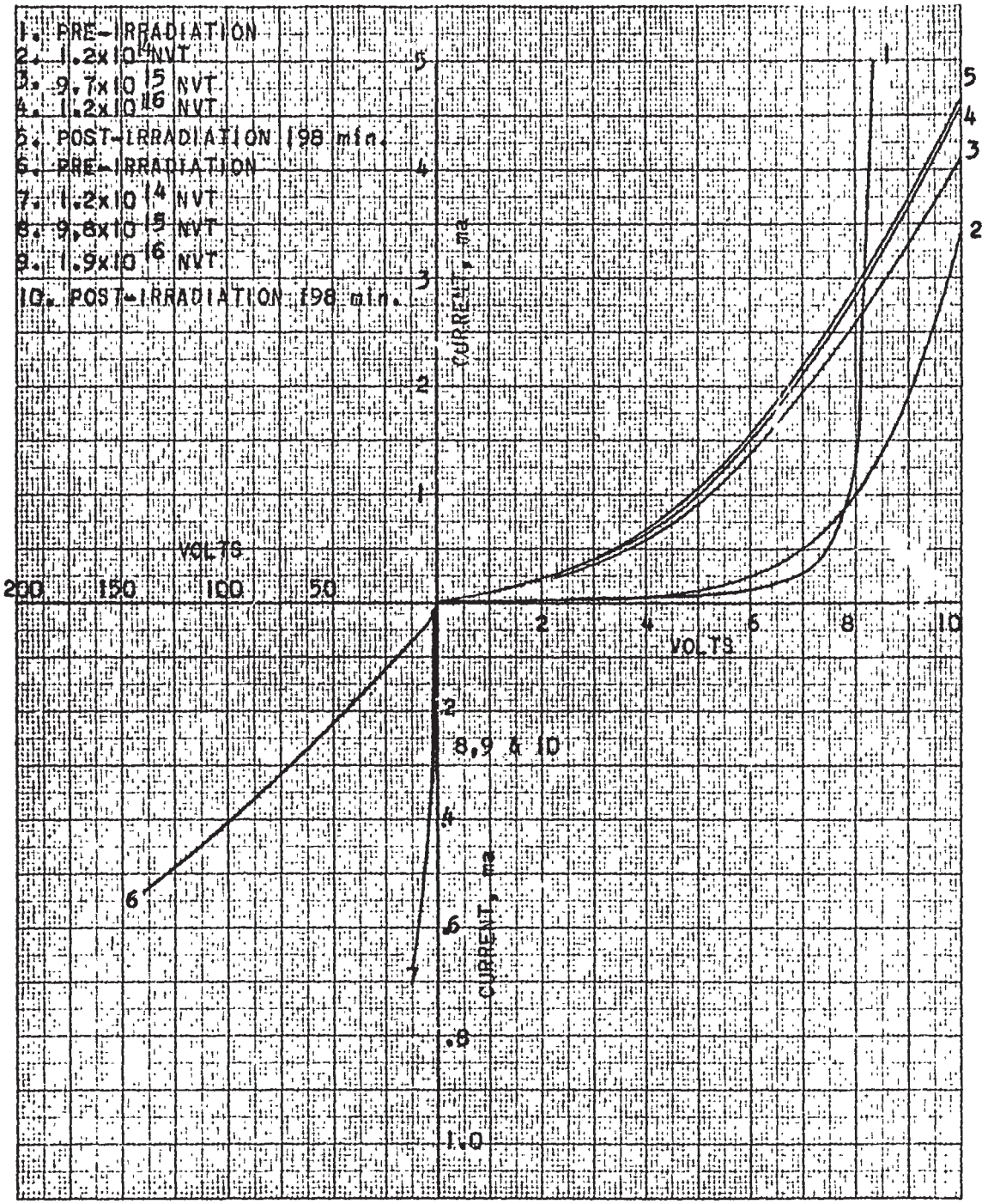

TYPICAL CHARACTERISTICS
OF INTERNATIONAL RECTIFIER IN-430-B

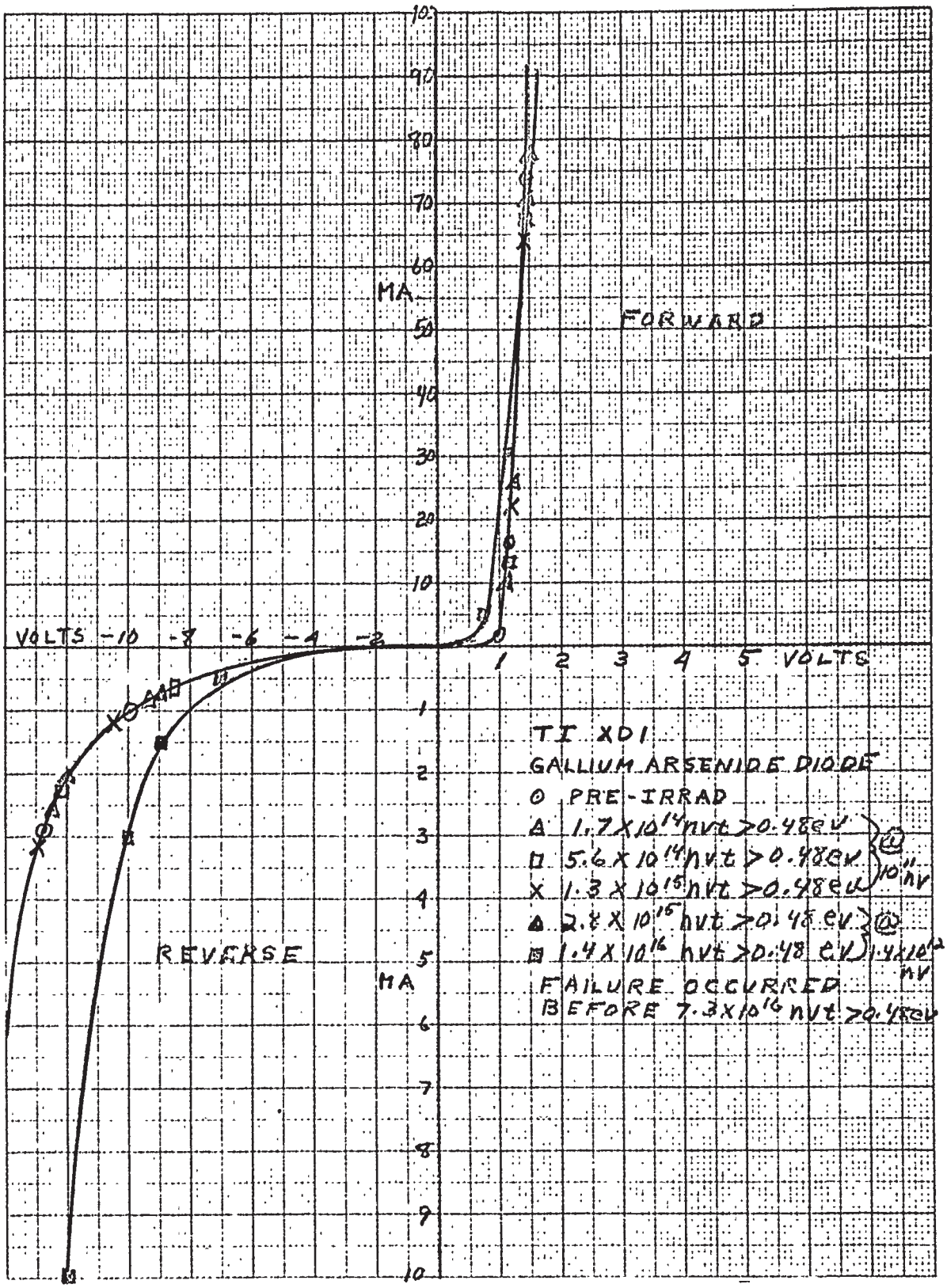

TABLE 4

INFRARED DETECTORS

Type	Manufacturer	Quantity	Maximum Operating Temperature (°F)	Identification Number
Lead Sulfide	Eastman Kodak	2	212	1,2
Lead Sulfide	Eastman Kodak	6	140	3,4,11,12,13,14
Lead Selenide	Eastman Kodak	2	140	5,10
Thermistor Bolometer	Barnes Engineering	1	140	7
Thermistor Bolometer	Barnes Engineering	1	392	8
Indium Antimonide PEM	Radiation Electronics Corporation	2	176	6,9

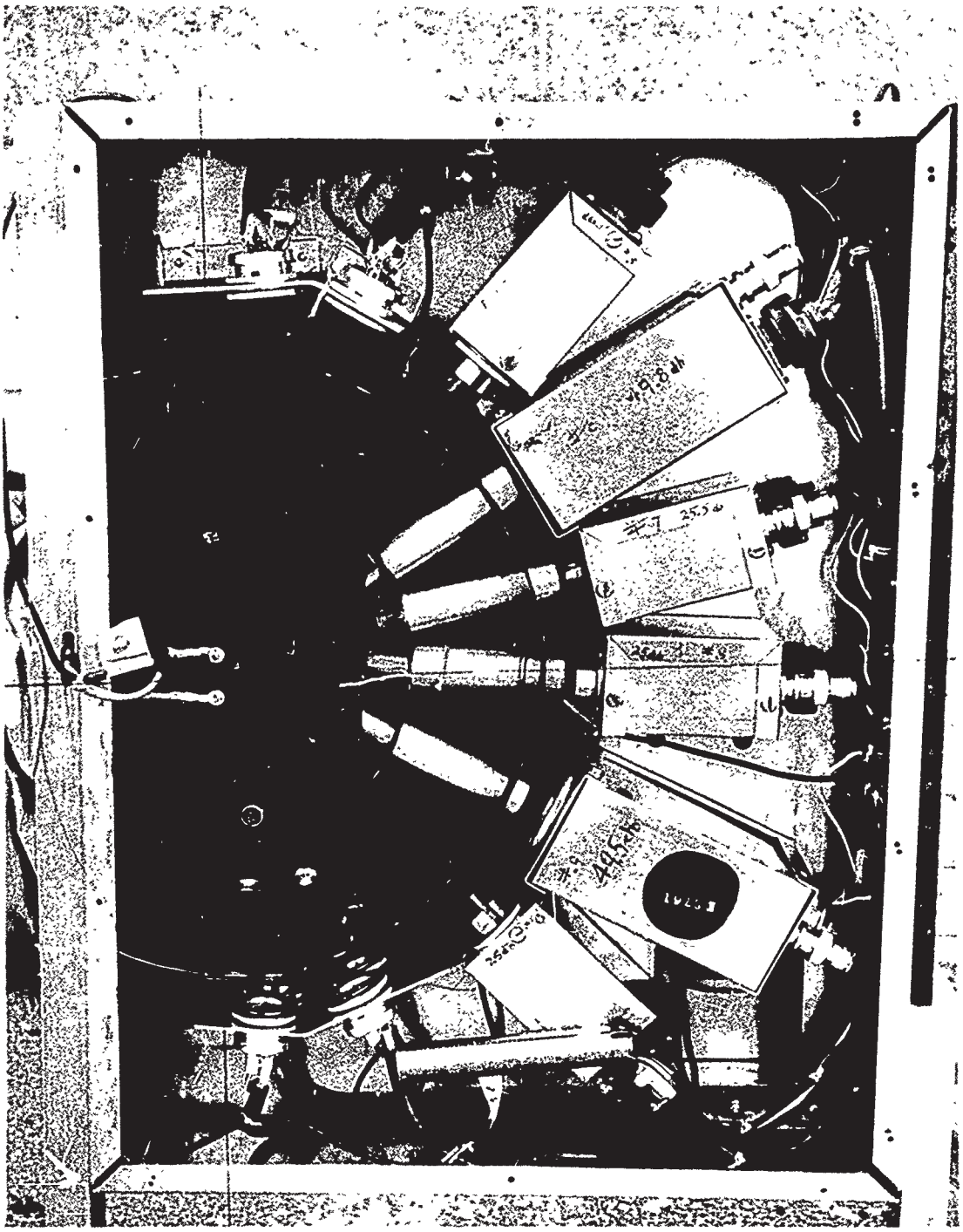

INFRA-RED CHAMBER CONVAIR FT. WORTH TEXAS

FIGURE 23

2. Results

Detailed data obtained on the fourteen infra-red detectors are tabulated in Appendix B. Examination of the signal level and the signal-to-noise ratio tabulations shows that most of the detectors began to deteriorate rapidly above an integrated flux of approximately 1.5×10^{14}nvt ($E > 0.48$ev). However, one lead selenide, one high-temperature lead sulphide, and one high-temperature thermistor bolometer continued to give an electrical signal output in response to an infrared signal throughout both the 0.040 and 3 megawatt levels of operation. The tabulated data on these detectors are shown in Tables 5, 6, and 7.

3. Conclusions

From these data, it is noted that the lead selenide detector tolerated up to 4×10^{15}nvt ($E > 0.48$ev), while the thermistor bolometer tolerated up to 1.6×10^{16}nvt ($E > 0.48$ev). It will also be noted that when the signal output began to drop, the resistance of the detector also began to decrease and became erratic as the integrated flux built up. An increase in the temperature of the ambient air in the test compartment occurred at the same point. It is possible that some of the effects attributed to nuclear irradiation may have been produced by the increase in detector temperature above its normal operating value. The exact reason for the increase in compartment temperature is unknown; however, it appeared to occur shortly after the reactor power was raised to three megawatts. This tends to indicate that the increase in temperature may have been due to increased gamma heating at the three megawatt power level. Later in the three megawatt power cycle, the temperature was restored to the initial values.

TABLE 5
LEAD SELENIDE INFRARED DETECTOR

140 °F

Integrated Flux n/cm^2 (E > 0.48 ev.)	Signal Level (Arbitrary Units)	S/N Ratio (Hum and Noise)	Resistance of Detector (ohms)	Temperature °F
Pre-Irradiation	1.0	--	530 K	135
1.6×10^{13}	0.97	--	420 K	135
3.5×10^{13}	0.77	49	410 K	135
5.1×10^{13}	0.68	36	420 K	135
6.8×10^{13}	0.68	34	420 K	135
1.03×10^{14}	0.61	41	410 K	135
1.2×10^{14}	0.64	27	410 K	135
7.8×10^{14}	0.13	--	105 K	152
3.3×10^{15}	0.0026	--	85 K	230
4.3×10^{15}	0.071	--	160 K	260
6.2×10^{15}	0.10	--	200 K	215
1.4×10^{16}	1.8	--	550 K	--
1.5×10^{16}	0.21	--	190 K	157
1.8×10^{16}	0.077	.92	100 K	156
Post-Irradiation	None	--	--	--

TABLE 6

LEAD SULPHIDE INFRARED DETECTOR

212°F

Integrated Flux n/cm^2 (E> 0.48 ev)	Signal Level (Arbitrary Units)	S/N Ratio (Hum and Noise)	Resistance of Detector (ohms)	Temperature (°F)
Pre-Irradiation	1.0	--	580 K	135
2.2×10^{13}	0.9	--	670 K	135
3.9×10^{13}	0.58	30	670 K	135
5.6×10^{13}	0.48	25	710 K	135
7.5×10^{13}	0.42	20	690 K	135
1.1×10^{14}	0.41	20	710 K	135
1.3×10^{14}	0.33	18	740 K	135
1.1×10^{15}	0.045	--	800 K	152
3.6×10^{15}	0.016	--	440 K	230
4.6×10^{15}	0.022	--	420 K	260
6.9×10^{15}	0.0022	--	610 K	215
1.9×10^{16}	--	--	7.9 M	156
Post-Irradiation	None	--	--	--

TABLE 7

THERMISTOR BOLOMETER INFRARED DETECTOR

392 °F

Integrated Flux n/cm^2 (E > 0.48 ev)	Signal Level (Arbitrary Units)	S/N Ratio (Hum and Noise)	Resistance of Detector (ohms)	Temperature °F
Pre-Irradiation	1.0	--	6.6 M	130
1.05×10^{13}	1.1	--	6.1 M	130
3.4×10^{13}	0.73	3.5	6.5 M	130
4.7×10^{13}	0.73	3.6	6.5 M	130
6.2×10^{13}	0.72	2.1	6.5 M	130
9.6×10^{13}	0.72	3.1	6.5 M	130
1.1×10^{14}	0.73	3.1	6.4 M	~ 130
7.2×10^{14}	0.58	--	3.1 M	~ 140
3.1×10^{15}	0.40	--	970 K	~ 200
3.9×10^{15}	0.49	--	540 K	~ 220
5.9×10^{15}	0.37	--	970 K	~ 200
1.2×10^{16}	0.49	--	--	--
1.4×10^{16}	0.92	--	2.6 M	~ 147
1.6×10^{16}	0.43	1.2	2.7 M	~ 147
Post - Irradiation	None	--	--	--

C. ION CHAMBERS

1. Types Investigated

For the Convair tests, two, commercial, gamma-compensated, ion chambers (Model GR-11) manufactured by General Electric were chosen. The chambers are rated for high temperature and relatively high flux operation; however, the ratings were based on pre-post tests rather than in-pile tests at temperature. Specifications for the chambers are given in Table 8. The chambers are of standard design using boron as a thermal nuetron sensitive coating in an annular chamber, together with a gamma compensating inner chamber. The chambers have a 1/v dependence on neutron energy and were operated in a high, fast t_{to} thermal flux field. Thus, the response due to epithermal neutrons approached or possibly exceeded that due to thermal neutrons.

The ion chambers were mounted in a controlled temperature chamber as shown in Figure 24 . The neutron flux levels were approximately 3×10^{11} neutrons/cm^2-sec epicadmium, and 3×10^8 neutrons/cm^2-sec thermal. A 150-foot length of coaxial cable was used to connect the chambers to two Fluke, 1000-volt power supplies and a Keithley Microammeter. Prior to irradiation, the units were checked with two 5 curie polonium-beryllium sources, and a 10 millicurie Co^{60} source. Chamber outputs and temperatures were monitored periodically during the irradiation. In addition, a curve of output current versus power was taken during the rise in power from 40 KW to 3 MW and again at the decrease in power at the end of the irradiation. During irradiations, one of the chambers was inoperable because of faulty leads. Thus, data obtained were for one chamber only.

Two prototype uncompensated stainless-steel ion chambers were fabricated by Marquardt (see Figure 25) for irradiation test work in the General Electric Vallecitos Test Reactor. One test unit was an all-welded chamber-and-cable type. The second test unit was mounted inside a standard aluminum test capsule. Varying thermal neutron flux fields were obtained by lowering the chamber units inside a irradiation guide tube that passed adjacent to the reactor core. The absolute thermal flux level inside the irradiation guide tube at different distances from the reactor core was determined by checking against known General Electric calibration curves.

2. Results

Figure 26 shows a plot of the G.E. chamber output versus reactor power at the beginning and end of the 3 MW runs at Convair. Figure shows chamber output normalized to unit flux versus exposure. Since the chambers were operated in a region where the fast-to-thermal ratio was approximately 1000 to 1, the data, for neutron fluxes at the energies of interest in computing ion chamber response, are somewhat uncertain.

TABLE 8

GENERAL ELECTRIC GR-11 ION CHAMBER DESIGN SPECIFICATIONS

Dimensions	
Sensitive Length	9-1/4 in.
Over-all Length	13-1/2 in.
Diameter (maximum)	3-1/16 in.
Materials	
Shell, Electrodes, and Connectors	Aluminum (2S)
Insulators	Mica and Aluminum
Electrode Coating	96% Boron-10
Filling Gas	Nitrogen
Operating Characteristics	
Neutron Flux Range	5.0×10^{2} to 10^{11} n/cm^2-sec
Neutron Sensitivity	2.2×10^{-14} amp/n/cm^2-sec
Gamma Sensitivity	2.2×10^{-11} amp/R/hr
Gamma Compensation	95%
Environment	
Temperature (maximum)	300°C (572°F)
Neutron Exposure (Life)	10^{19} nvt (for 10% reduction in sensitivity)

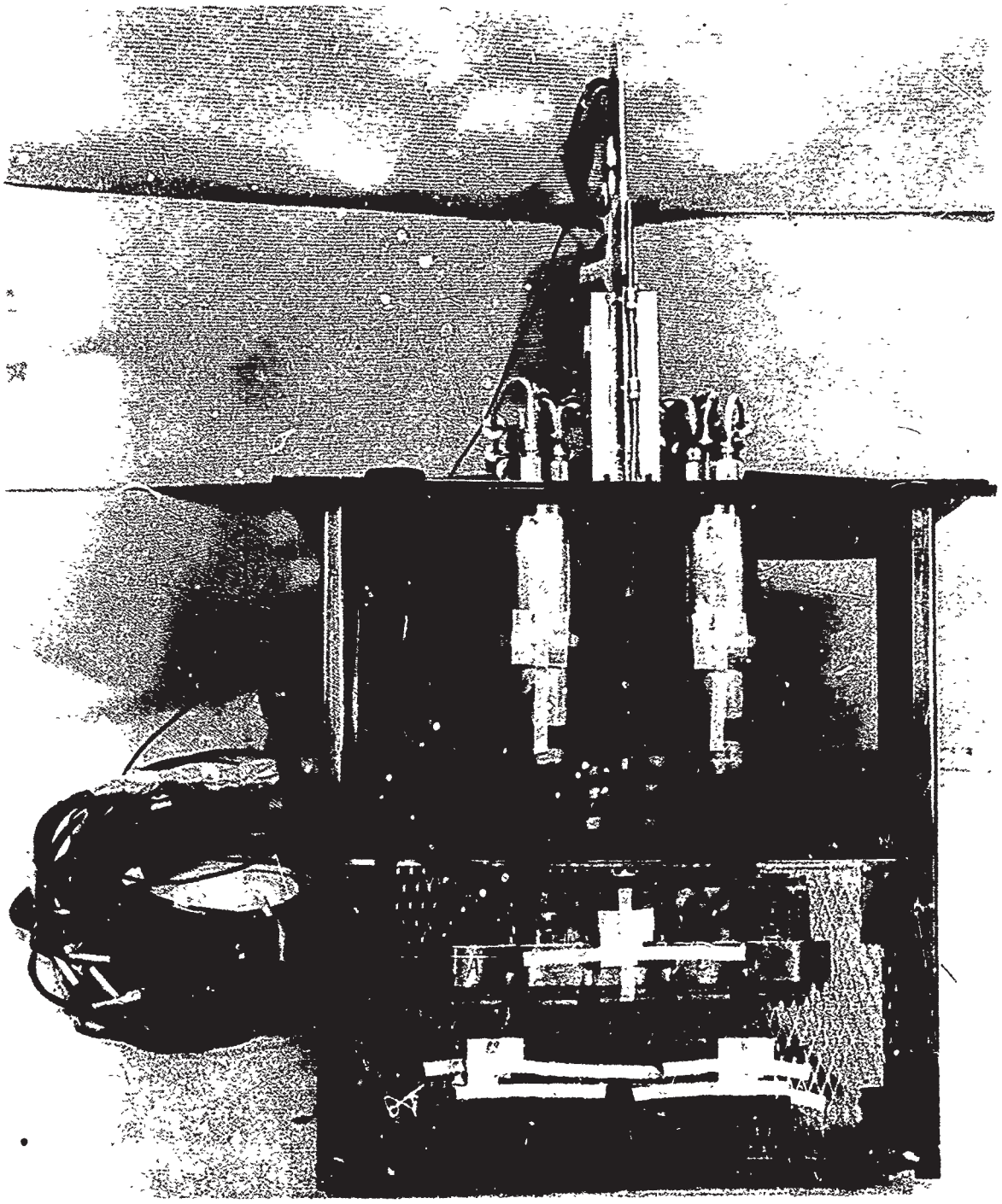

FIGURE 24

EXPERIMENTAL HIGH TEMPERATURE NEUTRON ION CHAMBER

FIGURE 25

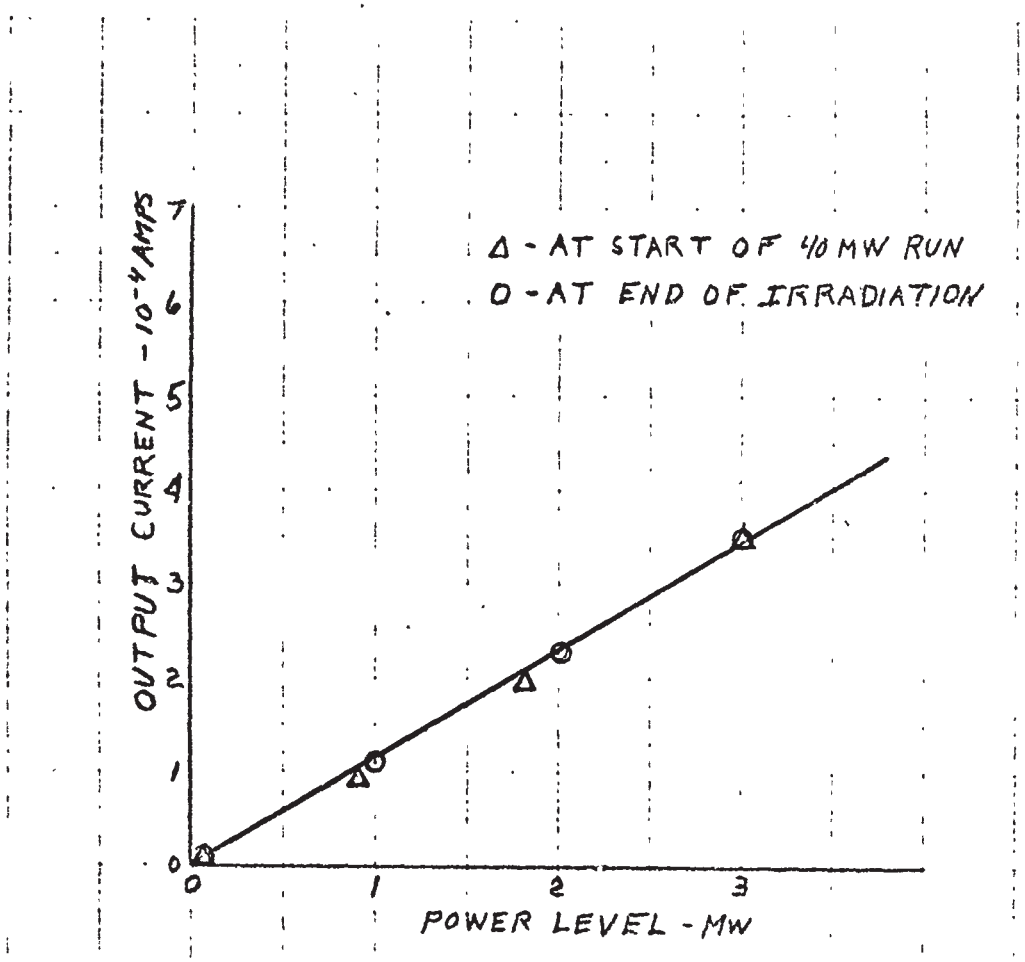

ION CHAMBER CURRENT vs. REACTOR POWER LEVEL

Thus, no accurate correlation between theoretical and measured output could be made. The curves show, however, that the chamber is quite stable, and the power level versus output does not vary more than ±10 percent from beginning to end of the irradiation. It is therefore reasonable to assume that no appreciable damage resulted since the variations in output could quite easily be due to control rod changes in the reactor producing a changing flux pattern. In tests of capacitors (described in Section III-D) where transient effects were noted, similar results were observed. These are indicated by a plot of percent change in capacitance versus time at 3 MW in Figure 27.

Figures 28 and 29 are plots of the Marquardt ion-chamber current as a function of thermal neutron flux for a fixed electrode voltage of 1600 volts. As shown by this plot, the chamber was capable of measuring neutron flux over a range of eight decades ($10^6 \times 10^{14}$), with an absolute sensitivity of 1×10^{-15} amps/nv. Figure 30 shows saturation curves that determine the relative linearity of the chamber as a function of chamber electrode voltage. As shown by these three curves, maintaining a voltage of 1800 volts on the electrodes permits operation of the chamber in neutron fluxes up to 9×10^{13}nv without serious nonlinearity.

In addition to these tests, the Marquardt chamber was operated for a period of eight and one-half hours in an ambient thermal flux field to 9×10^{13}nv without change in sensitivity or saturation characteristics.

3. Conclusions

The radiation data obtained during the GETR test indicate that the Marquardt prototype chamber will operate over a range of 7 decades (10^7nv to 10^{14}nv).

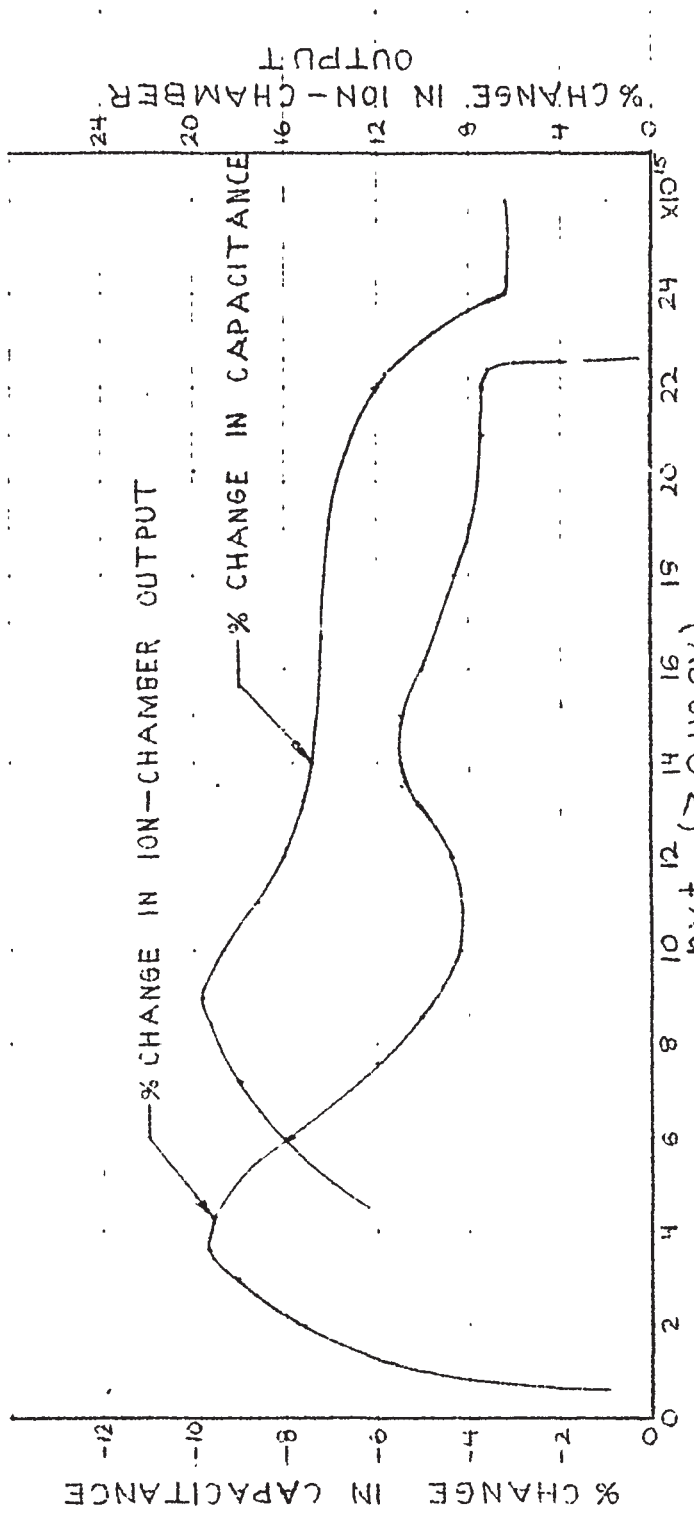

COMPARISON OF ION CHAMBERS WITH CAPACITORS

FIGURE III

FIGURE 27

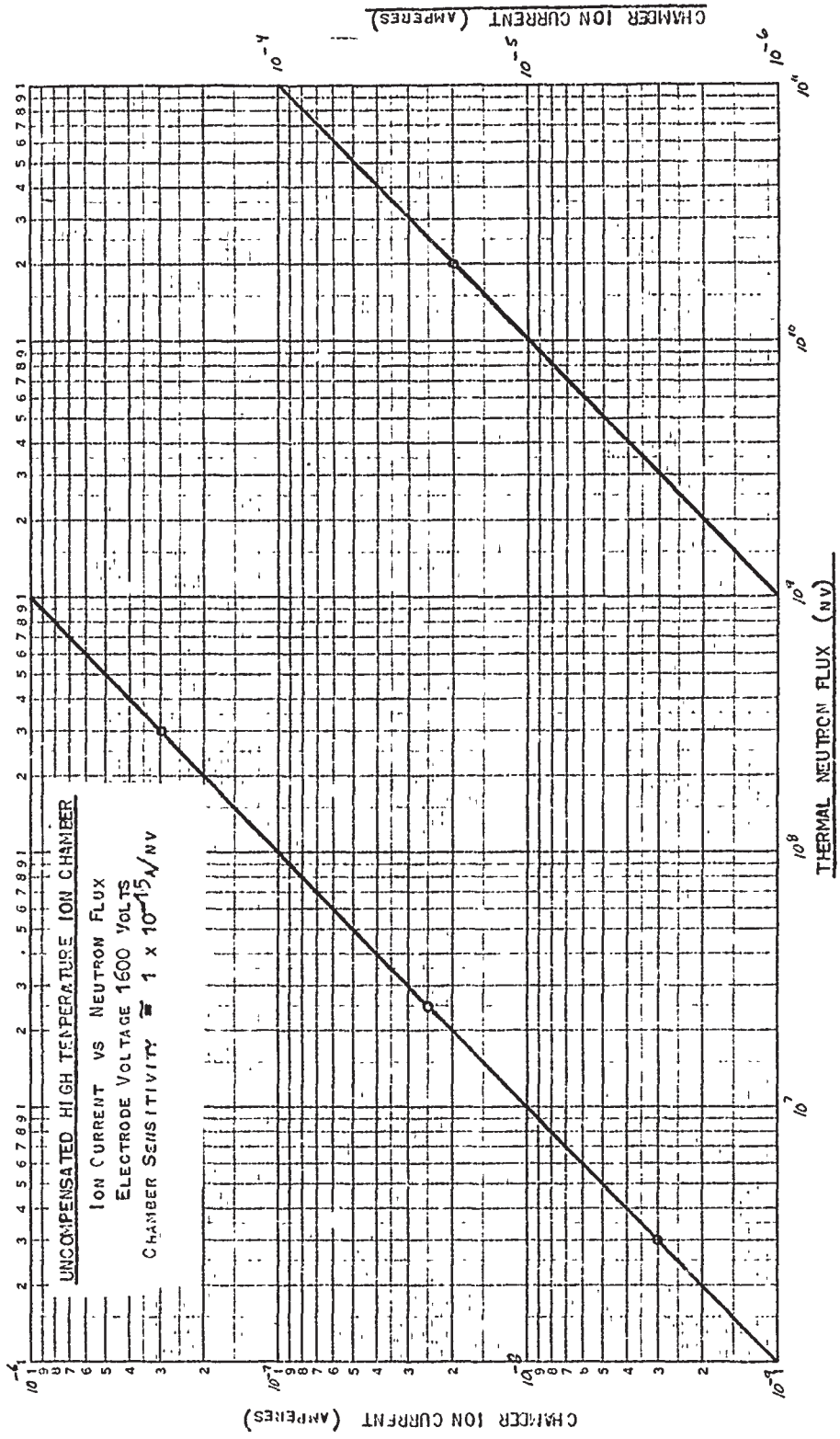

FIGURE 28

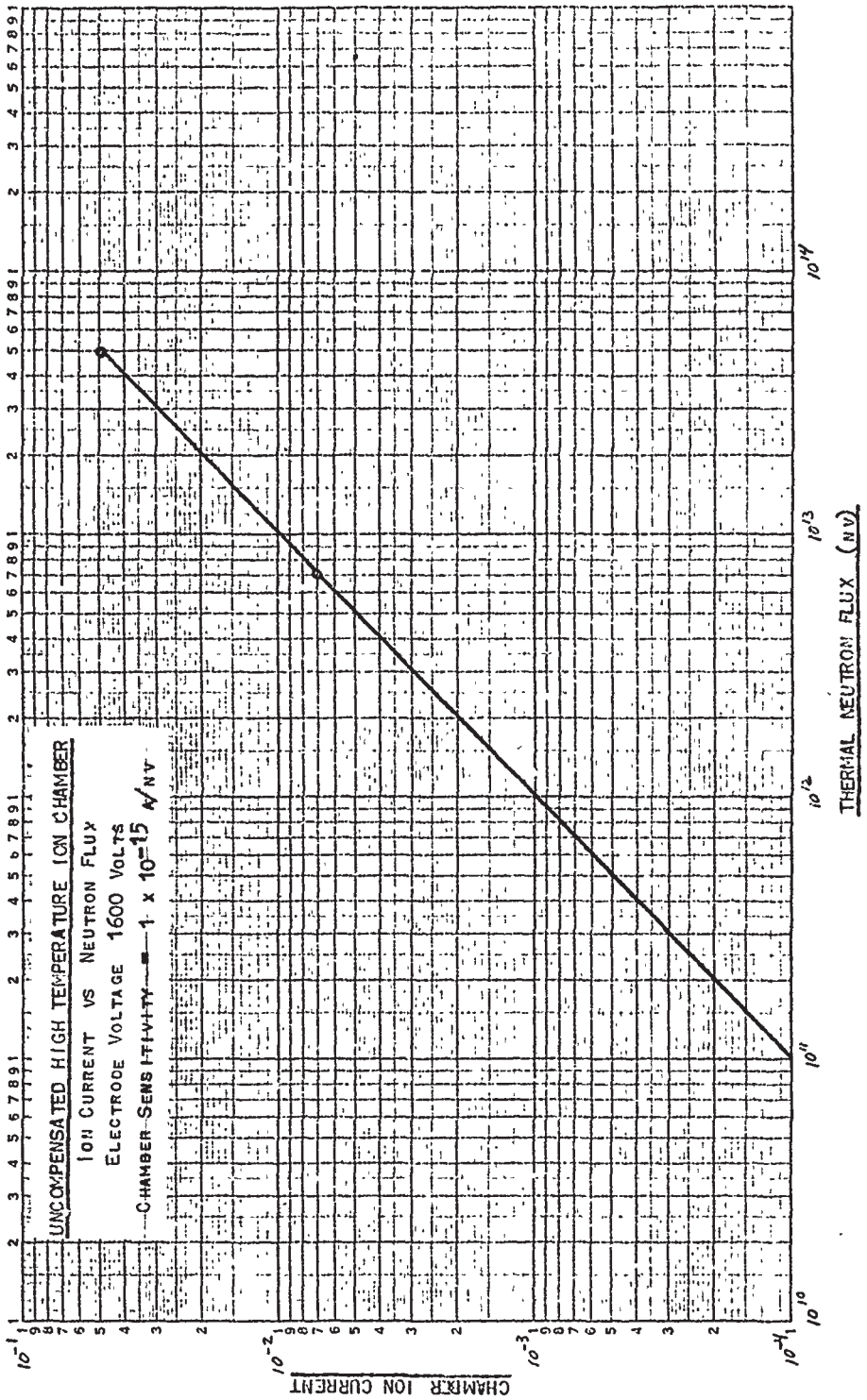

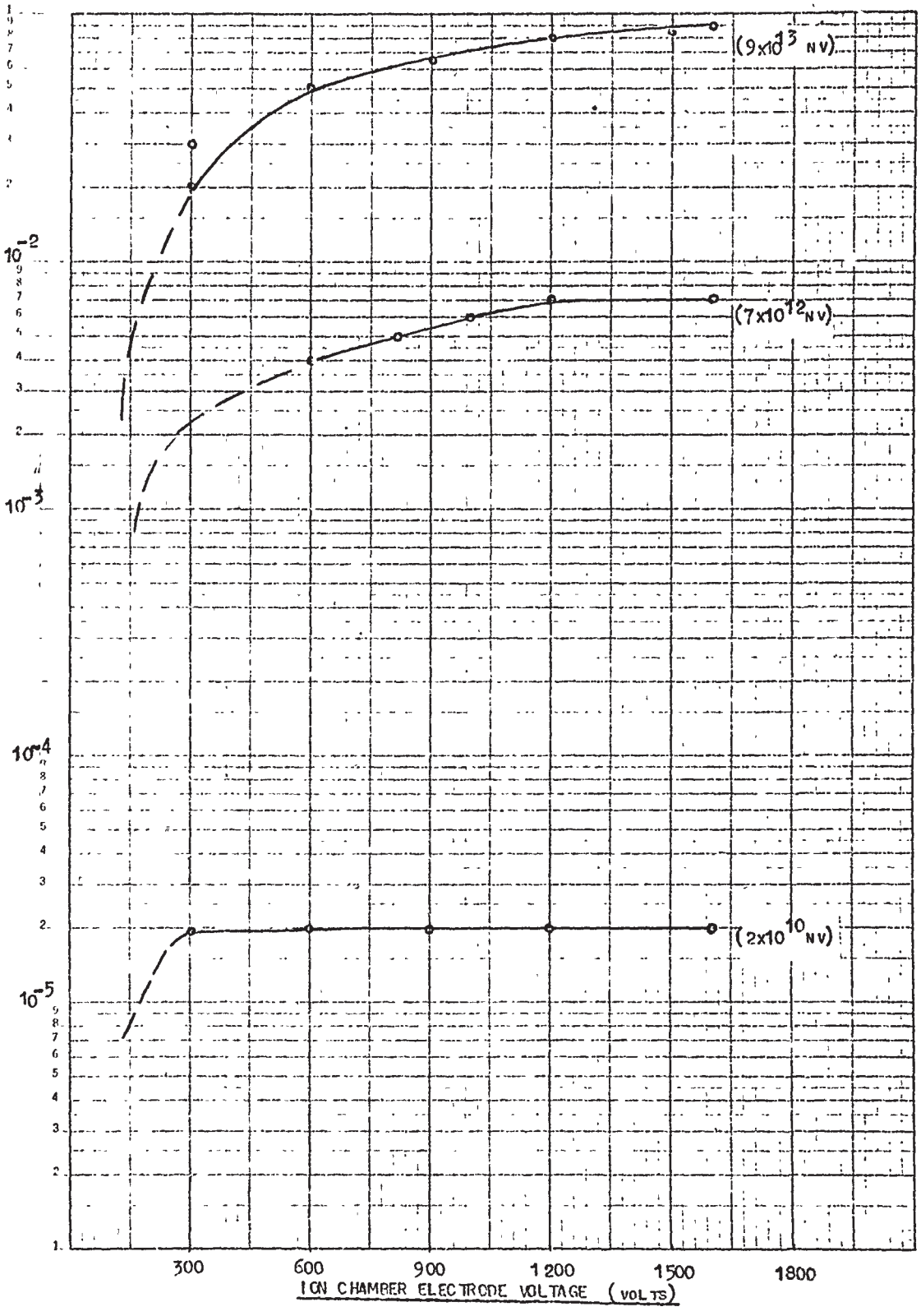

D. CAPACITORS

1. Types Tested

Two types of capacitors were tested. One was a mica dielectric encapsulated in a silicone resin compound. The other type was a mylar dielectric with a Kraft paper backing to distribute a silicone oil impregnant, all encapsulated in a soldered metal case. The mica capacitors were fabricated by Sprague Electric Company under the trade name "Fabmika" and were rated as follows:

Capacitor N	Capacitance	Voltage	Maximum Temperature
205M-105X-9172	1 mfd	1700 vdc	500°F
205M-105X-9401	0.47 mfd	400 vdc	500°F

The mylar capacitors were manufactured by Southern Electronic Corporation, and were rated at 0.3 mfd and 3000 vdc with a maximum operating temperature of 300°F.

The capacitors were mounted on vertical aluminum grid racks as shown in Figure 24 . The mylar capacitors were operated at an ambient temperature of 300°F and the Fabmika's at 500°F. A General Electric type 1610-A capacitance checker was used to measure capacitance and dissipation factor at 400 and 10,000 cps alternately. Direct-current voltages were maintained at about one half the rated voltage, and reversed every four hours. In the case of the mylar capacitors, it was necessary to reduce the d-c voltage during the test because of gross changes in leakage resistance during the test. The capacitors in each assembly were wired with one common bus, and open pin reference connections were made to check on changes in the leads.

2. Results

Both types of capacitors showed transient, as well as permanent changes from irradiation. The transient changes could be explained by assuming that a reversal occurs during irradiation; however, organic and silicone compounds as a general rule do not show such a reversal. Therefore, it seems more realistic to assume that the transients are the results of an ionization effect which is proportional to the irradiation flux. As indicated in Section IIIC, the variation in ion-chamber output at constant reactor power shows much the same shape as the changes in capacitance shown in Figure 27 .

The mylar-paper capacitors were affected more drastically and erratically in both capacitance and dissipation factor than were the Fabmika. The mylar capacitors showed transient changes in capacitance of 15 percent and permanent changes of 23 percent, while the Fabmika had corresponding changes of 10 percent and 3.5 percent, respectively. The dissipation factor in the mylar capacitors increased by as much as 2500 percent or more during irradiations, but the maximum change after irradiation was only 95 percent. The Fabmika capacitors increased 80 percent in dissipation factor during irradiation and had a 14 percent maximum increase after irradiation. All of these changes occurred in the 400 cps measurements. The changes, as measured at 10,000 cps, were lower in both cases, as shown in Table 9.

Gross changes and erratic behavior in the mylar-paper capacitors can be attributed in part to leakage of the silicone impregnant, and rupture of the cases (Figure 31). The leakage was noted in pre-irradiation tests and was attributed to expansion of the silicone oil. Actual internal temperatures during irradiation are estimated to have reached 400°F because of nuclear heating. Since this occurred fairly rapidly, it probably caused the ruptures of the metal shells. It is possible that this problem could be overcome by some minor changes in the mylar capacitor design. However, whether an improved capacitor of this type would be more resistant to radiation effects cannot be determined on the basis of persent data.

3. Conclusions

The Fabmika capacitors are apparently satisfactory for use under the test conditions. This point can be verified by actual circuit operation under similar conditions. The mylar capacitors are not satisfactory for use under the same conditions.

TABLE 9

Capacitor			Test Conditions		Change in Capacitance		% Change in Dissipation Factor		Neutron Exposure 0.4Mev	
Mfg.	Type	Capacity	Temp.	Frequency	Maximum Transient	Final	Maximum Transient	Final	Rate Neutrons/cm^2-sec (Au)	Dose Neutrons/cm^2(Au)
Southern Electronics Corp.	Mylar Paper	0.3 mfd.	300°F	400 cps	-16.7	-23.8	+2800	+61.4	3 x 10"	2.2×10^{16}
Southern Electronics Corp.	Mylar Paper	0.3 mfd.	300°F	10,000 cps	-31.6	-24.7	+119	-21.7	3 x 10"	2.2×10^{16}
Sprague Electronic Co.	Fabmika	0.47mfd.	500°F	400 cps	+1.7	+1.5	+16.3	-14	3 x 10"	2.2×10^{16}
Sprague Electronic Co.	Fabmika	0.47mfd.	500°F	10,000 cps	+1.7	+2.3	+17	+2.1	3 x 10"	2.2×10^{16}
Sprague Electronic Co.	Fabmika	1.0 mfd.	500°F	400 cps	-7.7	-3.9	+80.8	-14.8	3 x 10"	2.2×10^{16}
Sprague Electronic Co.	Fabmika	1.0 mfd.	500°F	10,000 cps	-10.1	-4.7	+20.1	-5.0	3 x 10"	2.2×10^{16}

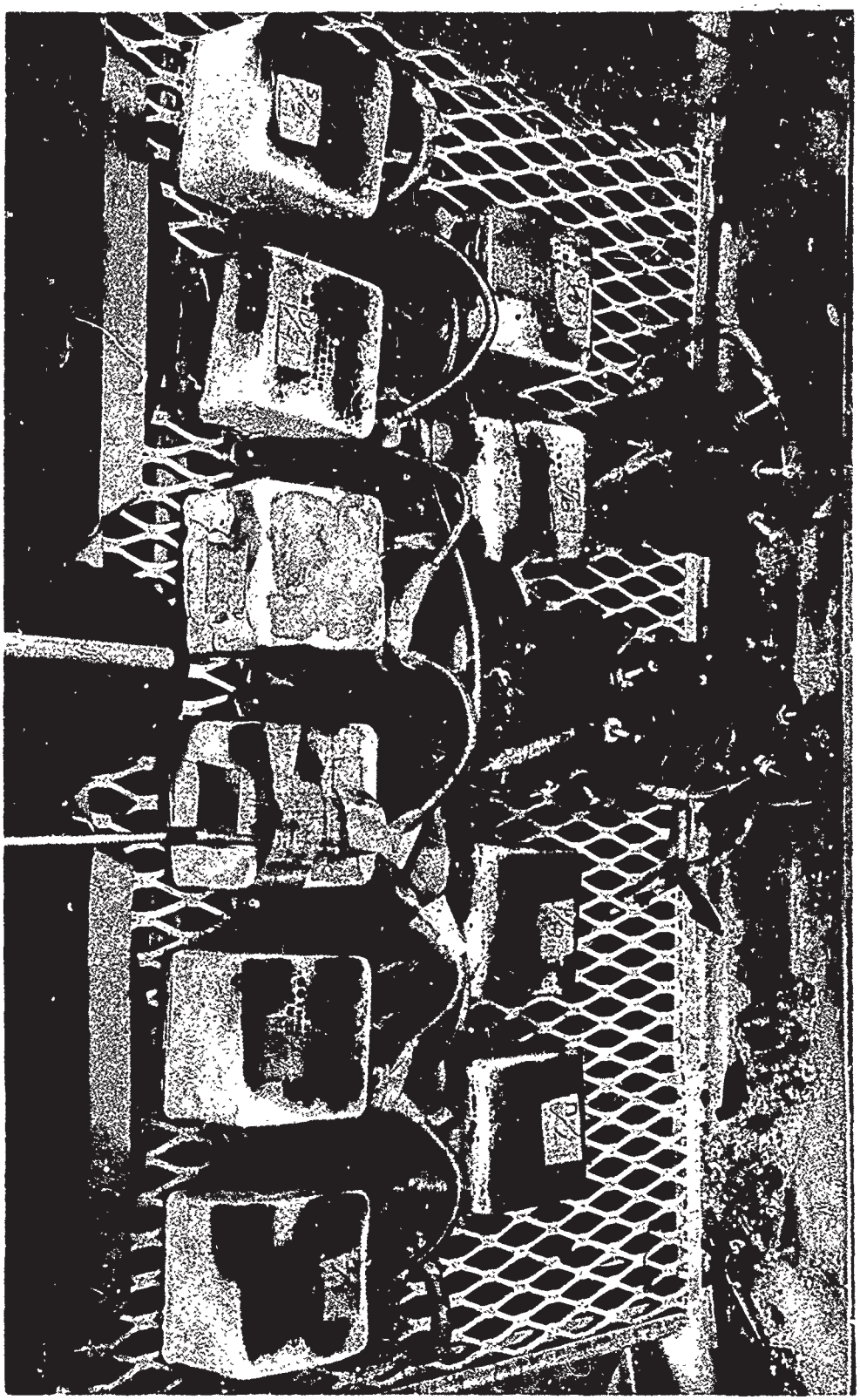

MYLAR CAPACITORS AFTER IRRADIATION AT 300°F

FIGURE 31

E. CERAMIC VACUUM TUBES

1. Types Tested

Six types of ceramic tubes were irradiated during the Marquardt GETR-1A tests. Two tubes of each of the following types were tested simultaneously:

Tube	Type	Status	Maximum Plate Voltage	Maximum Plate Current, Ma
G.E. 7077	Triode	In Production	250	10
G.E. Z2352	Triode	Eng. Prototype	300	15
G.E. Z2353	Triode	Eng. Prototype	300	8
Sylvania SN-2146B	Beam Power Pentode	Eng. Prototype	250	53
Sylvania SN-2225	Duo-Triode	Eng. Prototype	100	4.5

The tubes were fastenned to aluminum plates and assembled into capsules as shown in Figure 8. The capsules were then irradiated in the guide tube facility at GETR (Figure 4) at flux levels of 1×10^{11} nv and 1.4×10^{12} nv >0.48ev. Approximately 35 feet of leads were required between the capsule and test equipment. All data were taken statically using variable d-c power supplies and a curve plotter. Curves of plate voltage vs plate current at four grid biases were plotted at intervals during the irradiation.

2. Results

In all cases failure occurred below 1.3×10^{17} nvt > 0.48 ev. As shown in Figures 32 through 36, which are average values for two tubes at various radiation levels, the tubes all underwent slight though noticeable changes prior to failure.

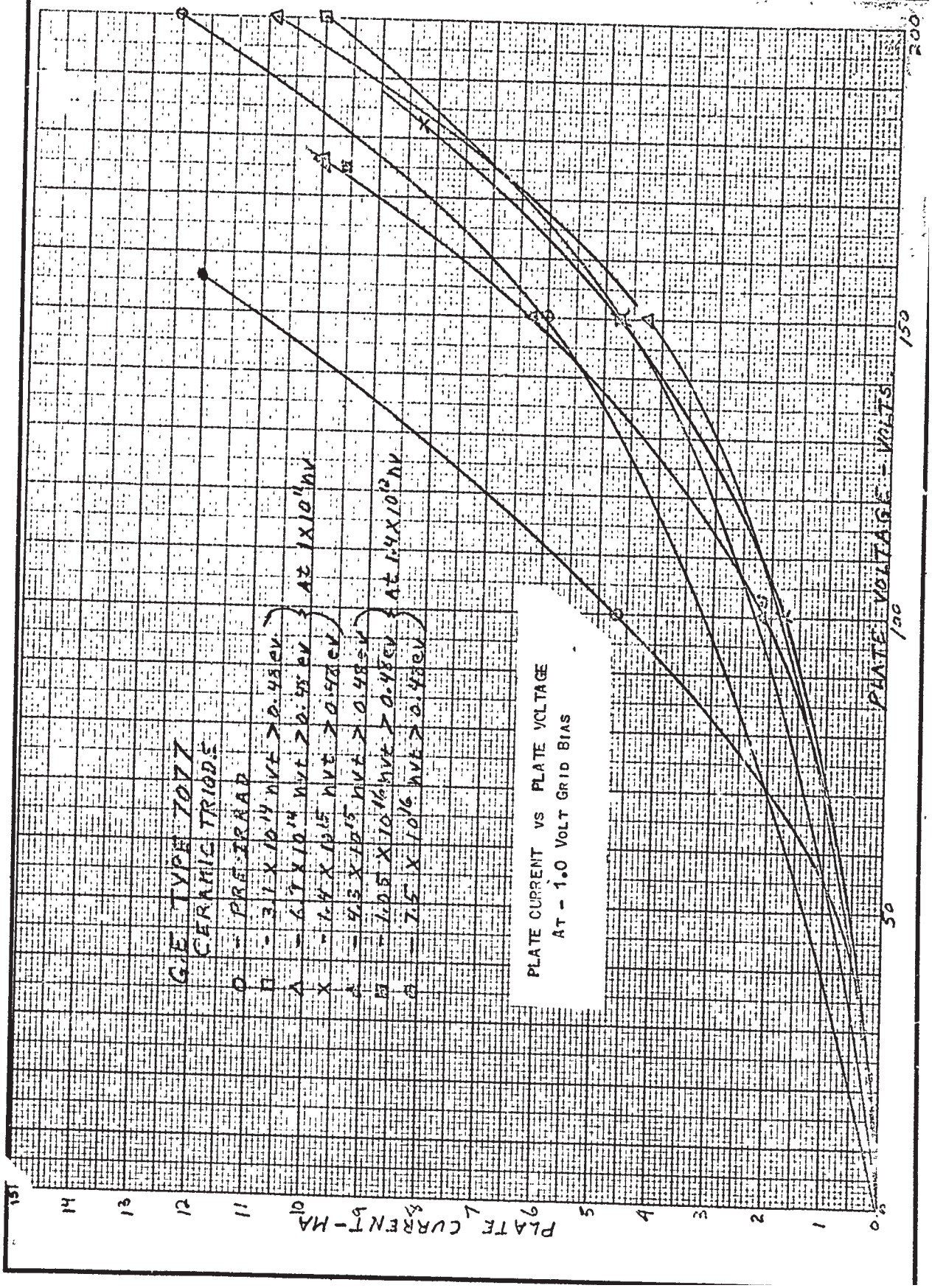

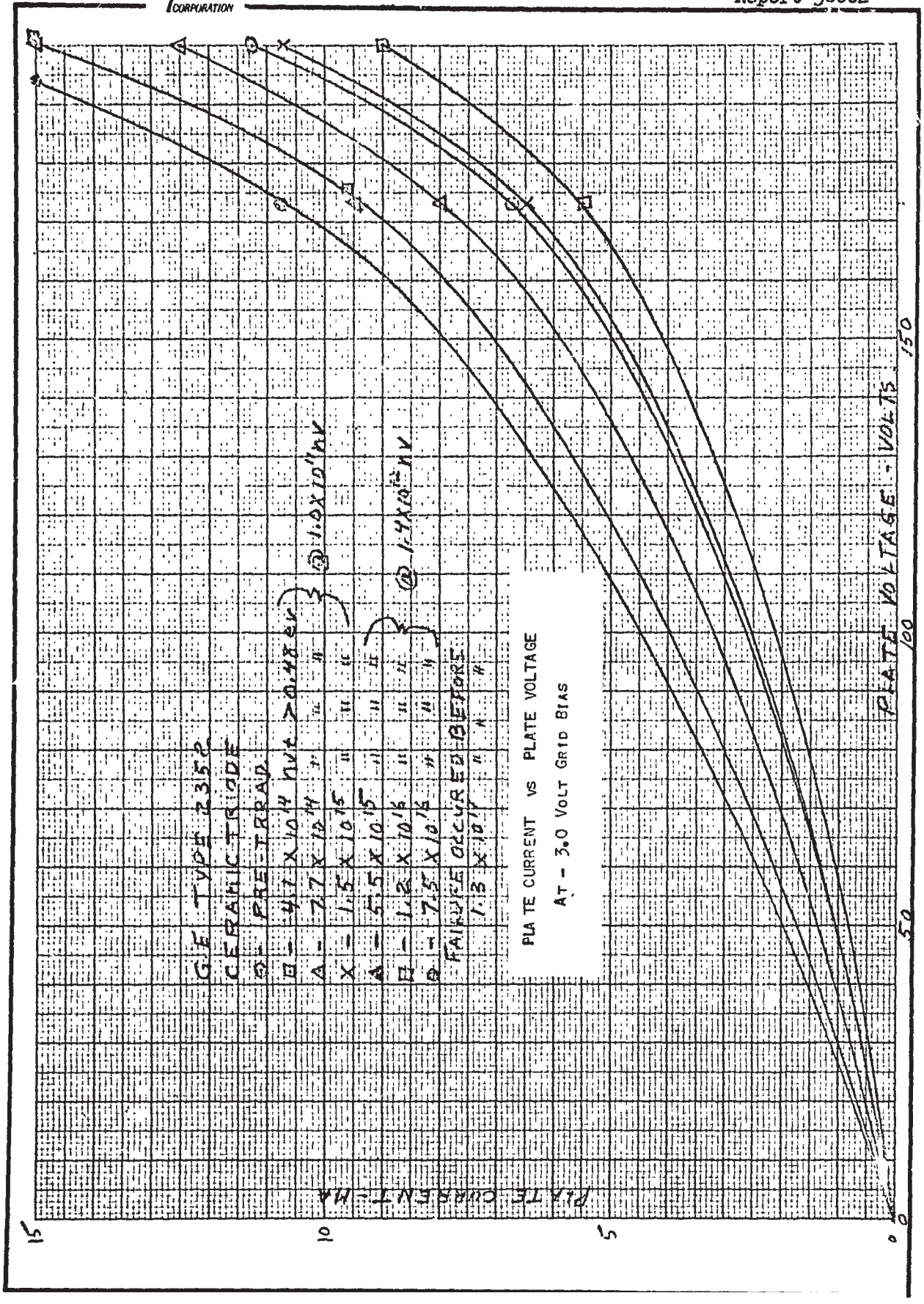

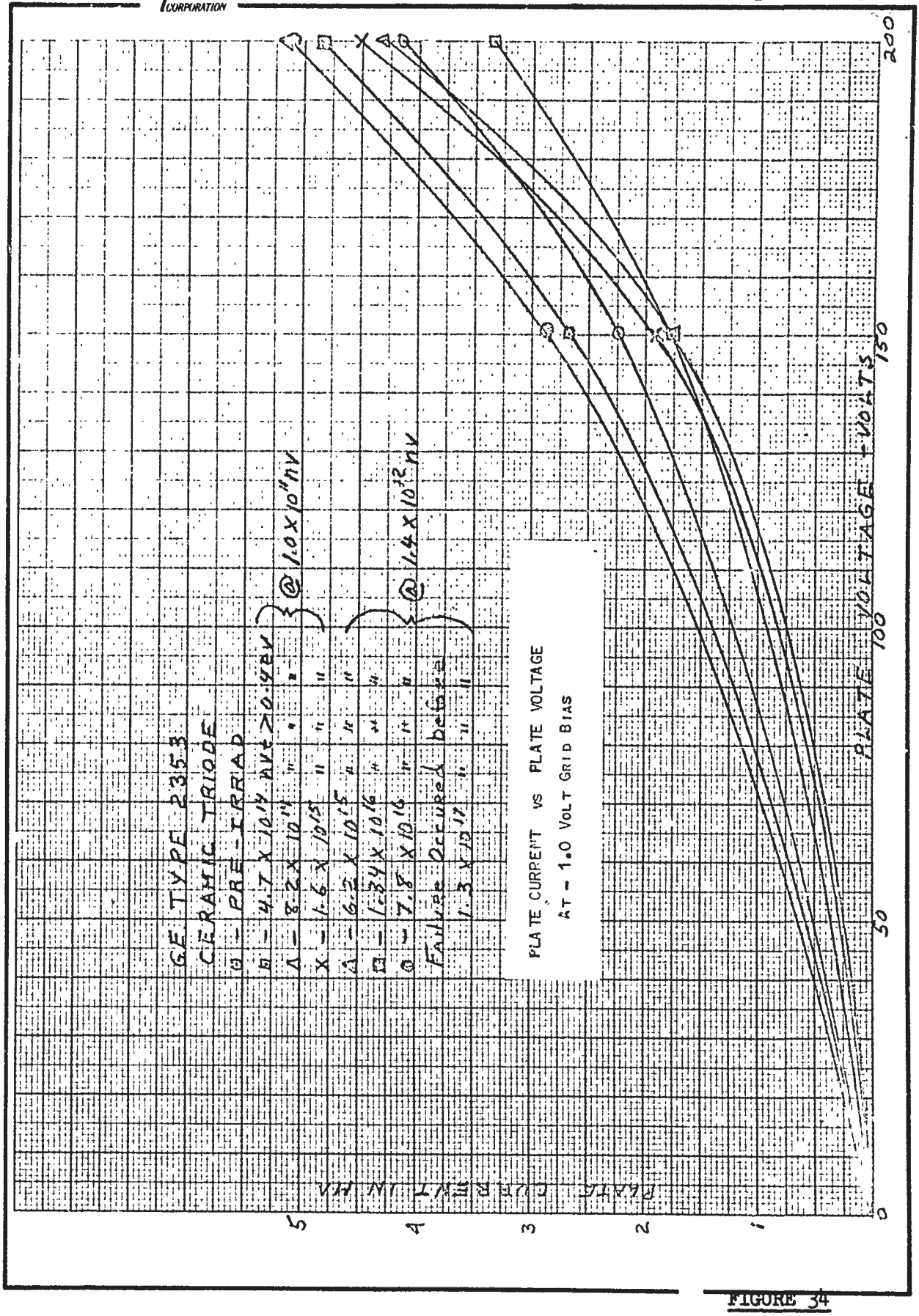

FIGURE 34

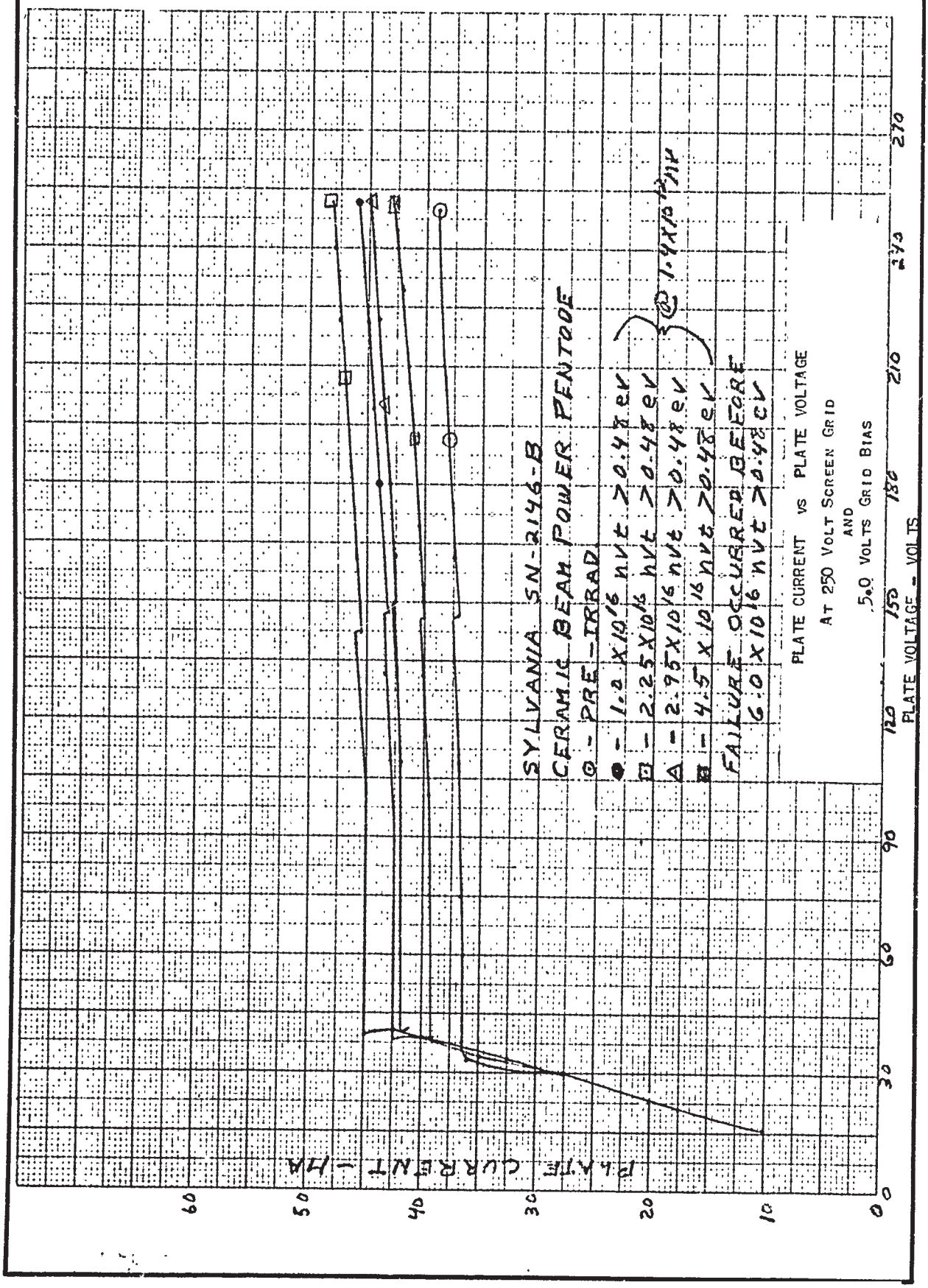

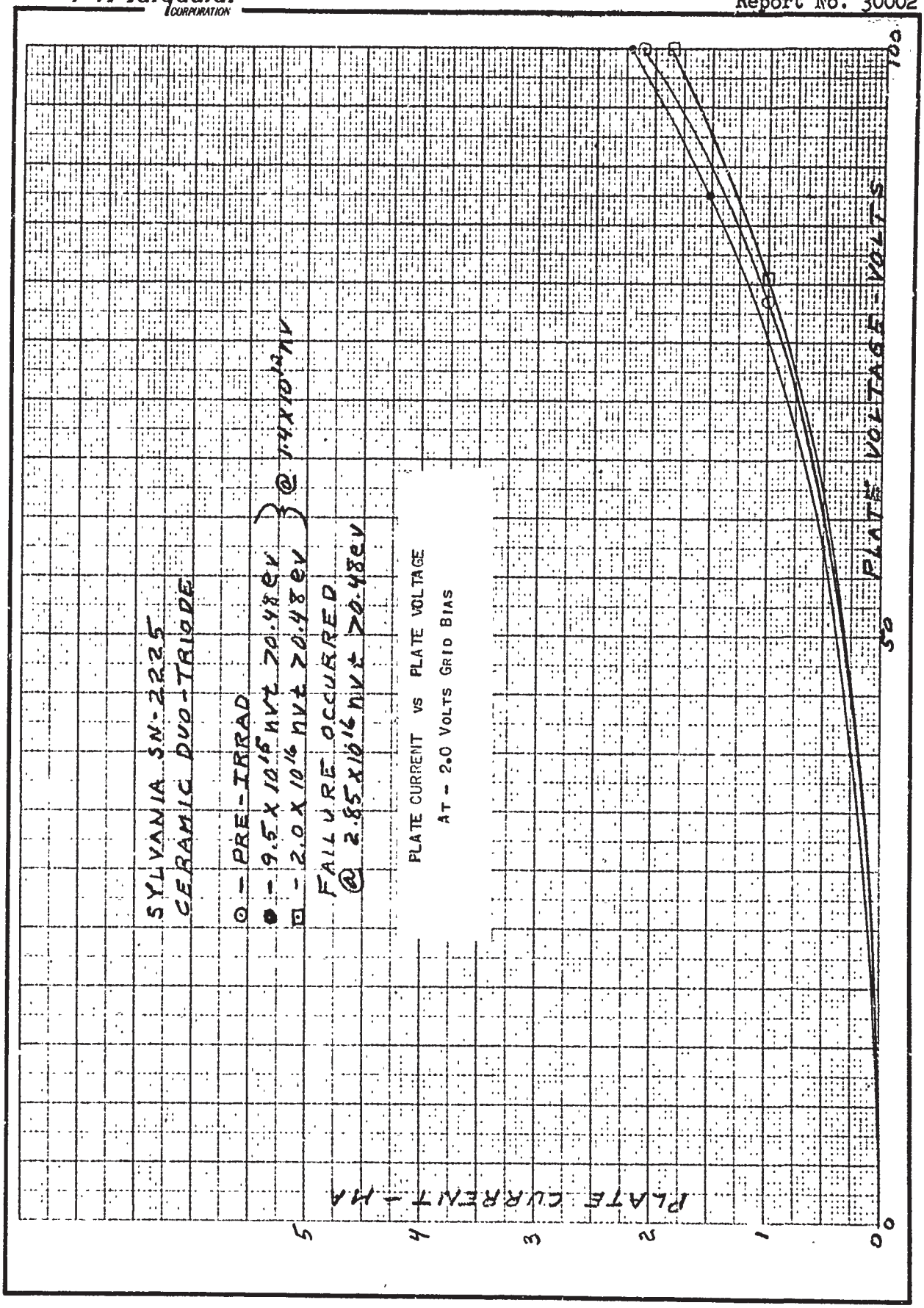

The G.E. Type 7077 failed before the other two G.E. tube types in the same capsule and showed the type of failure postulated for ceramic tubes, i.e., decreasing resistance of the ceramic causing the grid bias to become positive. Most of the types tested showed an initial decrease in plate current for a given plate voltage and grid bias following the onset of irradiation. Lead resistance changes caused by ionization effects could account for this and also for the ultimate failure of the tubes; however, this could not be definitely verified by post-irradiation measurements. In fact, the opposite effect was noted in one type of thermistor tested in the same capsules where the resistance increased by a factor of 10^5.

A comparison of the change in resistivity of Al_2O_3 vs. exposure as shown in Figure 12 with the exposures at which failure occurred in the ceramic tubes shows that failure could be expected at the doses received.

This does not agree with previous G.E. data; but the higher gamma and neutron dose rates in the present test might have had a pronounced effect.

3. Conclusions

Based on these tests, a preliminary operating limit of 1×10^{16} nvt can be set for ceramic tubes. This would allow a safety factor of at least five and insure reasonably reliable operation as far as neutron environments are concerned. Since the failures apparently occurred as a result of decreased resistivity of the ceramic, there is no reason to believe that reliability from the considerations of temperature and shock would be seriously affected. Actual use of the tubes would require that tests be conducted to verify this supposition.

F. SUBMINIATURE VACUUM TUBES

1. Types Tested

Three subminiature tubes types were tested as follows:

Tube	Type	Maximum Plate Voltage	Maximum Plate Current, Ma
G.E. 5902	Pentode	110	30
G.E. 6111	Duo-triode	100	8.5
G.E. 6112	Duo-triode	100	0.8

Only one each of these tube types were included, but both sections of the duo-triodes were checked. Testing methods were identical with the methods used for the ceramic vacuum tubes.

2. Results

The results of the tests are similar to the results of the ceramic tubes except that all the tubes failed between 4×10^{16} and 6×10^{16} nvt $>$ 0.48ev. There was an initial rise in plate current for a given plate voltage and at ultimate failure the tubes behaved like resistors. Figures 37 through 39 show plate current vs. plate voltage at a given grid bias for each of the tubes during the irradiation.

3. Conclusions

Subminiature tubes behaved more consistently than ceramic tubes and showed a more definite damage threshold. Because of the limited number tested under these conditions, their suitability for use as control components can only be estimated to be about the same as ceramic tubes.

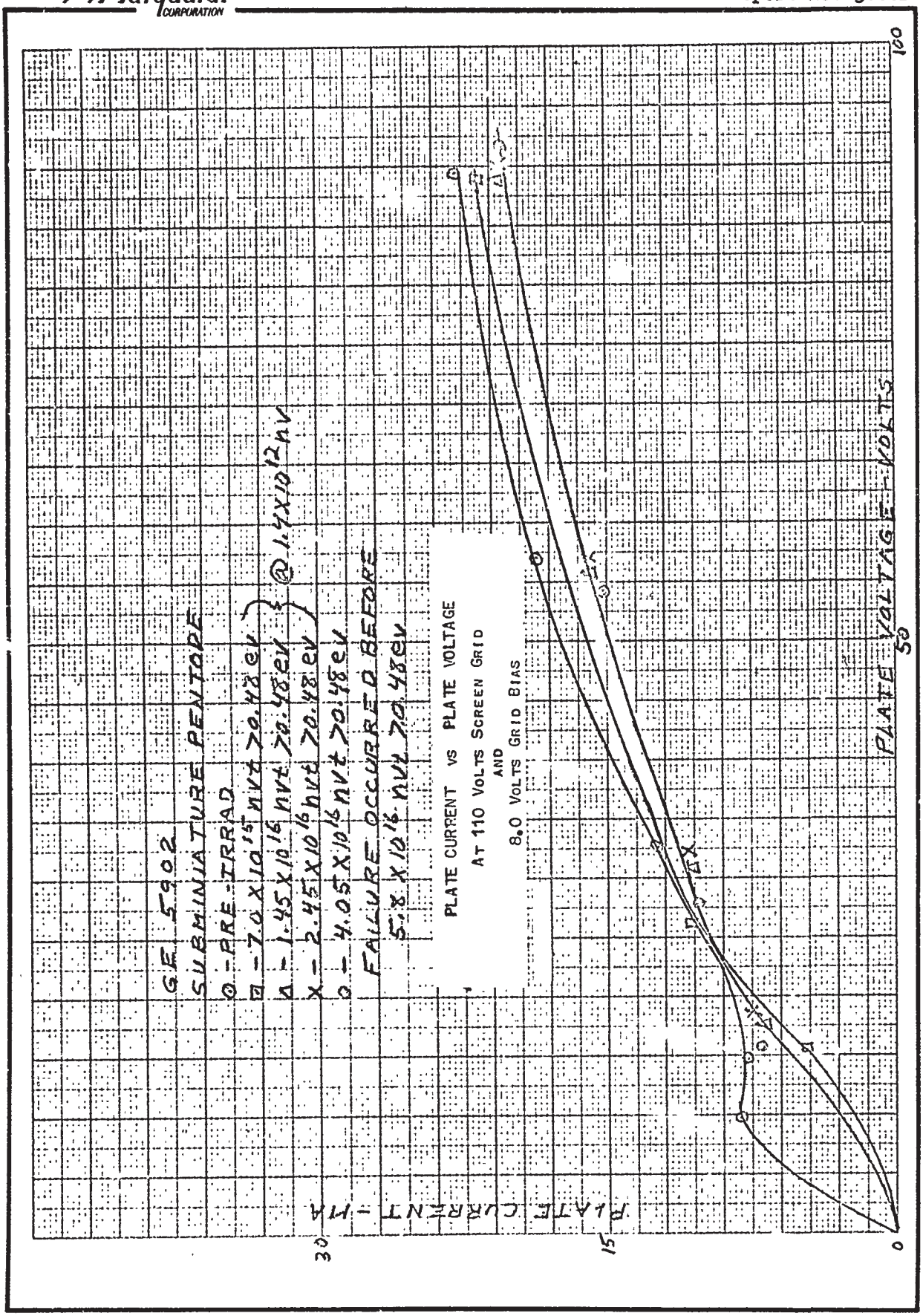

FIGURE 37

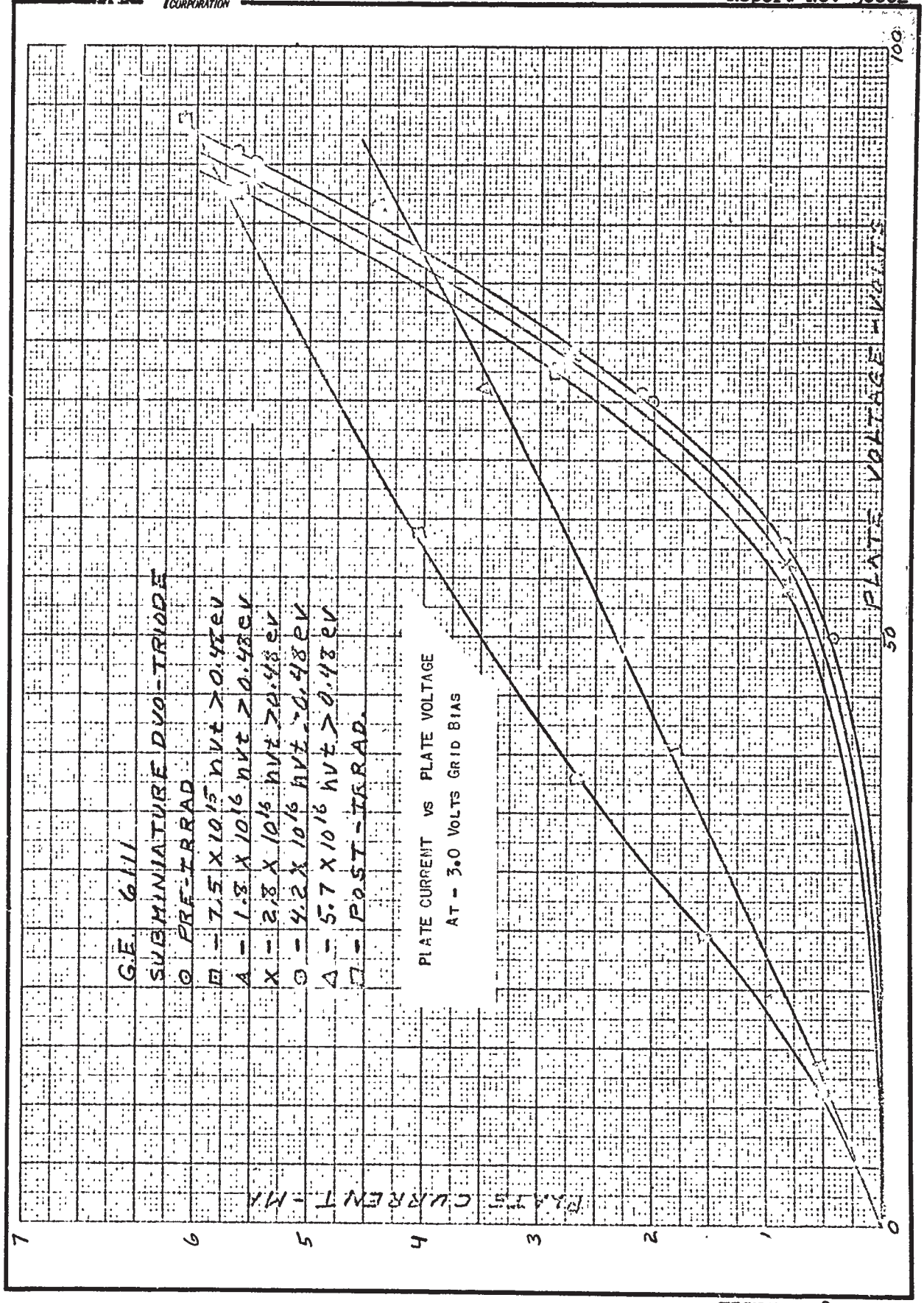

FIGURE 38

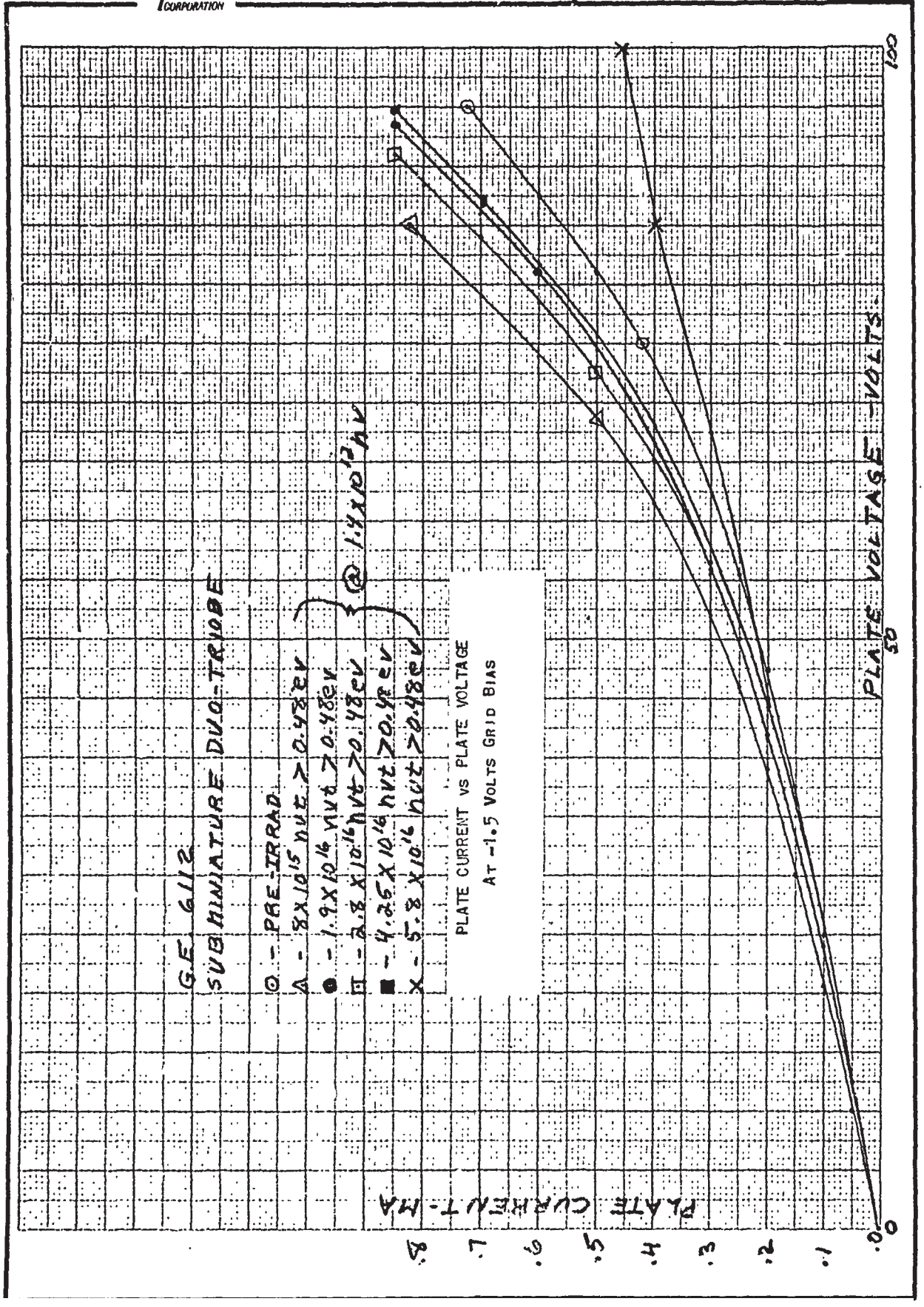

G. THERMISTORS

1. Types Tested

Two types of thermistors were tested. One was manufactured by Victory Engineering Corporation and had a negative temperature coefficient. The other was a silicon-type manufactured by Texas Instruments with a positive temperature coefficient. Specifications for each, are as follows:

Manufacturer	Type	Nominal Resistance, ohms	Temperature Coefficient Percent/°C	Maximum Temperature, °C
Texas Instruments	Silicon TM-1/4	100 ±10%	+0.7	150
VECO	21E2	100 ±10%	-3.8	125

Two samples of each type were operated at 60°C maximum temperature, in the GETR, at flux rates of 1.4×10^{12}nv (e) and exposures to 1.3×10^{17}nvt (e).

2. Results

The TM-1/4 sensistor showed a continuous increase in resistance with exposure with a final resistance of 1.2 megohms or approximately a million-fold increase, as shown in Figure 40 . There was no apparent effect of dose rate.

The VECO 21E2 thermistors showed much less change; however, readings became extremely erratic between 7.85×10^{16}nvt and 1.3×10^{17}nvt. In addition, a sharp change was observed when the dose rate was changed, as shown in Figure 41. A check of the heat transfer conditions indicates that a temperature differential of less than 1°C would result from increased nuclear heating, while the discontinuity represents an apparent temperature differential of approximately 10°C.

3. Conclusions

Neither thermistor type would be satisfactory for precise temperature measurements at the exposure levels of this test. For this temperature range and exposure, Chromel-Alumel thermocouples would be much better from the viewpoint of stability to nuclear radiation.

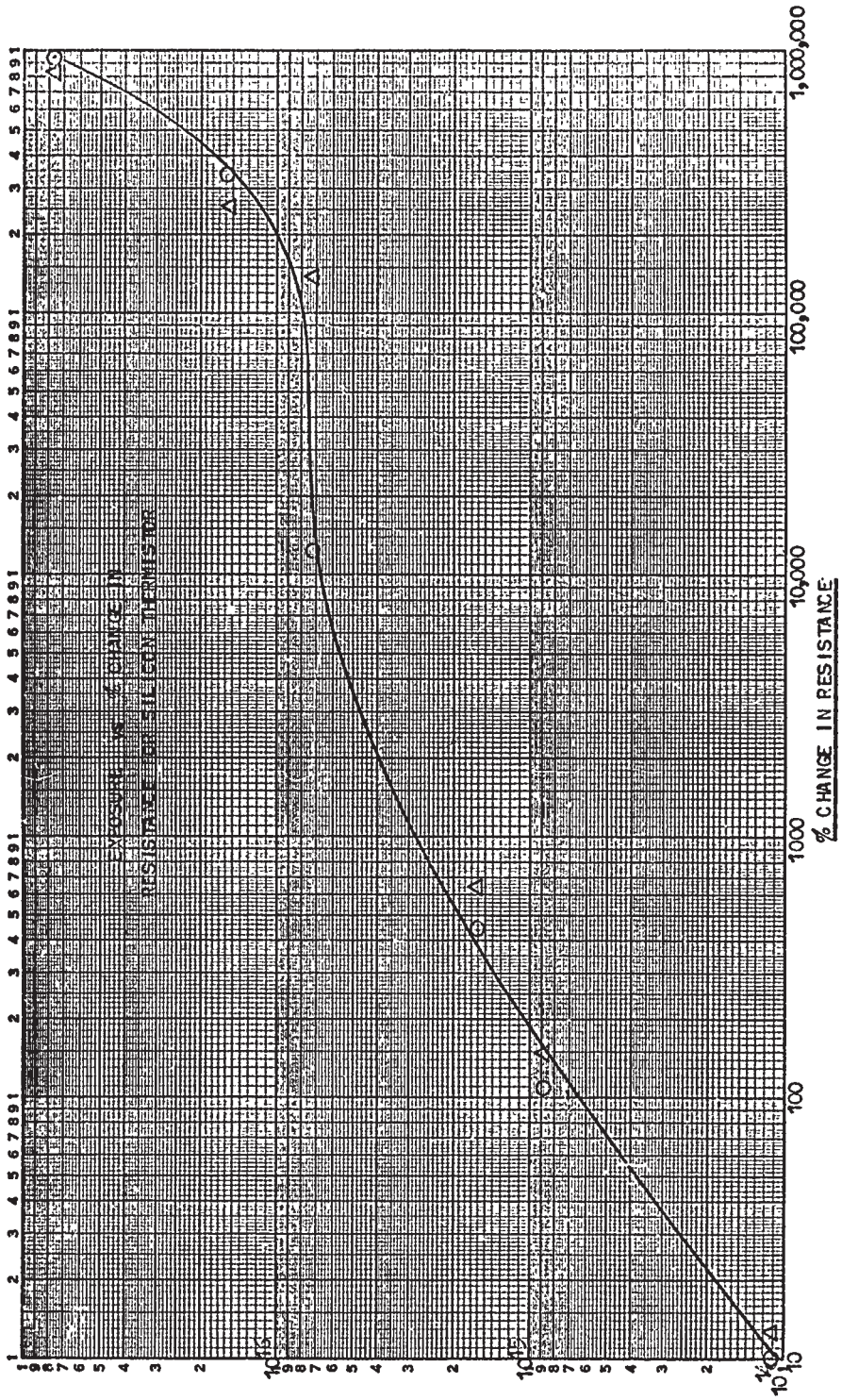

FIGURE 40

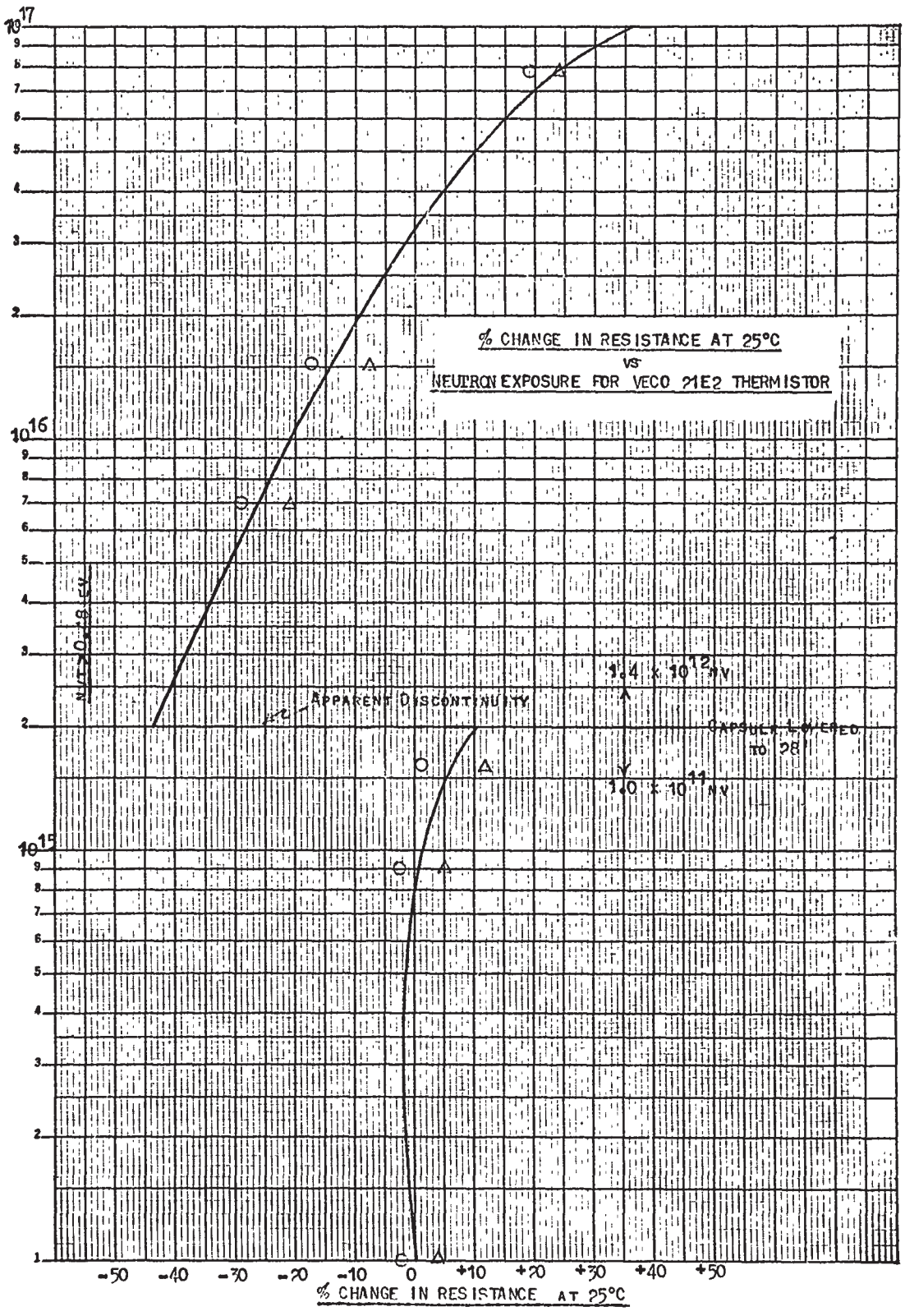

FIGURE 41

H. SUGGESTED FUTURE PROGRAMS

1. General Outline

Three important areas of radiation effects have been established by the present program. For the future, current results indicate:

a. Continuation of testing of materials and components to establish resistance to combined nuclear and high-temperature environments

b. Reliability studies and methods for pre-operational testing of components chosen as satisfactory for nuclear applications

c. Methods of modification of the temperature and nuclear environment to improve the factor of safety in the control systems

Item a. is a continuation of the tests developed to date and would include such items as:

(1.) Magnetic cores

(2.) High-temperature semiconductors

(3.) Temperature sensors

(4.) Improved infra-red sensors

(5.) Flux sensors

(6.) Any new devices or materials with applicability to reactor

(7.) Pneumatic components

Item "b" is the development of testing procedures to be included in actual specifications for operating components. The requirements are:

(a) Non-destructive tests which can be used on components and assemblies to determine their suitability for use in nuclear environments

(b) Statistical reliability tests which will give accurate reliability figures for design purposes

At present no practical method exists for meeting either of these requirements. Tests by Boeing, Cook Electric, and Admiral Corporation and others have shown that gamma irradiations can produce both transient and permanent changes in semiconductors; however, insufficient testing has been conducted to provide sufficient data to determine whether this form of testing can be used to determine ultimate reliability in any given nuclear environment. Conversely, no environment exactly duplicating the environment expected in PLUTO is available. Even were such an environment available, tests of large numbers of items from each individual batch would be required to provide good reliability data. At the present state-of-the-art for semiconductors, it might be expected to test 10 items for each item used. Thus, for a system with 10 diodes, irradiations would be required on 100 diodes of the same type from the same manufacturing batch.

Therefore, it is suggested Items A and B be combined to determine if performing gamma irradiations on 100 components, followed by neutron irradiation of a portion of those components which have proven satisfactory to a given level of gamma irradiation, can be used as a method of providing reliability statistics in the least expensive manner.

Item c. involves the philosophy of tailoring the environments to utilize existing proven components and is concerned primarily with the design and testing of shielding systems to reduce nuclear effects. This requires that actual systems be tested in an environment as similar as possible to that expected in PLUTO applications to determine if the shielding will produce the desired results and whether gamma heating problems can be overcome practically. One of the major problems is that high efficiency neutron shields have a tendency to harden the neutron spectrum, i.e., increase the average neutron energy. If neutron damage is a function of the energy flux rather than particle flux, the possibility then exists that the actual shield efficiency is less than calculated. The information presently available on semiconductors is far from complete on the effect of neutron energy on damage at the higher energy levels.

2. Specific Items To Be Tested During the Next Contract Period

a. Temperature Sensors

(1). Thermocouple Sensors

It is imperative that selected thermocouple materials (iridium/iridium-rhodium etc.) be tested under simultaneous high temperatures and fast neutron flux conditions to simulate the expected environment in the PLUTO reactor.

Measurements of these environments would consist of calibration, reproducibility, aging, and drift characteristics using a reference standard platinum versus platinum-rhodium thermocouple for comparison.

2. Thermocouple Insulators and Protection Tubes

Available data show a substantial reduction in resistance of such insulators as alumina, magnesia, beryllia, and thoria with increased temperature and nuclear irradiation. It is imperative to procure practical configurations of these insulators and protection tubes in the various materials Tests would be conducted under high temperature and nuclear irradiation conditions to measure resistance as a function of temperature and integrated flux, change in resistance with time (aging), and life.

3. Infra-red Sensors

Specifications on high-temperature, nuclear-resistant infra-red detectors were established during the present program; however, funds were not available for procuring sample units. These specifications should be re-issued during the coming contract period and efforts made to procure the most promising units for in-pile tests.

Effort should be directed toward improving the infra-red radiometer from the standpoint of high temperature and nuclear irradiation environments. The best approach to this effort would be directed toward improved infra-red detectors, optical systems, and electronic amplifier components.

4. Other Temperature Sensors

Pending results of the current investigation of resistance type and non-metallic type of thermocouples, the study should be extended to measure the effects of nuclear irradiation on these sensors.

b. Electronic Components

The irradiation of newly developed high-temperature and nuclear irradiation-resistant components like semiconductor diodes, transistors thermistors, tubes, and etc. should be continued to enable selection of most promising components for the control system. In addition to individual component irradiation, certain basic circuits should be irradiated to develop radiation tolerant circuits using radiation limited components. This may be accomplished by several methods. For example, two similar semiconductors may be used so that the deterioration in one is compensated by active feedback from the other.

APPENDIX A: Semiconductor Diode Curves

INDEX TO CURVES OF IRRADIATED SEMICONDUCTOR DIODES

Diodes Irradiated in Test No. 1

Diodes Irradiated in Test No. 2

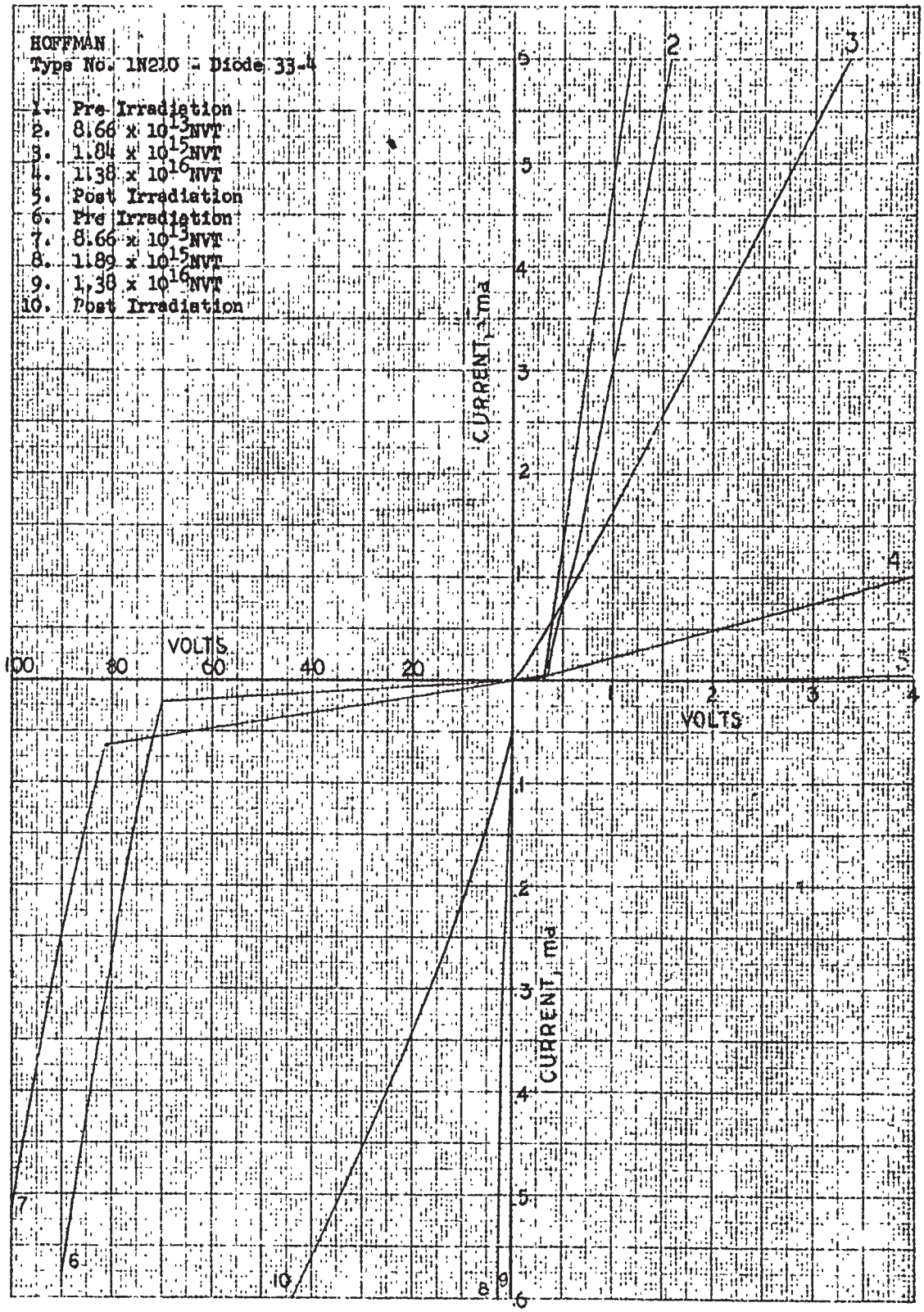

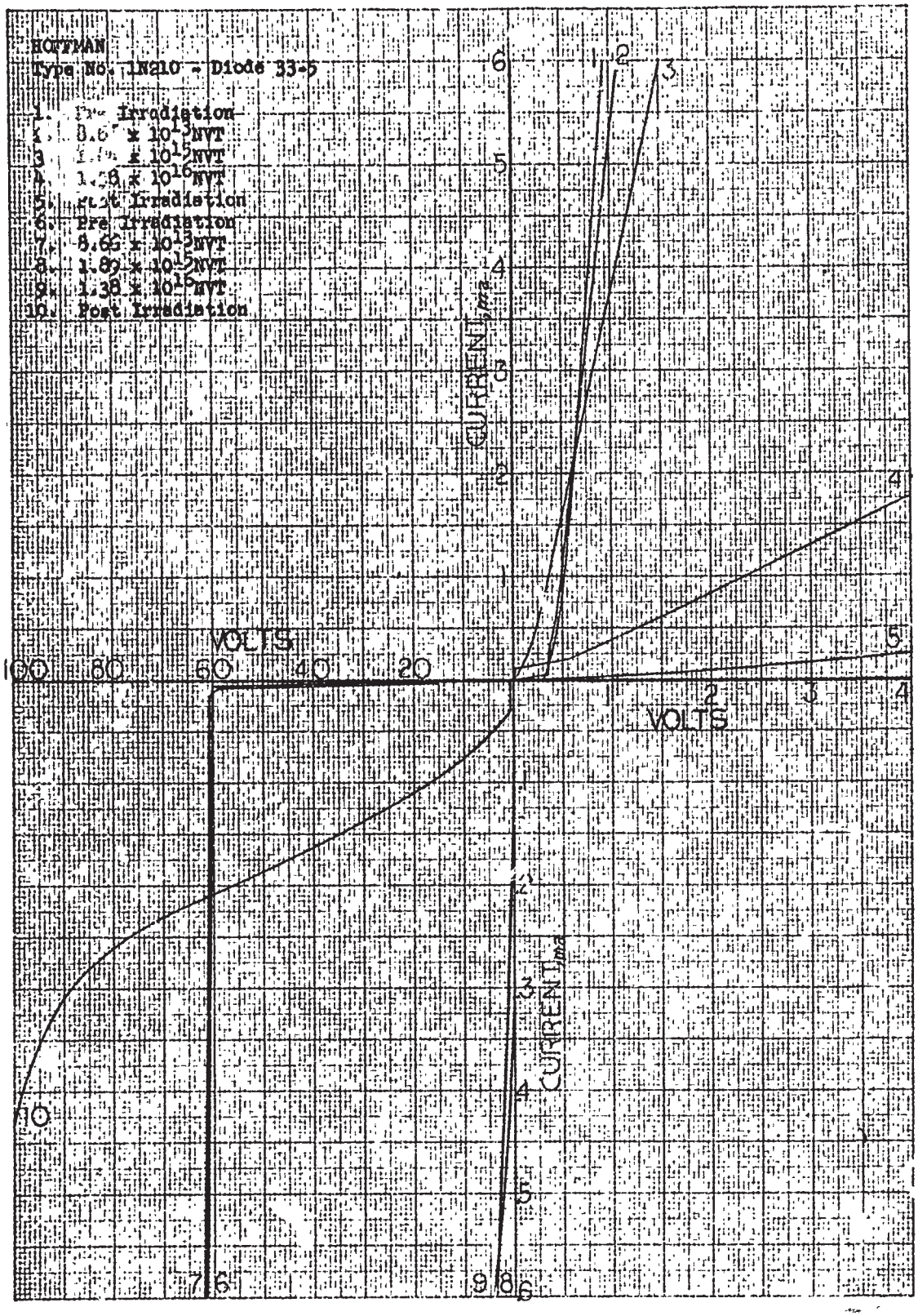

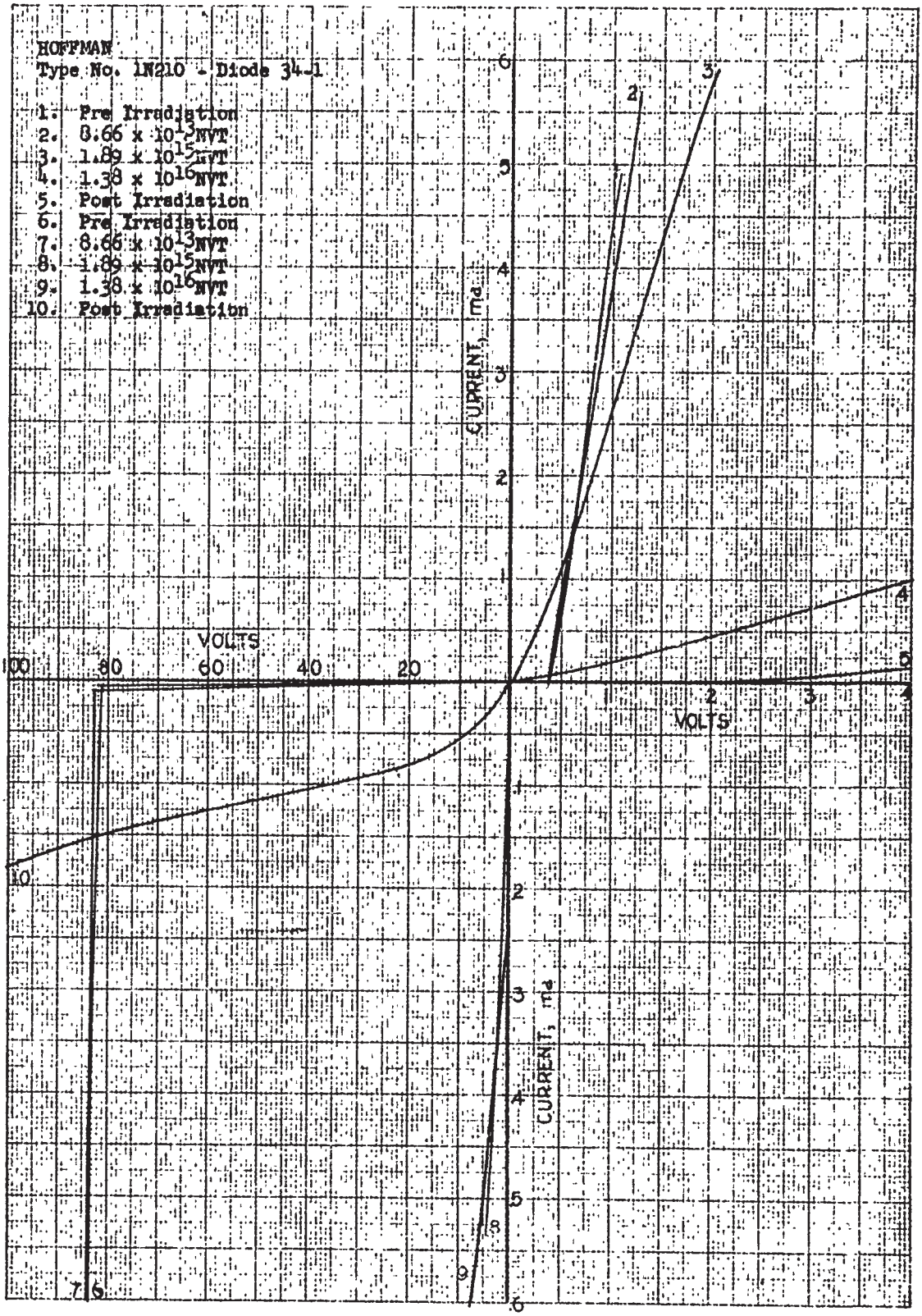

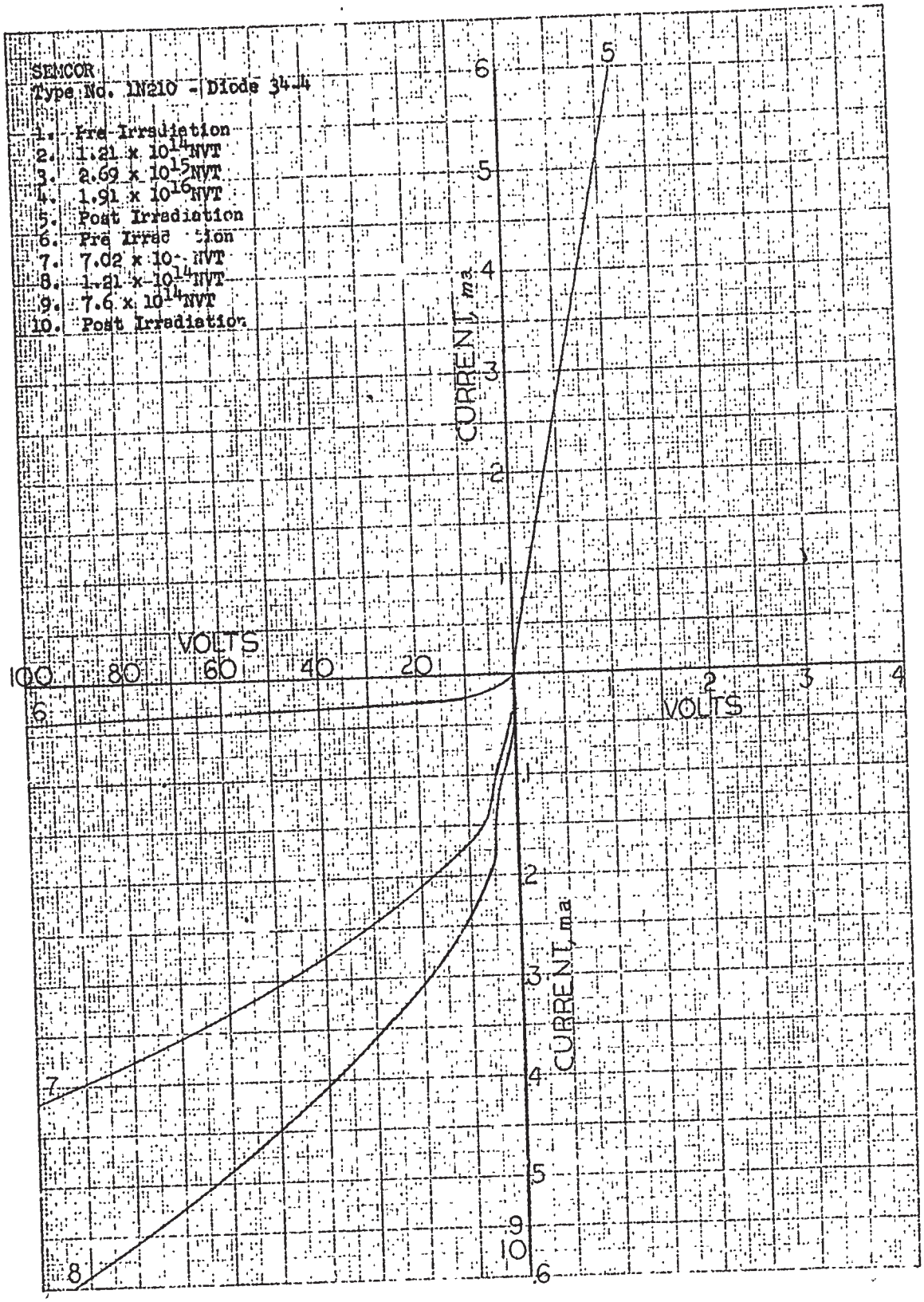

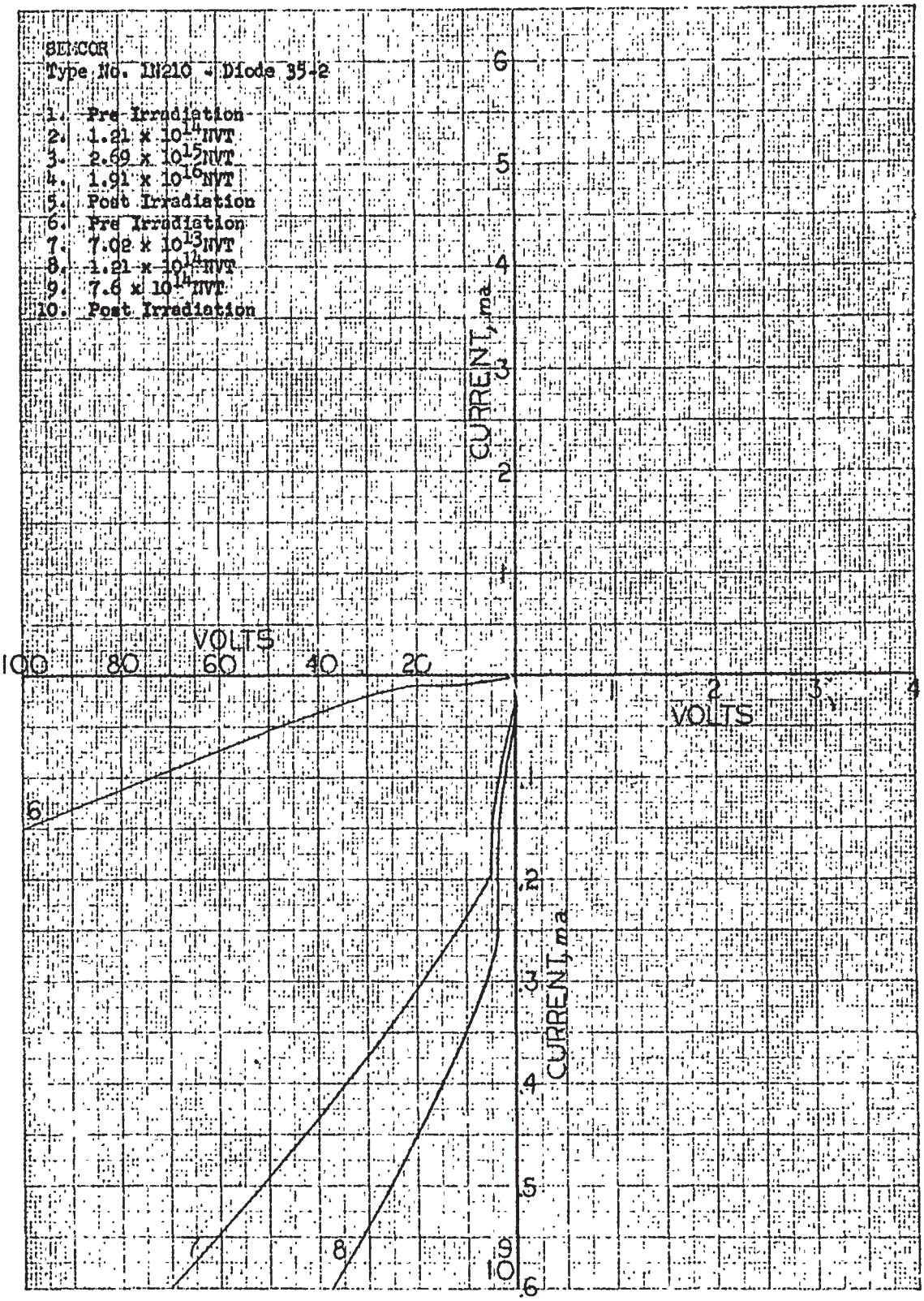

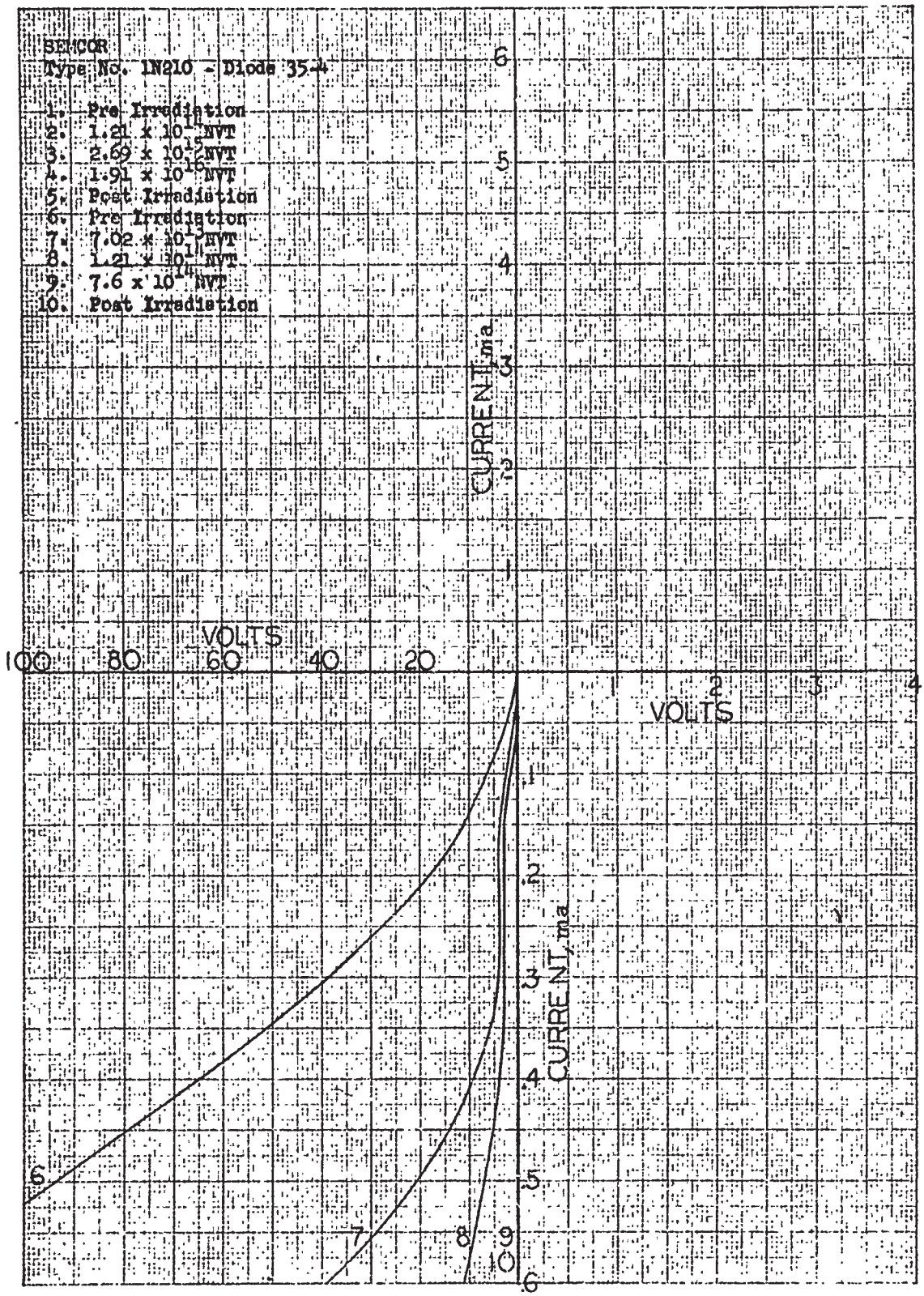

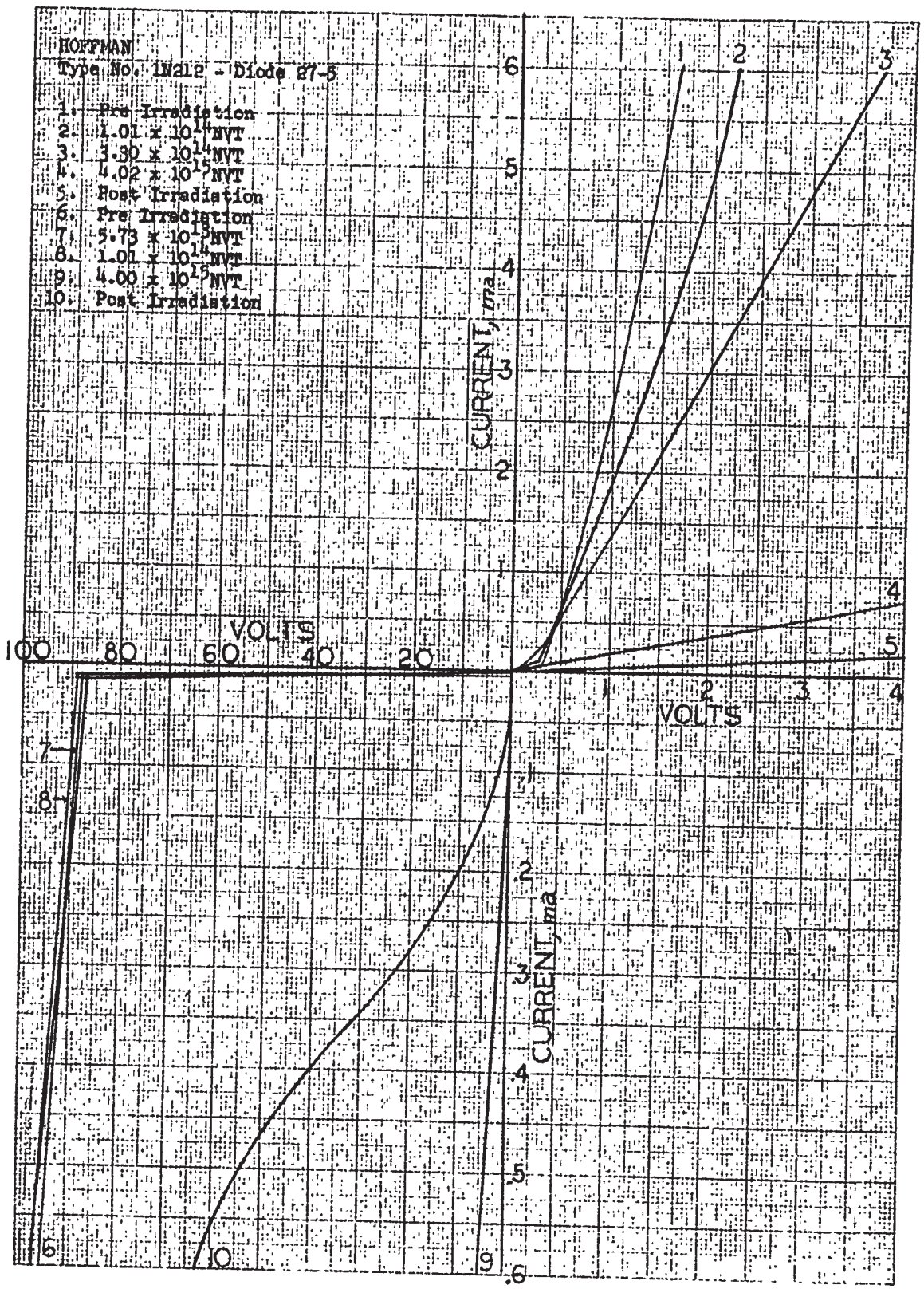

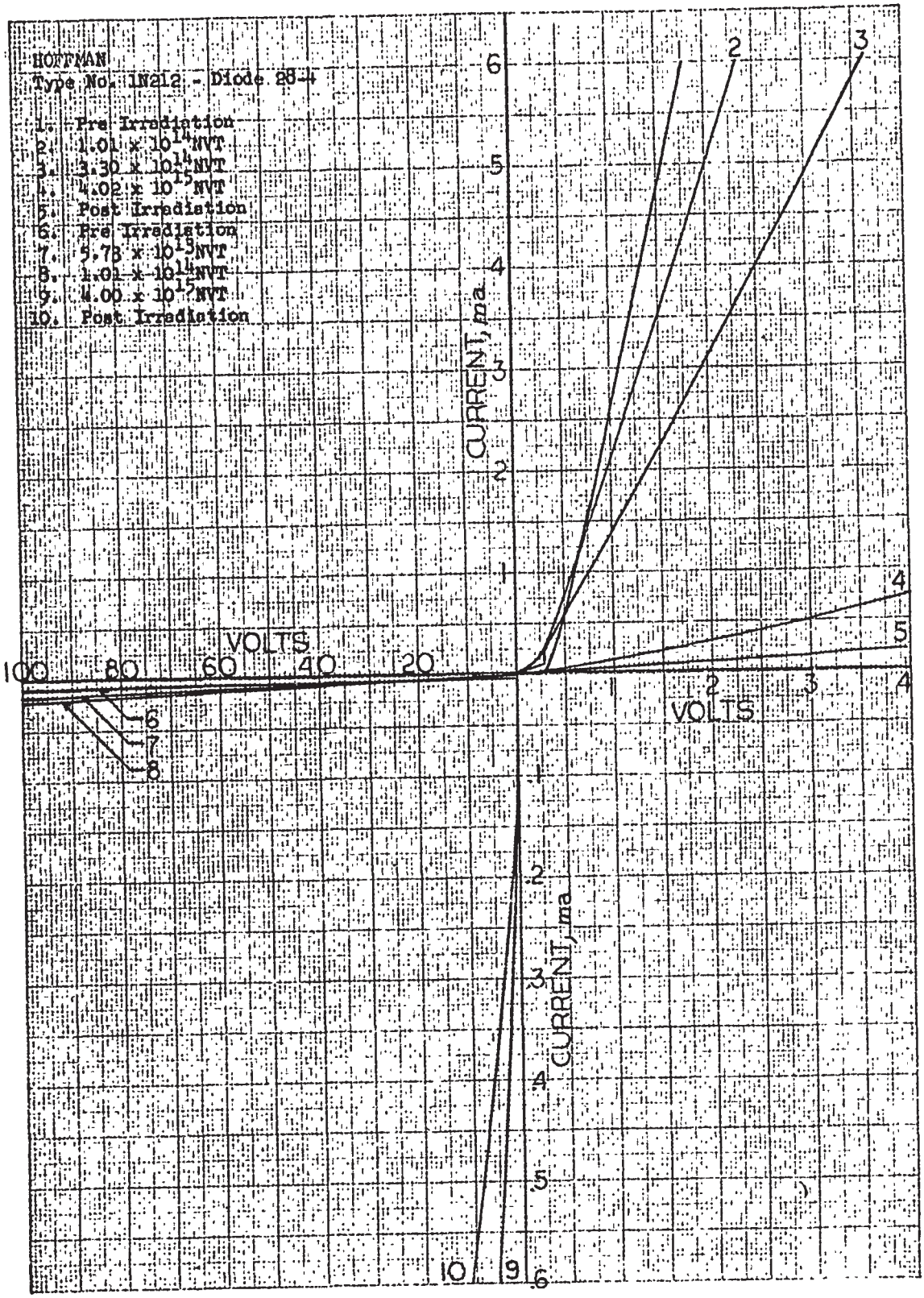

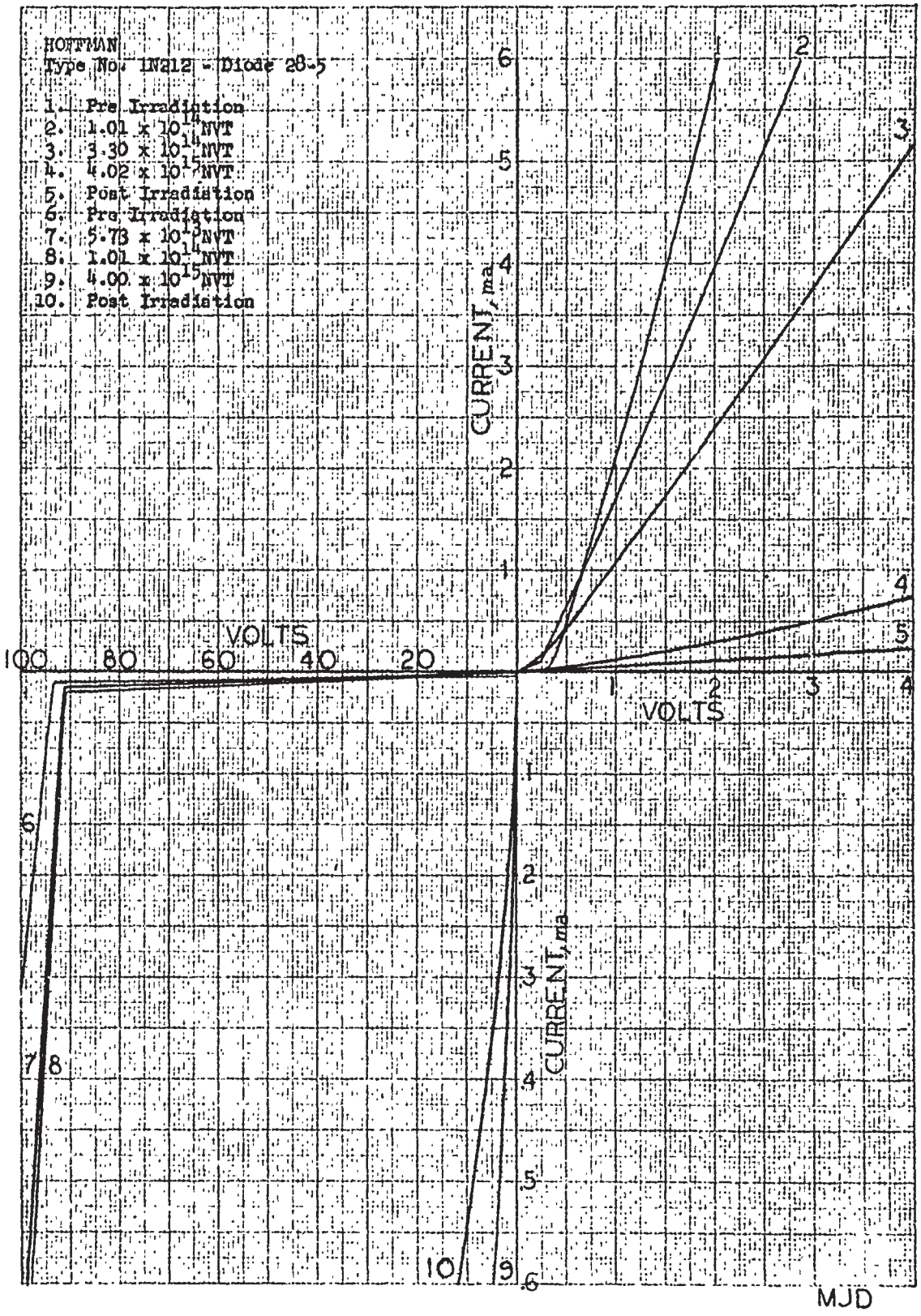

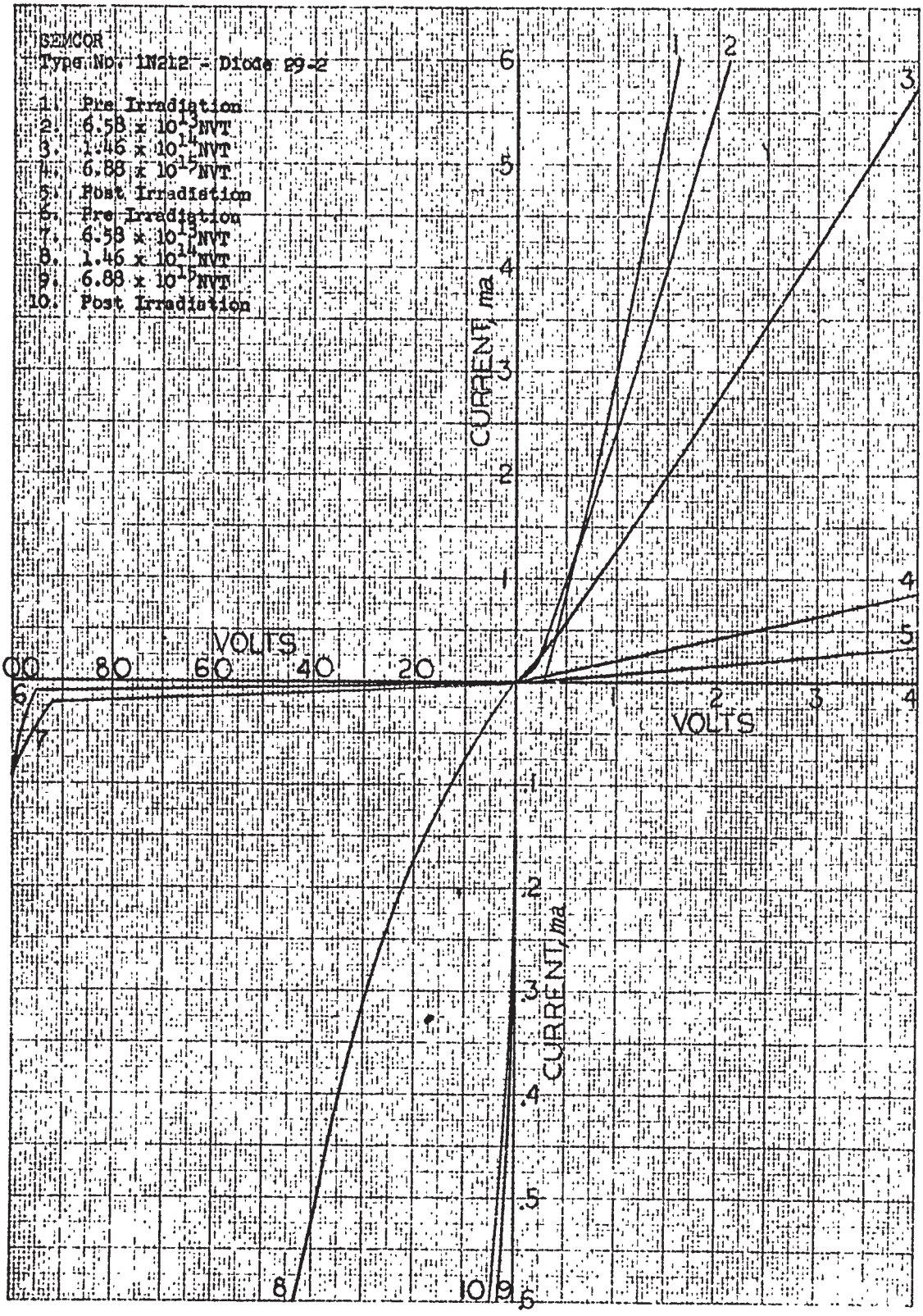

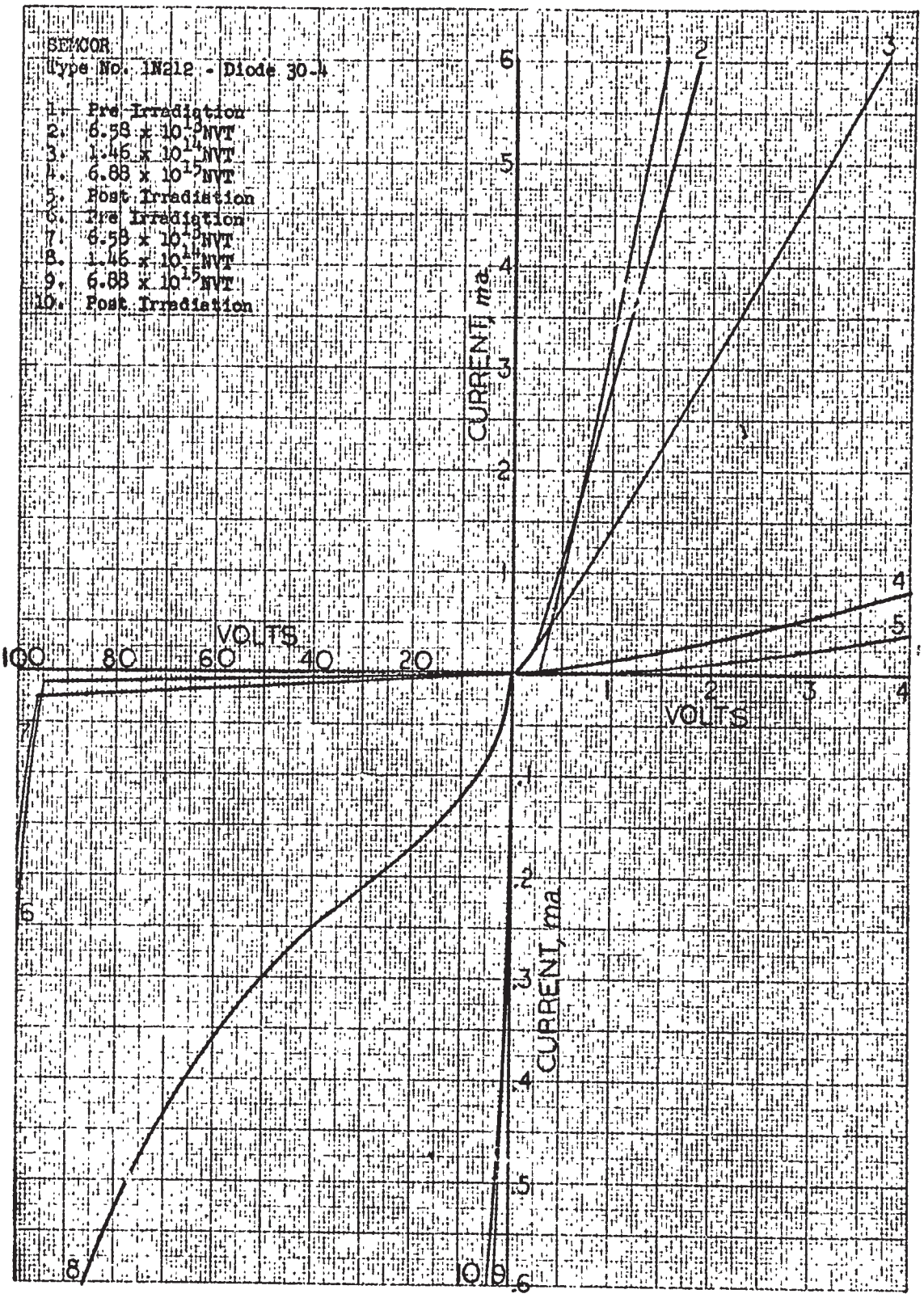

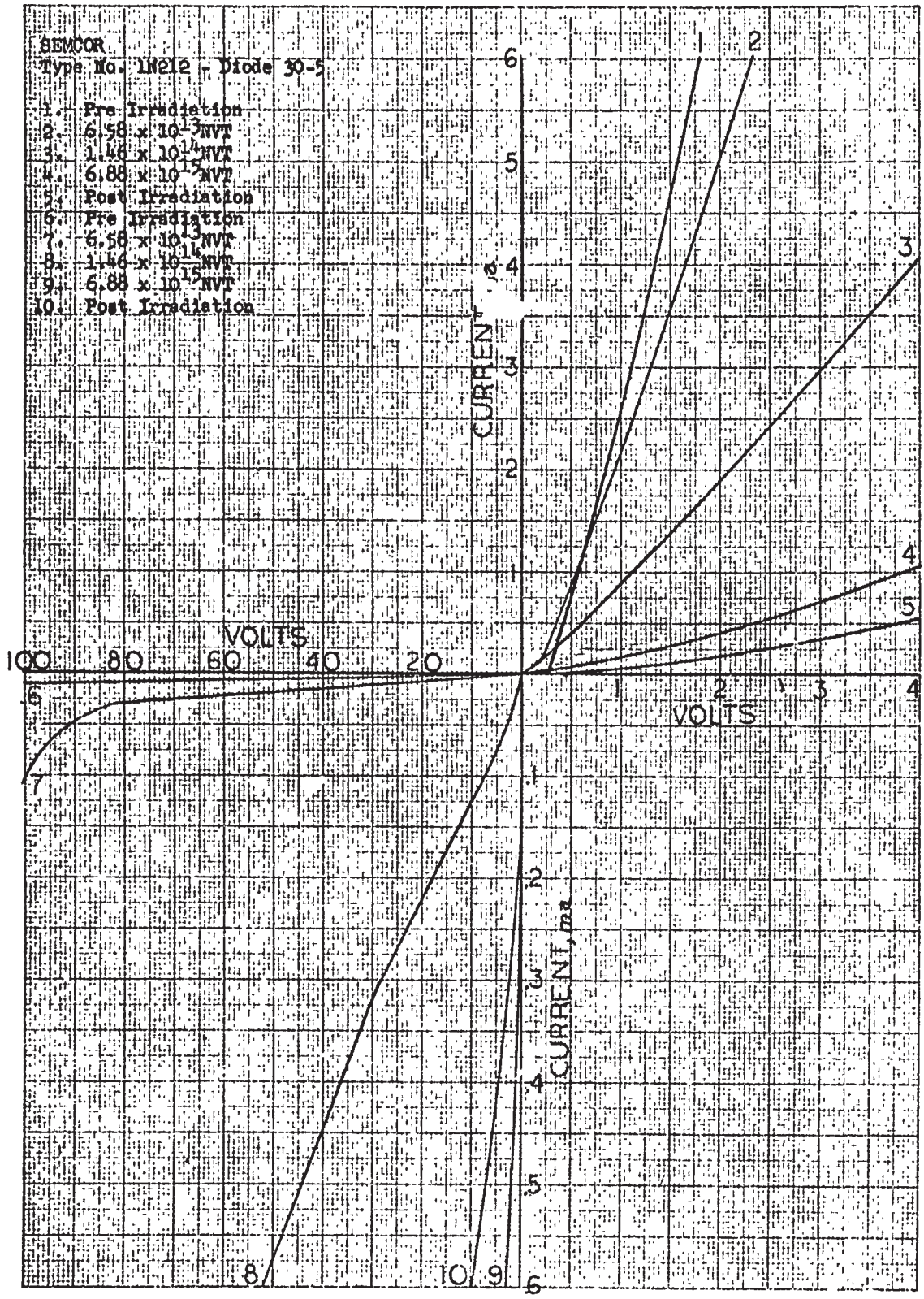

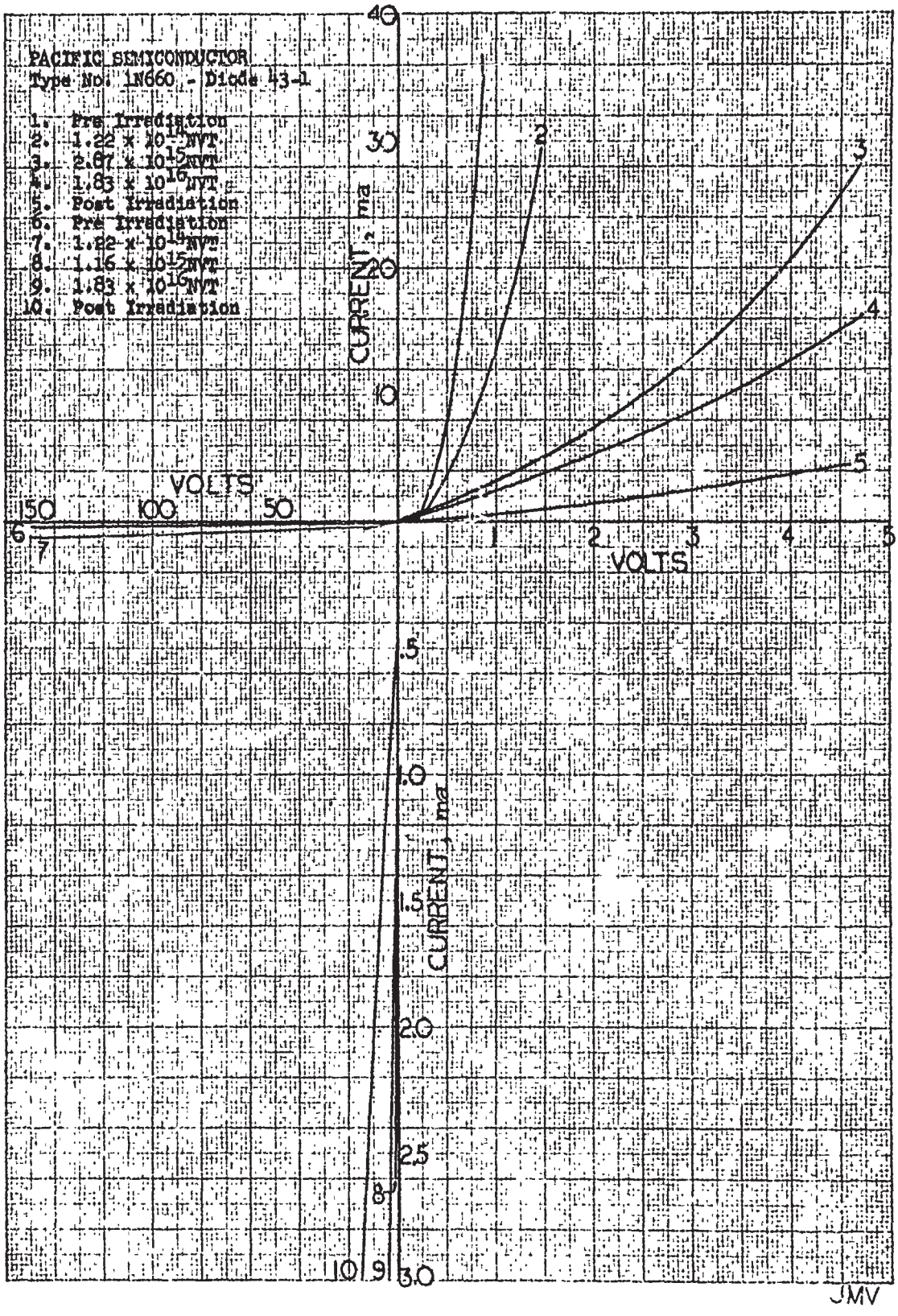

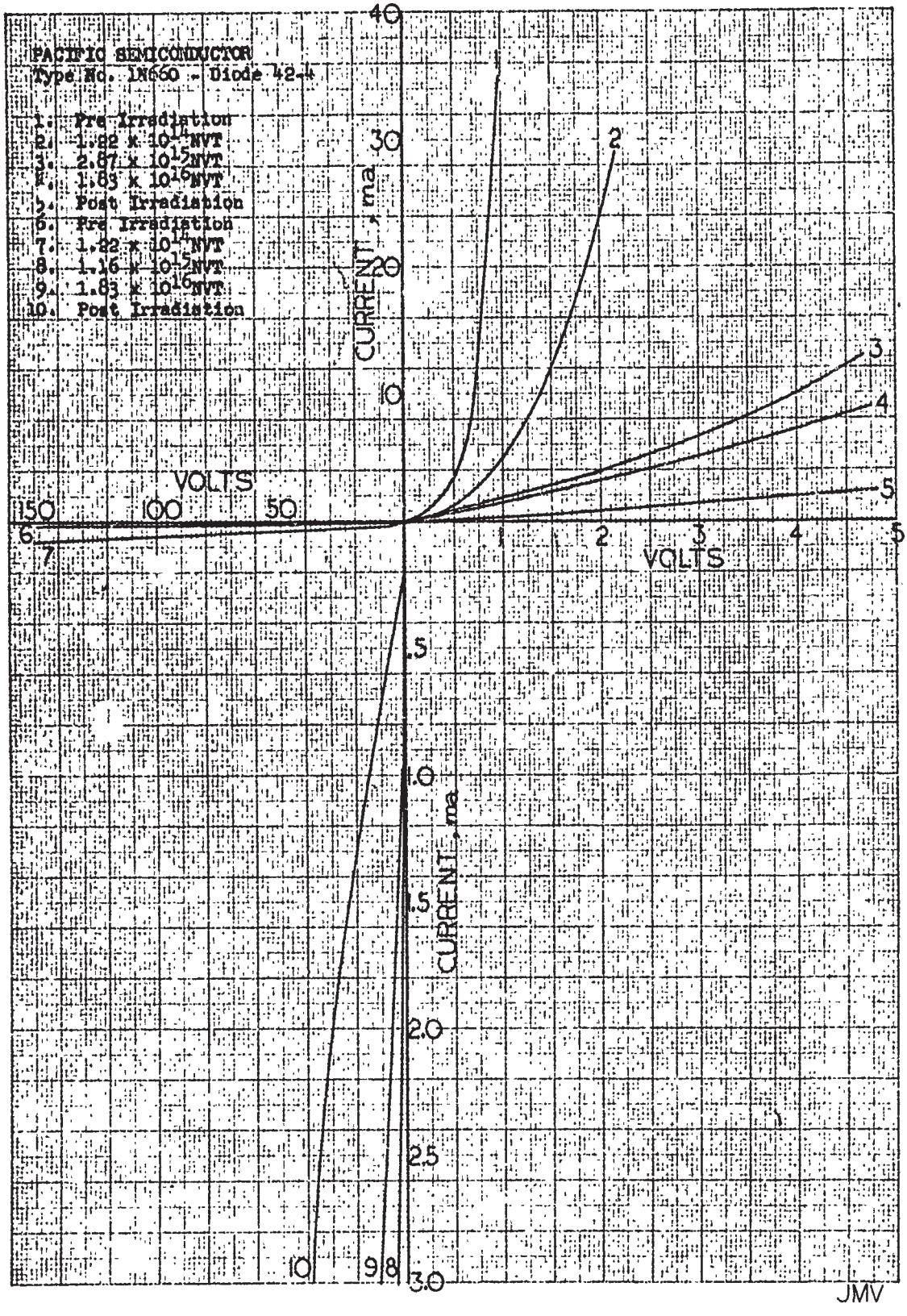

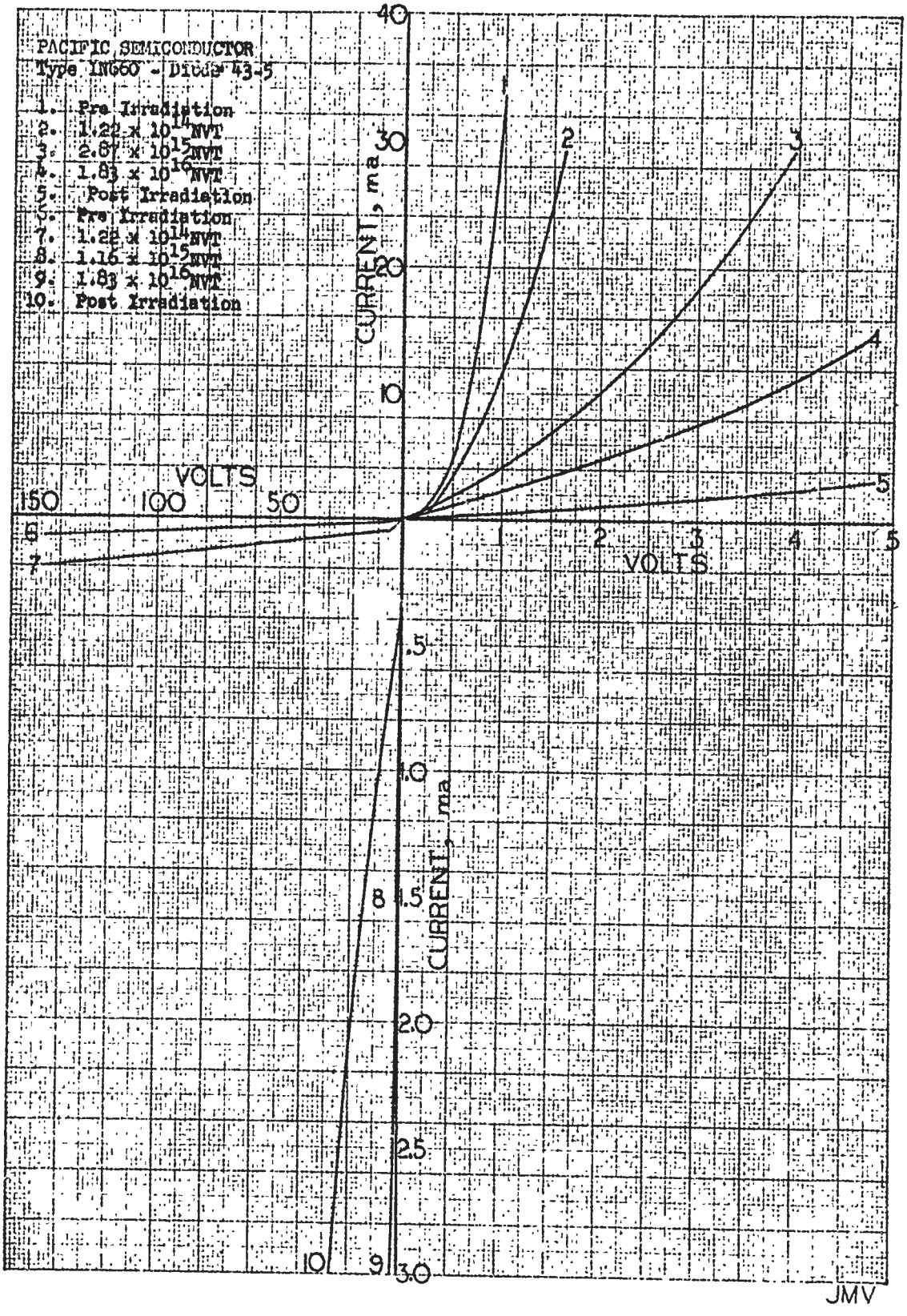

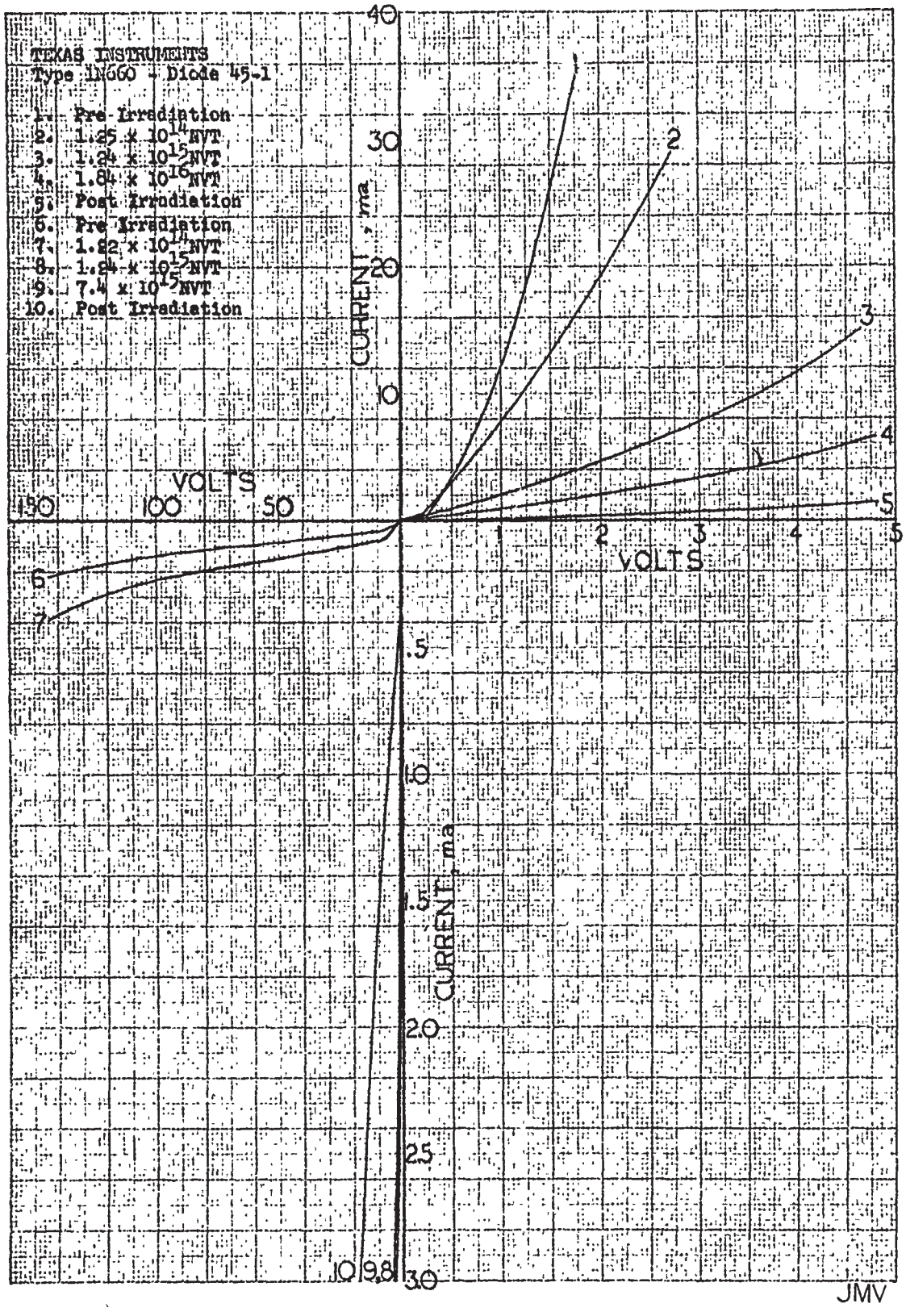

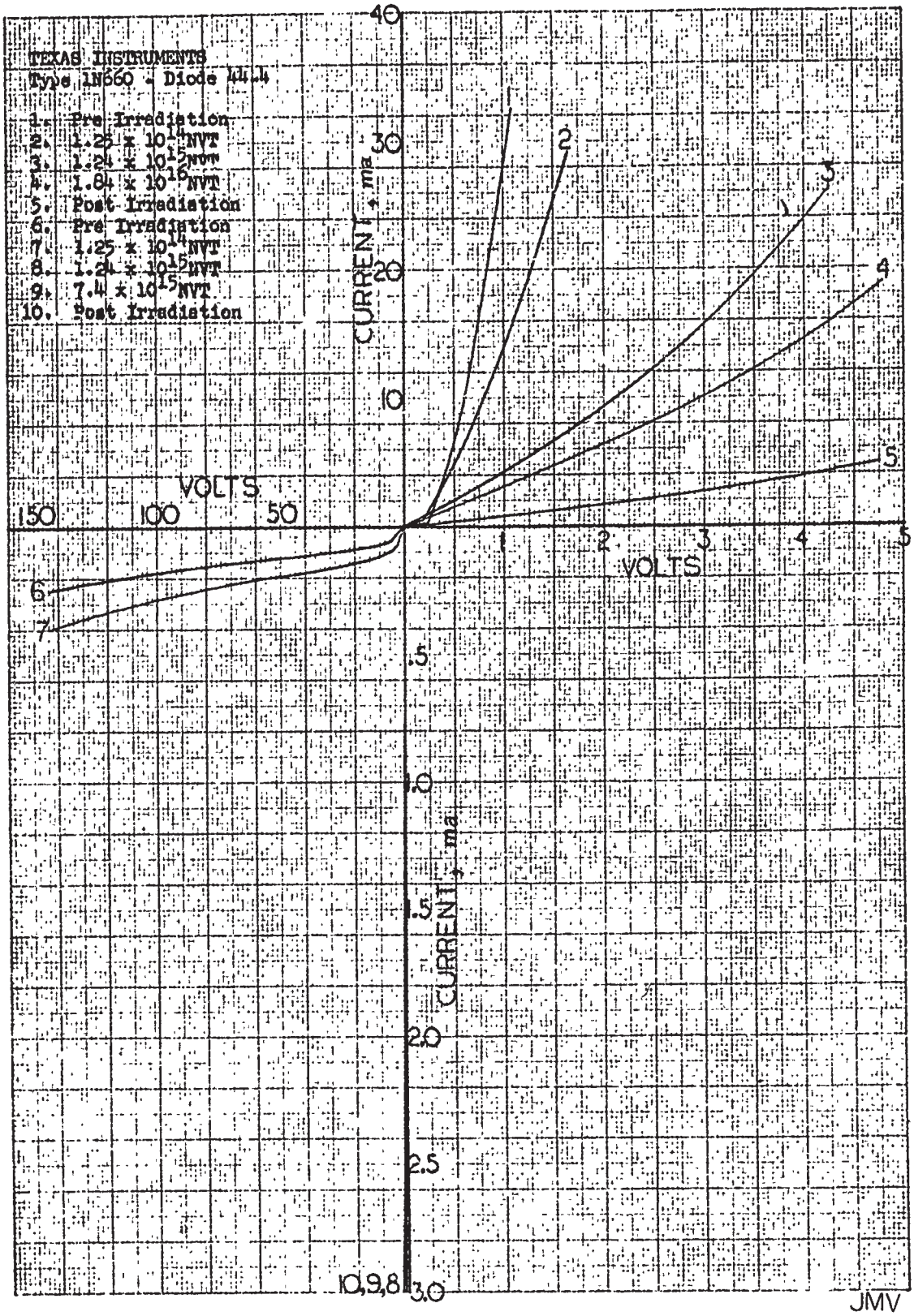

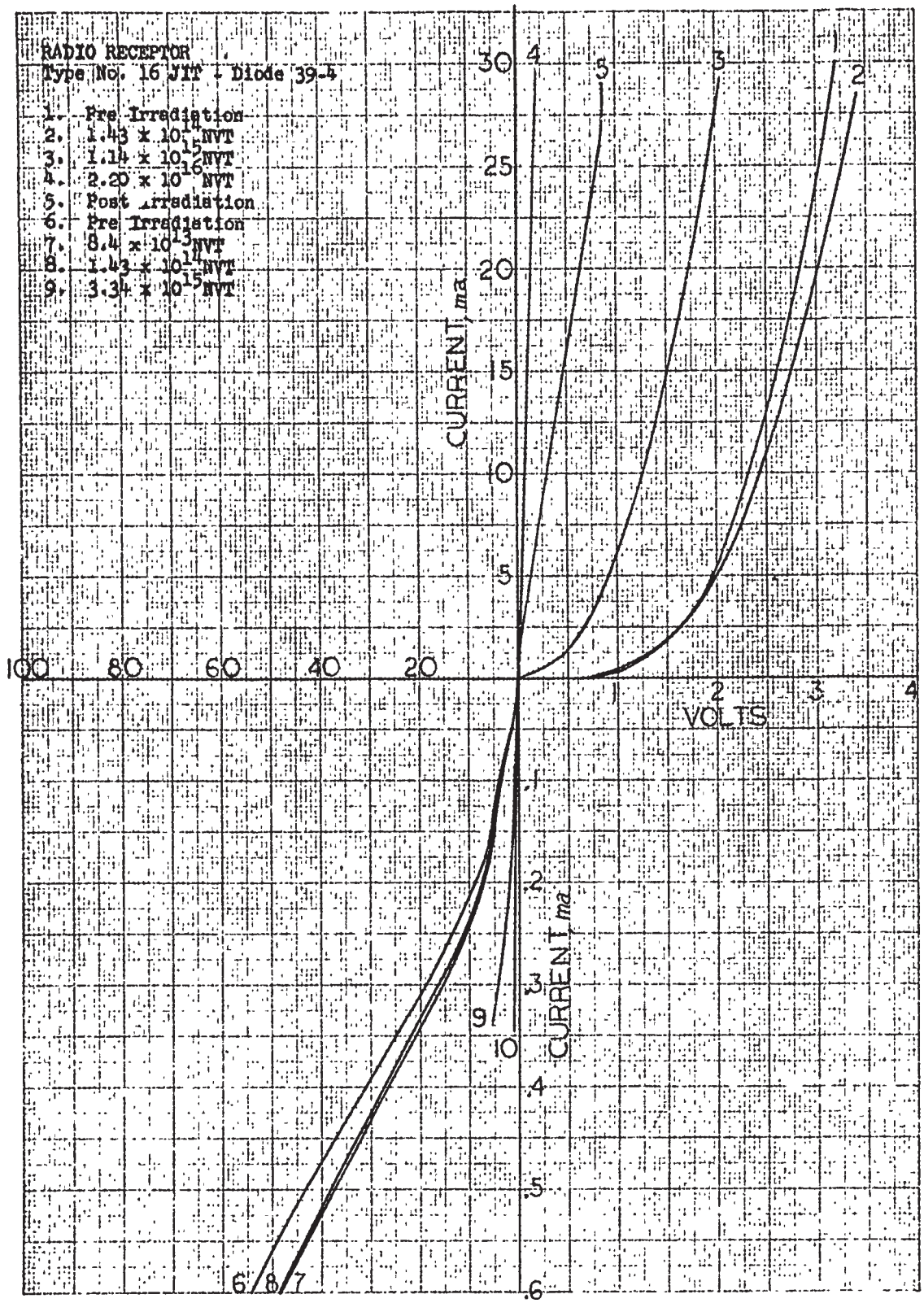

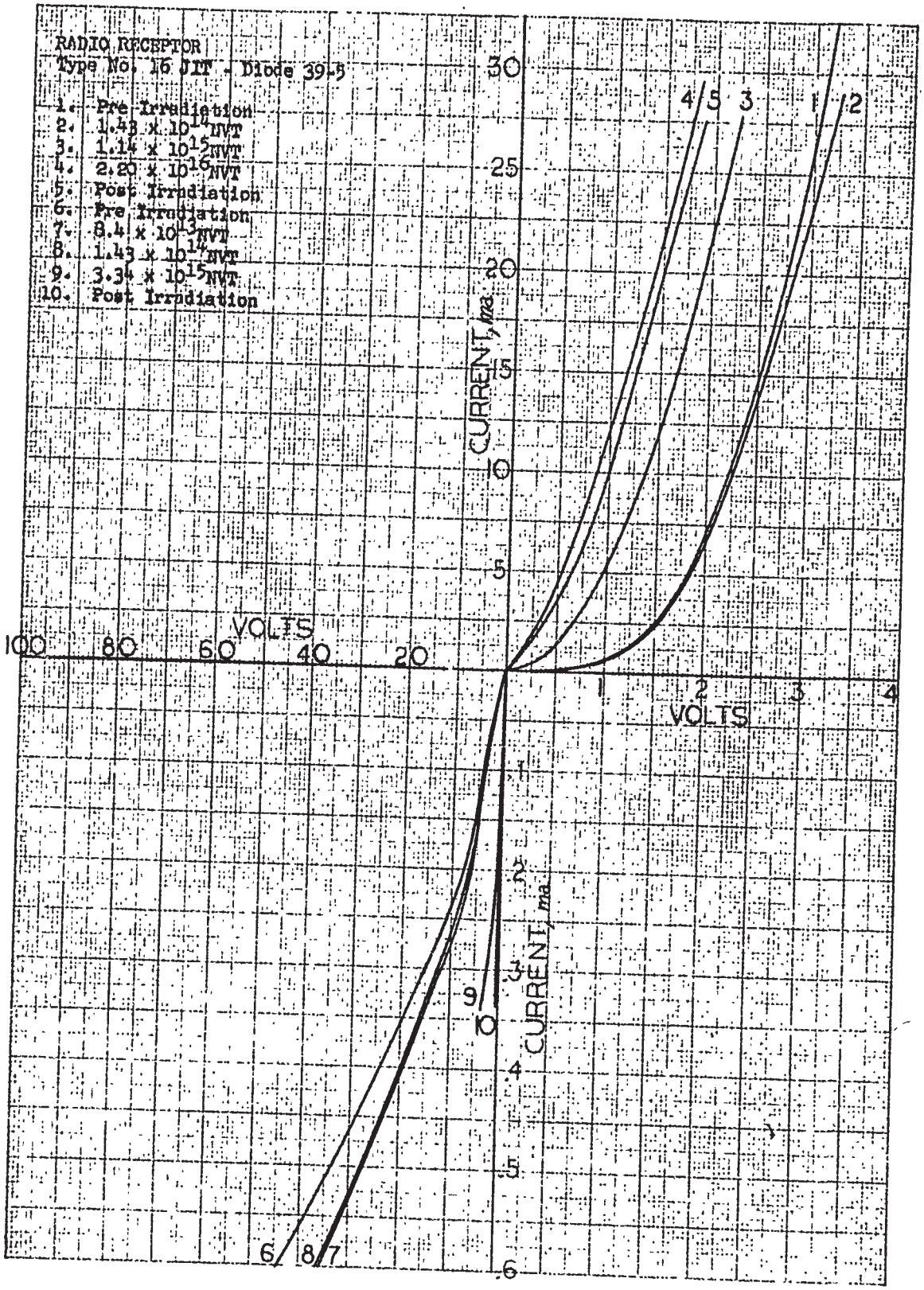

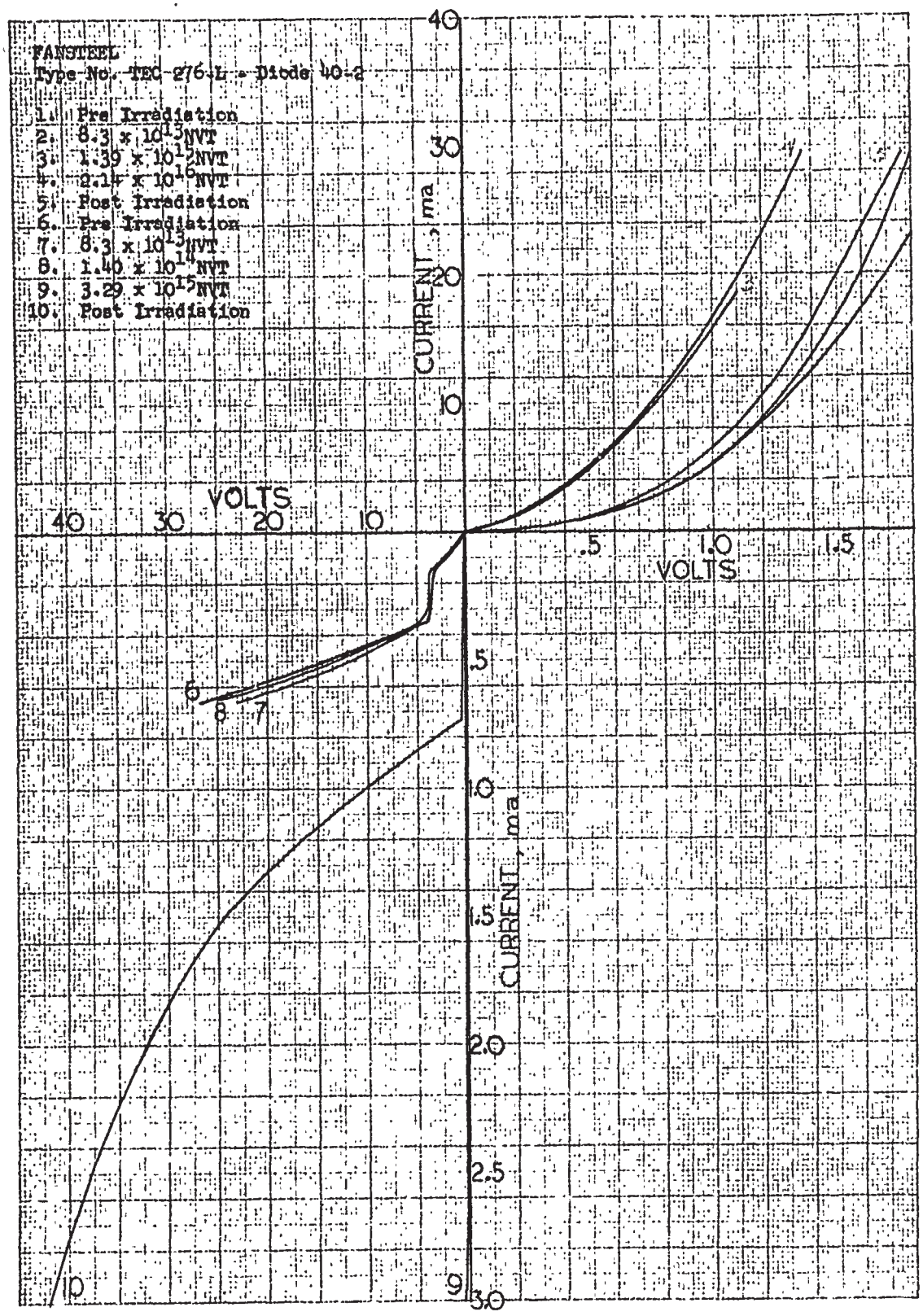

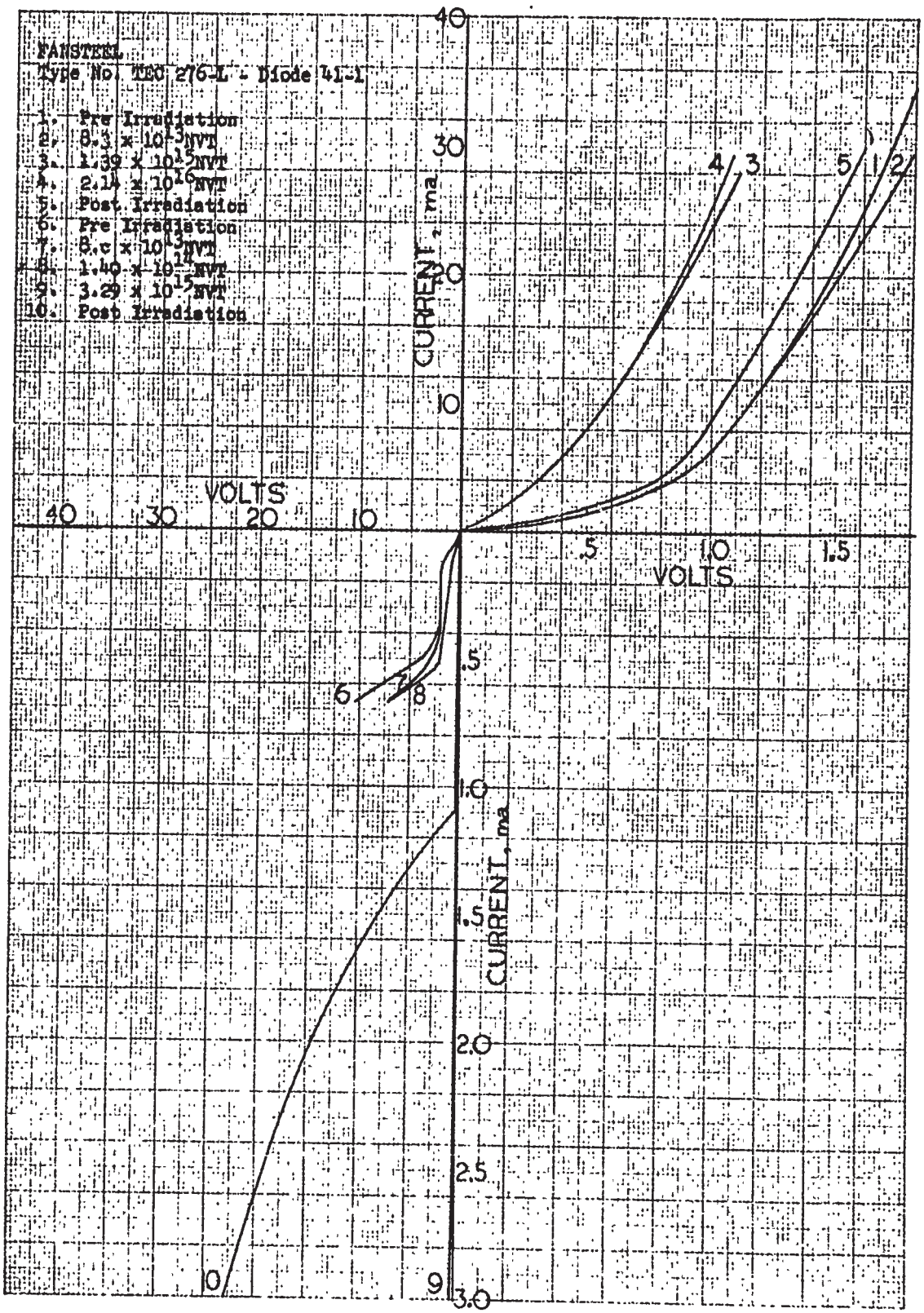

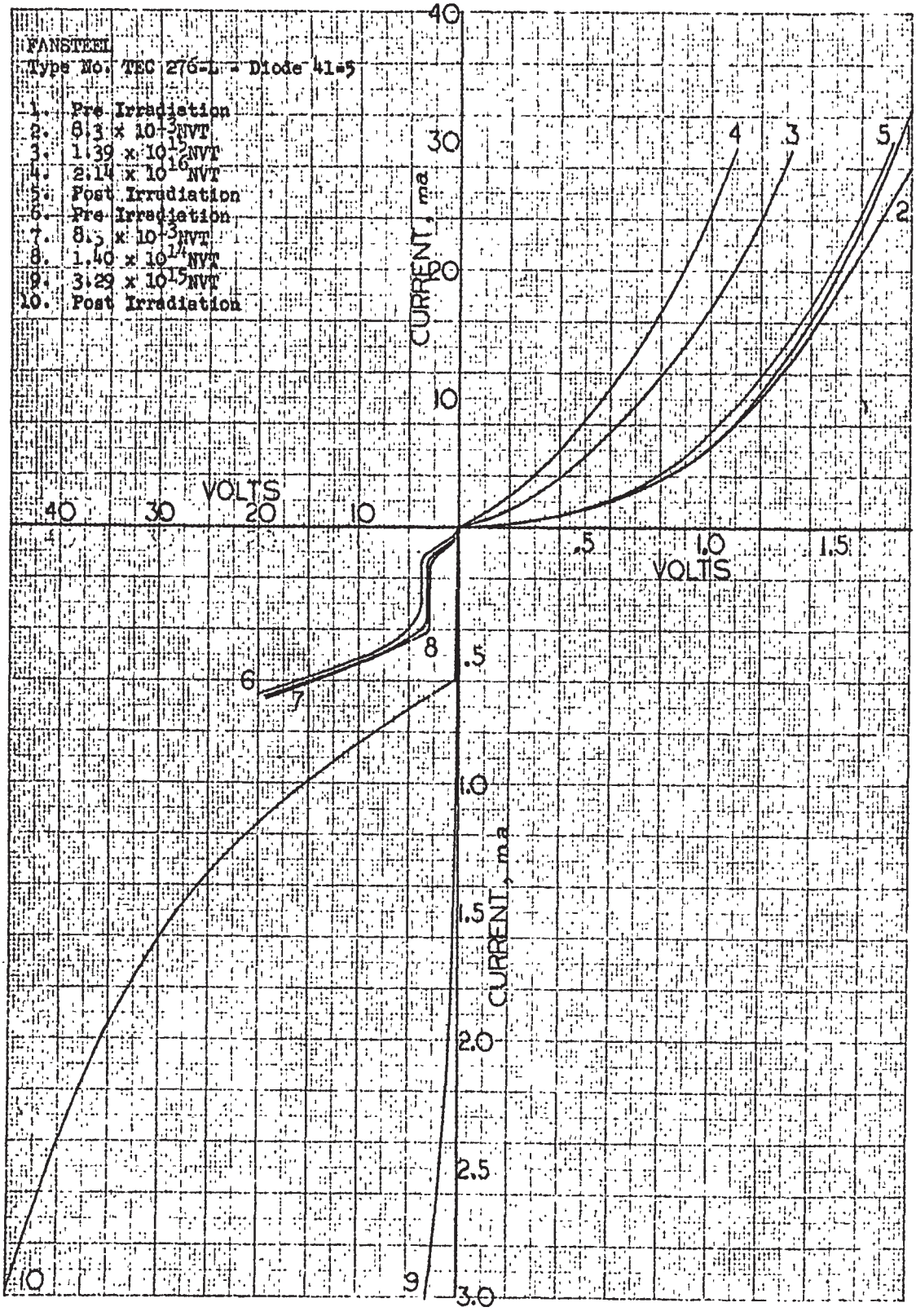

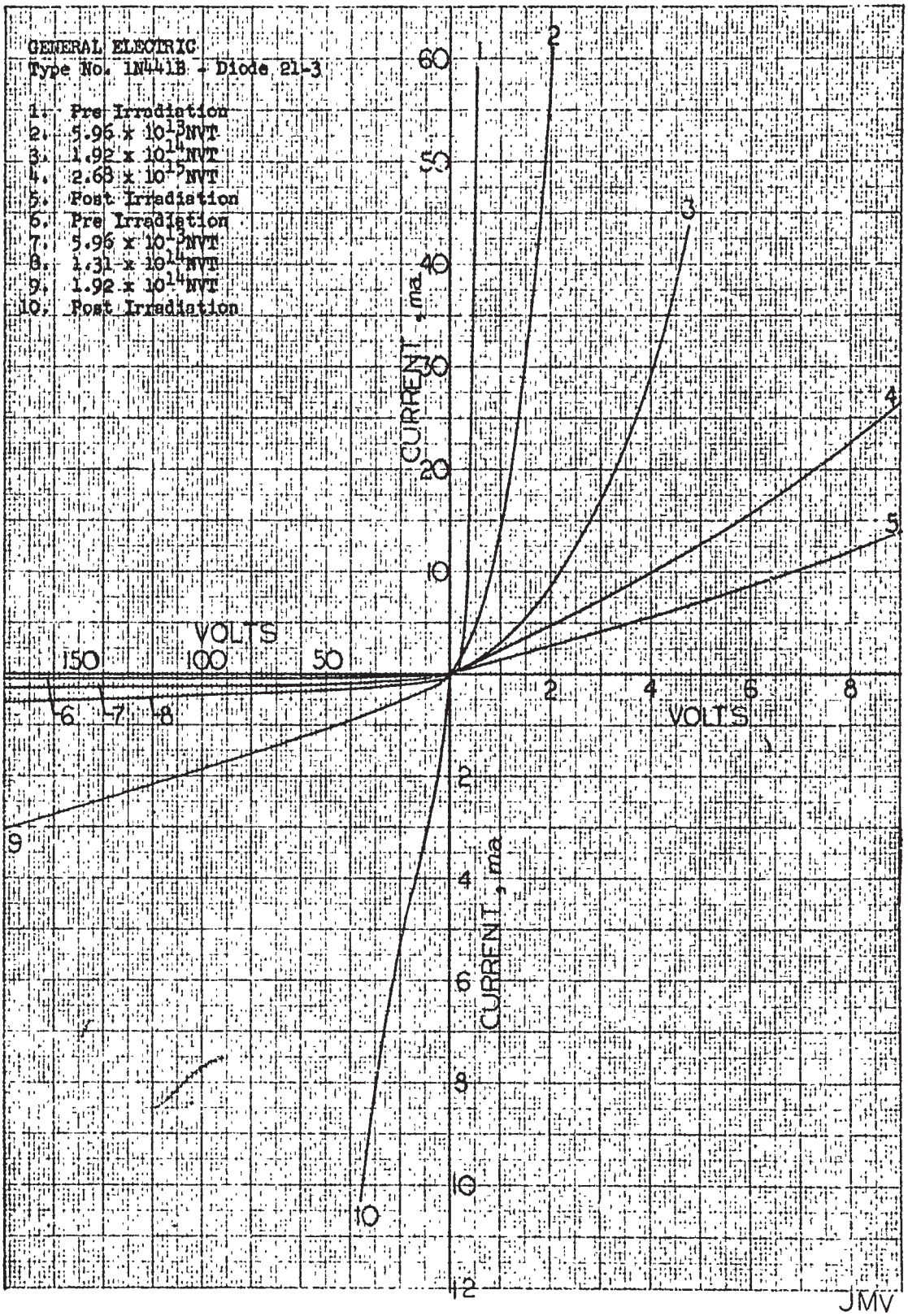

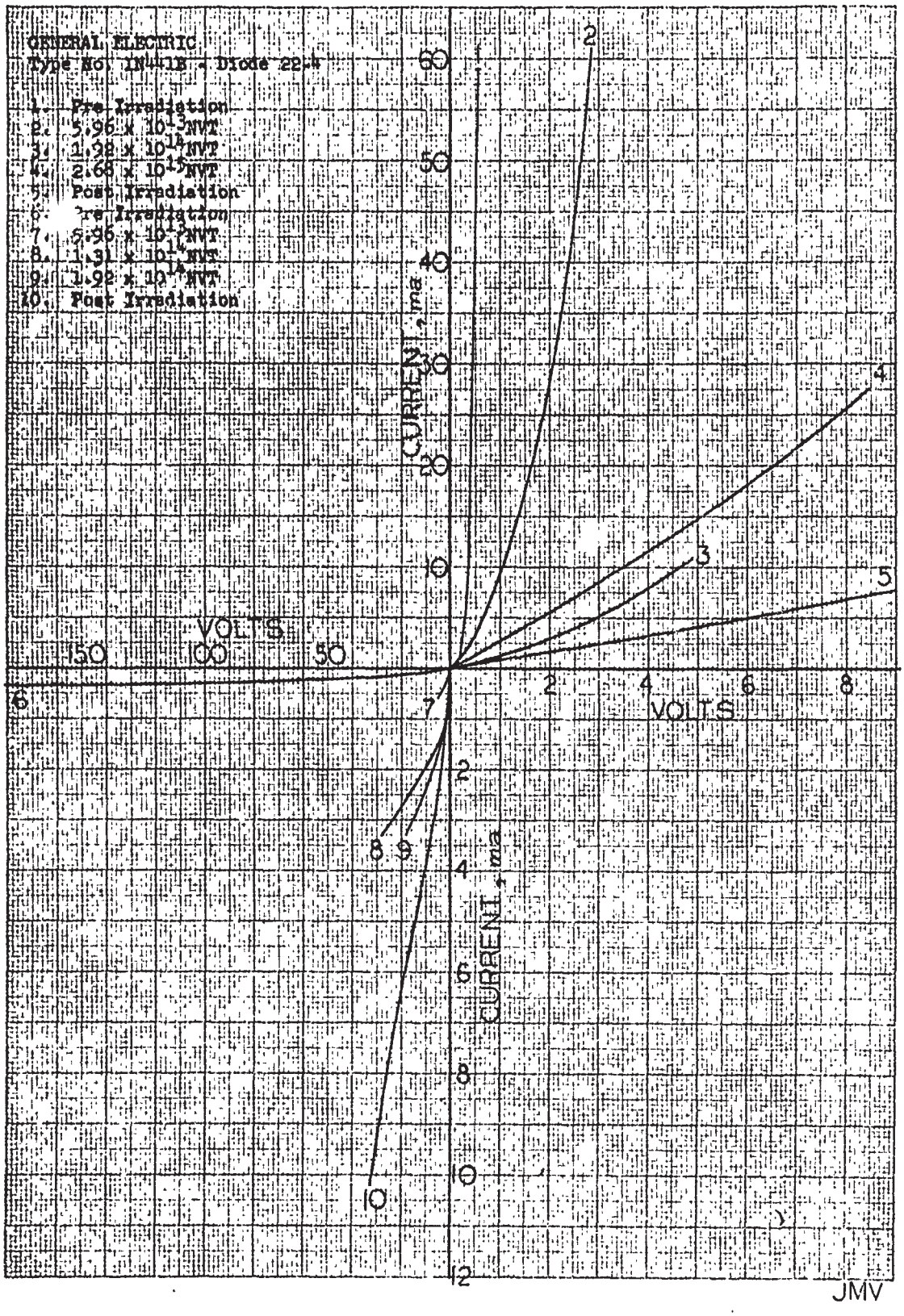

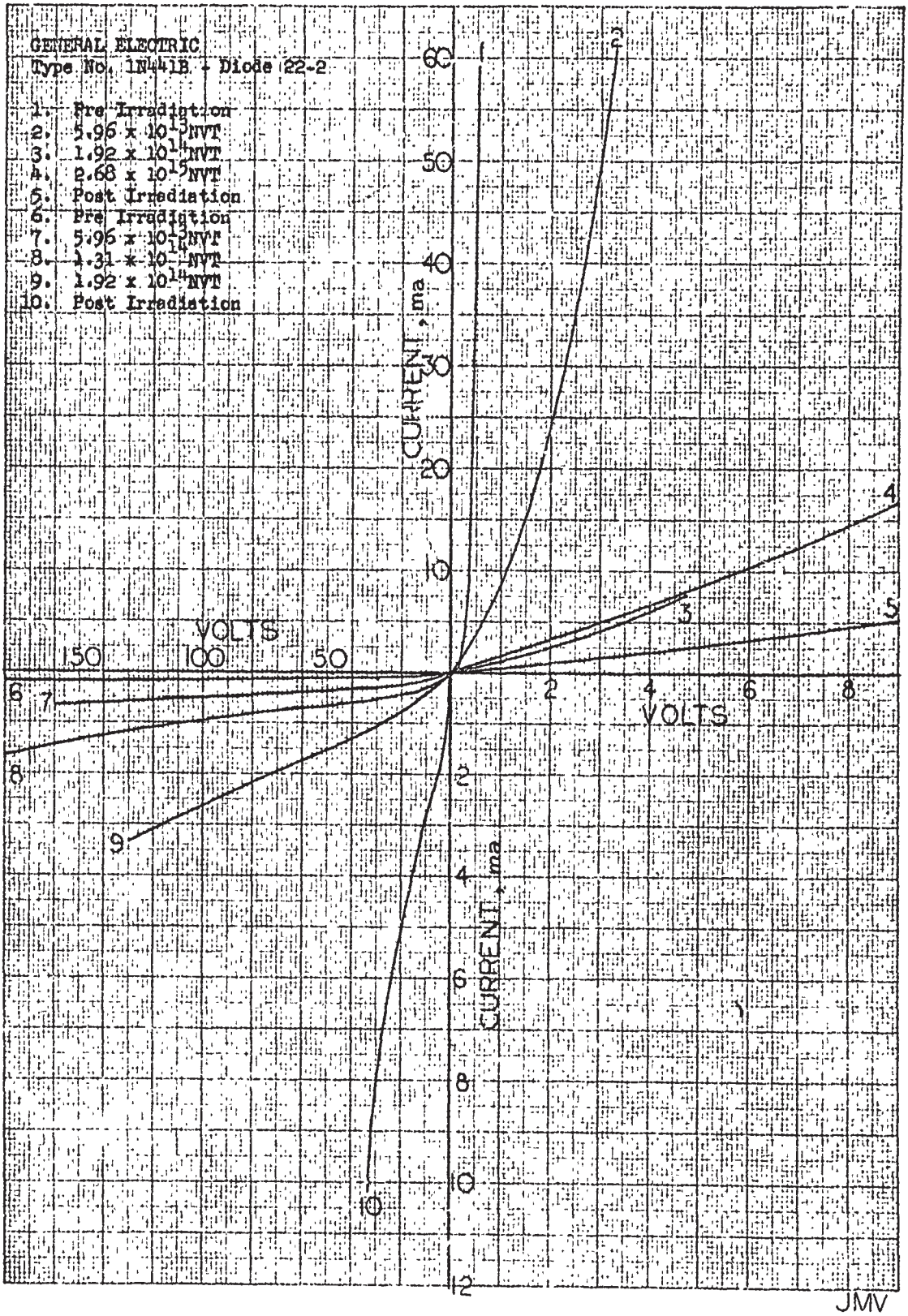

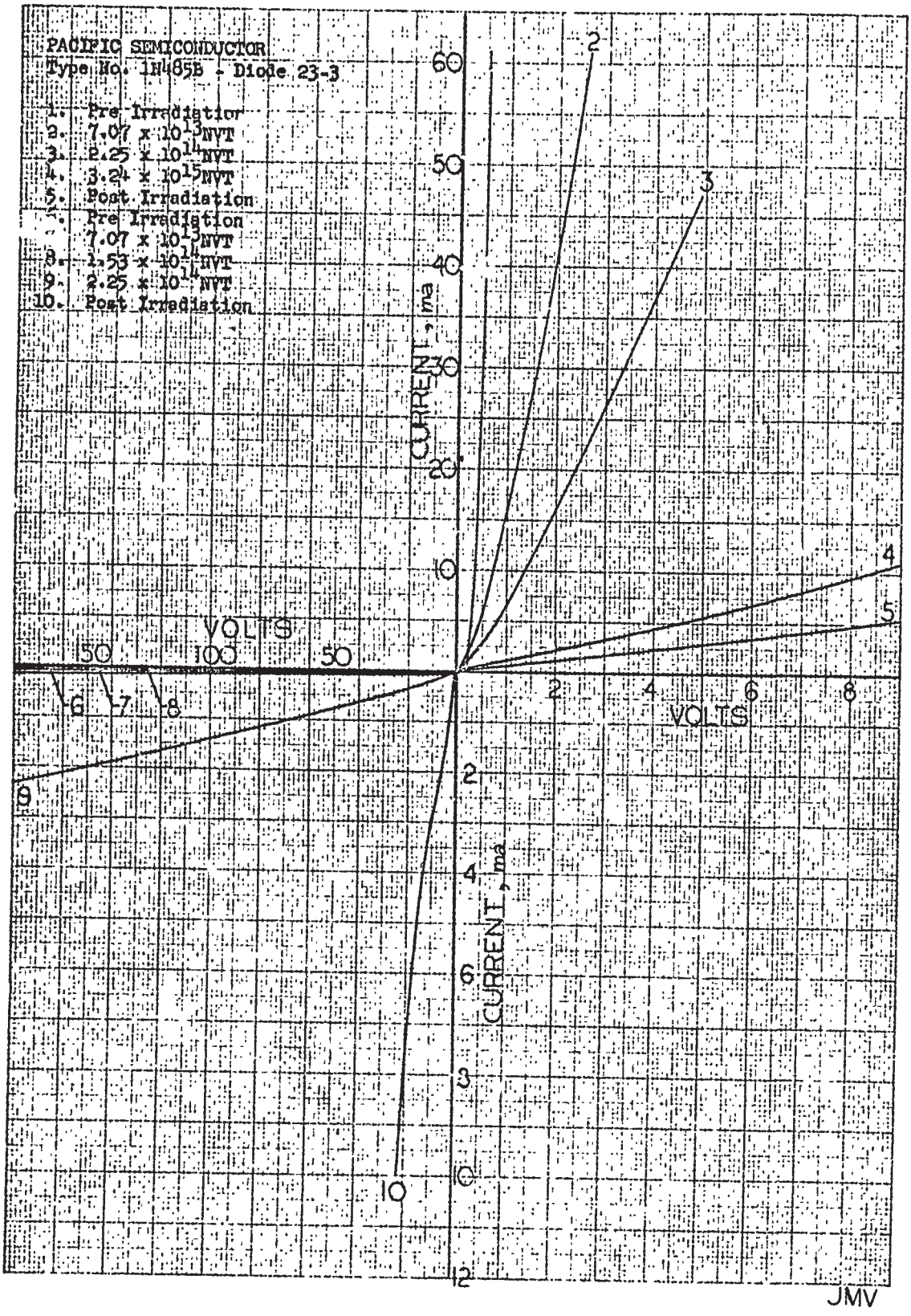

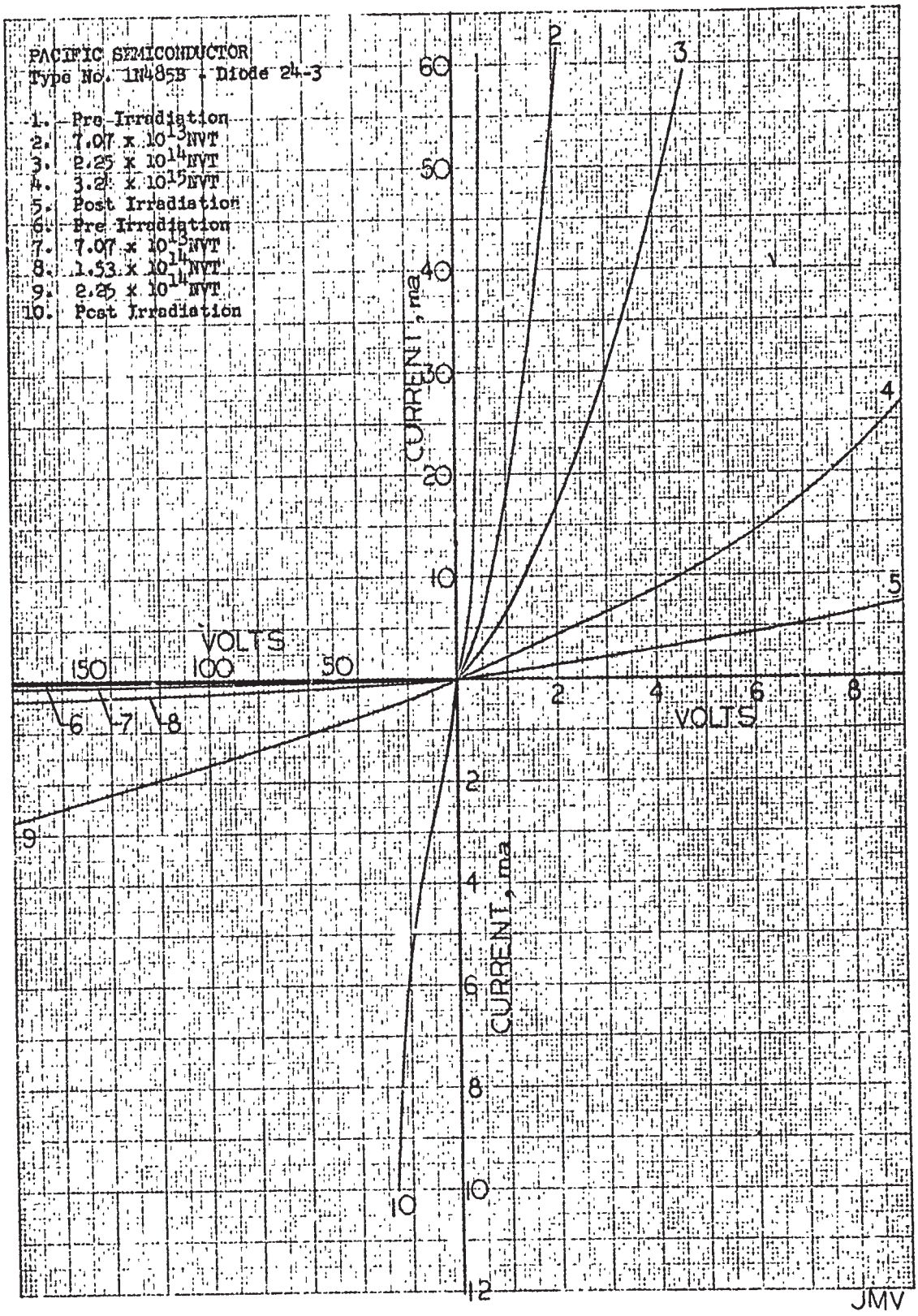

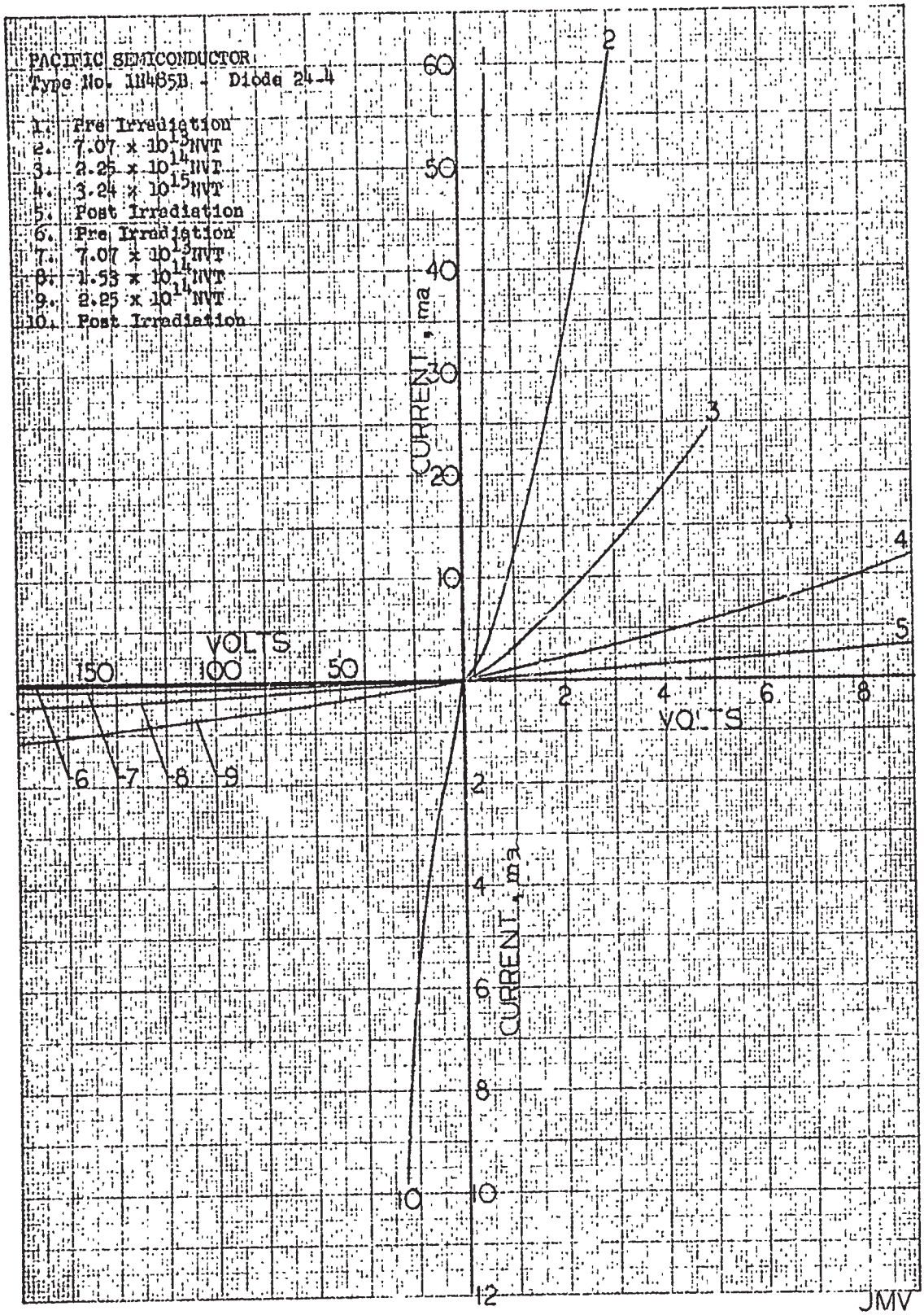

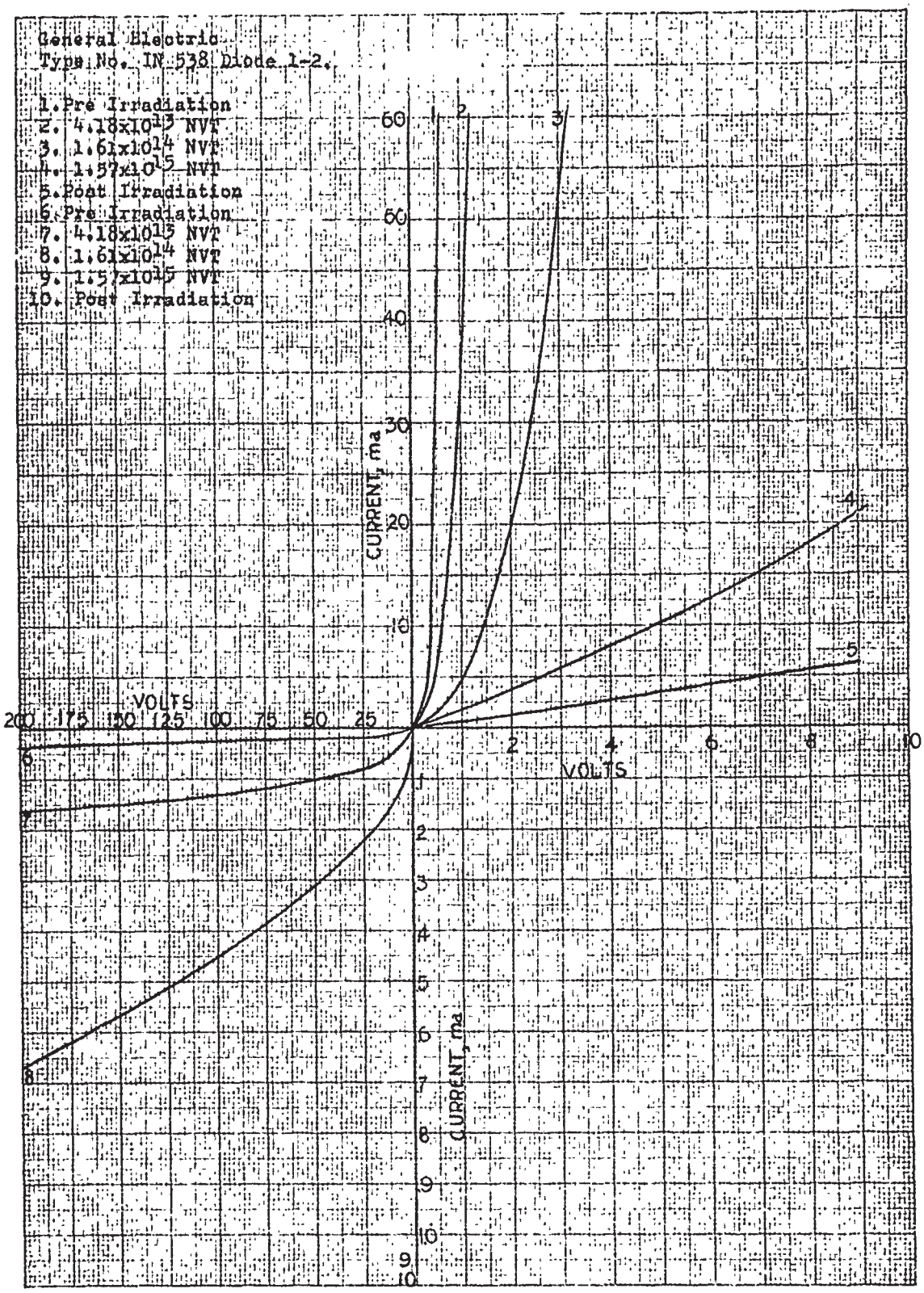

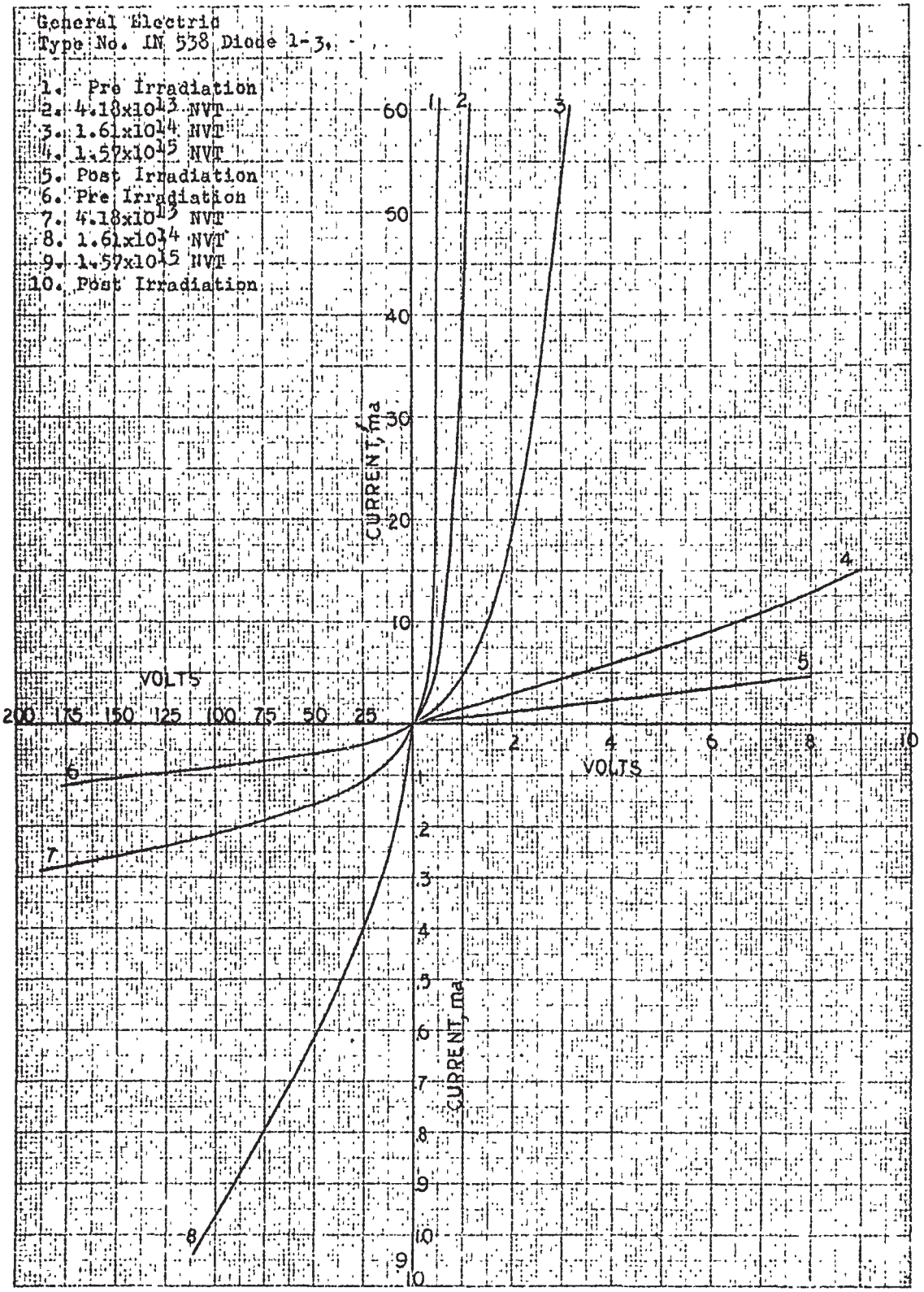

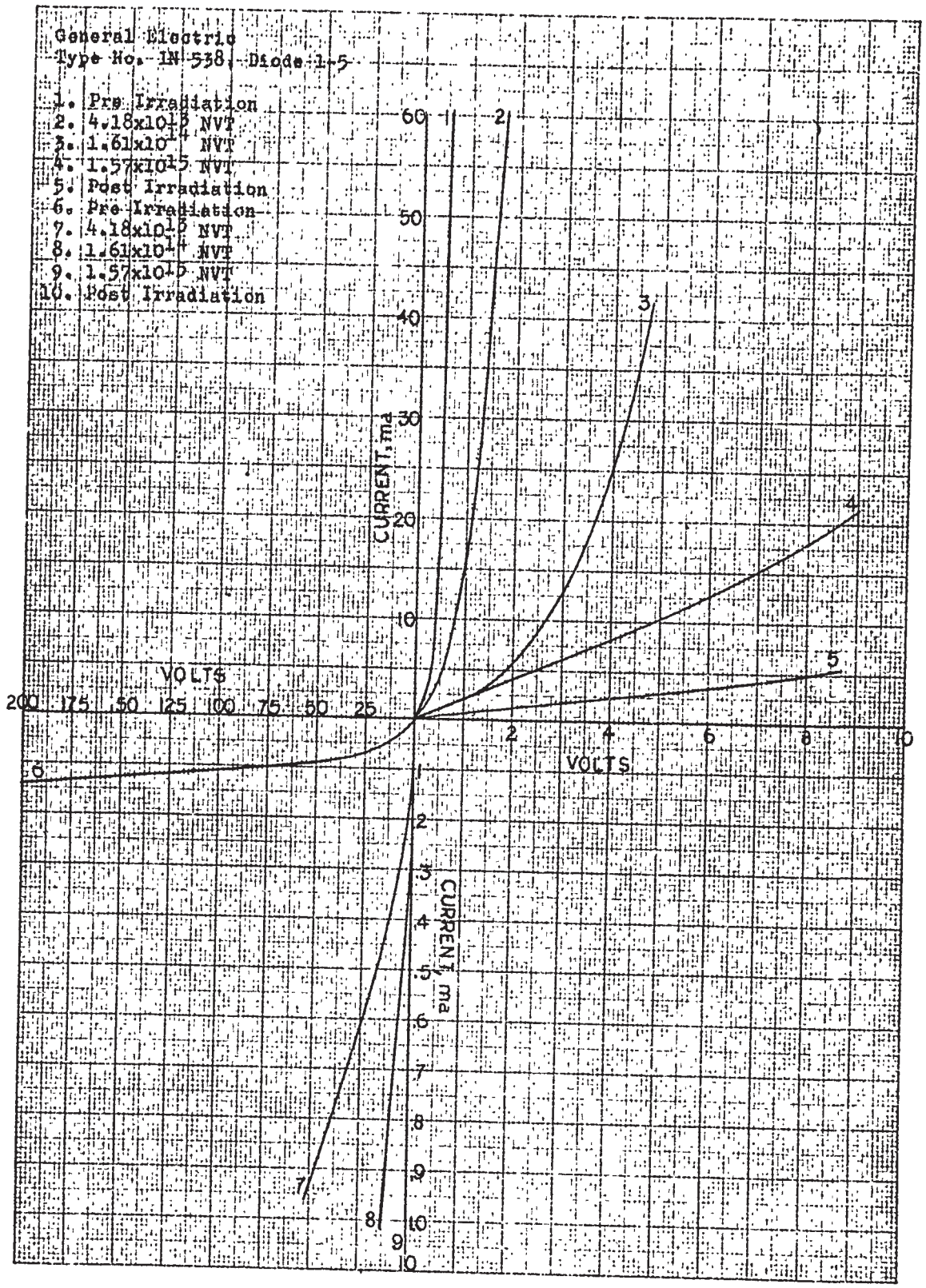

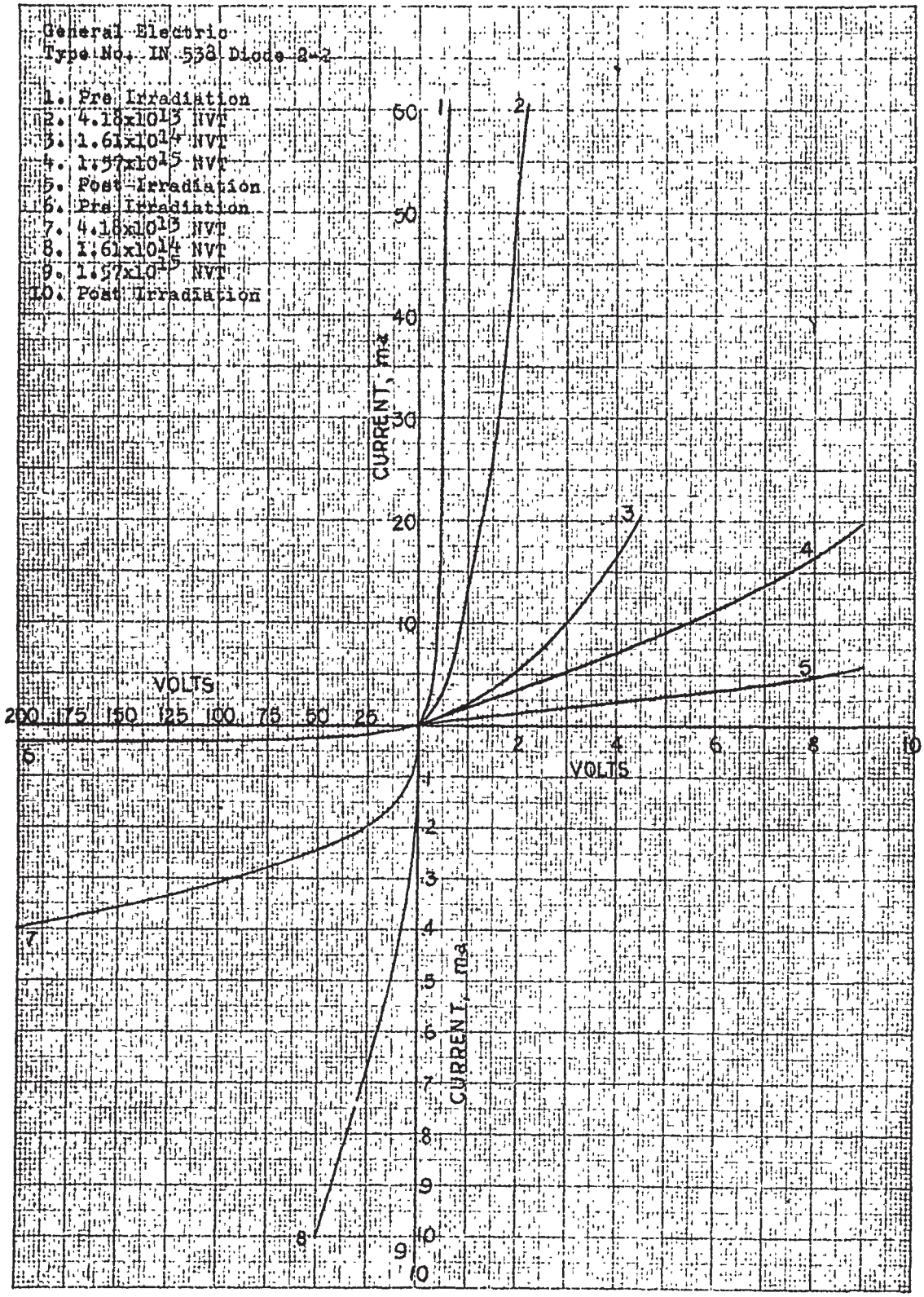

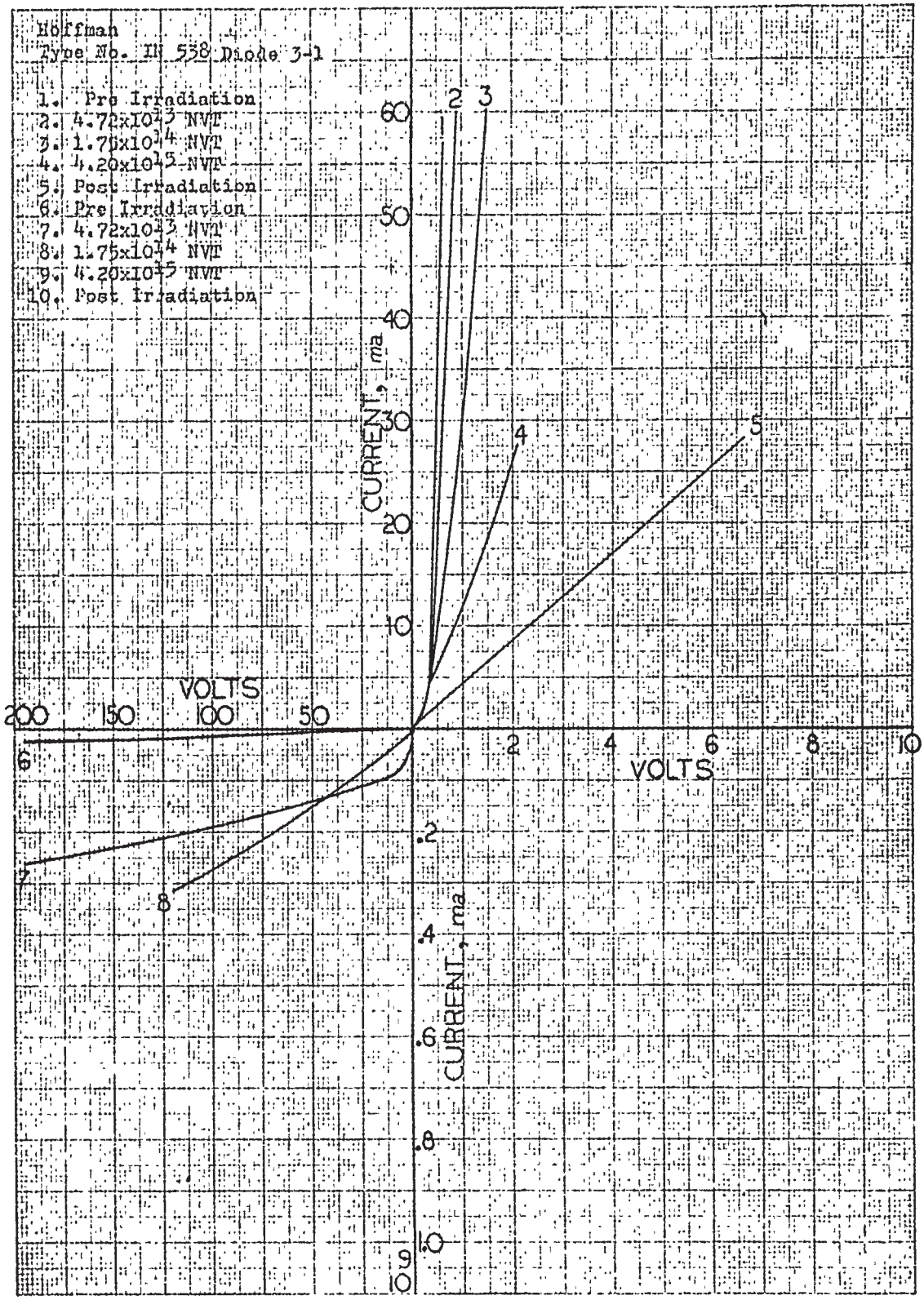

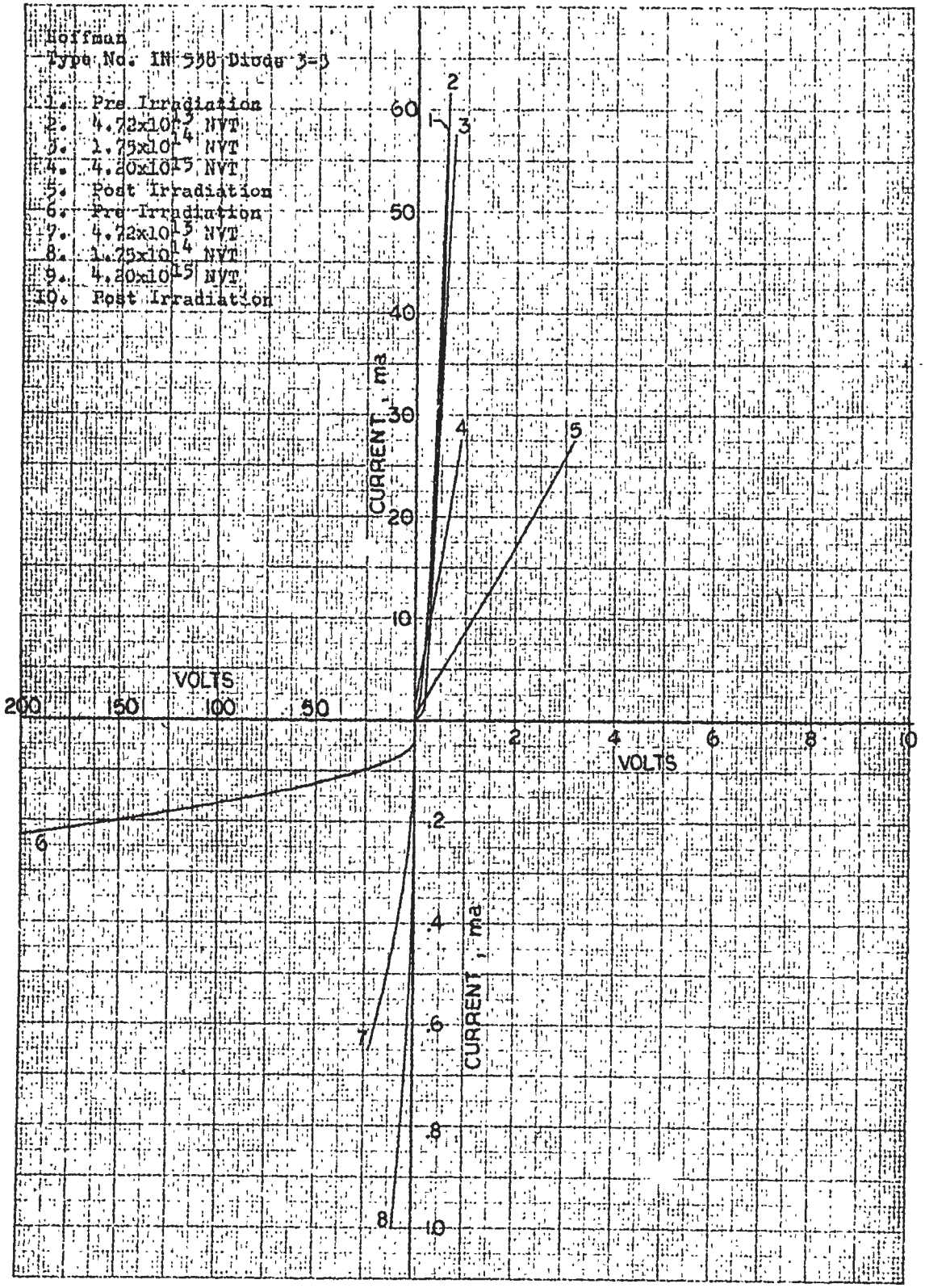

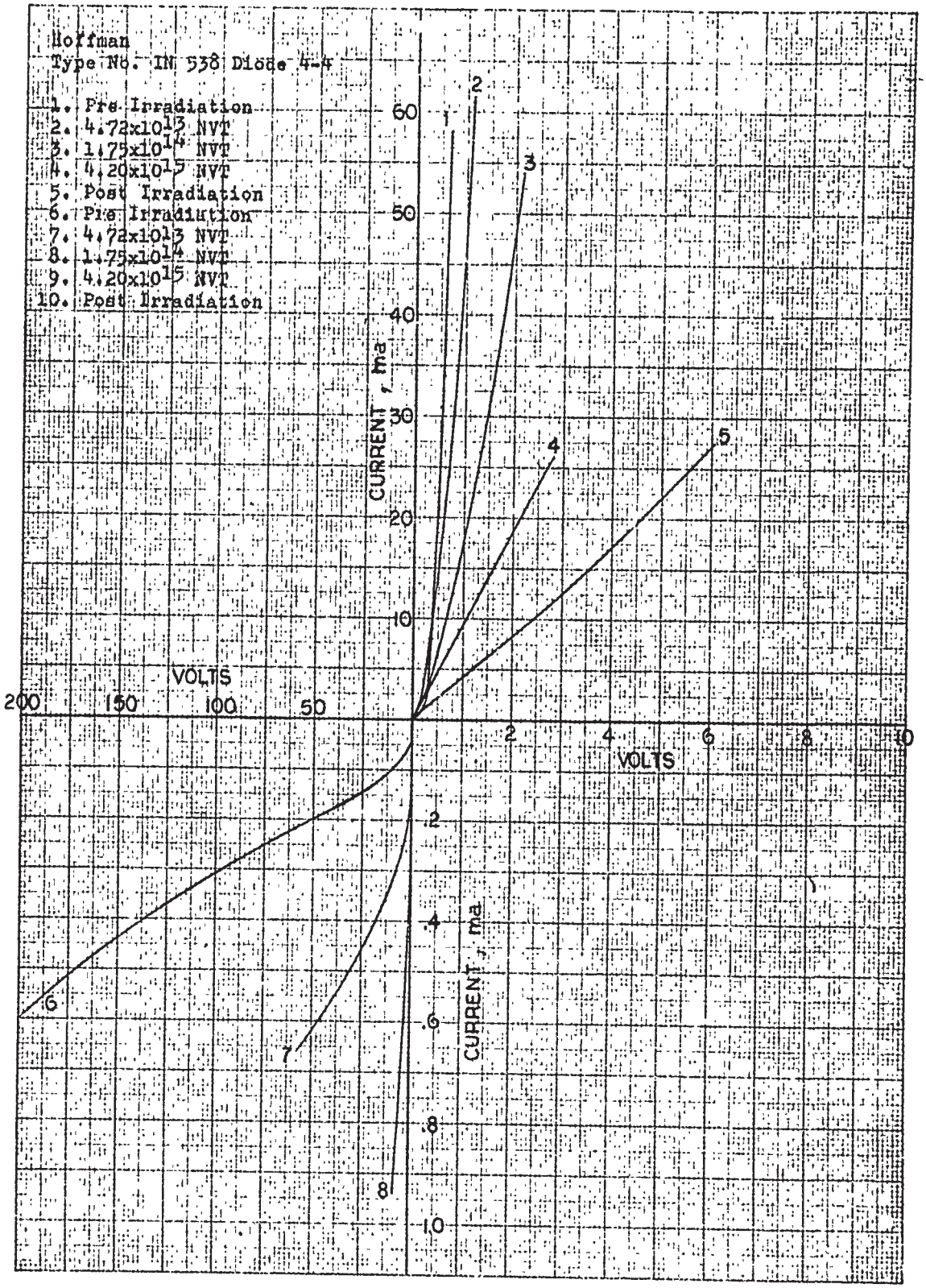

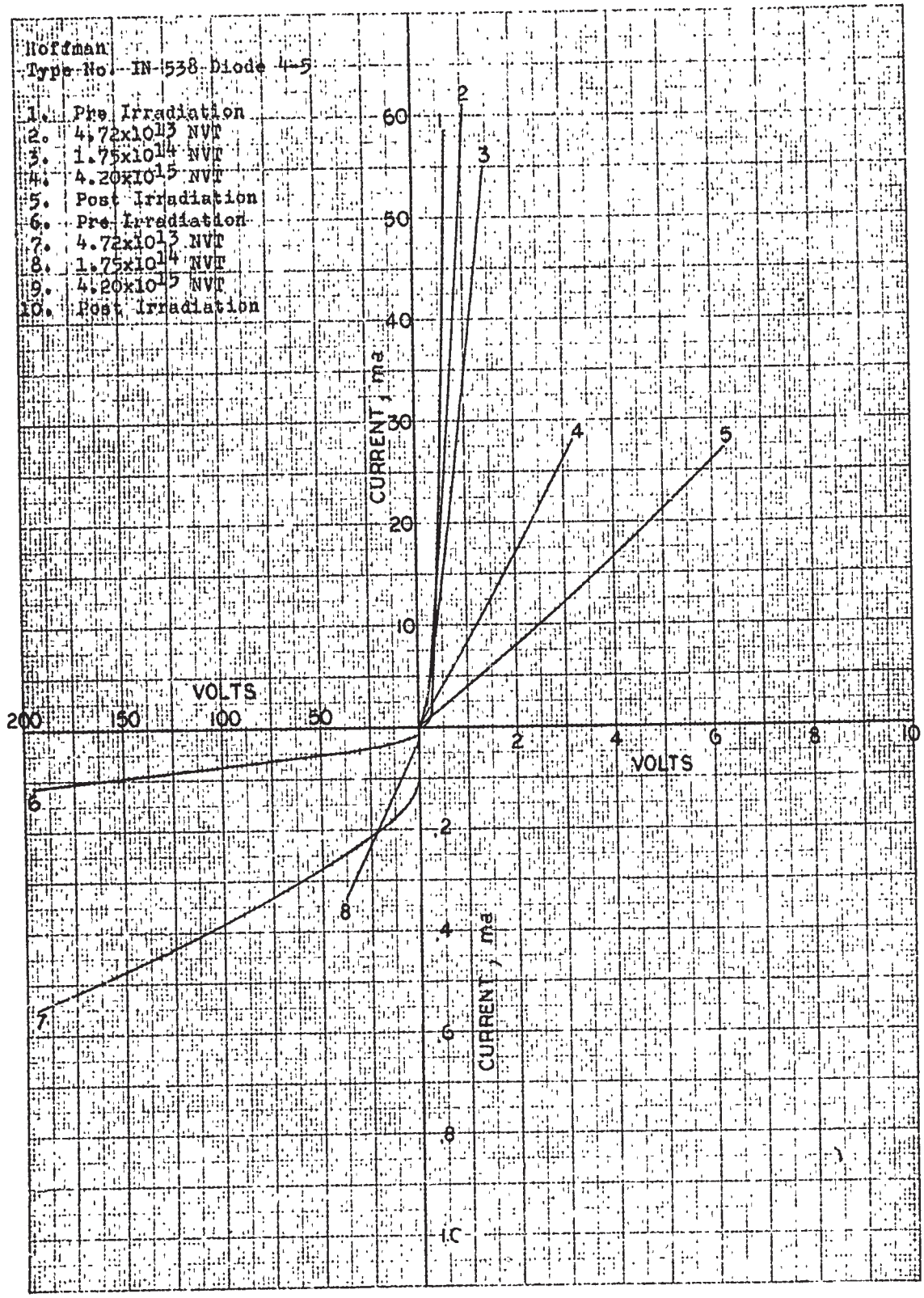

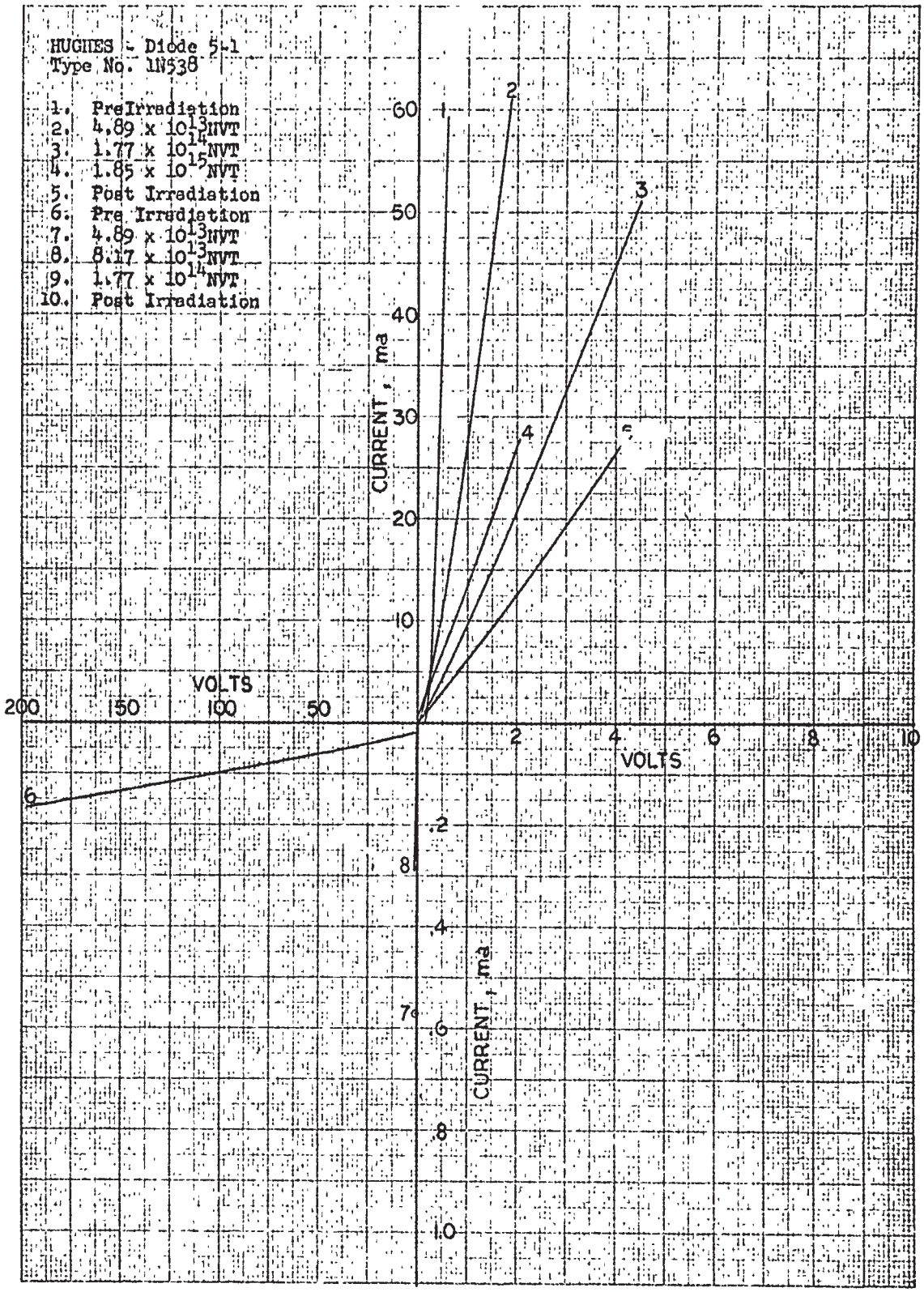

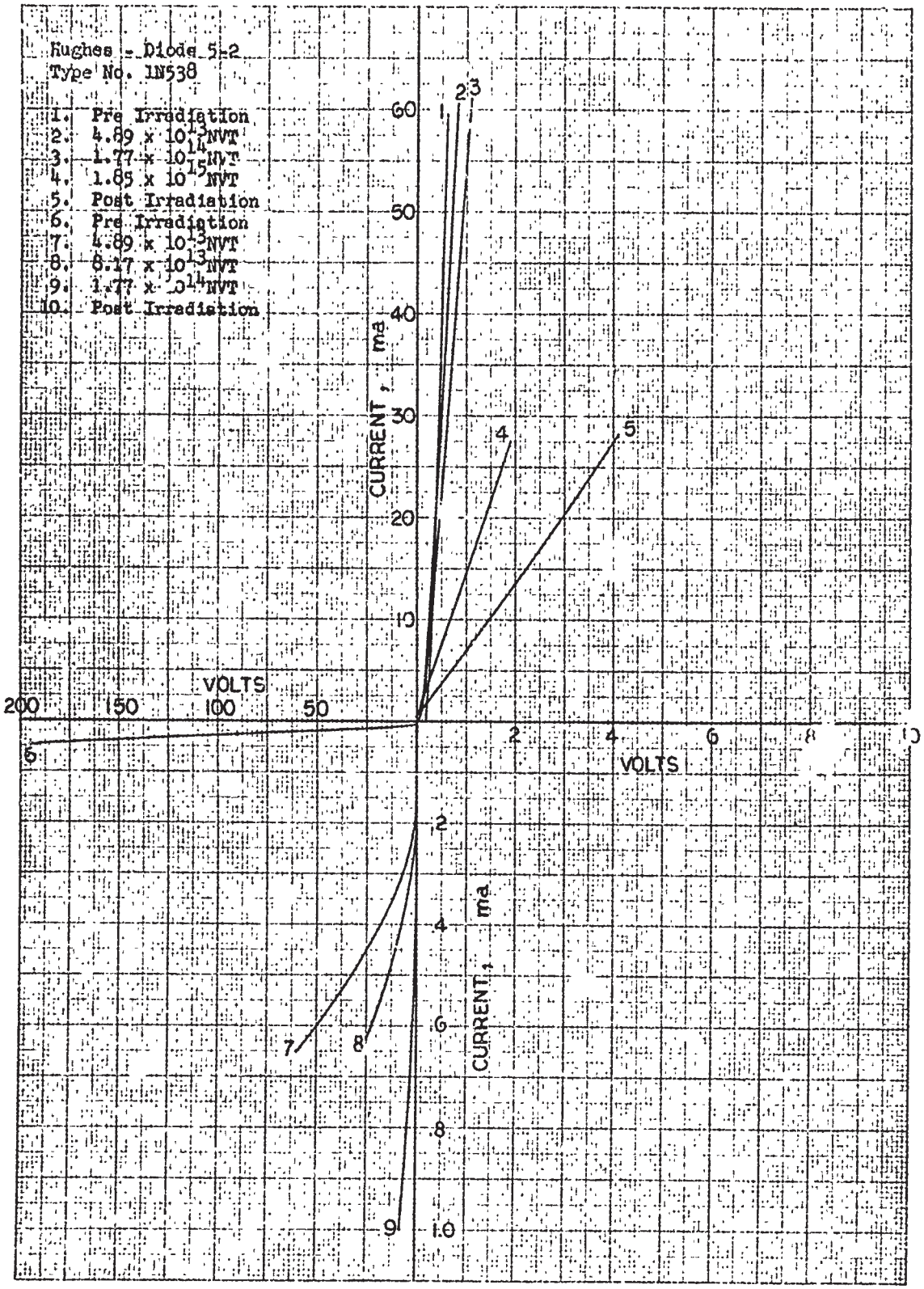

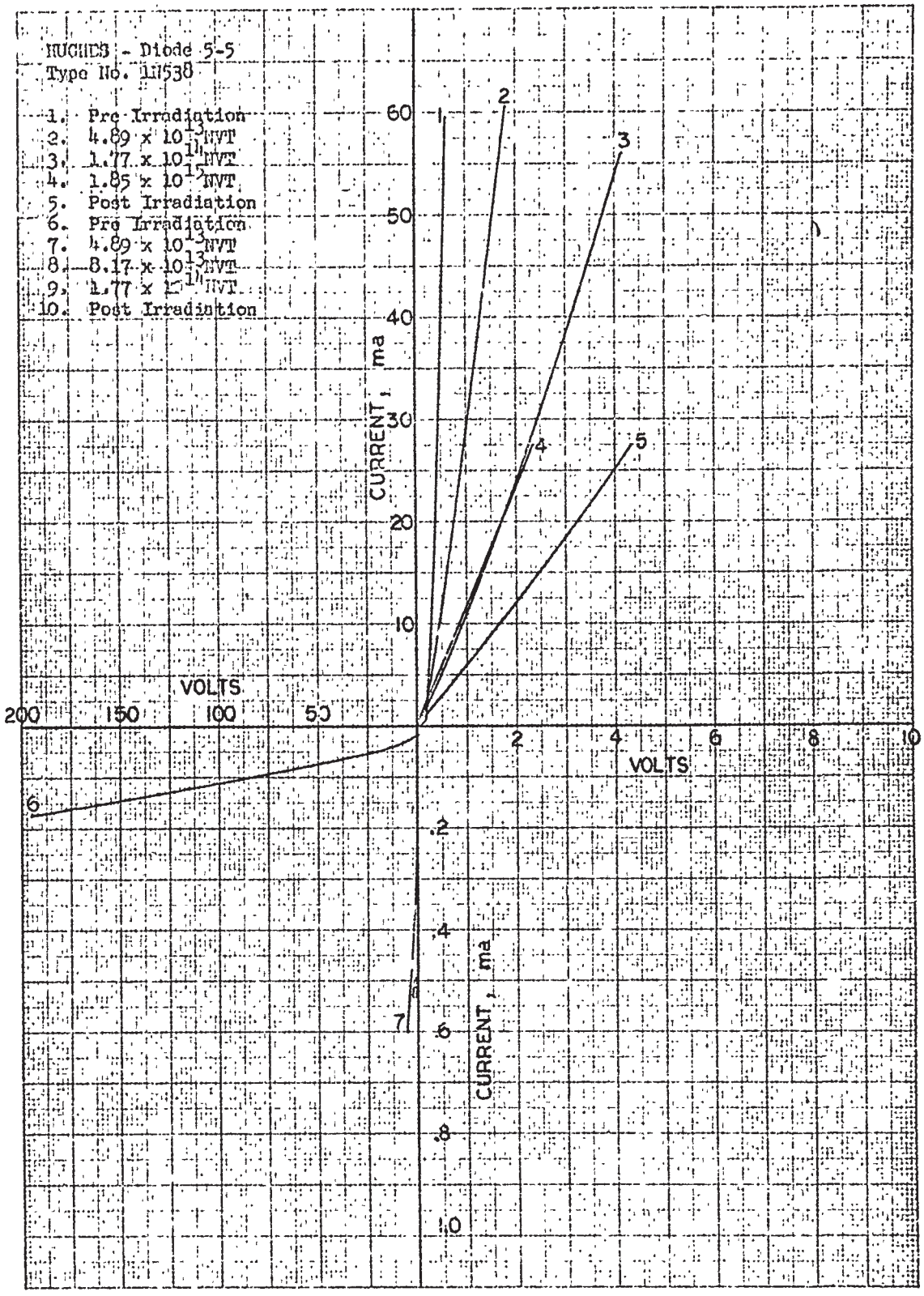

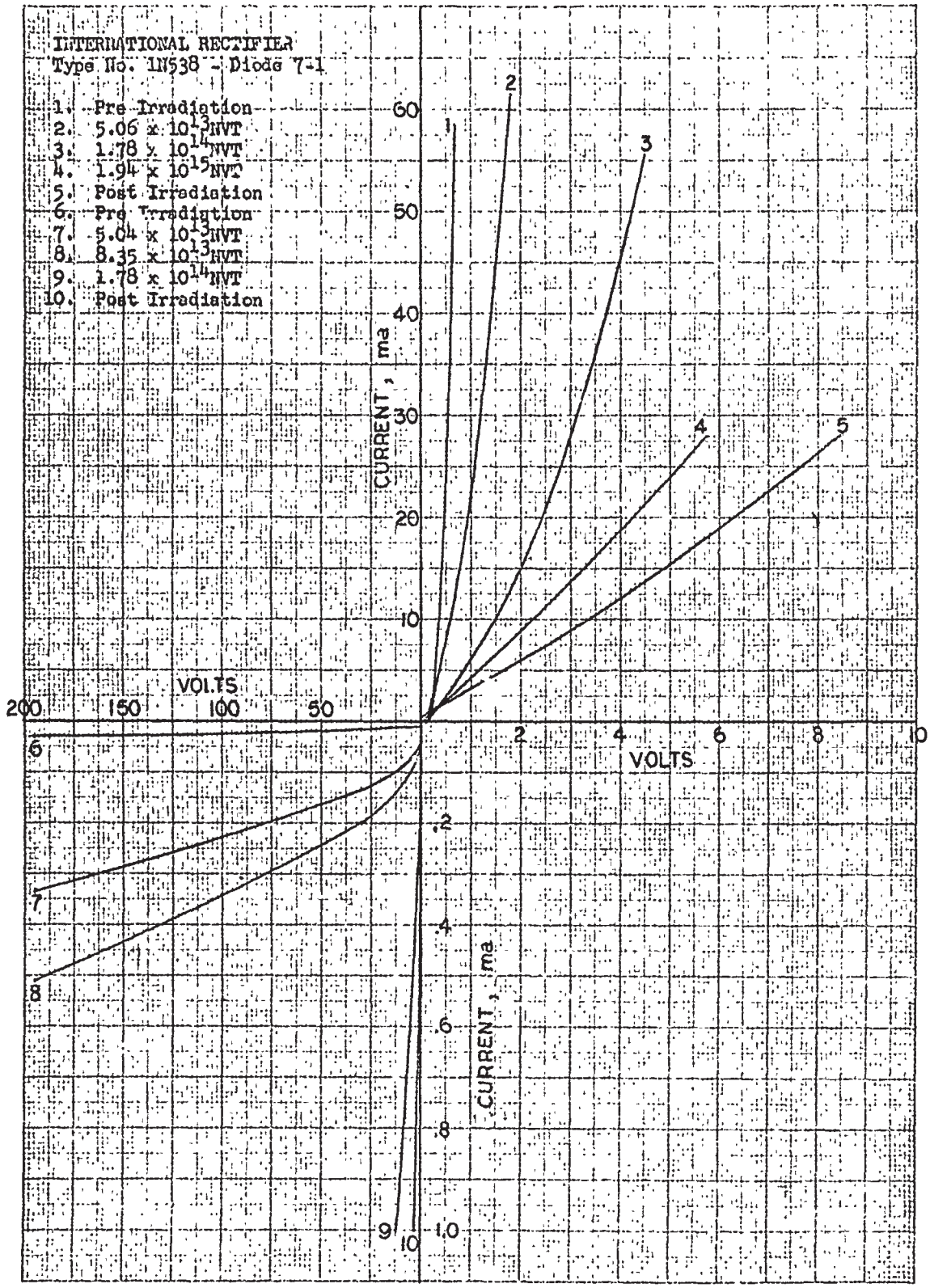

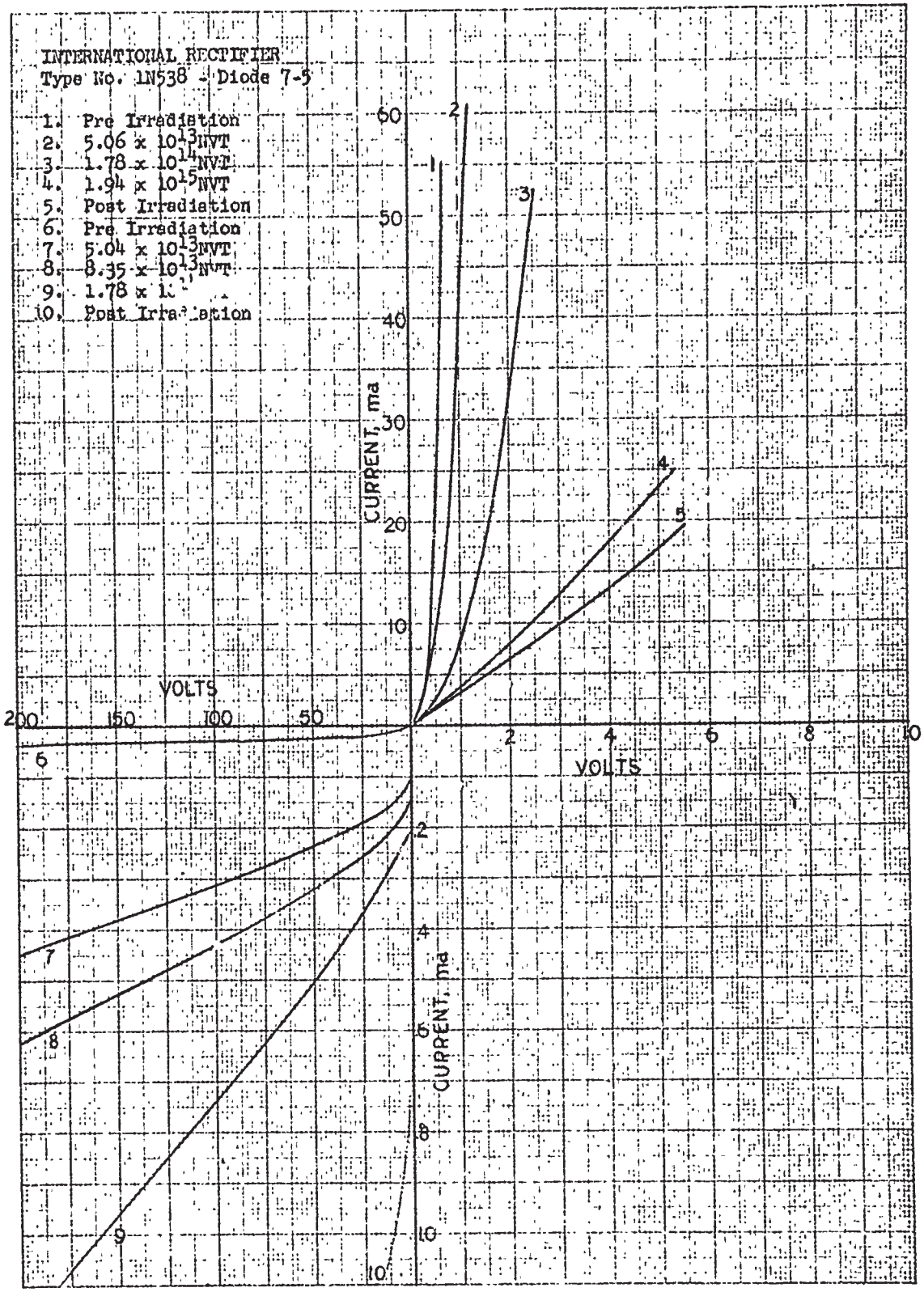

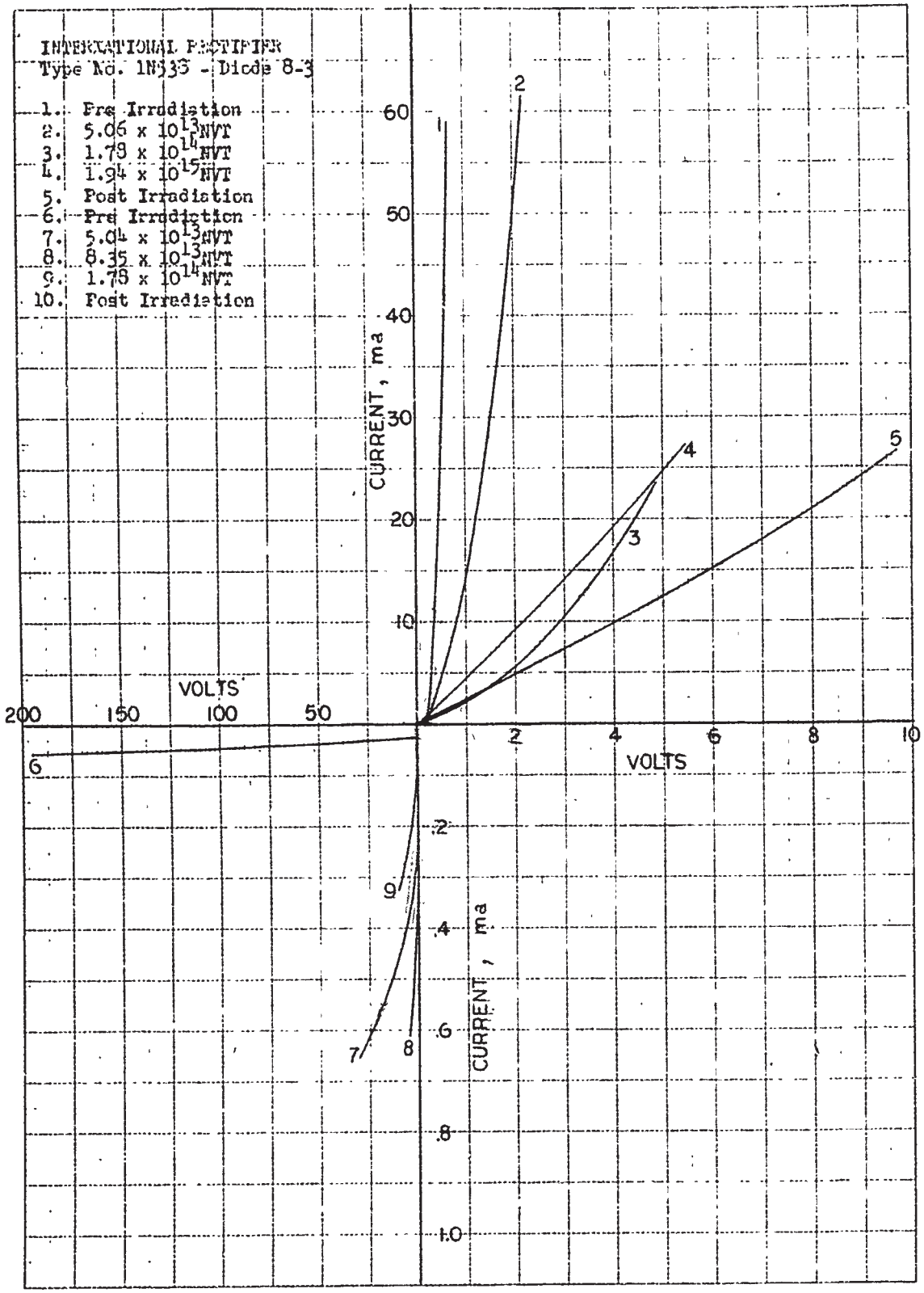

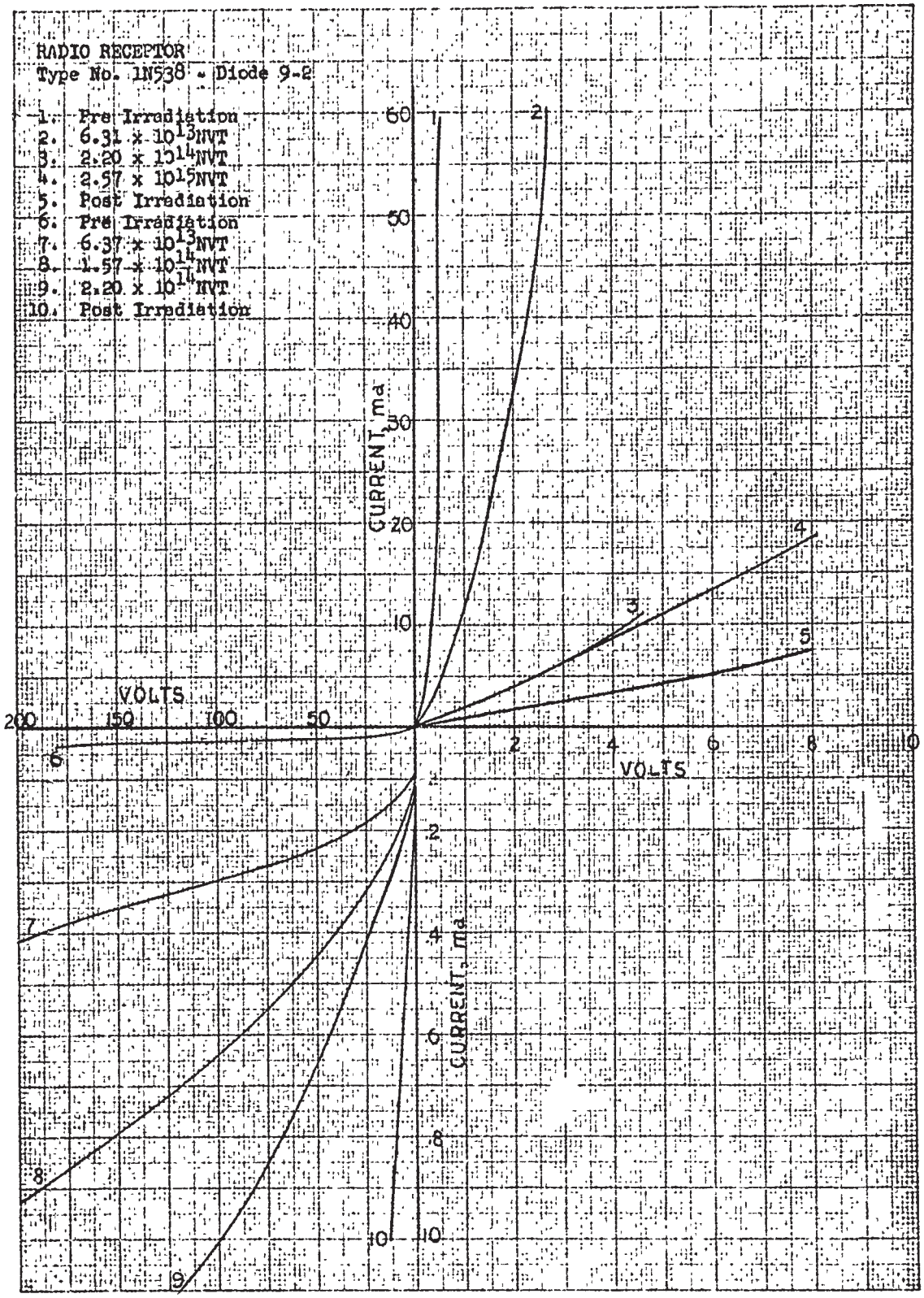

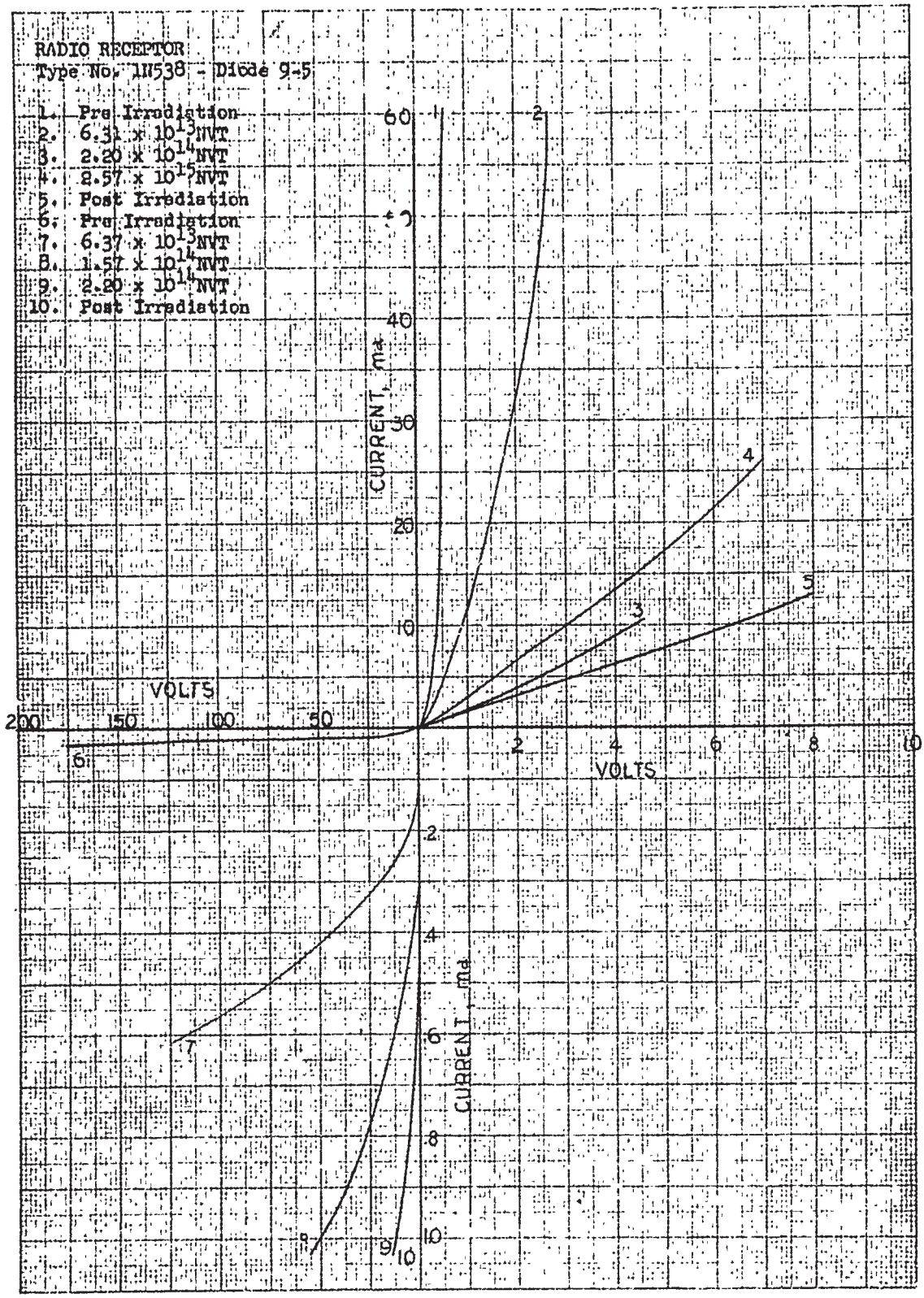

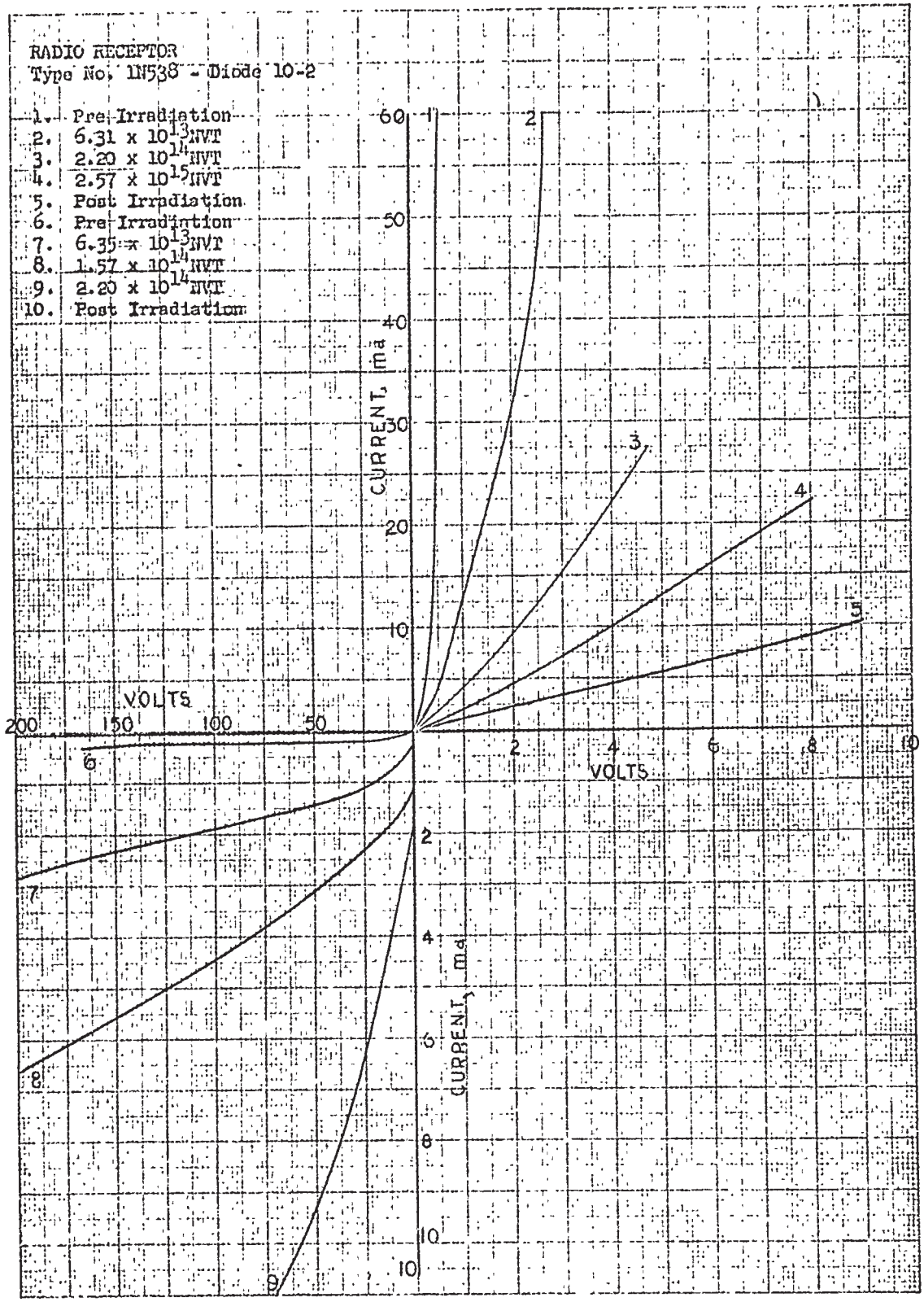

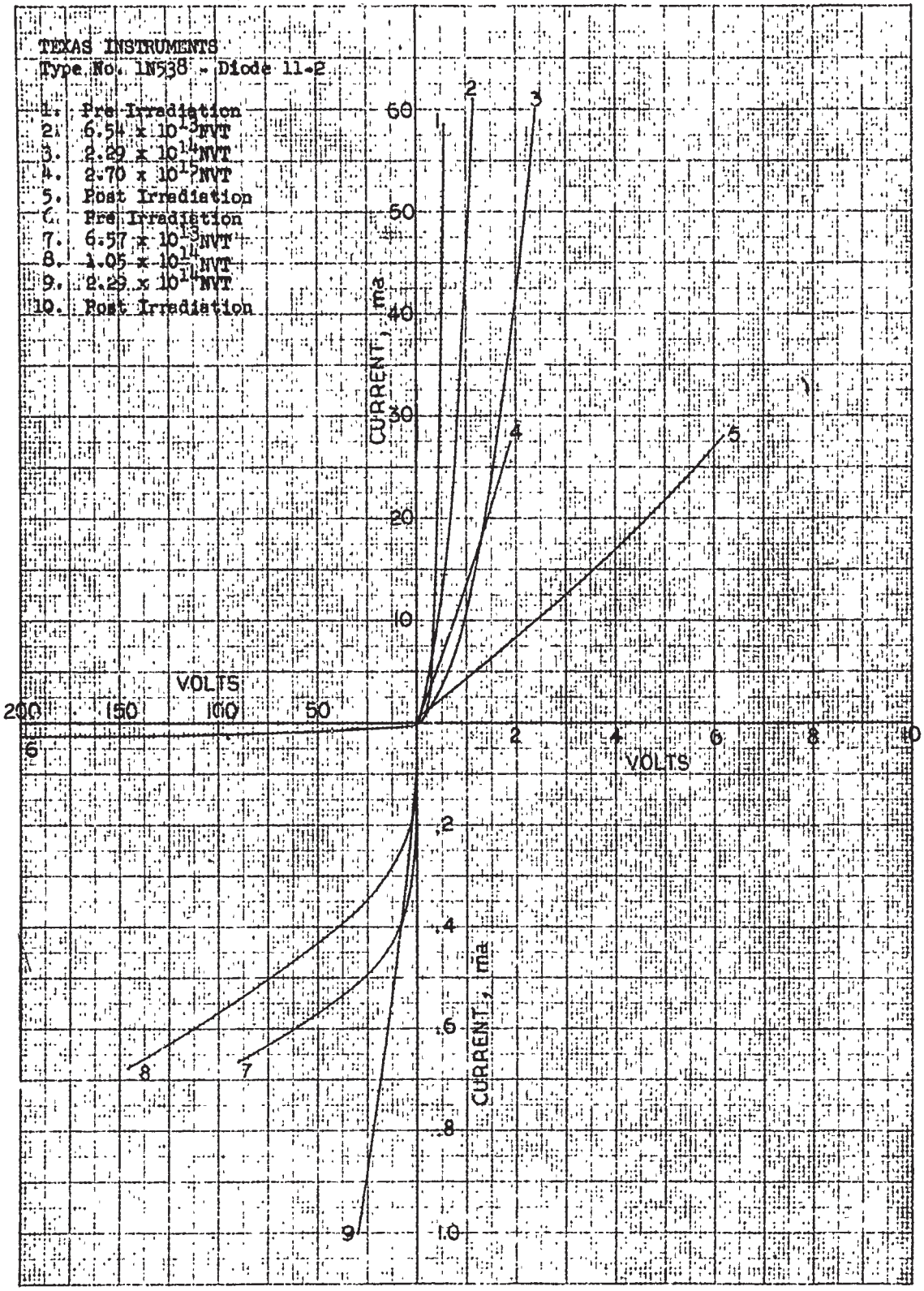

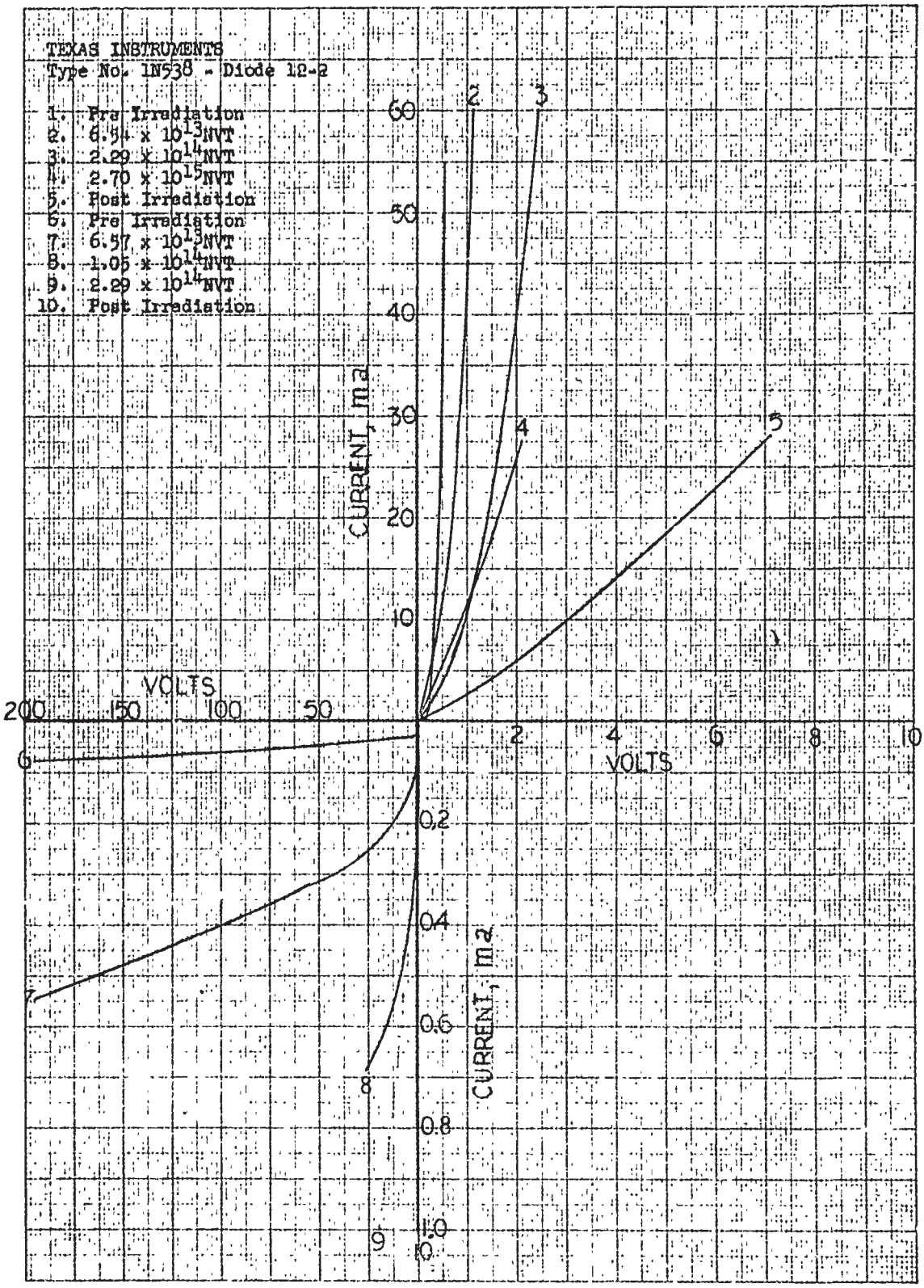

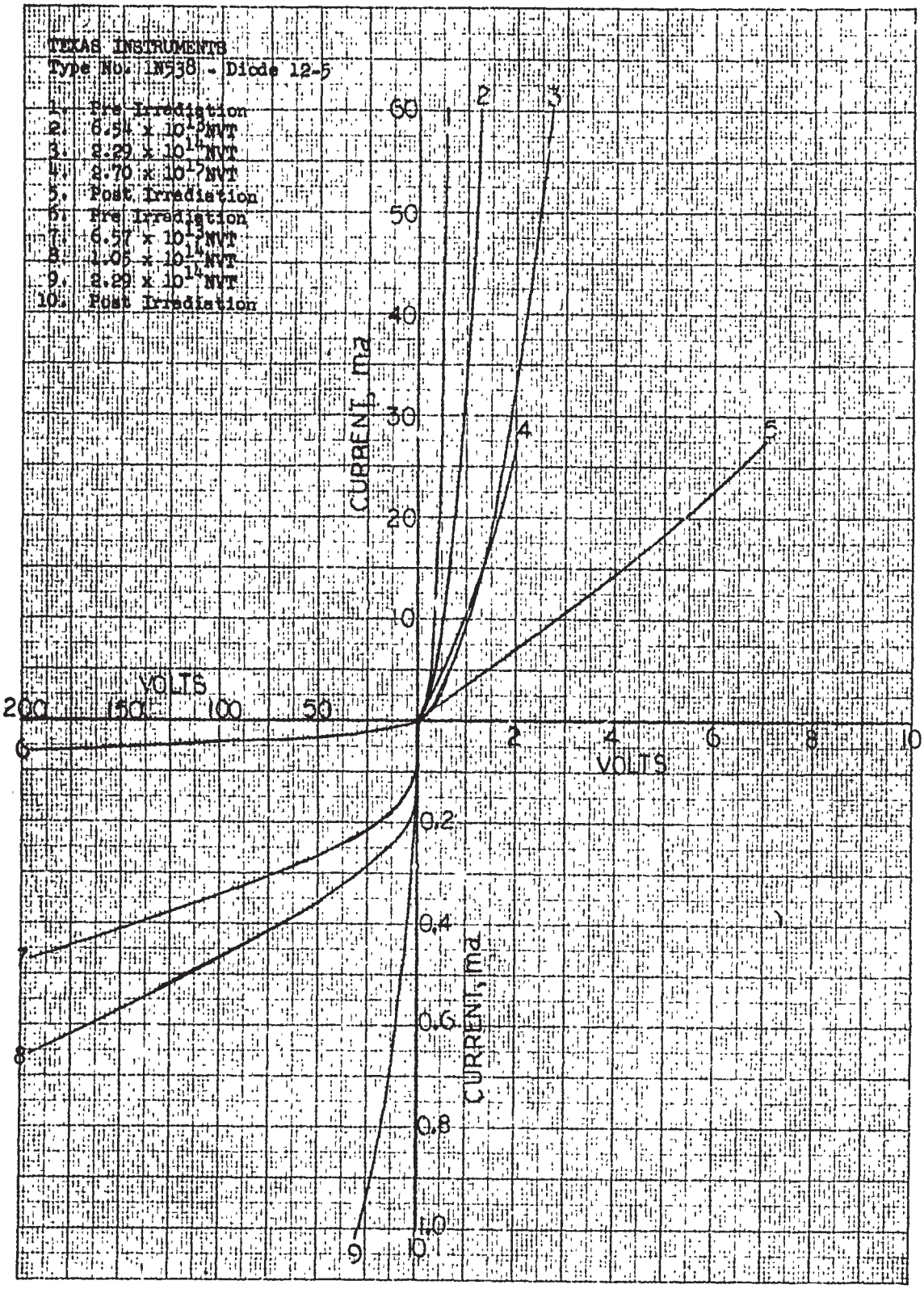

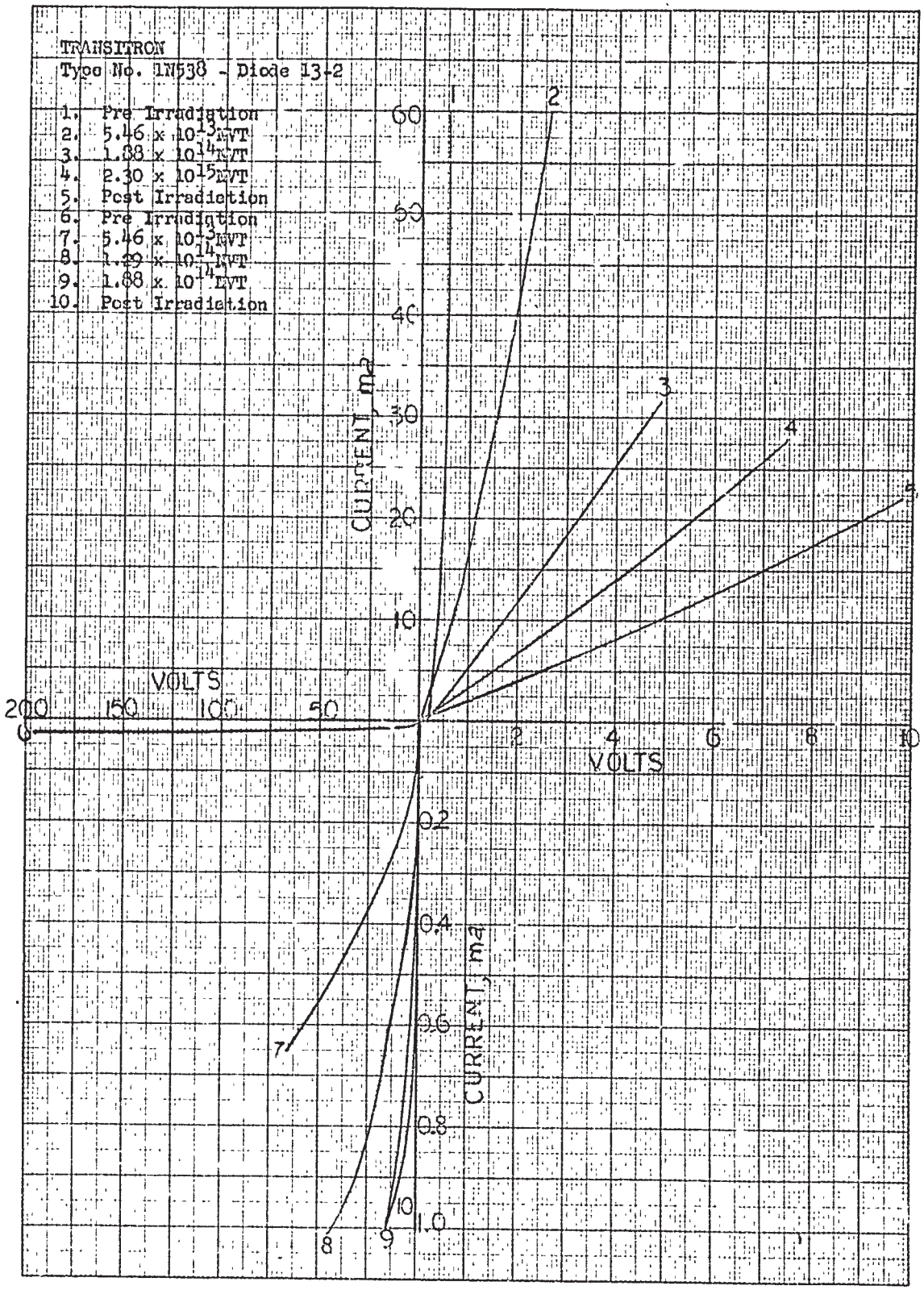

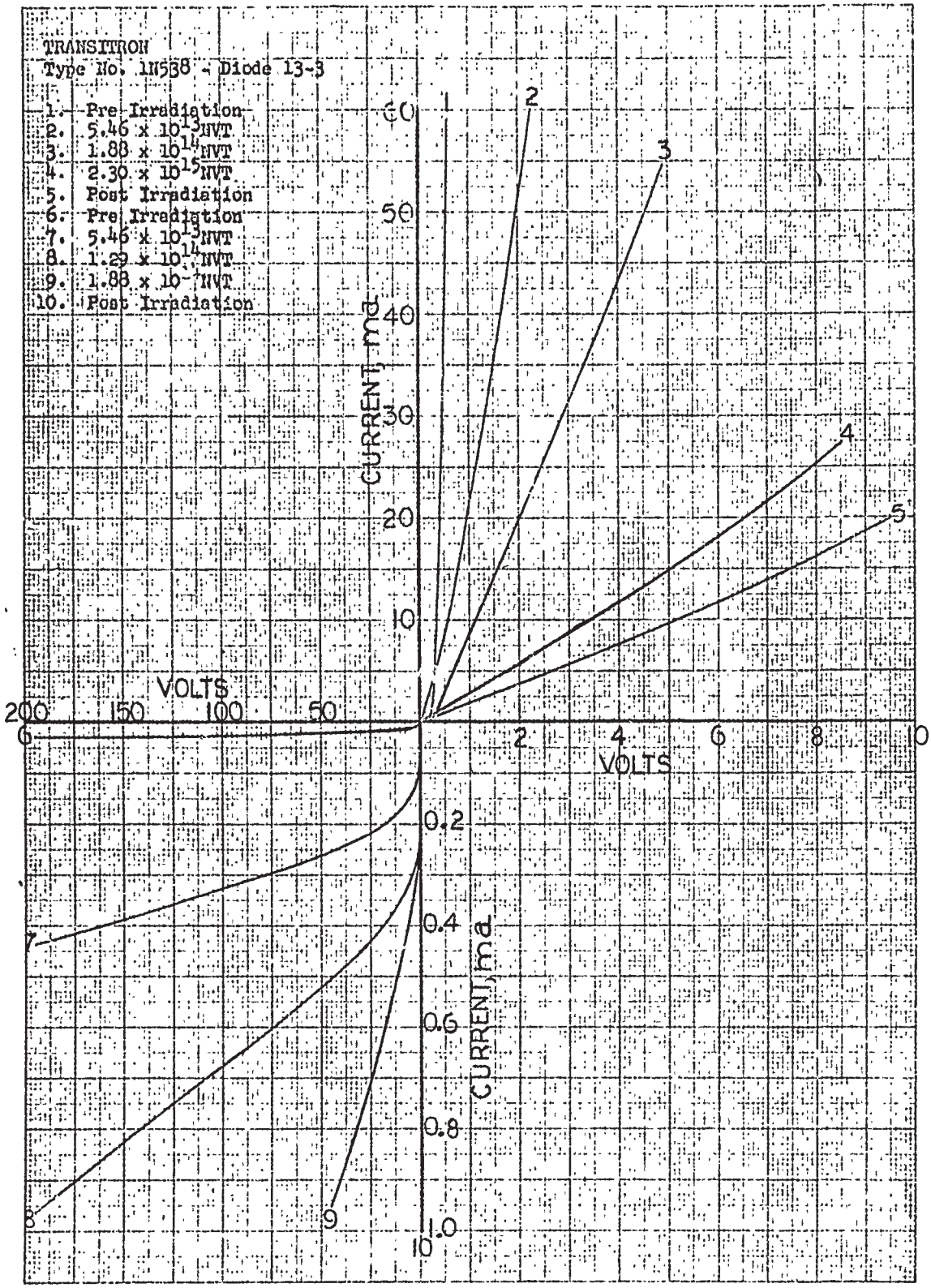

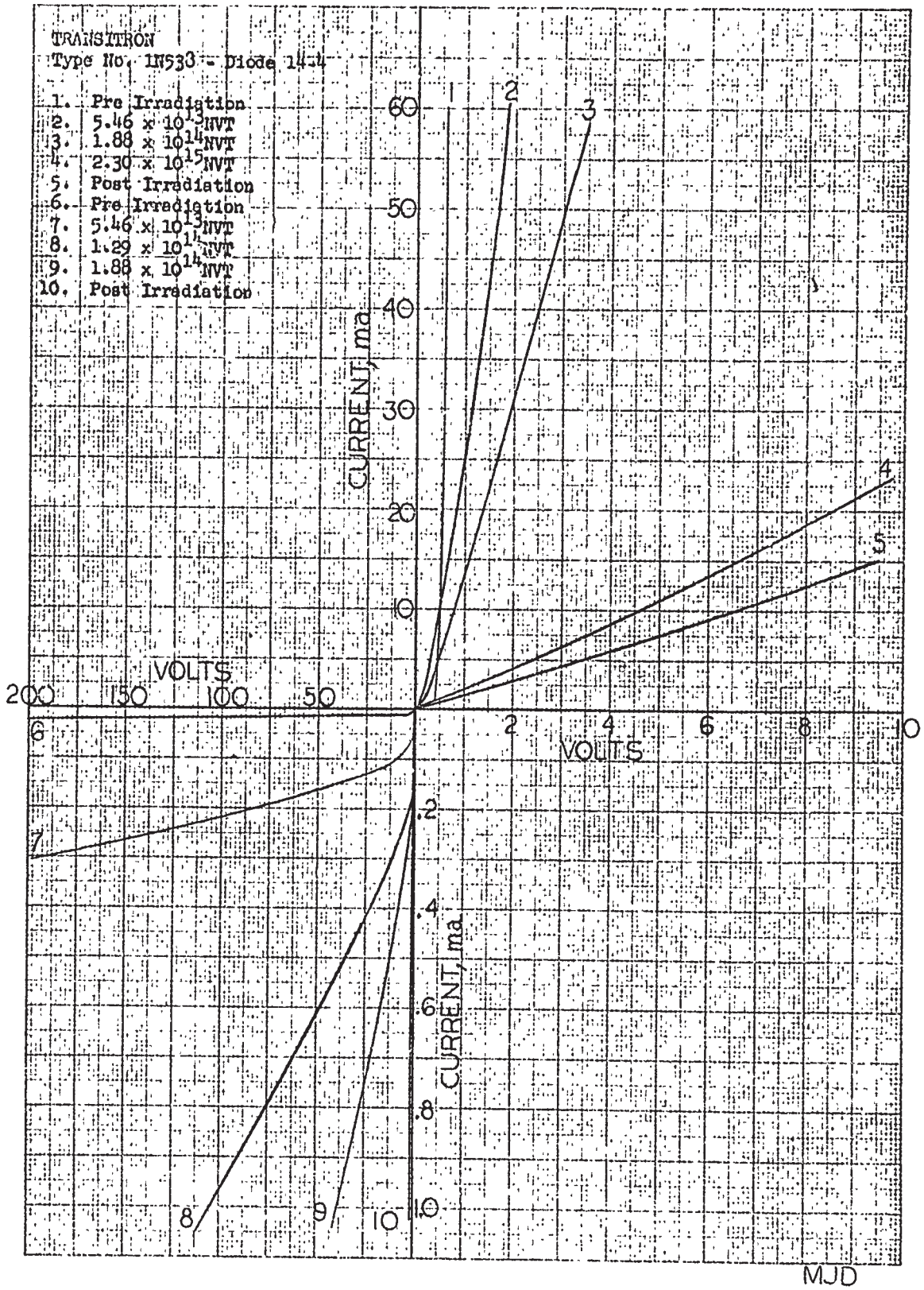

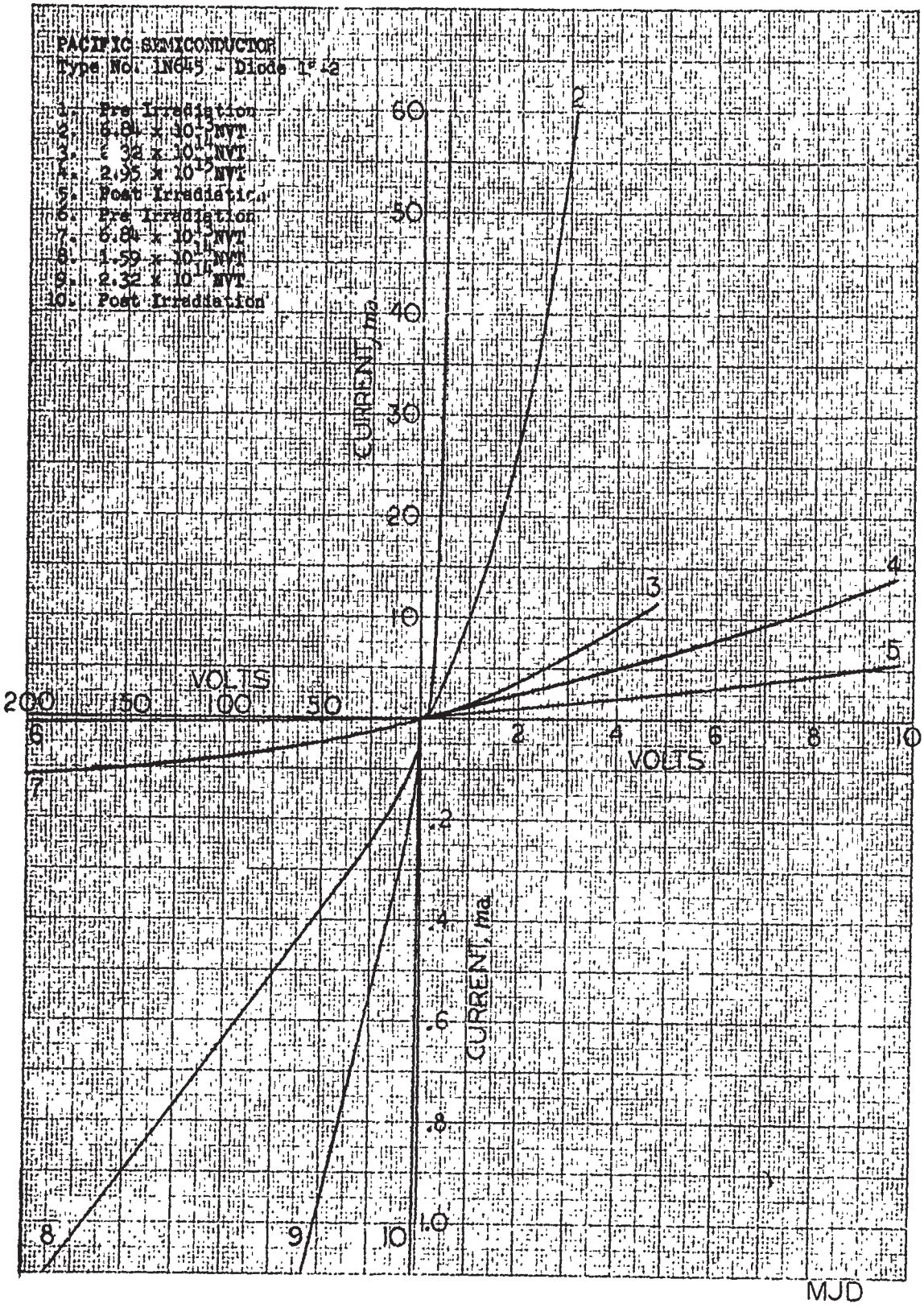

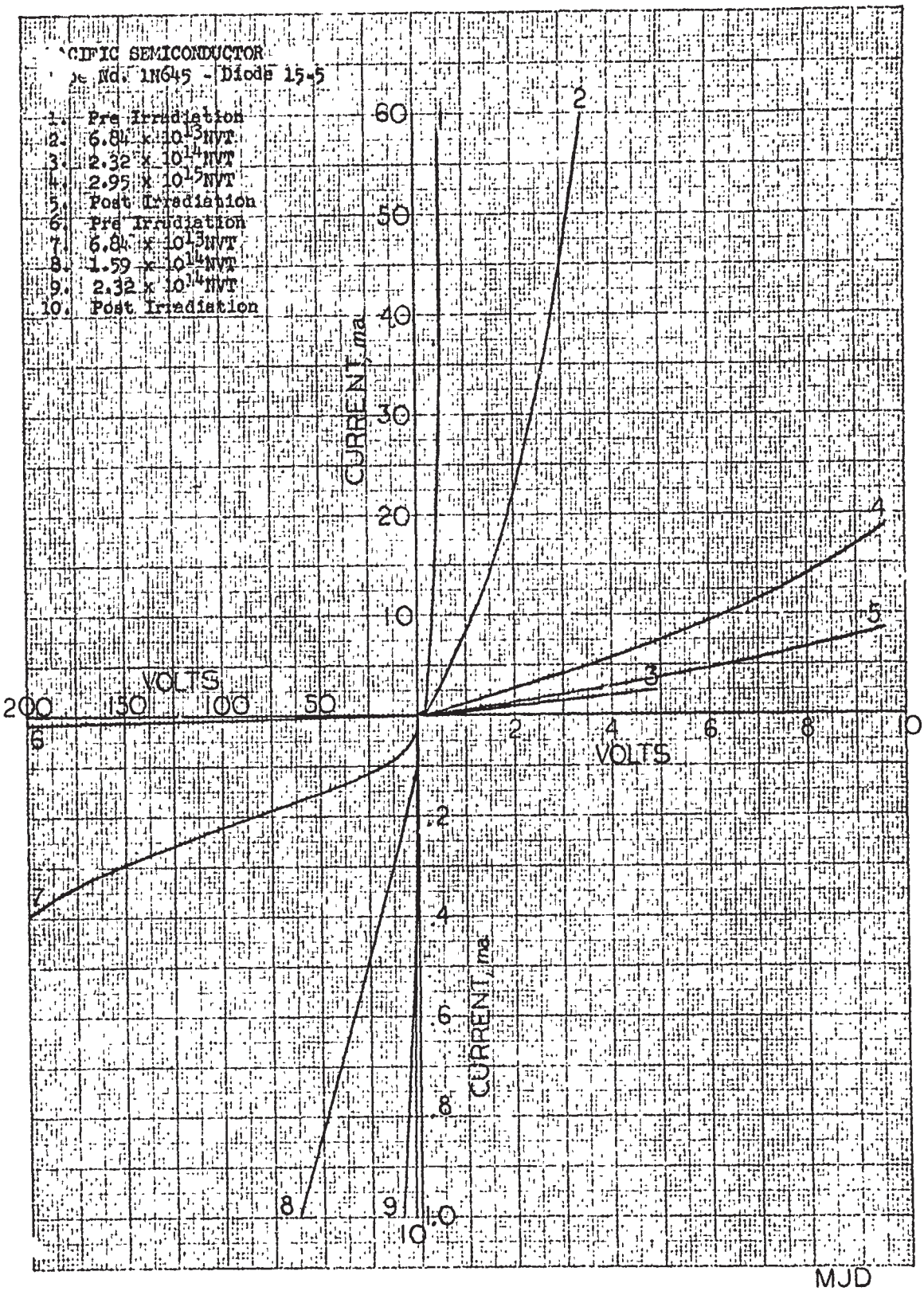

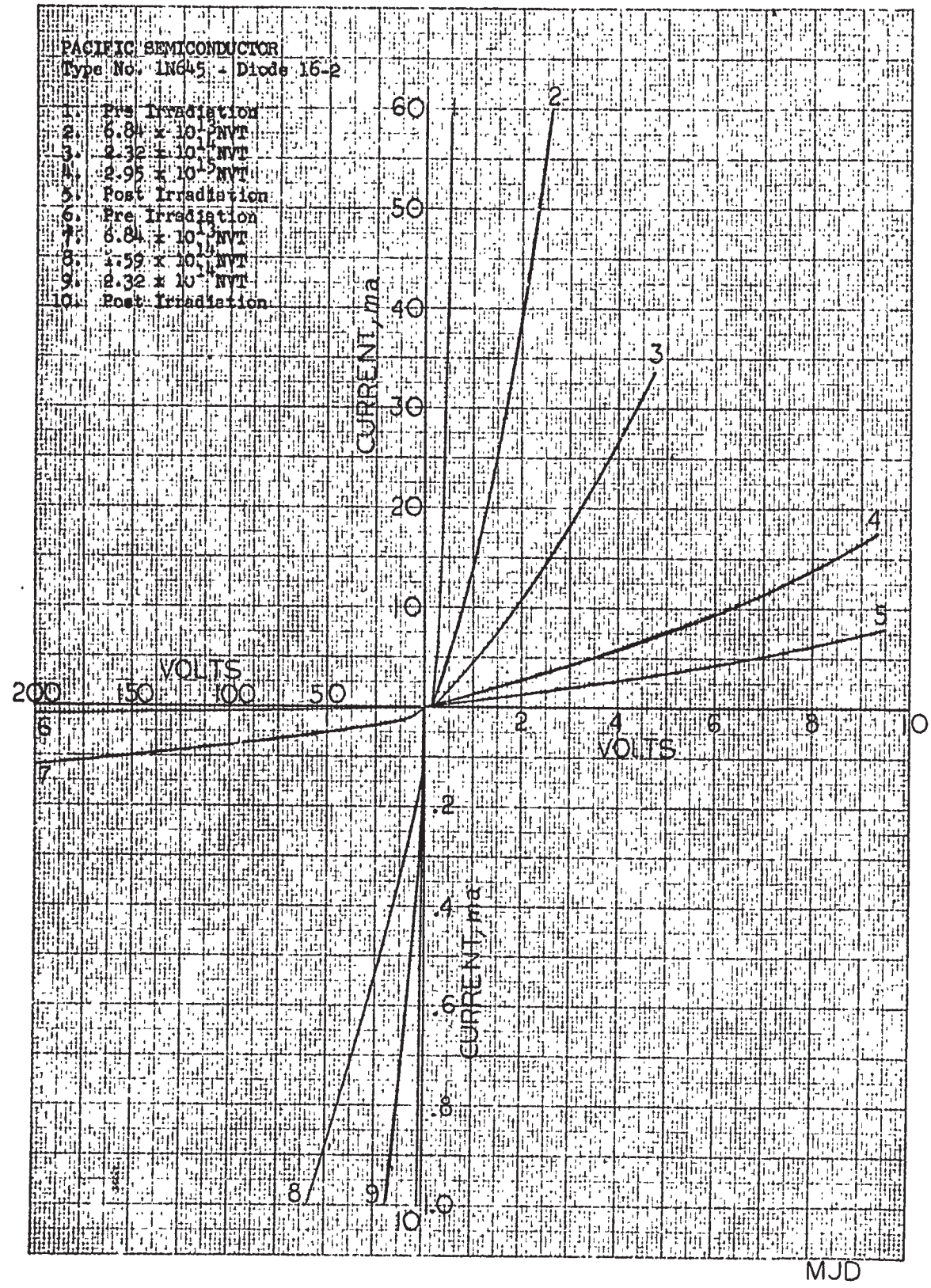

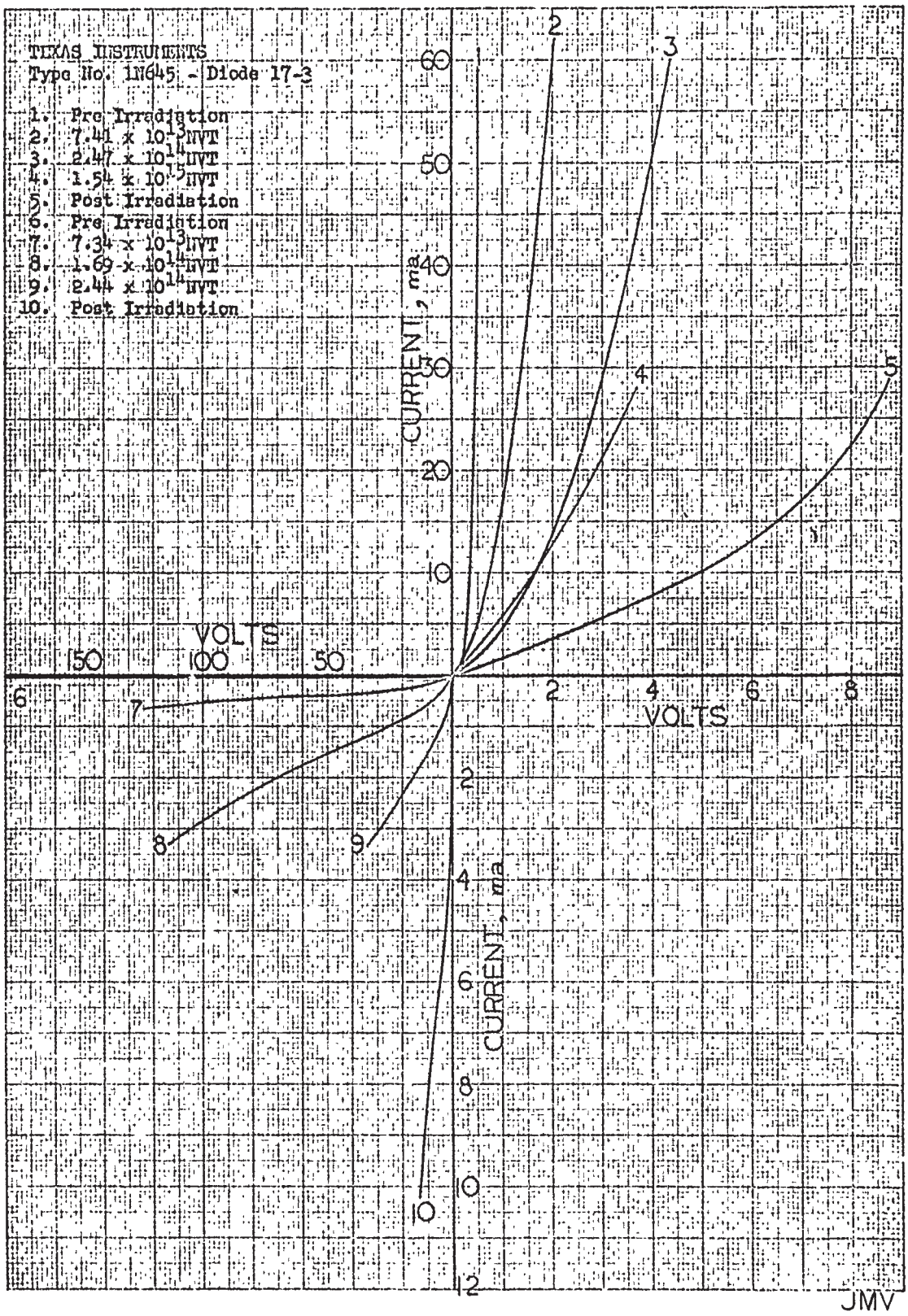

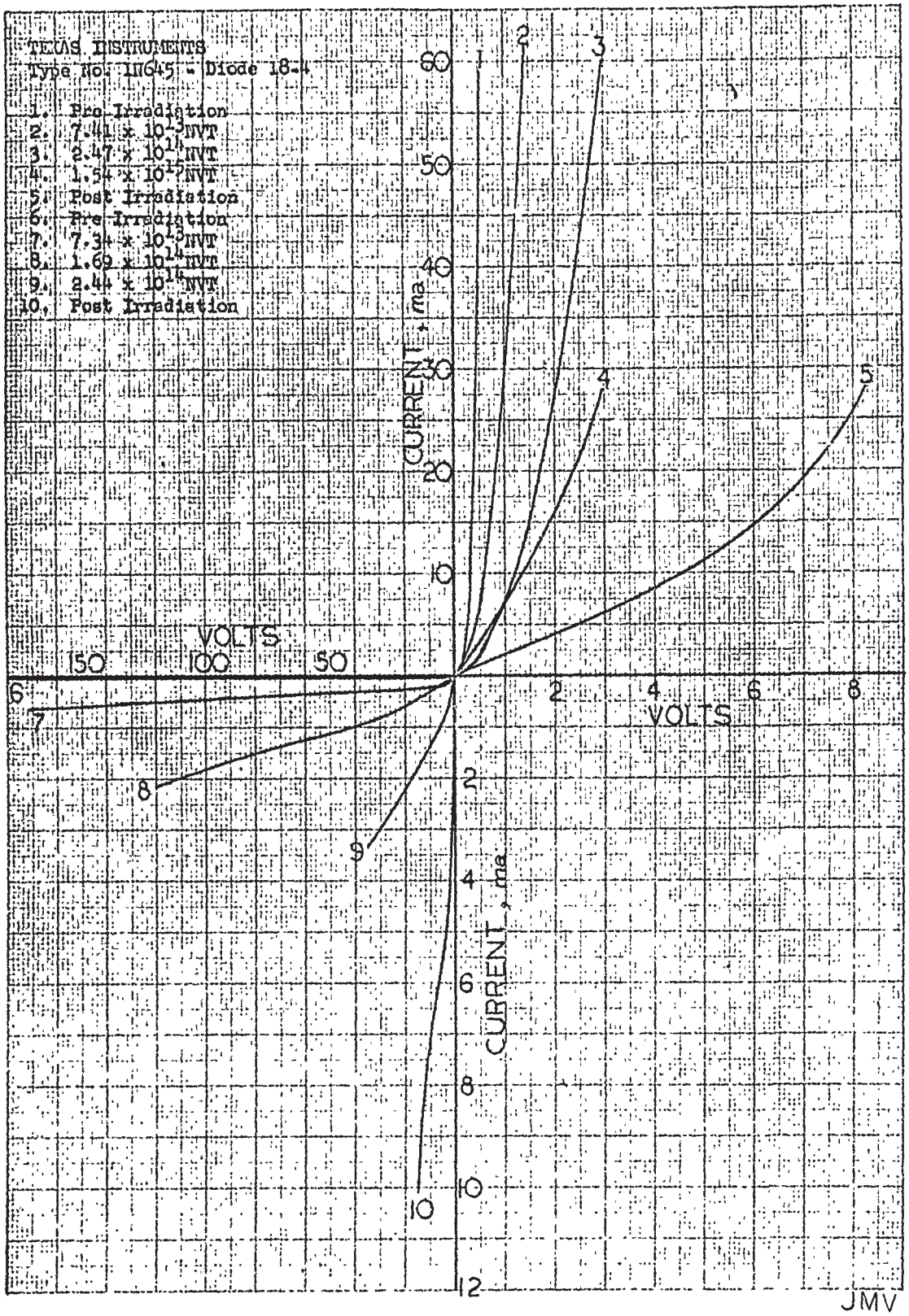

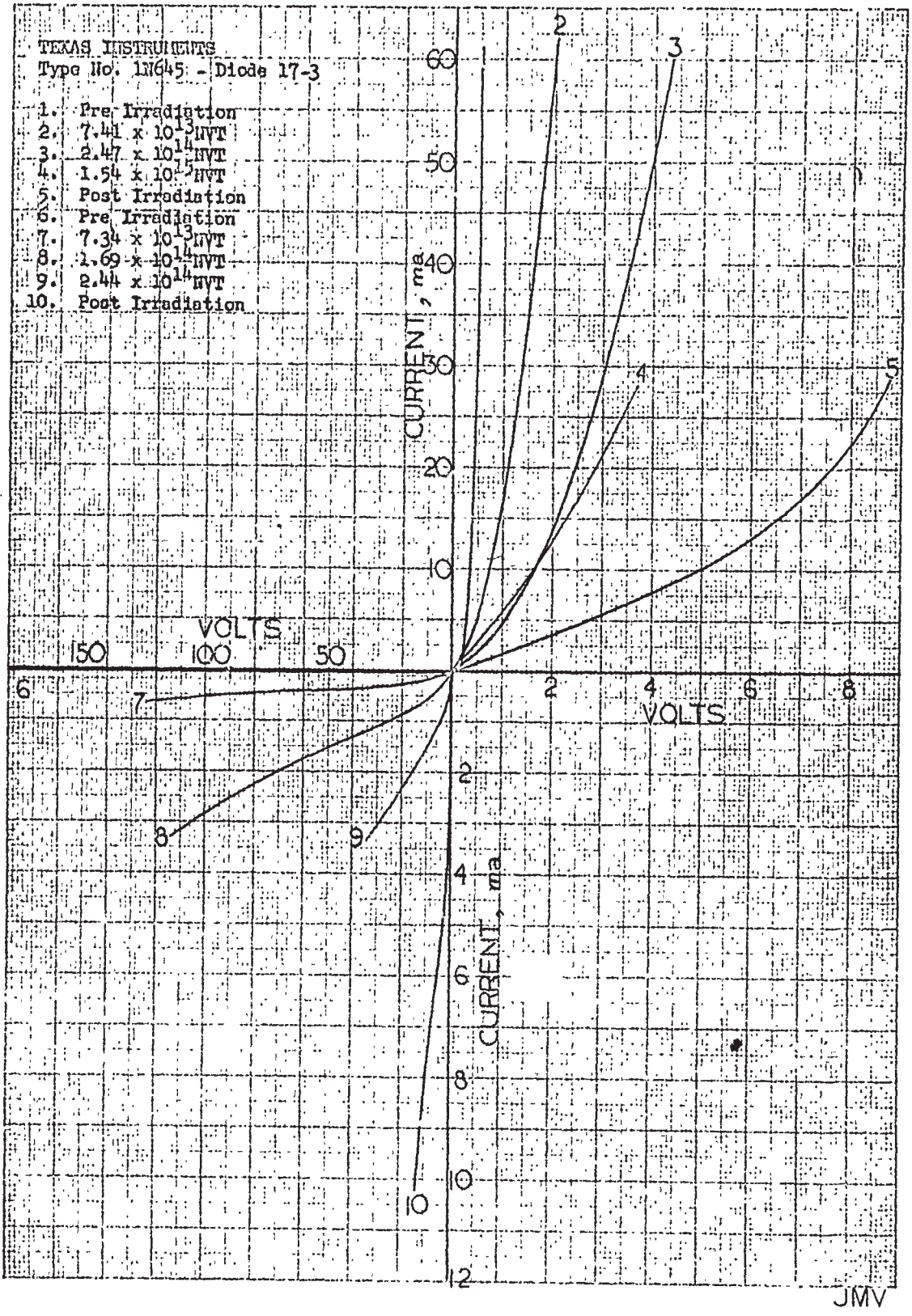

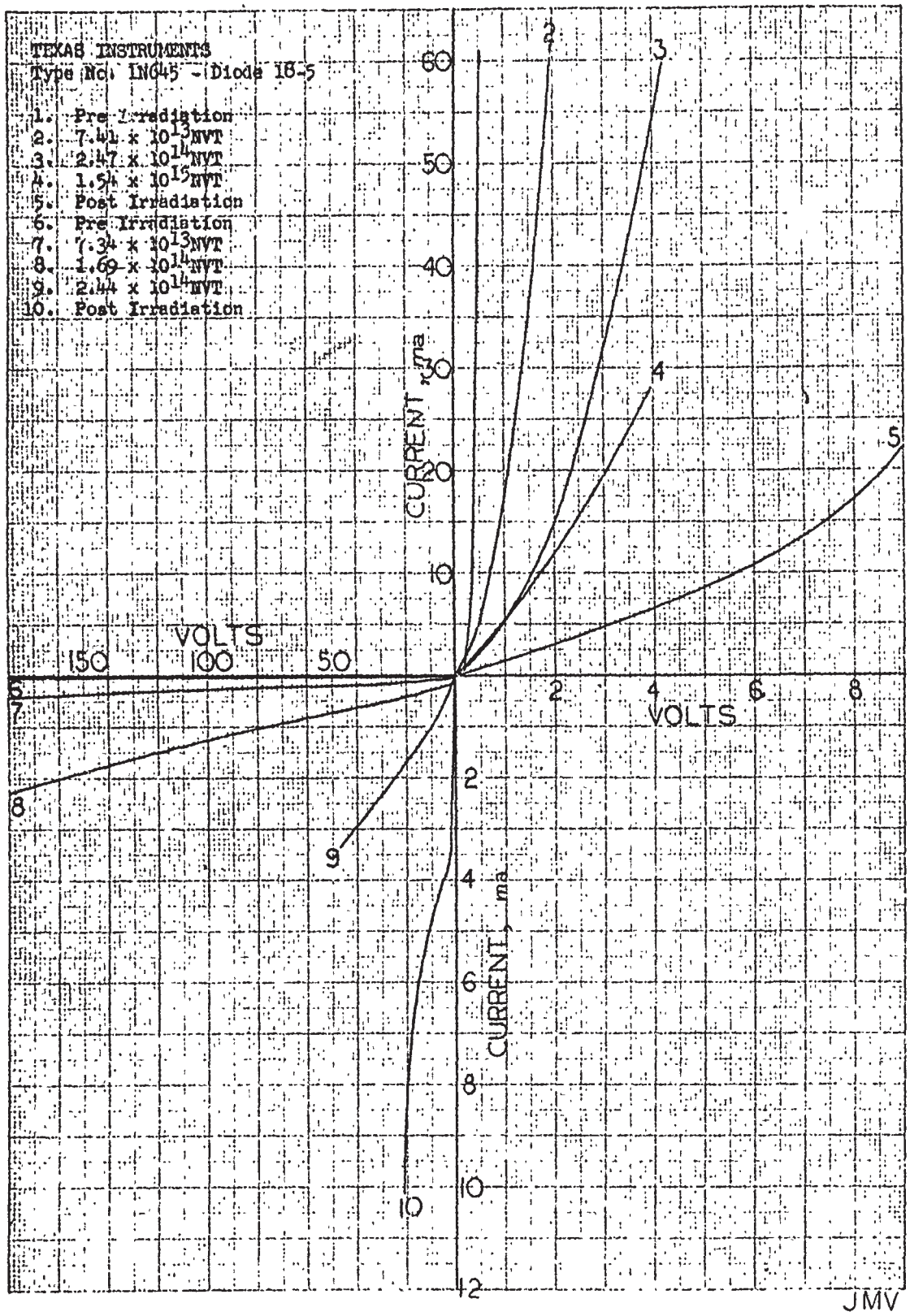

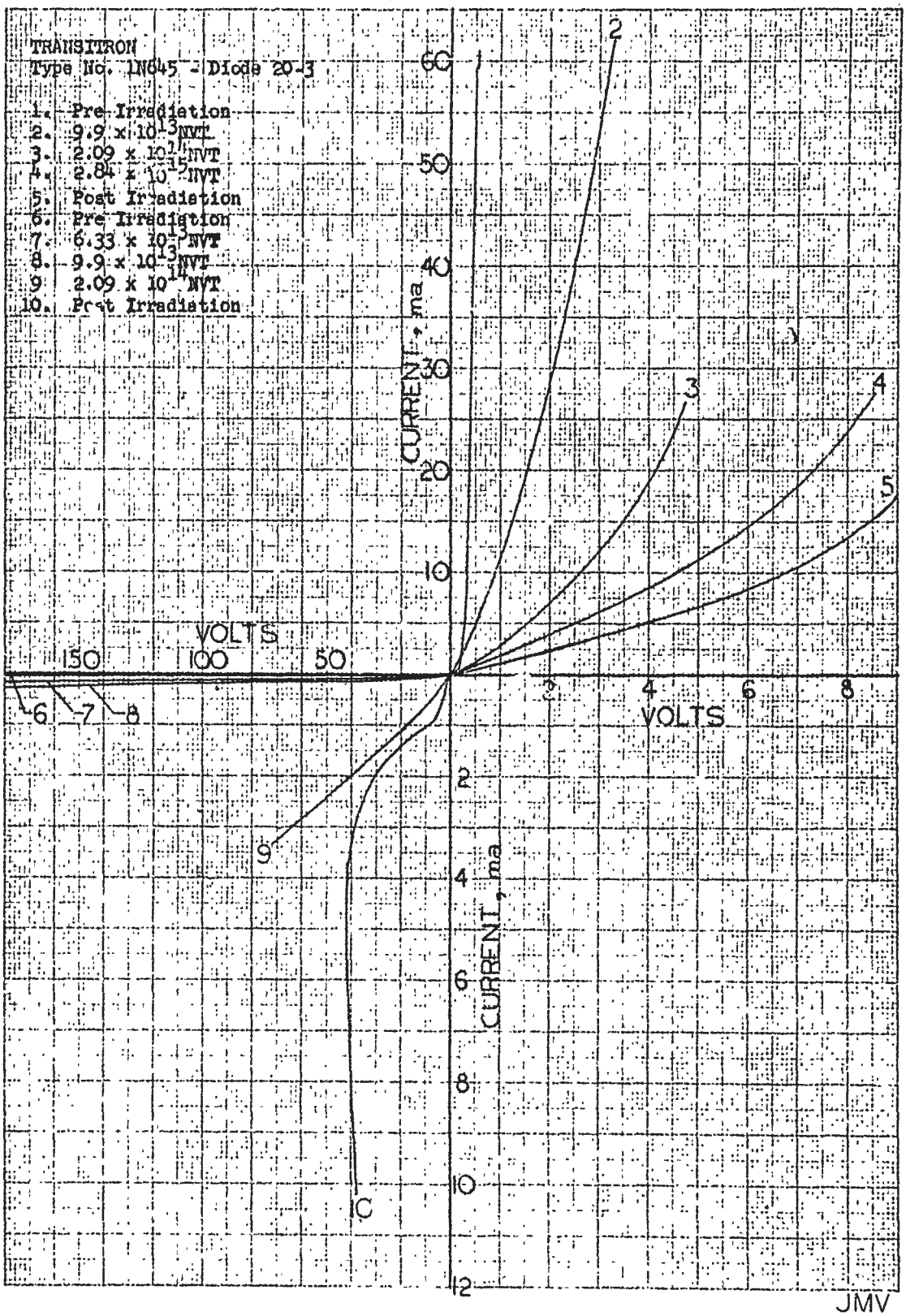

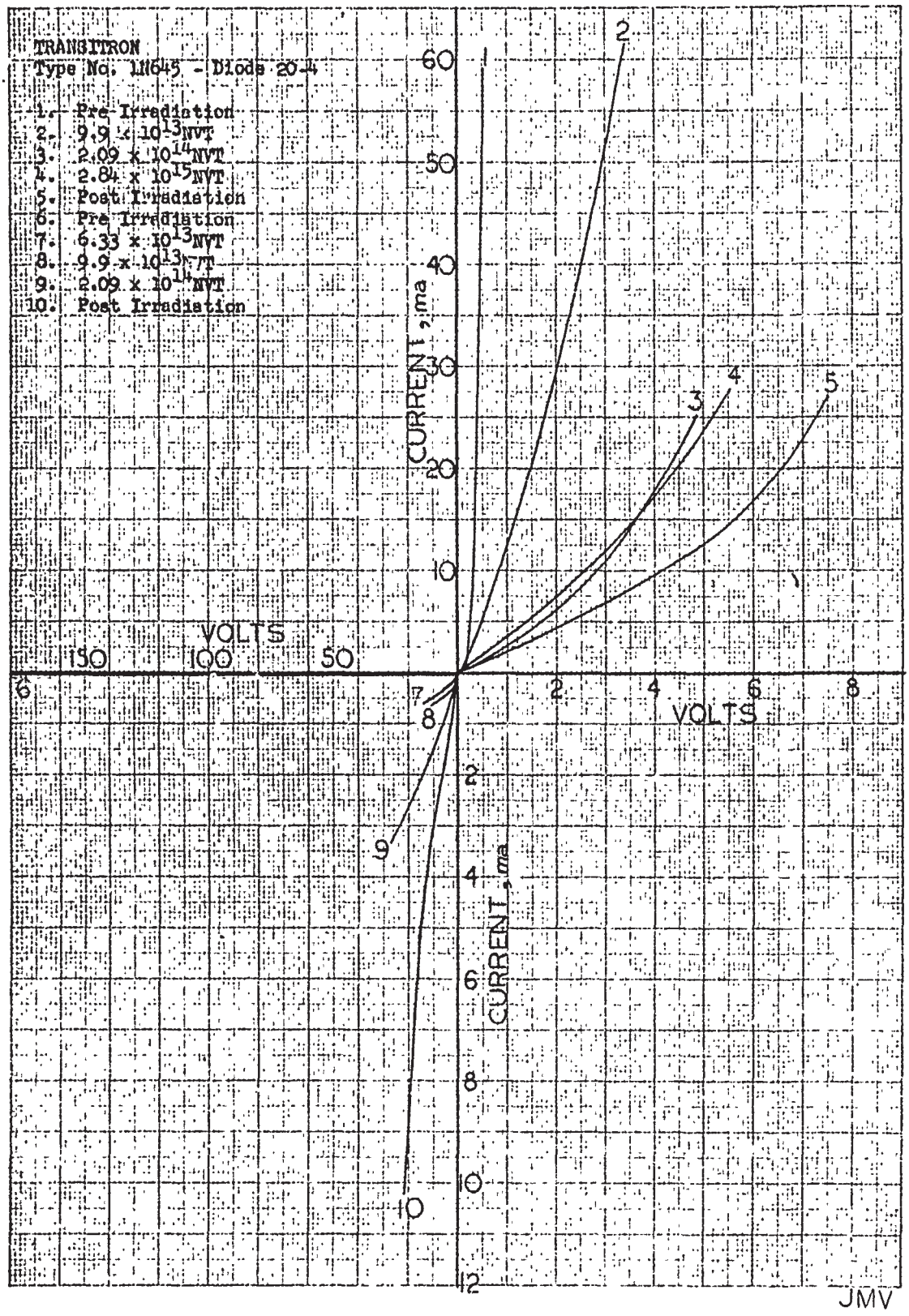

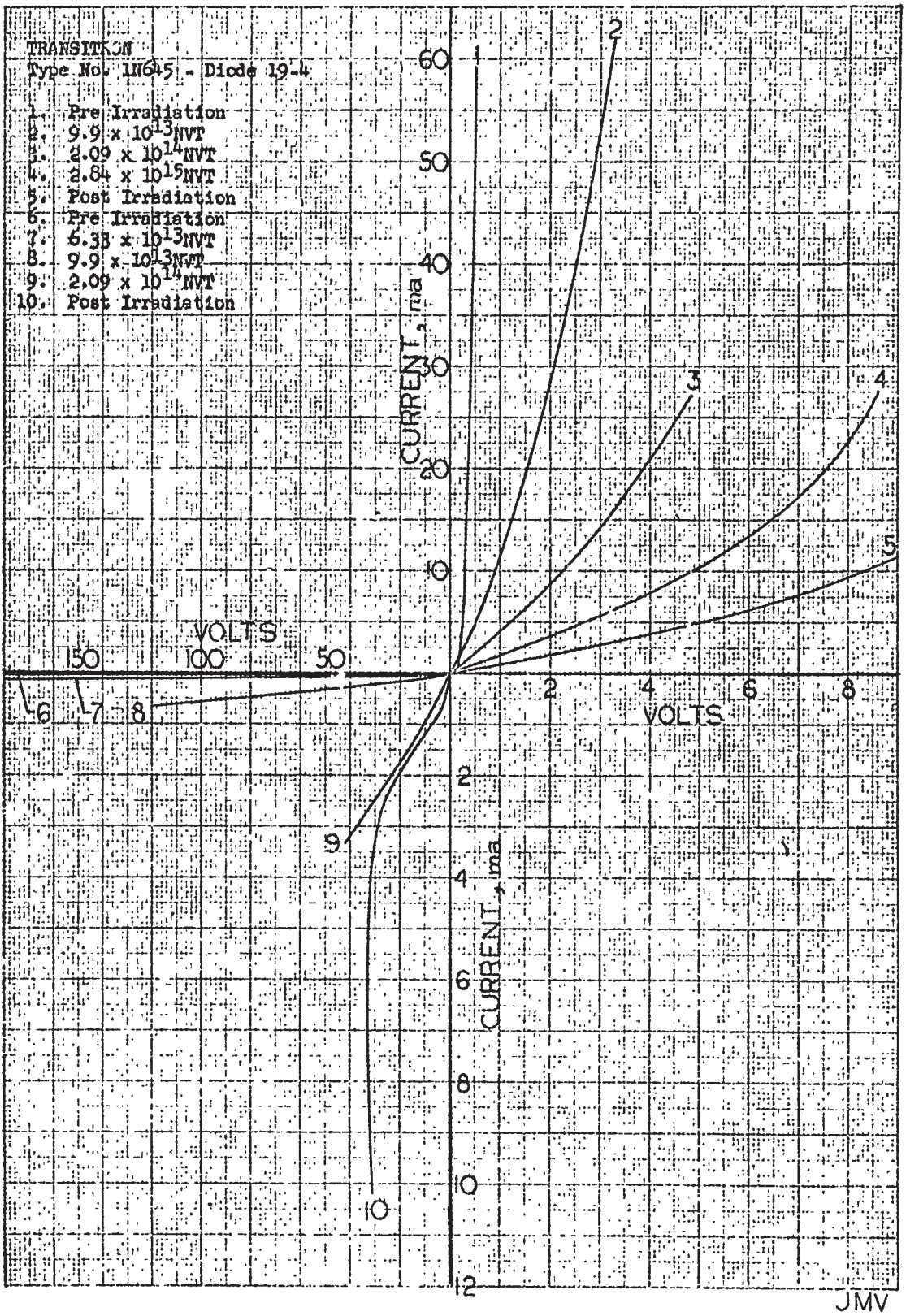

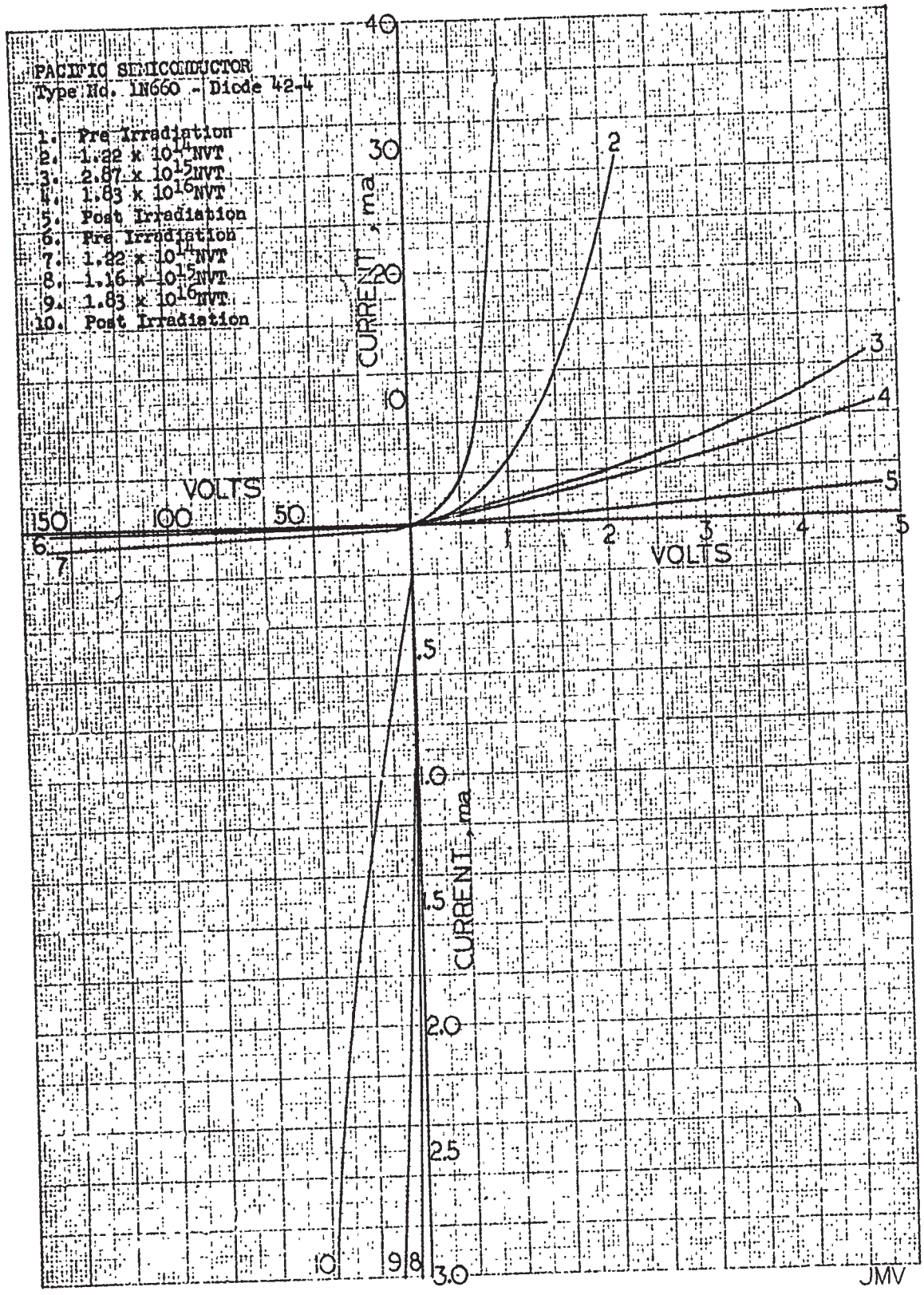

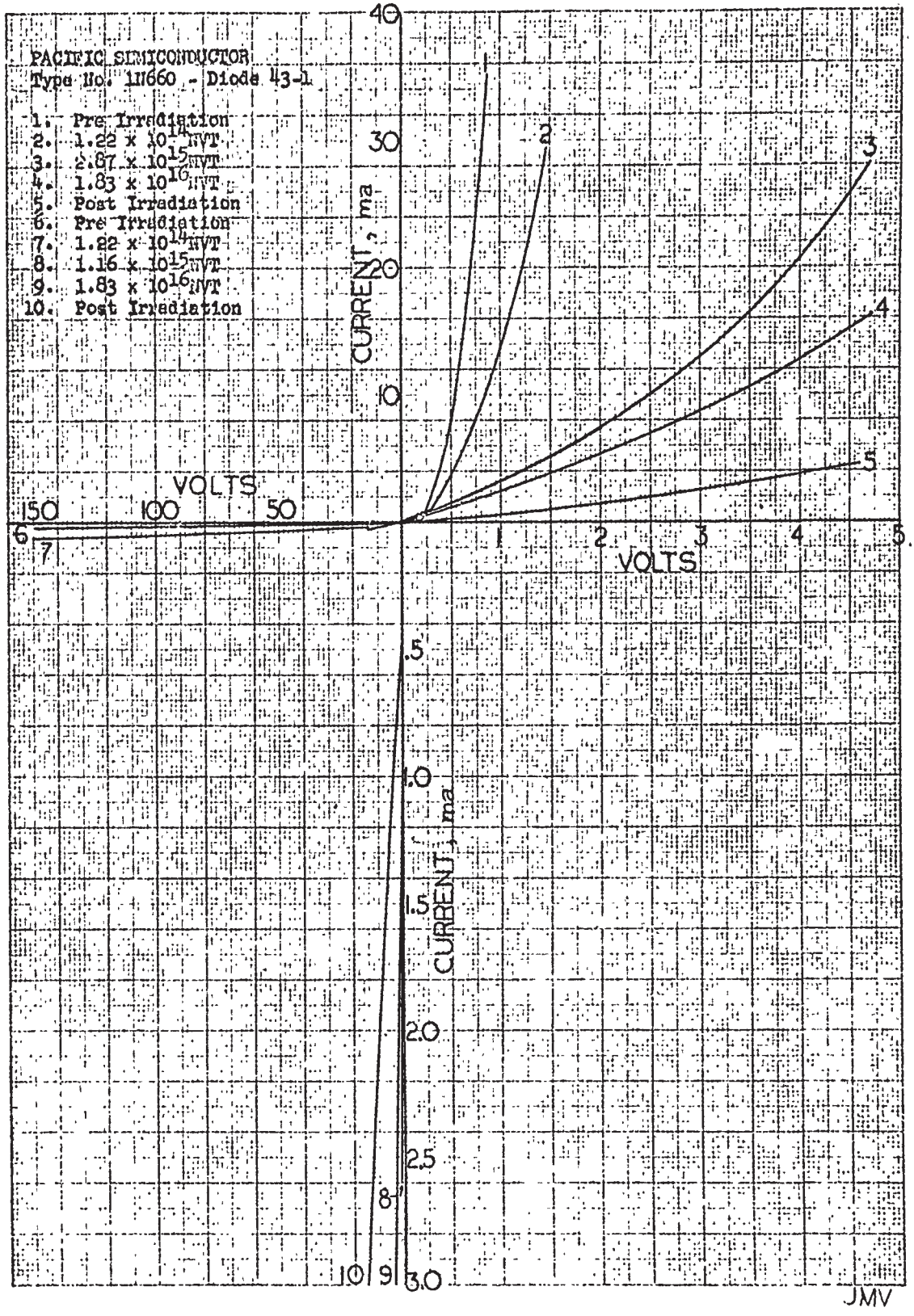

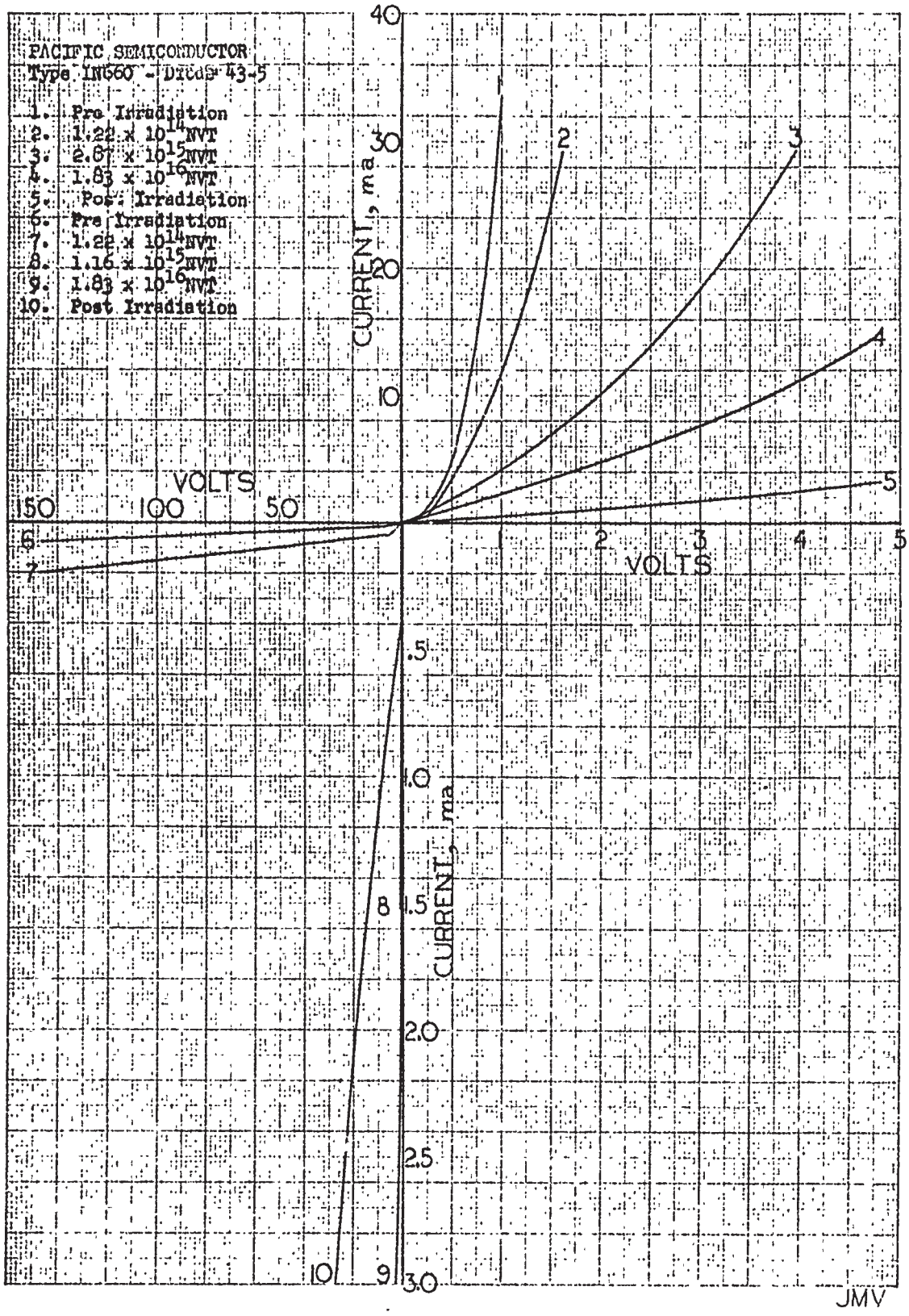

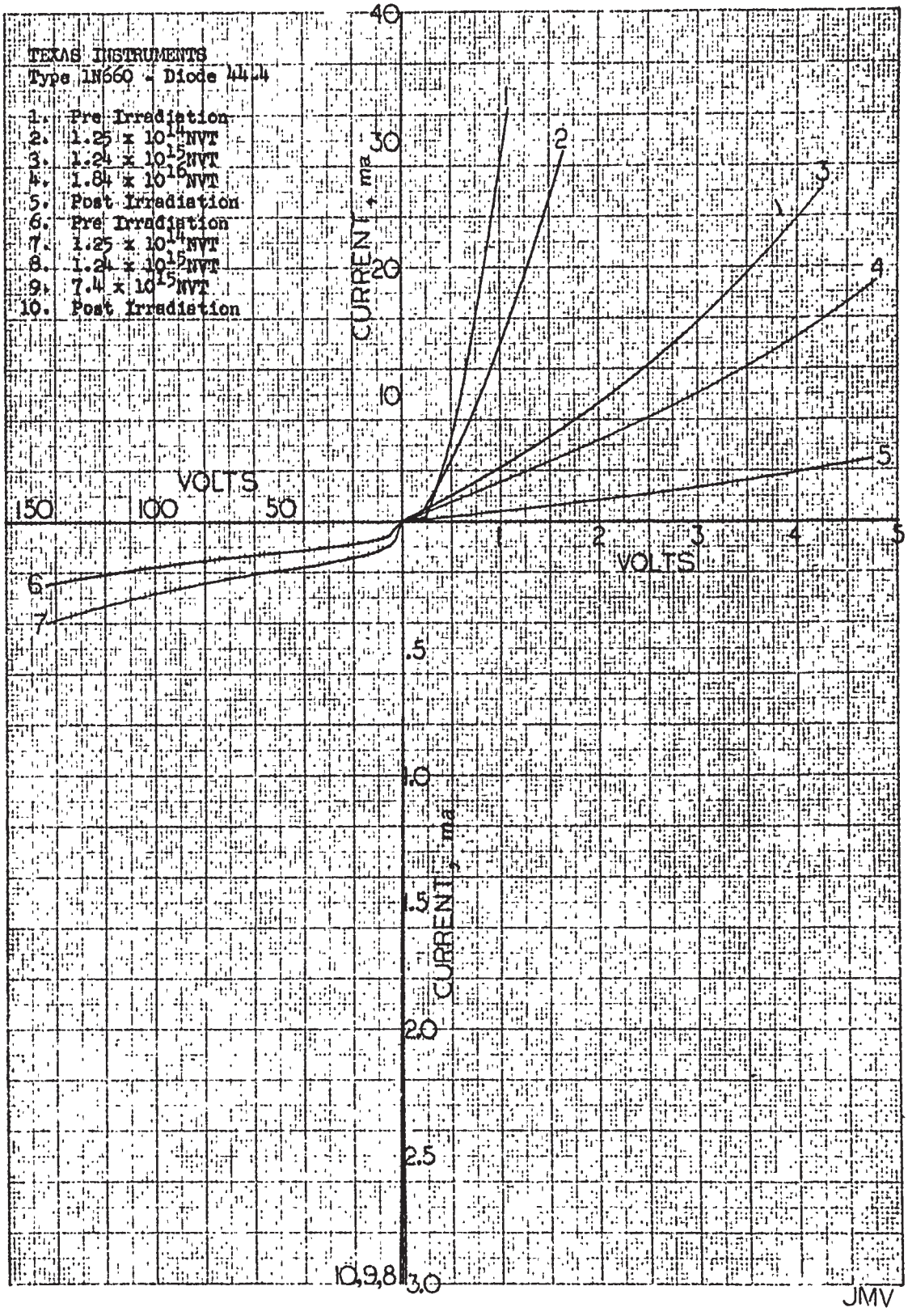

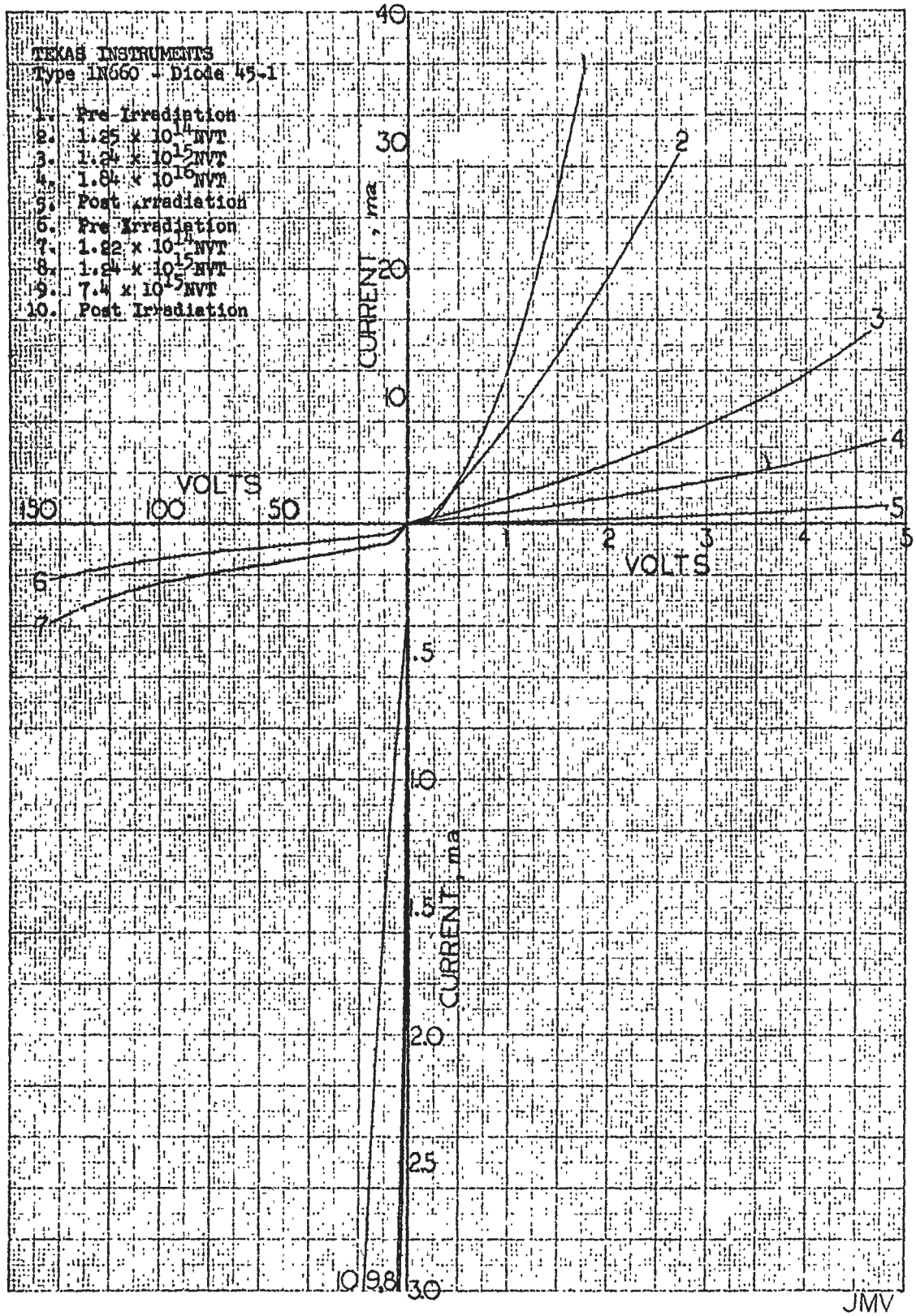

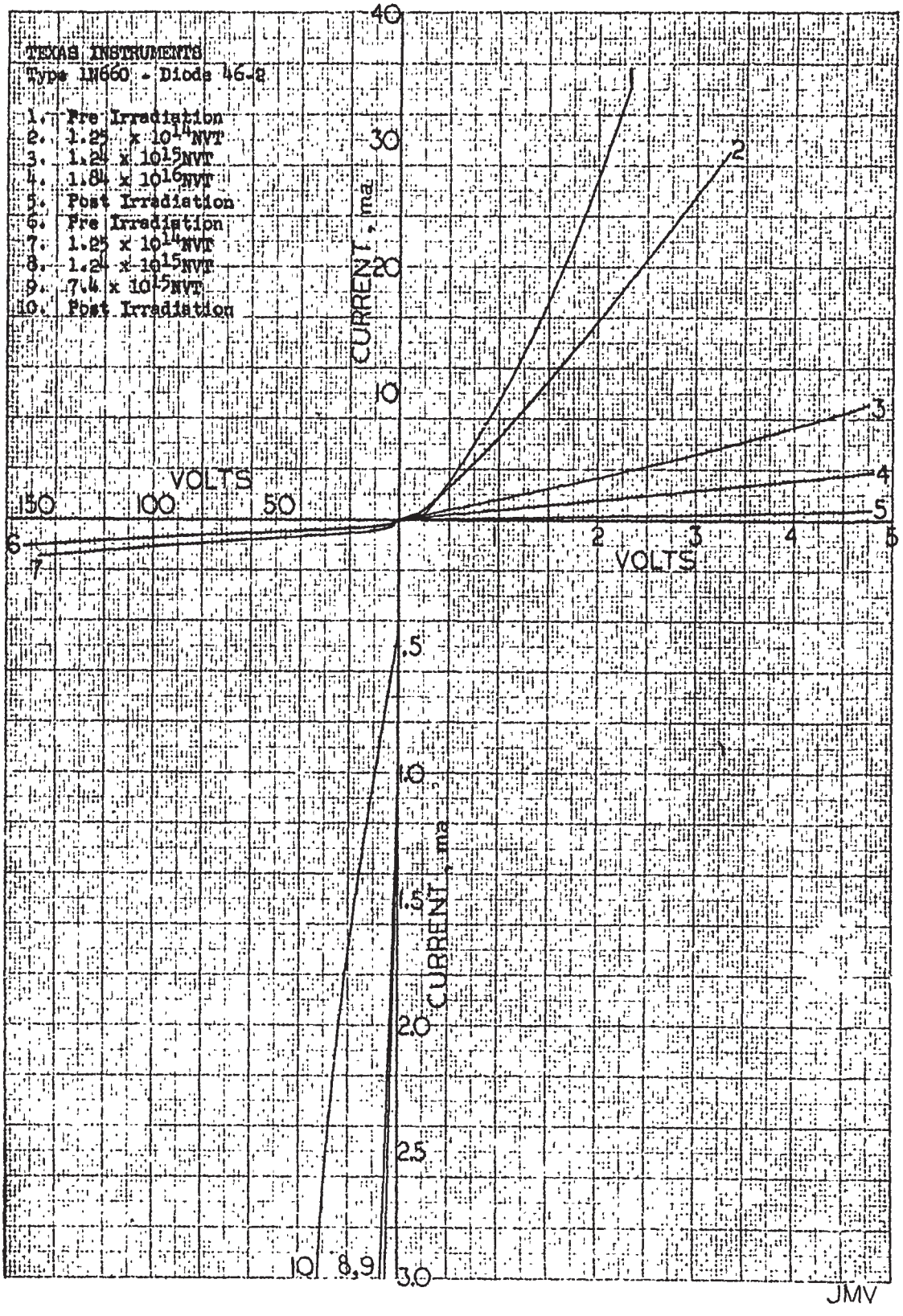

APPENDIX B: Infrared Detector Data

APPENDIX B

INFRARED DETECTOR DATA

UNIT NO. 1

Integrated Flux N/cm^2 $E>.48ev$	Signal Level (Arbitrary Units)	S/N Ratio (Hum and Noise)	Resistance of Detector (ohms)	Temperature °F
0	1.0	--	420 K	135
2.5×10^{13}	.69	--	440 K	135
4.4×10^{13}	.63	23	470 K	135
6.2×10^{13}	.53	20	470 K	135
8.3×10^{13}	.46	18	480 K	135
1.3×10^{14}	.38	16	510 K	135
1.5×10^{14}	.34	16	530 K	135
1.2×10^{15}	.048	--	530 K	152
4.1×10^{15}	.0046	--	650 K	230
5.2×10^{15}	.0085	--	560 K	260
7.3×10^{15}	.0067	--	18 K	215
2.0×10^{16}	--	--	360 K	156

UNIT NO. 2

Integrated Flux N/cm^2 $E>.48$ ev	Signal Level (Arbitrary Units)	S/N Ratio (Hum and Noise)	Resistance of Detector (ohms)	Temperature °F
0	1.0	--	580 K	135
2.2×10^{13}	0.90	--	620 K	135
3.9×10^{13}	0.58	30	670 K	135
5.6×10^{13}	0.48	25	710 K	135
7.5×10^{13}	0.42	20	690 K	135
1.1×10^{14}	0.41	20	710 K	135
1.3×10^{14}	0.33	18	740 K	135
1.1×10^{15}	0.045	--	800 K	152
3.6×10^{15}	0.016	--	440 K	230
4.6×10^{15}	0.022	--	420 K	260
6.9×10^{15}	0.0022	--	610 K	215
1.9×10^{16}	--	--	7.9 M	156

APPENDIX B

INFRARED DETECTOR DATA

UNIT NO. 3

Integrated Flux N/cm^2 $E>.48$ ev	Signal Level (Arbitrary Units)	S/N Ratio (Hum and Noise)	Resistance of Detector (ohms)	Temperature °F
0	1.0	--	580 K	135
2.2×10^{13}	0.73	--	570 K	135
4.3×10^{13}	0.78	16	570 K	135
6.0×10^{13}	0.65	14	590 K	135
8.0×10^{13}	0.54	14	630 K	135
1.2×10^{14}	0.43	13	670 K	135
1.4×10^{14}	0.38	11	720 K	135
1.1×10^{15}	0.038	--	1.1 M	152
3.6×10^{15}	0.016	--	580 K	230
4.6×10^{15}	0.018	--	590 K	260
6.8×10^{15}	0.014	--	960 K	215
1.9×10^{16}	--	--	140 K	156

UNIT NO. 4

Integrated Flux N/cm^2 $E>.48$ ev	Signal Level (Arbitrary Units)	S/N Ratio (Hum and Noise)	Resistance of Detector (ohms)	Temperature °F
0	1.0	--	450 K	135
2.2×10^{13}	1.0	--	400 K	135
4.3×10^{13}	0.53	22	690 K	135
6.0×10^{13}	0.47	18	700 K	135
8.0×10^{13}	0.82	15	390 K	135
1.2×10^{14}	0.73	16	410 K	135
1.4×10^{14}	0.71	16	410 K	135
1.1×10^{15}	0.010	--	480 K	152
3.6×10^{15}	0.0047	--	800 K	230
4.6×10^{15}	0.011	--	690 K	260
6.8×10^{15}	0.0044	--	1.6 M	215
1.9×10^{16}	--	--	270 K	156

APPENDIX B

INFRARED DETECTOR DATA

UNIT NO. 5

Integrated Flux N/cm^2 $E>.48$ ev	Signal Level (Arbitrary Units)	S/N Ratio (Hum and Noise)	Resistance of Detector (ohms)	Temperature °F
0	1.0	--	530 K	135
1.6×10^{13}	0.97	--	420 K	135
3.5×10^{13}	0.77	49	410 K	135
5.1×10^{13}	0.68	36	420 K	135
6.8×10^{13}	0.68	34	420 K	135
1.03×10^{14}	0.61	41	410 K	135
1.2×10^{14}	0.64	27	410 K	135
7.8×10^{14}	0.13	--	105 K	152
3.3×10^{15}	0.0026	--	85 K	230
4.3×10^{15}	0.071	--	160 K	260
6.2×10^{15}	0.10	--	200 K	215
1.4×10^{16}	1.80	--	550 K	--
1.5×10^{16}	0.21	--	190 K	157
1.8×10^{16}	0.077	.92	100 K	156

UNIT NO. 6

Integrated Flux N/cm^2 $E>.48$ ev	Signal Level (Arbitrary Units)	S/N Ratio (Hum and Noise)	Resistance of Detector (ohms)	Temperature °F
0	1.0	--	--	135
1.3×10^{13}	1.1	--	--	135
3.7×10^{13}	1.0	0.12	--	135
5.2×10^{13}	2.2	0.0	--	135
6.9×10^{13}	2.0	0.25	--	135
1.06×10^{14}	2.0	0.0	--	135
1.2×10^{14}	1.5	0.058	--	135
9.6×10^{14}	0.52	--	--	152
3.1×10^{15}	0.20	--	--	230
4.0×10^{15}	0.018	--	--	260
5.9×10^{15}	0.11	--	--	215
1.3×10^{16}	0.082	--	--	--

APPENDIX B

INFRARED DETECTOR DATA

UNIT NO. 7

Integrated Flux N/cm^2 $E>.48ev$	Signal Level (Arbitrary Units)	S/N Ratio (Hum and Noise)	Resistance of Detector (ohms)	Temperature °F
0	1.0	--	560 K	130
1.3×10^{13}	0.14	--	490 K	130
3.7×10^{13}	0.69	4.7	540 K	130
5.2×10^{13}	0.62	4.0	540 K	130
6.9×10^{13}	0.67	4.3	540 K	130
1.06×10^{14}	0.61	5.2	540 K	130
9.6×10^{14}	0.53	--	310 K	140
3.1×10^{15}	0.33	--	62 K	~ 200
4.0×10^{15}	0.42	--	33 K	~ 220
5.9×10^{15}	0.61	--	72 K	~ 200
1.3×10^{16}	0.61	--	--	--
1.4×10^{16}	0.67	--	300 K	~147
1.7×10^{16}	0.47	3.6	280 K	~147
2.1×10^{16}	0.67	2.3	720 K	110
2.2×10^{16}	0.67	1.4	730 K	110
2.22×10^{16}	0.61	2.2	800 K	110

UNIT NO. 8

Integrated Flux N/cm^2 $E>.48ev$	Signal Level (Arbitrary Units)	S/N Ratio (Hum and Noise)	Resistance of Detector (ohms)	Temperature °F
0	1.0	--	6.6 M	130
1.05×10^{13}	1.1	--	6.1 M	130
3.4×10^{13}	0.72	3.5	6.5 M	130
4.7×10^{13}	0.73	3.6	6.5 M	130
6.2×10^{13}	0.72	2.1	6.5 M	130
9.6×10^{13}	0.72	3.1	6.5 M	130
1.1×10^{14}	0.73	3.1	6.4 M	~ 130
7.2×10^{14}	0.58	--	3.1 M	~ 140
3.1×10^{14}	0.40	--	970 K	~ 200
3.9×10^{15}	0.39	--	540 K	~220
5.9×10^{15}	0.37	--	970 K	~200
1.2×10^{16}	0.49	--	--	--
1.4×10^{16}	0.92	--	2.6 M	~147
1.6×10^{16}	0.43	1.2	2.7 M	~147

APPENDIX B

INFRARED DETECTOR DATA

UNIT NO. 9

Integrated Flux N/cm^2 E>.48 ev	Signal Level (Arbitrary Units)	S/N Ratio (Hum and Noise)	Resistance of Detector (ohms)	Temperature °F
0	1.0	--	--	127
1.0×10^{13}	1.2	--	--	127
3.7×10^{13}	0.63	1.1	--	127
5.2×10^{13}	0.89	0.44	--	127
6.9×10^{13}	0.95	0.67	--	--
1.06×10^{14}	0.84	0.67	--	130
1.2×10^{14}	0.89	0.53	--	126
3.1×10^{15}	0.53	--	--	132
4.0×10^{15}	1.1	--	--	180
5.9×10^{15}	0.58	--	--	190
1.3×10^{16}	1.3	--	--	180

UNIT NO. 10

Integrated Flux N/cm^2 E>.48 ev	Signal Level (Arbitrary Units)	S/N Ratio (Hum and Noise)	Resistance of Detector (ohms)	Temperature °F
0	1.0	--	560 K	127
9.5×10^{12}	0.91	--	420 K	127
3.9×10^{13}	0.68	7.4	510 K	127
5.5×10^{13}	0.59	7.3	440 K	127
7.2×10^{13}	0.60	9.0	480 K	127
1.1×10^{14}	0.60	9.0	440 K	130
1.3×10^{14}	0.57	6.1	440 K	126
1.0×10^{15}	0.39	--	40 K	132
3.3×10^{15}	0.42	--	17 K	180
4.2×10^{15}	0.24	--	8.5 K	190
6.2×10^{15}	0.043	--	40 K	180
1.3×10^{16}	0.012	--	--	--
1.4×10^{16}	1.3	--	280 K	--
1.5×10^{16}	0.013	--	51 K	137
1.8×10^{16}	--	--	--	137

APPENDIX B

INFRARED DETECTOR DATA

UNIT NO. 11

Integrated Flux N/cm^2 $E>.48$ ev	Signal Level (Arbitrary Units)	S/N Ratio (Hum and Noise)	Resistance of Detector (ohms)	Temperature °F
0	1.0	--	350 K	127
8.6×10^{12}	1.3	--	340 K	127
4.3×10^{13}	0.67	24	340 K	127
6.0×10^{13}	0.56	17	360 K	127
7.9×10^{13}	0.48	17	360 K	--
1.2×10^{14}	0.33	15	390 K	130
1.4×10^{14}	0.26	15	390 K	126
1.1×10^{15}	0.074	--	1.6 M	132
3.6×10^{15}	0.027	--	1.0 M	180
4.6×10^{15}	0.0081	--	860 K	190
6.8×10^{15}	0.070	--	1.8 M	180
1.9×10^{16}	--	--	440 K	137

UNIT NO. 12

Integrated Flux N/cm^2 $E>.48$ ev	Signal Level (Arbitrary Units)	S/N Ratio (Hum and Noise)	Resistance of Detector (ohms)	Temperature °F
0	1.0	--	310 K	127
5.8×10^{12}	1.0	--	330 K	127
4.3×10^{13}	0.57	22	330 K	127
6.0×10^{13}	0.50	15	350 K	127
7.9×10^{13}	0.40	16	360 K	--
1.2×10^{14}	0.31	12	390 K	130
1.4×10^{14}	0.23	12	360 K	126
1.1×10^{15}	0.067	--	1.4 M	132
3.6×10^{15}	0.023	--	1.0 M	180
4.6×10^{15}	0.0067	--	820 K	190
6.8×10^{15}	0.019	--	1.9 M	180
1.9×10^{16}	--	--	760 K	137

APPENDIX B

INFRARED DETECTOR DATA

UNIT NO. 13

Integrated Flux N/cm^2 $E>.48$ ev	Signal Level (Arbitrary Units)	S/N Ratio (Hum and Noise)	Resistance of Detector (ohms)	Temperature °F
0	1.0	--	470 K	127
2.5×10^{12}	0.95	--	510 K	127
4.6×10^{13}	0.52	44	500 K	127
6.5×10^{13}	0.45	31	530 K	127
8.6×10^{13}	0.38	30	550 K	--
1.3×10^{14}	0.28	29	570 K	130
1.5×10^{14}	0.21	26	600 K	126
1.2×10^{15}	0.38	--	2.0 M	132
3.9×10^{15}	0.012	--	1.2 M	180
5.0×10^{15}	0.0011	--	750 K	190
7.3×10^{15}	0.0089	--	2.0 M	180
2.1×10^{16}	--	--	500 K	137

UNIT NO. 14

Integrated Flux N/cm^2 $E>.48$ ev	Signal Level (Arbitrary Units)	S/N Ratio (hum and Noise)	Resistance of Detectors (ohms)	Temperature °F
0	1.0	--	400 K	127
1.3×10^{12}	1.0	--	420 K	127
4.6×10^{13}	0.48	130	420 K	127
6.5×10^{13}	0.42	48	430 K	127
8.6×10^{13}	0.32	53	460 K	--
1.3×10^{14}	0.020	64	490 K	130
1.5×10^{14}	0.12	87	530 K	126
1.2×10^{15}	0.054	--	700 K	132
3.9×10^{15}	0.024	--	1.0 M	180
5.0×10^{15}	0.0046	--	860 K	190
7.3×10^{15}	0.013	--	2.1 M	180
2.1×10^{16}	--	--	610 K	137